



**HAL**  
open science

# Comprehensive study of the effects of formulation and processing parameters on structural and functional properties of active bio-based packaging films

Mia Kurek

► **To cite this version:**

Mia Kurek. Comprehensive study of the effects of formulation and processing parameters on structural and functional properties of active bio-based packaging films. Other. Université de Bourgogne; Sveučilište u Zagrebu (Hrvatska), 2012. English. NNT : 2012DIJOS095 . tel-01624565

**HAL Id: tel-01624565**

**<https://theses.hal.science/tel-01624565>**

Submitted on 26 Oct 2017

**HAL** is a multi-disciplinary open access archive for the deposit and dissemination of scientific research documents, whether they are published or not. The documents may come from teaching and research institutions in France or abroad, or from public or private research centers.

L'archive ouverte pluridisciplinaire **HAL**, est destinée au dépôt et à la diffusion de documents scientifiques de niveau recherche, publiés ou non, émanant des établissements d'enseignement et de recherche français ou étrangers, des laboratoires publics ou privés.



**UNIVERSITÉ DE BOURGOGNE**  
**SVEUČILIŠTE U ZAGREBU**  
UMR PAM-PAPC  
*Faculty of Food Technology and Biotechnology*



## ***Doctoral dissertation***

*Presented in Fulfilment of the Requirements for  
the Degree Doctor of Philosophy in the joint supervision between University of  
Burgundy and University of Zagreb*

# ***Comprehensive study of the effects of formulation and processing parameters on structural and functional properties of active bio-based packaging films***

*presented by*

***MIA KUREK***

*Publicly presented and defended on 24 October 2012 in Dijon*

*Thesis supervisors:*

***Professor Frédéric DEBEAUFORT***  
***Professor Kata GALIĆ***

*Dissertation Committee:*

<i>Mr. Stéphane Desobry</i>	<i>Université de Lorraine, France</i>	<i>Reviewer</i>
<i>Mr. Srećko Valić</i>	<i>University of Rijeka, Croatia</i>	<i>Reviewer</i>
<i>Ms. Nadia Oulahal</i>	<i>Université Claude Bernard Lyon I, France</i>	<i>Examiner</i>
<i>Mr. Damir Ježek</i>	<i>University of Zagreb, Croatia</i>	<i>Examiner</i>
<i>Ms. Kata Galić</i>	<i>University of Zagreb, Croatia</i>	<i>Supervisor</i>
<i>Mr. Frédéric Debeaufort</i>	<i>Université de Bourgogne</i>	<i>Supervisor</i>

**CONFIDENTIAL**





*To my parents*



## *Abstract*

---

### **Comprehensive study of the effects of formulation and processing parameters on structural and functional properties of active bio-based packaging films**

---

The aim of this study is the analysis of structure and transfer mechanisms through chitosan based food packaging materials with incorporated carvacrol as a model of antimicrobial active substance. Integration of composition parameters, structure, processing and drying of chitosan systems is correlated to its physico-chemical and functional properties. Understanding and detailed analyses of processing parameters is crucial in production of active chitosan coatings applied on conventional materials such as polyethylene. So, the knowledge of composition and microstructure in association to environmental conditions, control the retention and the release kinetics of carvacrol from chitosan film. Water vapour was crucial parameter that strongly influenced adsorption, swelling and plasticization of chitosan based films, as well as thermal, surface and mechanical properties. By changing the matrix structure, penetrating water molecules decreased gas barrier efficiency and increased release of carvacrol. Furthermore, release of carvacrol in the headspace was correlated to the antimicrobial efficiency and to the organoleptic impact on packed food products. Such investigation highlights the transfer mechanism within bio-based materials, prior to efficiency prediction for their industrial development.

In dry conditions, all chitosan films were fairly good gas barriers (about  $10^{-17}$  g/m·s·Pa). Chitosan coated polyethylene films were up to 10000 times less permeable than uncoated PE. Increase in the environmental humidity above 60% and up to 96% (that represents the conditions of a real fresh food packaging system), significantly increased gas permeability of all chitosan films. Mechanical tests confirmed that when relative humidity increased, structural changes were induced. Therefore, extensive water plasticization of chitosan matrix was observed.

Diffusion coefficients of carvacrol from chitosan film increased up to 1000 times when humidity increased from 0% to 100%. Water vapour triggers the release of carvacrol in the vapour phase. This indicates the importance of controlling the environmental conditions in the packaging at the time of the application but also during the active film storage.

Films with carvacrol concentrations in the vapour phase above  $2 \times 10^{-7}$  g/mL<sub>air</sub> were efficient against large spectrum of bacteria, including some Gram-positive bacteria, Gram-negative bacteria and fungi. In some instances the concentration that was required for carvacrol antimicrobial efficiency was not organoleptically acceptable to consumers.

**Keywords:** chitosan, active packaging, mass transfer, water vapour, permeability, release, antimicrobial efficiency, headspace

## *Sažetak*

---

### **Sveobuhvatno istraživanje utjecaja formulacije i procesnih parametara na strukturna i funkcionalna svojstva aktivnih ambalažnih biomaterijala**

---

Cilj ovog rada je analiza strukture i mehanizama prijenosa tvari kroz ambalažne materijale za pakiranje hrane na bazi kitozana s inkorporiranim karvakrolom kao modelnom aktivnom antimikrobnom tvari. Integrirani sastavni parametri, struktura, proizvodnja i sušenje kitozanskog sustava korelirani su sa njegovim fizikalno-kemijskim i funkcionalnim svojstvima. Razumijevanje i detaljna analiza procesnih parametara predstavlja ključan korak u proizvodnji aktivnih kitozanskih prevlaka na konvencionalnim materijalima kao što je polietilen. Dakle, poznavanje sastava i mikrostrukture u ovisnosti o okolnim uvjetima, osnovni je preduvjet za kontrolirano zadržavanje i otpuštanje karvakrola iz filmova na bazi kitozana. Vodena para predstavlja ključni parametar koji značajno utječe na adsorpciju, bubrenje i plastifikaciju kitozanskih filmova, kao i na njegova toplinska, površinska, i mehanička svojstva. Penetracijom (prodiranjem) molekula vode dolazi do promjene strukture matriksa, smanjuje se učinkovitost barijernih svojstava prema plinovima i povećava otpuštanje karvakrola. Otpuštanje karvakrola u zračnom prostoru u korelaciji je sa antimikrobnom učinkovitošću i organoleptičkim svojstvima upakiranih prehrambenih proizvoda. Ovo istraživanje prije svega naglašava značaj poznavanja mehanizma prijenosa tvari unutar biomaterijala koji je neophodan za predviđanje učinkovite primjene na industrijskoj razini.

**Ključne riječi:** kitozan, aktivno pakiranje, prijenos mase, vodena para, propusnost, otpuštanje, antimikrobna efikasnost, plinovito stanje

## *Résumé*

---

### **Contribution à la compréhension de l'influence des paramètres de formulation et de procédé sur la structure et les propriétés fonctionnelle de films actifs à base de bio-polymères**

---

Cette étude porte sur l'analyse du mécanisme de transfert du carvacrol (molécule antimicrobienne volatile) au travers de films à base de chitosan. La composition, la structure, les paramètres de procédés et de séchage de la couche de chitosan ont été corrélés aux propriétés physico-chimiques et fonctionnelles des films. La compréhension de ces facteurs et de leurs influences est cruciale à l'optimisation de la production de films actifs à base de polyéthylène enduits de chitosan. En effet, composition, microstructure et condition environnementale (température, humidité) conditionnent la rétention puis la libération contrôlée du carvacrol. La présence d'humidité induit absorption, gonflement, et plastification du chitosan, et par conséquent influe sur la structure, ses propriétés thermiques et de surface. L'absorption d'humidité, due au changement de structure, entraîne une forte augmentation de la perméabilité aux gaz et à la vapeur d'eau, et favorise ainsi la libération du carvacrol, nécessaire à une efficacité antimicrobienne rapide. Cette dernière, ainsi que l'impact sensoriel sur l'aliment emballé, sont directement corrélés aux aspects cinétiques et de partage des vapeurs de carvacrol. Ces travaux ont ainsi mis en évidence l'importance de la compréhension de mécanismes de transfert dans les emballages à base de bio-polymères sur leur production et application industrielles.

**Mots-clés:** chitosane, emballages actifs, transfert de matière, eau, perméabilité, libération contrôlée, activité antimicrobienne, phase vapeur



## *List of publications and communications*

### **Publications from PhD work:**

1. **Kurek, M.**, Descours, E., Galić, K., Voilley, A., & Debeaufort, F. (2012). How composition and process parameters affect volatile active compounds in biopolymer films. *Carbohydrate Polymers*, 88, 646-656.
2. **Kurek, M.**, Ščetar, M., Voilley, A., Galić, K., & Debeaufort, F. (2012). Barrier properties of chitosan coated polyethylene. *Journal of Membrane Science*, 404-405, 162-168.
3. **Kurek, M.**, Brachais, C-H., Ngumjeu, C.M., Bonnotte, A., Voilley, A., Galić, K., & Debeaufort, F. (2012). Structure and thermal properties of a chitosan coated polyethylene bilayer film. *Polymer Degradation and Stability*, 97(8), 1232-1240.
4. **Kurek, M.**, Brachais, C-H., Ščetar, M., Voilley, A., Galić, K., Couvercelle, J.P., & Debeaufort, F. (2012). Carvacrol affects interfacial, structural and transfer properties of chitosan coated polyethylene, *Carbohydrate Polymers*, submitted in March 2012.
5. **Kurek, M.**, Moundanga, S., Favier, C., Galić, K., & Debeaufort, F. (2012). Antimicrobial efficiency of carvacrol vapour related to mass partition coefficient when incorporated in chitosan based films aimed for active packaging. *Food Control*, DOI 10.1016/j.foodcont.2012.11.049.
6. **Kurek, M.**, Guinault, A., Voilley, A., Galić, K., Debeaufort, F. (2012). Effect of relative humidity on carvacrol release and permeation properties of chitosan based films and coatings. *Food Chemistry*, accepted.
7. **Kurek, M.**, Karbowski, T., Galić, K., Voilley, A., & Debeaufort, F. Water vapour sorption isotherms of chitosan based films and coatings. *Biomacromolecules*, will be submitted.
8. **Kurek, M.**, Endrizzi, A., Delaitre, J.M., Galić, K., & Debeaufort, F. Application of carvacrol as active compound on real food products: Validation of sensory impact. *Food Technology and Biotechnology*, will be submitted.

### **Publications from collaboration:**

1. **Kurek, M.**, Klepac, D., Ščetar, M., Galić, K., Valić, S., Liu, Y., Yang, W. (2011). Gas barrier and morphology characteristics of linear low-density polyethylene and two different polypropylene films. *Polymer Bulletin*, 67, 1293-1309.



2. Galić, K., Ščetar, M., & **Kurek, M.** (2011). The benefits of processing and packaging, *Trends in Food Science & Technology*, 22(2–3), 127-137.
3. Ščetar, M., **Kurek, M.**, & Galić, K. (2010). Trends in meat and meat products packaging - a review. *Croatian Journal of Food Science and Technology*, (1) 32-48.
4. Ščetar, M., **Kurek, M.** & Galić, K. (2010). Trends in fruit and vegetable packaging - a review. *Croatian Journal of Food Technology, Biotechnology and Nutrition* 5(3-4): 69-86.
5. Klepac, D., Ščetar, M., **Kurek, M.**, Mallon, P.E., Luyt, A.S., Galić, K., & Valić, S. (2011). Oxygen permeability, ESR, DSC and PALS studies of uniaxially deformed PE-LLD film. *Polymer international*.
6. Descours, E., Hambleton, A., **Kurek, M.**, Voilley, A., Debeaufort, F., & Seuvre, A.M. (2012). Impact of steam cooking process on aroma behaviour in starch model matrix. *Carbohydrate Polymers*, submitted in November 2012.
7. Ščetar, M., Kovačić, E., **Kurek M.**, & Galić, K. (2012). The shelf life study of sliced dry fermented sausage under vacuum and protective nitrogen atmosphere. *Meat Science*, accepted.
8. Debeaufort, F., **Kurek, M.**, & Voilley, A. (2012). Stabilisation des aliments par les emballages: la maîtrise des transferts d'eau. IAA, La revue des industries alimentaires & agricoles.

### **Congress communications (\*oral communications):**

1. **Kurek, M.**, Karbowski, T., Voilley, A., Galić, K., Debeaufort, F. (2012). Influence of relative humidity on the functional and barrier properties of bio-based packaging films and active coatings. *International Symposium on Food Packaging-Scientific Developments supporting Safety and Innovation*, Berlin, Germany, 14.11.2012-16.11.2012.
2. **\*Kurek, M.**, Galić, K., Voilley, A., Debeaufort, F. (2012). Influence of processing parameters in the retention of the active volatile compound and physicochemical properties of biopolymer coatings. *April 2012, Matbim 2012, Dijon, France*.
3. **\*Kurek, M.**, Galić, K., Voilley, A., Debeaufort, F. (2012). Influence of relative humidity on the functional and barrier properties of active chitosan films used for food packaging, *7th International Conference on Water in Food, June 2012, Helsinki, Finland*.

4. **Kurek, M.**, Moundanga, S., Galić, K., Debeaufort, F. (2012). Antibacterial activity of volatile compound/chitosan based films in the vapour phase against *Escherichia coli*. April 2012, Matbim 2012, Dijon, France.
5. **Kurek, M.**, Endrizzi, A., Delaitre, J.M., Debeaufort, F. (2012). Impact of aroma compounds included in active packaging films on the sensory properties of packed food products. April 2012, Matbim 2012, Dijon, France.
6. Galuš, S., **Kurek, M.**, Debeaufort, F. (2012). Characterization of edible bilayer films from whey protein and chitosan. April 2012, Matbim 2012, Dijon, France.
7. Descours, E., **Kurek, M.**, Mint-Dah, F.V., Debeaufort, F., Voilley, A., Seuvre, A.M. (2012). Steam cooking using a PET packaging pouch, Matbim 2012, France. Best Poster Prize: 1st Place.
8. \***Kurek M.**, Endrizzi, A., Debeaufort F. (2012). Qualiment, Development of active food packaging materials. 28 June 2012, Dijon.
9. \***Kurek M.**, Debeaufort, F. (2012). Procède d'incorporation de substances volatiles naturelles et antimicrobiennes dans des films d'emballage. EMABIO Programme de la recherche, restitution des résultats. Bourg en Bresse, 29 June 2012.
10. **Kurek, M.**, Voilley, A., Galić, K., Debeaufort, F. (2011). Drying temperature influence on the aroma retention in biopolymer based-edible films. Book of abstracts of 7th International Congress of Food Technologists, Biotechnologists and Nutritionists. Opatija, Croatia.
11. **Kurek, M.**, Ščetar, M., Voilley, A., Galić, K., Debeaufort, F. (2011). Influence of biopolymer layers and aroma compound on the polyolefin-based film permeability. Book of abstracts of 7th International Congress of Food Technologists, Biotechnologists and Nutritionists. Opatija, Croatia, 178-178.
12. **Kurek, M.**, Voilley, A., Delaitre, J.M., Debeaufort, F. (2011). Influence of contaminant aroma vapours on the sensory properties of food products. Book of abstracts of 7<sup>th</sup> International Congress of Food Technologists, Biotechnologists and Nutritionists, Opatija, Croatia, 94-94.
13. **Kurek, M.**, Voilley, A., Galić, K., Debeaufort, F. (2011). Influence of different proceeding parameters on the aroma retention in biopolymer based-edible films. 3<sup>rd</sup> International Conference on Biodegradable and Biobased polymers, Strasbourg, France.
14. Nguimjeu, C., **Kurek, M.**, Delaitre, J.M., Vroman, I., Brachais, C.H., Couvercelle, J.P. (2011). Incorporation of thymol and carvacrol in polymers matrix for food packaging.
15. Ščetar, M., Ptiček Siročić, A., **Kurek, M.**, Hrnjak-Murgić, Z., Galić, K., Lelas, V. (2011). Low density polyethylene film for food packaging modified by zeolite and nanoclay. Book of abstracts of 7th International Congress of Food Technologists, Biotechnologists and Nutritionists, Opatija, Croatia, 183-183.
16. Ščetar, M., **Kurek, M.**, Lelas, V., Galić, K. (2010). Gas permeation properties of modified PE-LD with zeolite and nanoclay aimed for food packaging. Proceedings of the EFFoST Conference 2010 EFFoST Annual Meeting - Food and Health.

17. Klepac, D., Ščetar, M., Valić, S., **Kurek, M.**, Galić, K. (2010). Mechanical Degradation of Food Packaging Polymeric Materials. Book of Abstracts of 15<sup>th</sup> World Congress of Food Science and Technology, Cape Town: South African Association for Food Science and Technology. 290-290.
18. Ščetar, M., Kovačić, E., **Kurek, M.**, Galić, K. (2010). The influence of packaging on dry meat sausage shelf-life. Book of abstracts of 5<sup>th</sup> Central European Congress on food, Bratislava, Slovakia, p. 105.
19. Ščetar, M., **Kurek, M.**, Galić, K. (2009). Schematic overview of dry food packaging material selection. Proceedings of the EFFoST Conference New Challenges in Food Preservation-Processing-Safety-Sustainability, Budapest, Hungary.
20. **Kurek, M.**, Galić, K. (2008). Effect of External Parameters on Barrier Characteristics of Polyethylene Film for Food Packaging. Book of Abstracts of Symposium on Food Packaging Scientific Developments supporting Safety and Quality, Associations: International Life Sciences Institute-ILSI Europe. Prag, 187-187.
21. **Kurek, M.**, Hruškar, M., Galić, K. (2008). Determination of mass content of proline and invertase activity in different honey samples. Book of Abstracts of The 2008 Joint Central 4th Central European Congress on Food and 6th Croatian Congress of Food Technologists, Biotechnologists, and Nutritionists. Cavtat, Croatia, p. 185.
22. **Kurek, M.**, Lalović, M., Špralja, A., Galić, K. (2008). Absorption of food stimulants in polyolephinic packaging materials. Book of Abstracts of 14th World Congress of Food Science and Technology. Shanghai, China, pp 491-491.
23. Valić, S., Ostojić, S., **Kurek, M.**, Klepac, D., Galić, K. (2008). Thermal and barrier characterisation of polyethylene film as food packaging material. Book of Abstracts of 14<sup>th</sup> World Congress of Food Science and Technology. Shanghai, China, pp. 493-493.

# Acknowledgements

*"Twenty years from now you will be more disappointed by the things that you didn't do than by the ones you did do. So throw off the bowlines. Catch the trade winds in your sails. Explore. Dream. Discover!" - Mark Twain*

Life challenges come with no guarantees, no time out, and no second chances. All life is an experiment. The more experiments you make, the better (*Ralph Waldo Emerson*). Undertaking this doctoral thesis research program was like an exciting journey, during which I long to reach the destination even though on the way there were some problems and difficulties to deal with. This exciting and demanding challenge that was full of ups and downs, required great engagements and efforts to be accomplished, but there were many people who supported me like "the wind beneath my wings". It is my great pleasure and honour to express my acknowledgements to those who have supported me throughout these three years.

First of all, I would like to express my gratitude to the members of Jury:

Professor Stéphane Desobry and Professor Srećko Valić for accepting to review my doctoral dissertation.

To Dr. Nadia Oulahal and Professor Damir Ježek for agreeing to participate in this thesis jury and judge this work.

I would like to express my sincere appreciation, gratitude and respect to Kata and Fred, for their guidance, valuable time, efforts and patience throughout my doctoral program. Fred, first of all I must say thank you for giving me the opportunity to work with you, for all the guidance, support and the confidence you gave me. It was honour to work with you. Kata, since we started working together, and from the very first day when I started speaking about studying in France, you have always been encouraging, believing in me, supporting me and giving me scientific and moral support. I have at least a billion of reasons to say Thank you both since in all these years you were my professors, mentors, my Friends.

I am deeply grateful to Faculty of Food Technology and Biotechnology, University of Zagreb, administrative and research staff and especially to Ms. Mirjana Hruškar, for encouraging and supporting me to study abroad.

This work was supported by the Ministère de l'Enseignement Supérieur et de la Recherche, the Ministère de l'Economie, de l'Industrie et de l'Emploi, by the way of Fond Unique Interministériel (project EMAC N09 290 6395), the Conseil Régional de Bourgogne, Generale de la Competitivite de l'Industrie et des Services DGCIS, Conseil régional Franche-Comté, Conseil Régional Picardie, Conseil Général Côte d'Or, Conseil Général du Jura, le Grand Dijon, the competitive clusters Vitagora, IAR et Plastipolis.

I would like to gratefully acknowledge all private partners involved in the project, Mr. Georgeault et Mr. Hatte (Lactalis), Mr. Mougin and Mr. Fahfouhi (AFT Plasturgie), Ms Bigot and Mr Sabatier (Salaisons Dijonnaises), Mr. Berning and Mr. Caret (Chazal), Mr. Joubert and Mr. Gruet (Plastilax/Groupe Lacroix), Mr. Ferchaud (CVG). Special thanks to Mr. Antoine Cassel (Wipak) and Mr. Jean Marie Delaitre (Welience). I would also like to thank Dr. Jean Pierre Couvercelle (ICMUB), Dr. Patrick Gervais (UMR-PAM), and Ms. Lan Tighzert (ESIEC).

To Ms Sylvie Moundanga I express my sincere appreciation for her contribution in supervision of my work. Thank you for your guidance, precious time, for everything that you thought me and for huge help in the world of microbes. I thank also her research staff from the Laboratory PAM-PMB.

I want to express my deepest gratitude to Professor Jean Pierre Gay, first of all for being a friend of mine and for his grateful help in English language support and teaching.

I'm also very grateful to Emeritus Professor Andree Voilley for her precious advices and scientific support. Special thanks to Dr. Thomas Karbowiak for his advices, support and guidelines. I have also appreciated the warm welcome, as well as the scientific assistance, from all the staff from the Equipe PAM-PAPC, especially Dr. Bernard Colas, Dr. Gaelle Roudaut, Dr. Anne Marie Seuvre and Ms. Alexandra Da Silva. Special thanks to Dr. Claire-Helene Brachais for her precious advices and help, to Dr. Alain Guinault for his help and warm welcome in Laboratory CNAM-PIMM Paris, to Ms. Aline Bonnotte, to Ms. Anne Endrizzi and Ms. Karen Joly who all together helped me in realizing my goals.

I want to thank all the staff from IUT-Dijon, for giving me the opportunity to teach. Especially to Ms. Isabelle Vialet for giving me confidence to work with students.

This journey was really full of happiness and tears. Nothing in my life would not be achieved without the greatest support, love and advices from my parents. Mami and Tatko, who never doubted, constantly supported, and always loved, that have been with me through every up, as well as every down, that walked the kilometres for me and guided me through the dark, that were all that they you could be. You made my life beautiful. You mean the world to me, and I could not have become the person I am today without you both in my life. I love you. Anči, you were my support, my big/little sis far away but always making me smile and providing only joy and happiness. Thanks a lot to my Nono, who encouraged me and showed me that the scientific world is not so far from reality. I hope that you would be proud of your Mijanić exactly like the last words that you said to me. I will never forget you. To Njanja who despite hard times provided me only joy, love and happiness. To my Nana and Deda who supported me all journey long, for the wishes and love that you have for me. Love you so much.

To whole my family, to Tea, Davor, Andrea, none of this could have been achieved without your everlasting love, unconditional support, deep appreciation,

overwhelming encouragement and true understanding during my long term away from home. You all mean so much to me.

Thanks for believing in me, for showing that you care, for supporting me at each step, for loving me and saying „...you can do it: go and make it...“. Thank you Miško for being there all the time, whenever I needed you.

This PhD experience has represented for me not only an important life step to improve my scientific and professional skills, but more than this a period of friendship enrichment thanks to my colleagues Emilie, Christelle, Jean Luc, Ashish, Manal, Coralie, Fatma, Nasreddine. Special thanks to Mario who was my friend, support, mate and arms in Zagreb. Thanks to all trainees that helped me during these three years: Charline, Coralie, Wichien, Marion, Fanny and Jeromine.

There are so many people who made my stay in Dijon easier as well as wonderful. Great thanks to all my friends from DUC Family: Caro, Anne Marie, Charline, Aurelie, Marie, Lionel, one page is not enough for all the names! You helped me to change my ideas, to enter once again to a sports competition world and make me feel like I was sixteen.

Thanks a lot to my „couples d’amis“ Emilie and Seb, Eve and Jeremy for your love and care that helped me survive difficult times during my studies. Emilie I cannot think about how I could manage if you weren't there, in the lab, at home, at a phone, to smile and cry, to encourage and cheer. I won't forget to look back on the tears that make us smile today and hope that you will finish our lab anecdotes book.

Thanks a lot to all my Croatian friends, the list is long so I'll just say thanks for being exactly who you are.

Finally, Julien, I know I was not made of honey all time long. It's hard to find people that will love you no matter what. Thanks for being you, for giving me the joys and smiles from day one, for helping me enjoy the atmosphere here, for lending me your ears when I was upset, wiping the tears of my eye away, for keeping me going and getting me out, for giving my words a proper mean (you must be a “pro” now), for helping me try and cope with people around, for giving me the courage to stand up on my own, for the love and care you showed, for breathing, listening, smiling, crying and living my thesis with me. Merci Cheri.



# *Table of Contents*

Abstract-Sažetak-Résumé	
List of Publications and Communications	
Acknowledgments	
Table of Contents	
List of Abbreviations	
List of Figures	
List of Tables	
<b>Chapter 1 Introduction</b>	<b>1</b>
<b>Chapter 2 Bibliographic review</b>	<b>7</b>
2.1. Conventional packaging versus modern technologies	9
2.2. Consumer's requirements and safety considerations	11
2.2.1. Consumer requirements	11
2.2.2. Safety considerations	11
2.3. Active packaging – basic concept	15
2.4. Antimicrobial food packaging	17
2.5. Essential oils as antimicrobial agents for active packaging systems	21
2.6. Biopolymers in food packaging	23
2.7. Chitosan	24
2.7.1. Deacetylation, crystallinity and molecular weight	24
2.7.2. Chitosan solubility	25
2.7.3. Chitosan crystals diversity	26
2.7.4. Chitosan films and their application	31
2.8. Efficacy, structure and distribution of active compound in the polymer matrix	34
2.8.1. Influence of antimicrobial compound on the structure of polymer/biopolymer matrices	34
2.8.2. Parameters influencing gas transfers through biopolymer films	36
2.8.3. Influence of polymer matrix on the retention and antimicrobial activity of incorporated compound	43



---

<b>Chapter 3 Materials and Methods</b> .....	47
3.1. Materials and reagents .....	49
3.1.1. Film forming materials .....	49
3.2. Film formation .....	52
3.2.1. Self standing chitosan films .....	52
3.2.2. Chitosan coated polyethylene films .....	54
3.3. Characterization of film forming solutions .....	56
3.3.1. Rheological behaviour of film forming solutions .....	56
3.3.2. Structure and dispersion of film forming solutions .....	57
3.4. Physico-chemical characterization of chitosan based films and coatings .....	59
3.4.1. Aroma compound retention and release .....	59
3.4.2. Structure properties of chitosan films and coatings .....	61
3.4.3. Mechanical properties .....	62
3.4.4. Thermal properties .....	63
3.4.5. Surface properties .....	64
3.5. Transfer measurements .....	70
3.5.1. Theoretical background .....	70
3.5.2. Gas permeability measurements .....	74
3.5.3. Water vapour permeability measurement .....	75
3.5.4. Moisture sorption isotherms .....	76
3.5.5. Calculation of water vapour diffusion coefficient in film .....	80
3.6. Antimicrobial properties of chitosan films and coatings .....	80
3.6.1. Microbial cultures .....	80
3.6.2. Inoculation .....	81
3.6.3. Experimental design .....	82
3.7. Sensory evaluation .....	84
3.8. Statistical analysis .....	87
<b>Chapter 4 How composition and process parameters affect volatile active compounds in biopolymer films</b> .....	89
4.1. Characterization of the film forming solutions .....	92
4.1.1. Rheological behaviour of film forming solutions .....	92

---

---

4.1.2. Particle size distribution .....	93
4.2. Drying process .....	96
4.3. Film macroscopic appearance .....	102
4.4. Film properties as a function of composition and drying conditions .....	102
4.4.1. Influence on mass partition coefficient .....	103
4.4.2. Influence of chitosan concentration .....	106
4.4.3. Influence of additives .....	109
4.5. Conclusions of the Chapter 4 .....	111
<b>Chapter 5 Barrier properties of chitosan coated polyethylene .....</b>	<b>115</b>
5.1. Water vapour permeability .....	118
5.1.1. Influence of coating process on the water vapour permeability of polyethylene .....	119
5.1.2. Influence of casting solvent and glycerol on WVP of self-standing chitosan films .....	119
5.2. Oxygen, carbon dioxide and air permeability .....	122
5.2.1. Influence of coating process on gas permeability of coated PE .....	122
5.2.2. Influence of casting solvent and glycerol on gas permeability of chitosan self-standing films .....	125
5.3. Conclusion of Chapter 5 .....	128
<b>Chapter 6 Structure and thermal properties of a chitosan coated polyethylene bilayer film .....</b>	<b>129</b>
6.1. Thermal properties .....	132
6.1.1. Characterization of the chitosan coating .....	133
6.1.2. Comparative thermal stability of PE, coated PE and CSE film .....	135
6.1.3. Comparative thermal stability of glycerol plasticized and unplasticized samples .....	136
6.2. Film microstructure and surface analysis .....	137
6.3. Conclusions of Chapter 6 .....	144

---

---

<b>Chapter 7 Carvacrol affects interfacial, structural and transfer properties of chitosan coated polyethylene</b> .....	147
7.1. Liquid surface tension of the film forming solutions and critical surface tension of polyethylene and chitosan films.....	149
7.1.1. Critical surface tension and surface free energy of PE films .....	151
7.1.2. Wettability of polyethylene films by the coating solutions.....	153
7.2. Effect of glycerol on the surface tension of film forming solutions and its spreadability/adhesivity on polyethylene .....	155
7.3. Surface free energy and critical surface tension of dry chitosan self standing films .....	158
7.4. Molecular interactions in the films.....	159
7.5. Film microstructure .....	162
7.6. Thermal properties of coated PE and self standing carvacrol/chitosan films....	163
7.7. Water vapour permeability .....	167
7.8. Oxygen, carbon dioxide and air permeability.....	169
7.9. Conclusions of Chapter 7 .....	171
<b>Chapter 8 Effect of relative humidity on carvacrol release and permeation properties of chitosan based films and coatings</b> .....	173
8.1. Hydrophobicity and wettability of chitosan surfaces.....	176
8.2. Influence of glycerol on surface properties of chitosan films .....	181
8.3. Thermal properties of chitosan based films influenced by relative humidity....	184
8.4. Water vapour permeability of carvacrol/chitosan films and coatings at high RH differentials .....	185
8.5. Oxygen and carbon dioxide permeability.....	187
8.6. Influence of glycerol and relative humidity on the gas and water vapour permeability of chitosan films with carvacrol .....	190
8.7. Carvacrol release from chitosan films .....	192
8.8. Conclusion of Chapter 8.....	195
<b>Chapter 9 Water vapour sorption isotherms of chitosan based films and coatings: influence on their barrier and mechanical properties</b> .....	197
9.1. Water vapour sorption kinetics in chitosan based films .....	199
9.2. Water vapour sorption isotherms .....	210

---

---

9.3. Correlation between water vapour moisture isotherms and oxygen permeability in the relative humidity range from 0% to 96% of chitosan-based films and coatings .....	216
9.4. Effect of relative humidity on mechanical properties of chitosan based films and coatings .....	220
9.5. Conclusions of the Chapter 9 .....	223
<b>Chapter 10 Antimicrobial efficiency of carvacrol vapour related to mass partition coefficient when incorporated in chitosan based films aimed for active packaging .....</b>	<b>225</b>
10.1. Film characterization .....	228
10.2. Antimicrobial efficiency .....	231
10.2.1. Macroscopic observations .....	231
10.2.2. Chitosan/carvacrol film antimicrobial efficiency in lag phase of bacterial growth.....	233
10.2.3. Chitosan/carvacrol film antimicrobial efficiency in the exponential phase of bacterial growth .....	238
10.3. Antimicrobial efficiency of chitosan based films against <i>Penicillium camemberti</i> .....	241
10.4. Antimicrobial efficiency of three polyethylene coated film with different concentrations of carvacrol in the vapour phase.....	245
10.5. Conclusions of Chapter 10 .....	248
<b>Chapter 11 Application of carvacrol as active compound on real food products: Validation of sensory impact .....</b>	<b>251</b>
11.1. Impact of essential oils on packaged food products .....	253
11.2. Effect of carvacrol/chitosan coated polyethylene on sensory quality of jambon blanc (ham), „jambon persillé“ (parsley ham), „paté en croute“(meat paté pie), „terrines“ and feta cheese .....	256
11.3. Conclusion of Chapter 11.....	262
<b>Chapter 12 Overall conclusions and perspectives.....</b>	<b>265</b>
<b>References.....</b>	<b>275</b>



---



---

## *List of Abbreviations*

CSA	Chitosan solubilised in the aqueous acetic acid
CSACVC	Chitosan solubilised in the aqueous acetic acid and activated with carvacrol
CSAGLY	Chitosan solubilised in the aqueous acetic acid and plasticized with glycerol
CSAGLYCVC	Chitosan solubilised in the aqueous acetic acid and both activated with carvacrol and plasticized with glycerol
CSE	Chitosan solubilised in the hydroalcoholic acetic acid
CSECVC	Chitosan solubilised in the hydroalcoholic acetic acid and activated with carvacrol
CSEGLY	Chitosan solubilised in the hydroalcoholic acetic acid and plasticized with glycerol
CSEGLYCVC	Chitosan solubilised in the hydroalcoholic acetic acid and both activated with carvacrol and plasticized with glycerol
PE	Polyethylene
PECSE	Polyethylene coated with chitosan solubilised in the hydroalcoholic acetic acid
PECSECVC	Polyethylene coated with chitosan solubilised in the hydroalcoholic acetic acid and activated with carvacrol
“support side”	side of a film in contact with glass Petri dish during drying
„air side“	side of a film in contact with air during drying
Å	angstrom
A	film area exposed to moisture transfer
a*	Hunter's colour parameter (between red and green)
A <sub>B</sub>	base area of the water drop on the tested surface
AG	Arabic Gum
A <sub>S</sub>	surface area of the water droplet on this reference material
ATR	Attenuated Total Reflectance
a <sub>w</sub>	water activity
b*	hunter's colour parameter (between yellow and blue)
BET	Brunauer-Emmett-Teller sorption model
BHI	Brain Heart Infusion
C	concentration
C (microbiology)	cultivability
C <sub>OGAB</sub>	Arrhenius type constant to express temperature dependence of C <sub>GAB</sub>
C <sub>f</sub>	concentration of the volatile compound in the film
CFU	Colony Forming Unit
C <sub>g</sub>	concentration of the volatile compound in the vapour phase
C <sub>GAB</sub>	constant related to adsorption energies of first and second layers
CMC	Carboxyl methylcellulose
C <sub>o</sub>	initial concentration
CS	Chitosan
CVC	Carvacrol
D	Diffusion coefficient

---

$D_0$	Pre-exponential factor
$d_1$	the initial colony size diameter
$d_{3,2}$	surface-average diameter
$d_{4,3}$	volume/mass diameter
DA	Deacetylation degree
db	dry basis
DSC	Differential Scanning Calorimetry
$d_x$	the average colony size diameter
e	thickness
E	elongation at break
$E_a$	activation energy
EC	European Commission
$E_D$	Activation energy for diffusion
EFSA	European Food Safety Agency
EM	Elastic Modulus
EP	Activation energy of permeation
EPA	Environmental Protection Agency
ESEM	Environmental Scanning Electron Microscopy
EVAL	Ethylene Vinyl Alcohol
$F_{abS}$	absorption flux
FDA	Food and Drug Administration
$F_{eva}$	evaporation flux
FFS	Film Forming Solution
FIFRA	Federal Insecticide, Fungicide and Roetendicide Act
FTIR	Fourier Transform Infrared Spectroscopy
GAB	Guggenheim-Anderson-de Boer sorption model
GC	Gelose Columbia
GC-FID	Gas Chromatography-Flame Ionisation Detector
GLY	Glycerol
GRAS	Generally Recognized As Safe
HDPE	High Density Polyethylene
HPMC	Hydroxypropyl Methylcellulose
IUPAC	International Union of Pure and Applied Chemistry
J	transfer rate
$K_{GAB}$	constant related to the adsorption energies of second and subsequent layers
$K_{mass}$	mass partition coefficient
L	thickness
$L^*$	Hunter's colour parameter (lightness)
LB	Luria Broth
LDPE	Low Density Polyethylene
LLDPE	Linear low density polyethylene
$m_a$	adsorbed mass
MAP	Modified Atmosphere Packaging
MC	Methylcellulose

---

MIC	Minimal Inhibitory Concentration
$m_m$	monolayer water content
MRS	Man Rogosa Sharpe
$M_t/M_\infty$	mass ratio
$n$	Flow behaviour index
$N$	total number of cells in the colony
NC	Nanoclays
OML	Overall Migration Limit
OPP	Oriented Polypropylene
$p$	partial pression
$P$	Permeability coefficient
$P_0$	Pre-exponential factor
$p_0$	saturated pression
PA-6	Polyamide-6
$P_{air}$	air permeability
PCA	Principal Component Analysis
$PCO_2$	carbon dioxide permeability
PDA	Potato Dextrose Agar
p.d.m.	Polymer dry matter
PE	Polyethylene
PEG	Polyethylene glycol
PET	Polyethylene terephthalate
$PO_2$	oxygen permeability
PP	Polypropylene
PS	Polystyrene
PVDC	Polyvinylidene chloride
RH	relative humidity
rpm	rotations per minute
$S$	Solubility coefficient
$S_0$	Pre-exponential factor
SFE	Surface Free Energy
STP	Standard pressure
sw	swelling index
$T$	Temperature
$t$	time
$T_D$	degradation temperature
$T_d$	dehydration temperature
$T_{DS}$	dissociation temperature
$T_g$	glass transition temperature
TGA	thermal gravimetric analysis
$T_m$	melting temperature
TS	tensile strength
$V$	droplet volume
$V_{abs}$	absorbed volume



---

$V_{\text{eva}}$	evaporated volume
$W$	Wettability
$W_a$	Work of adhesion
$W_c$	Work of cohesion
$W_s$	spreading coefficient
WVP	Water Vapour Permeability
WVTR	Water vapour Transmission Rate
$x$	thickness
$\alpha$	permselectivity
$\gamma$	shear rate
$\gamma$	surface tension
$\gamma_c$	critical surface tension
$\gamma_{LV}$	surface tension at the liquid-vapour interface
$\gamma_s^D$	dispersive component of surface tension
$\gamma_s^L$	surface tension at the solid-liquid interface
$\gamma_s^P$	polar component of surface tension
$\gamma_s^V$	surface tension at the solid-vapour interface
$\delta$	deformation
$\Delta E$	total colour difference
$\Delta H$	enthalpy
$\Delta H_d$	enthalpy of dehydration
$\Delta H_D$	enthalpy of degradation
$\Delta H_{DS}$	enthalpy of dissociation
$\Delta H_{GAB1}$	adsorption enthalpy of the first layer
$\Delta H_{GABn}$	adsorption enthalpy of subsequent layers
$\Delta H_m$	enthalpy of melting
$\Delta H_s$	enthalpy of sorption
$\Delta m$	mass difference
$\Delta p$	pression difference
$\Delta t$	time difference
$\Delta V$	the droplet volume variation
$\eta$	visosity
$\theta$	contact angle
$K$	consistency index
$v_{as}$	asymmetrical stretching
$v_s$	symmetrical stretching
$\rho$	rocking
$\tau$	shear stress
$\omega$	wagging

## *List of Figures*

<b>Figure 2.1.</b> Protective function of food packaging .....	9
<b>Figure 2.2.</b> Different modes of active releasing mechanisms (Dainelli et al., 2008) ...	15
<b>Figure 2.3.</b> Soluble and insoluble structure of chitosan monomer (Kumirska et al., 2011) .....	25
<b>Figure 2.4.</b> Crystalline transformation of chitosan (Ogawa et al., 2000) .....	27
<b>Figure 2.5.</b> Plausible parallel packing structure of chitosan molecules in the Type II form projected (a) along the b-axis and (b) along the c-axis (Okuyama et al., 2000) ..	28
<b>Figure 2.6.</b> Molecular structure of hydrated (a, b) and anhydrous chitosan (c, d). (Okuyama et al., 2000) .....	29
<b>Figure 2.7.</b> Bonding sites in chitosan crystal (Okuyama et al., 1997) .....	29
<b>Figure 2.8.</b> Schematic representation of dehydration of chitosan crystal (Okuyama et al., 2000) .....	30
<b>Figure 2.9.</b> Oxygen (a), carbon dioxide (b) and water vapour (c) permeability for several biopolymers and synthetic polymers as evaluated at 25°C and in dry environment (for PO <sub>2</sub> and PCO <sub>2</sub> ) .....	37
<b>Figure 2.10.</b> Oxygen (a) and carbon dioxide (b) permeability for several biopolymers and synthetic polymers as evaluated at 25°C and in humid environment .....	42
<b>Figure 3.1.</b> Chitosan based films preparation .....	54
<b>Figure 3.2.</b> Coating system for obtaining chitosan coated polyolefin films .....	54
<b>Figure 3.3.</b> Schema of (a) chitosan coated and (b) activated chitosan coated polyethylene .....	55
<b>Figure 3.4.</b> Schema of chitosan coatings on BIAKER 65 XX HFP .....	55
<b>Figure 3.5.</b> Flexoprinter Carint (a) Anonymous; b) Wipak, Bousbecque .....	56
<b>Figure 3.6.</b> a) Diffraction of a laser beam by small and large particles and b) laser scattering measurement principle .....	58

---

<b>Figure 3.7.</b> a) Schema of a module used for testing mechanical properties and b) evolution of constraint/deformation curves in function of polymer glass transition temperature ( $T_g$ ) (adapted from Gibson and Ashby, 1988) .....	62
<b>Figure 3.8.</b> Contact angle of a drop of liquid deposited on a solid surface and the surface tension at the contact point of three phases .....	65
<b>Figure 3.9.</b> Schema of the experimental system used for contact angle measurements .....	66
<b>Figure 3.10.</b> The Zisman plot design .....	67
<b>Figure 3.11.</b> Wetting of a solid surface .....	69
<b>Figure 3.12.</b> Transfer mechanism through polymer film .....	71
<b>Figure 3.13.</b> Diffusion flow around a thin polymer membrane .....	73
<b>Figure 3.14.</b> Water vapour permeation cell .....	76
<b>Figure 3.15.</b> Types of water vapour sorption isotherms (IUPAC, 1985) .....	77
<b>Figure 3.16.</b> Schema of isolation procedure and preparation of a culture .....	81
<b>Figure 3.17.</b> Photos of a) replica platter, b) microplate, c) inoculated Petri dish .....	82
<b>Figure 3.18.</b> Schema of Petri dishes used in the experiments. A control test; B test with pure aroma compound; C test with activated chitosan films/coatings .....	83
<b>Figure 3.19.</b> Five food products used in this study .....	85
<b>Figure 3.20.</b> Re-packaging of food products under sterile conditions and using active or control films .....	86
<b>Figure 4.1.</b> Typical flow curves, at 20°C, of the film forming solutions prepared in the aqueous acidic media (continuous lines) or in the hydroalcoholic acid media (dashed lines) .....	92
<b>Figure 4.2.</b> Particle size distribution of a) chitosan film forming solution and film before and after addition of Triton X-100; b) chitosan/carvacrol film forming solution and film .....	94
<b>Figure 4.3.</b> Drying curves of the chitosan slutions .....	99
<b>Figure 4.4.</b> Water content ( $g_{H_2O}/100$ g d.m.) and relative carvacrol release (% of initially added amount) from chitosan based films during drying .....	101

---

<b>Figure 4.5.</b> Relationship between the carvacrol retention during the film processing and the air/film partition coefficient during the film storage .....	104
<b>Figure 4.6.</b> Carvacrol retention (A) and the air/biopolymer partition coefficient (K <sub>mass</sub> ) (B) in the chitosan based films with or without the addition of nanoclays when dried at temperature scale from 20 to 100°C .....	106
<b>Figure 4.7.</b> Retention and partition coefficient (K <sub>mass</sub> ) of carvacrol as a function of the film composition and the drying temperature .....	110
<b>Figure 4.8.</b> Overview of the mechanism and the main parameters influencing active packaging film performances.....	112
<b>Figure 5.1.</b> Oxygen permeability of polyethylene (PE) and PE chitosan coated samples (PECSE).....	122
<b>Figure 5.2.</b> Carbon dioxide permeability of polyethylene (PE) and PE chitosan coated samples (PECSE).....	123
<b>Figure 5.3.</b> Changes in oxygen permeability of polyethylene and chitosan coated polyethylene films as a function of temperature and relative humidity .....	124
<b>Figure 6.1.</b> TGA thermograms of polyethylene (PE), chitosan coated polyethylene (PECSE) and chitosan coating (CSE) .....	135
<b>Figure 6.2.</b> TGA thermograms of chitosan powder and chitosan films .....	137
<b>Figure 6.3.</b> Micrograph of cross section of chitosan coated polyethylene (A); cross section (B), air side surface (C) and support side surface (D) of CSA film; cross section (E), air side surface (F) and support side surface (G) of CSE film; cross sections of glycerol plasticized samples-CSAGLY (H) and CSEGLY (I) and air side surface (J) and support side surface (K) of CSEGLY .....	139
<b>Figure 6.4.</b> FTIR-ATR spectra of polyethylene (PE), chitosan film prepared with hydroalcoholic acid solvent (CSE), chitosan coated polyethylene - side polyethylene (PECSE-PE), chitosan coated polyethylene - side chitosan film (PECSE-CSE).....	142

---

<b>Figure 6.5.</b> FTIR-ATR spectra of raw chitosan powder (CS), chitosan film prepared with aqueous acid solvent (CSA), chitosan film prepared with aqueous acid solvent and plasticized with glycerol (CSAGLY), chitosan film prepared with hydroalcoholic acid solvent (CSE) and chitosan film prepared with hydroalcoholic acid solvent and plasticized with glycerol (CSEGLY) .....	143
<b>Figure 7.1.</b> Pictures of solvents and chitosan film forming solutions when applied to polyethylene film .....	150
<b>Figure 7.2.</b> Zisman plot of polyethylene surface .....	153
<b>Figure 7.3.</b> ESEM cross sections of PECSECVC film (A), CSECVC coating layer (B), CSECVC film (C) and surfaces of chitosan films – support side surface of CSACVC (D) and CSECVC (E) and air side surface of CSECVC (F,H) and CSACVC (G) .....	155
<b>Figure 7.4.</b> Changes in the drop volume of the film forming solution containing glycerol (GLY) and/or carvacrol (CVC) deposited onto the polyethylene as a function of the solvent nature (CSA=aqueous acetic acid solvent, or CSE=hydroalcoholic acid solvent) .....	157
<b>Figure 7.5.</b> Water vapour (WVP), oxygen, carbon dioxide and air permeability of polyethylene (PE), chitosan coated (PECSE) and chitosan+carvacrol coated (PECSECVC) polyethylene film .....	167
<b>Figure 7.6.</b> Changes in gas permeability of chitosan films in dry environment (0% RH) as influenced by the addition of carvacrol .....	171
<b>Figure 8.1.</b> Shape and volume changes of water drop deposit on: (a) chitosan based films prepared with aqueous acetic solvent and (b) chitosan films prepared with hydroalcoholic acid solvent; (c) chitosan coated polyethylene; and (d) activated chitosan coated polyethylene .....	178
<b>Figure 8.2.</b> Comparison of the total surface free energy and its polar component in chitosan based films as influenced by glycerol addition .....	182
<b>Figure 8.3.</b> Micrographs of cross section of CSAGLYCVC (a) and (b); CSEGLYCVC (c) and (d); and (e) air and (f) support surface of CSEGLYCVC .....	184

---

<b>Figure 8.4.</b> Water vapour permeability (WVP) at 20°C and three humidity differentials ■ 100-30% RH, ■ 75-30% RH and ■ 33-0% RH of chitosan films and carvacrol activated chitosan films compared to chitosan coated PE films.....	186
<b>Figure 8.5.</b> Oxygen and carbon dioxide permeability influenced by relative humidity of a) polyethylene and chitosan coated polyethylene films and b) chitosan and carvacrol activated chitosan self standing film. ■ O <sub>2</sub> dry (0% RH), ■ O <sub>2</sub> humid (>96% RH), ■ CO <sub>2</sub> dry (0% RH), ■ CO <sub>2</sub> humid (>96% RH).....	188
<b>Figure 8.6.</b> Oxygen and carbon dioxide permeability of carvacrol containing chitosan films in dry and humid environment as affected by the addition of glycerol: a) chitosan films prepared in aqueous acetic acid solvent (CSACVC); b) chitosan films prepared in hydroalcoholic acetic acid solvent (CSECVC).....	191
<b>Figure 8.7.</b> Water vapour permeability of chitosan films with carvacrol and glycerol at three different humidity differentials (CSAGLYCVC and CSEGLYCVC).....	191
<b>Figure 8.8.</b> Kinetic of carvacrol release from chitosan based film during 2 months influenced by relative humidity (0, 75 and >96%) and temperature a) 4°C, b) 20°C and c) 37°C.....	193
<b>Figure 8.9.</b> Influence of temperature and relative humidity on the diffusivity of carvacrol in chitosan film.....	194
<b>Figure 9.1.</b> Curves of water sorption kinetics for (a) chitosan powder and (b) chitosan based film (CSA). db= dry basis.....	200
<b>Figure 9.2.</b> Curves of water desorption kinetics for (a) chitosan powder and (b) chitosan based film (CSA).....	202
<b>Figure 9.3.</b> Water vapour sorption in chitosan based films. a) CSAGLY, ΔRH 70-80%; b) CSAGLY, ΔRH 50-60% c) CSEGLY, ΔRH 70-80%; d) CSEGLY, ΔRH 50-60%. Experimental data (o) and fitting data (-).....	206
<b>Figure 9.4.</b> Water vapour sorption in CSAGLY film in relative humidity range 10-20%. Experimental data (o) and fitting data (-).....	207
<b>Figure 9.5.</b> Diffusion of water in chitosan based films as a function of relative humidity: a) chitosan film prepared in aqueous acetic acid solvent, and b) chitosan films prepared in hydroalcoholic acid solvent.....	208
<b>Figure 9.6.</b> Water vapour sorption and desorption isotherms of chitosan powder....	210

---

<b>Figure 9.7.</b> Water vapour sorption isotherms of a) chitosan based films prepared with the aqueous acetic acid solvent (CSA); b) chitosan based films in hydroalcoholic acid solvent (CSE).....	211
<b>Figure 9.8.</b> Water vapour desorption isotherms of a) chitosan based films prepared in aqueous acetic acid solvent (CSA); b) chitosan based films in hydroalcoholic acid solvent (CSE); containing carvacrol (CVC) or glycerol (GLY) or both (CVCGLY).....	213
<b>Figure 9.9.</b> GAB model fitting of a) chitosan powder; b) CSA film; c) CSACVC film; d) CSAGLY film; and e) CSACVCGLY film. Experimental (o) and fitted (-) .....	214
<b>Figure 9.10.</b> Oxygen permeability of chitosan based films as influenced by different relative humidities: a) chitosan based films prepared in aqueous acetic acid solvent (CSA); b) chitosan based films in hydroalcoholic acid solvent, containing either carvacrol (CVC) or glycerol (GLY) .....	217
<b>Figure 9.11.</b> Relationship between water vapour sorption isotherms (symbols) and oxygen permeability (lines) of polyethylene (PE, blue), chitosan coated polyethylene (PECSE, green) and chitosan-carvacrol coated polyethylene (PECSECVC, red).....	219
<b>Figure 9.12.</b> Tensile stress-strain curves of chitosan films as a function of relative humidity and composition.....	222
<b>Figure 10.1.</b> Photos of a) <i>Bacillus subtilis</i> 168 BGSC 1A, b) <i>Salmonella Enteritidis</i> CIP 81.3, c) <i>Escherichia coli</i> TG1 K12 and d) <i>Listeria innocua</i> DSM 20649 after the exposure to the vapour of two antimicrobial films AF1* and AF5* and control film (chitosan-based film without carvacrol).....	232
<b>Figure 10.2.</b> Average colony size diameter of bacterial strains put in the vapour contact with five active chitosan-based films, control film and pure carvacrol vapours at $t_0$ during seven days exposure of a) <i>Bacillus subtilis</i> 168 BGSC 1A; b) <i>Escherichia coli</i> TG1 K12; c) <i>Listeria innocua</i> DSM 20649; and d) <i>Salmonella Enteritidis</i> CIP 81.3.....	235
<b>Figure 10.3.</b> Average colony size diameter ratio of bacterial strains put in the vapour contact with five active chitosan-based films, control film and pure carvacrol vapours at $t_1$ during seven days exposure of a) <i>Bacillus subtilis</i> 168 BGSC 1A; b) <i>Escherichia coli</i> TG1 K12; c) <i>Listeria innocua</i> DSM 20649; and d) <i>Salmonella Enteritidis</i> CP 81.3.....	240

---

<b>Figure 10.4.</b> Photos of <i>Penicillium camemberti</i> DSM 1233 after the exposure to the vapour of two antimicrobial films AF1* and AF5* and control film (chitosan-based film without carvacrol) .....	242
<b>Figure 10.5.</b> Inhibition of <i>Penicillium camemberti</i> DSM 1233 at a) $t_0$ and b) $t_1$ .....	244
<b>Figure 10.6.</b> Antimicrobial efficiency of three chitosan coated polyethylene films against (a,b) <i>B. subtilis</i> 168 BGSC 1A, (c,d) <i>E. coli</i> TG1 K12, (e,f) <i>L. plantarum</i> and (g,h) <i>P. Camemberti</i> DSM 1233 .....	247
<b>Figure 11.1.</b> Schematic view of tests performed in order to characterize the influence of active films on organoleptic impact in food products .....	257
<b>Figure 11.2.</b> Mass of carvacrol in different films after 15 days of storage of ham, “paté en croûte”, “jambon persillé”, “terrine” and feta cheese .....	258
<b>Figure 11.3.</b> The amounts of carvacrol found in food products after the storage in three different active films .....	259
<b>Figure 11.4.</b> Results from taste and odour triangle test of five products packed in three packaging materials with different concentration of carvacrol .....	260
<b>Figure 11.5.</b> Changes in odour and taste of different product packed in chitosan coated AF2 after sensory evaluation .....	262
<b>Figure 12.1.</b> Schema of the most important parameters influencing active bio-based film production and application .....	268





## *List of Tables*

<b>Table 2.1.</b> Antimicrobial biopolymer based films with essential oils.....	18
<b>Table 3.1.</b> Structure and physico-chemical characteristics of carvacrol.....	50
<b>Table 3.2.</b> Saturated salt solutions used to control water activity (Bell and Labuza, 2000).....	51
<b>Table 3.3.</b> Culture media used in microbiology experiments .....	51
<b>Table 3.4.</b> Composition of film forming solutions/dry films and their abbreviations .....	53
<b>Table 3.5.</b> Composition and codification of multilayer packaging films .....	56
<b>Table 4.1.</b> Mean diameter ( $d_{3,2}$ and $d_{4,3}$ ) and type of particle size distribution before (FFS) and after film drying (film).....	94
<b>Table 4.2.</b> Colour parameters of chitosan films influenced by the composition. Samples were dried at 20°C and 30% RH .....	97
<b>Table 4.3.</b> Influence of drying temperature on the colour parameters and the drying time of the chitosan based films. All films were plasticized with glycerol (30% w/p.d.m.) and dried at 30% RH .....	98
<b>Table 4.4.</b> Composition of the chitosan based films and its influence on the thickness, drying time, carvacrol retention and the air/biopolymer partition coefficient when dried at 20°C and 30% RH.....	108
<b>Table 5.1.</b> Water vapour permeability ( $WVP \times 10^{-13}$ (g/m·s·Pa)) at 25°C of PE films coated with chitosan compared to chitosan self standing films prepared with different casting solvents and plasticizers .....	120
<b>Table 5.2.</b> Oxygen, carbon dioxide, air permeability and $CO_2/O_2$ permselectivity at 25°C and 0% (dry gas) and >96% (humid gas) of chitosan films influenced by casting solvent and glycerol addition in film formulation.....	126

---

<b>Table 6.1.</b> Thermal properties of chitosan powder, chitosan based films, PE, and PE coated films obtained by DSC analysis .....	132
<b>Table 6.2.</b> FTIR-ATR absorbance bands ( $\text{cm}^{-1}$ ) of raw chitosan powder and different chitosan films after processing.....	141
<b>Table 7.1.</b> Surface tension ( $\gamma_L$ ), dispersive ( $\gamma_L^D$ ) and polar ( $\gamma_L^P$ ) surface tension components, adhesion ( $W_A$ ), cohesion ( $W_C$ ) and spreading coefficient ( $W_S$ ) of standard liquids and chitosan film forming solutions (FFS) on the PE at equilibrium after 30 s ( $\Theta_{30s}$ ) .....	151
<b>Table 7.2.</b> Comparison of surface free energy and the dispersive ( $\gamma_S^D$ ) and polar ( $\gamma_S^P$ ) components of polyethylene film and chitosan self standing films. Measurement were done at air drying surface (air) and support drying surface (support).....	152
<b>Table 7.3.</b> Surface tension of chitosan film forming solutions and their change with the addition of glycerol .....	156
<b>Table 7.4.</b> Adhesion ( $W_A$ ), cohesion ( $W_C$ ) and spreading ( $W_S$ ) coefficients of chitosan/glycerol film forming solutions onto polyethylene surface at equilibrium ( $\Theta_{30s}$ ).....	158
<b>Table 7.5.</b> FTIR-ATR absorbance bands ( $\text{cm}^{-1}$ ) of raw chitosan powder and different chitosan films after processing.....	160
<b>Table 7.6.</b> Thermal properties of chitosan coated PE, chitosan /carvacrol coated PE and chitosan self standing films .....	164
<b>Table 7.7.</b> Water vapour (WVP), oxygen ( $\text{PO}_2$ ), carbon dioxide ( $\text{PCO}_2$ ) and air permeability ( $P_{\text{air}}$ ) and permselectivity ( $\alpha$ ) of chitosan self-standing films.....	169
<b>Table 8.1.</b> Contact angle at time 0 s ( $\theta_{t0}$ ), and at 30 s ( $\theta_{t30}$ ), absorption flux ( $F_{\text{abs}}$ ), time delay before swelling and swelling percentage data for the analysed films .....	177
<b>Table 8.2.</b> Contact angle at time 0 s ( $\theta_{t0}$ ) and at 30 s ( $\theta_{t30}$ ), absorption flux ( $F_{\text{abs}}$ ), time delay before swelling and swelling percentage data for chitosan based films as influenced by the addition of carvacrol .....	181

---

<b>Table 9.1.</b> Diffusion coefficients of water vapour in chitosan based films .....	205
<b>Table 9.2.</b> GAB model fitting parameters .....	215
<b>Table 9.3.</b> Elongation at break (E), tensile strength (TS) and Young (elastic) modulus (EM) of chitosan-based films as a function of relative humidity .....	221
<b>Table 9.4.</b> Classification <sup>a</sup> of mechanical properties and film structures as a function of ambient relative humidity and film composition.....	222
<b>Table 10.1.</b> Properties of chitosan based films used in antimicrobial study .....	230
<b>Table 10.2.</b> Cultivability (expressed as percentage of bacterial cells having reproduction ability, %) and inactivation ability of carvacrol in various chitosan-based antimicrobial films against <i>Bacillus subtilis</i> 168 BGSC 1A, <i>Escherichia coli</i> TG1 K12, <i>Listeria innocua</i> DSM 20649 and <i>Salmonella Enteritidis</i> CIP 81.3 .....	236
<b>Table 11.1.</b> Collected data on sensory impact of carvacrol and carvacrol containing essential oils in different food products. The upper part of a table gives the acceptable scores, while the lower part gives literature data for unacceptable sensory score .....	255
<b>Table 11.2.</b> Characteristics of three active packaging films used in sensory evaluation .....	257
<b>Table 11.3.</b> Odour thresholds of carvacrol.....	260
<b>Table 11.4.</b> Odour and taste descriptors after triangle tests performed with AF2 after 3 and 15 days of storage .....	261
<b>Table 11.5.</b> Odour and taste descriptors after triangle tests performed with AF3 after 3 and 15 days of storage .....	261



*Chapter 1*  
*Introduction*

---



Packaging is one vector of innovation for food product development. The packaging industry occupies an important place in the food supply chain. It is an essential strategy for launching new products and its differentiation for market competition. New packaging systems and materials with innovative features are technical, security, marketing and sales tools to improve the business competitiveness. The packaging industry presents about 9% of final sale price of consumer products. Main functions of a packaging are: protection (mechanical, thermal and physicochemical), customer service (information and convenience) and industrial features (handling, storage, information functions, presentation, labelling, technical and communication actions).

In recent years, consumers have become more concerned about what they eat. Foods are sources of nutritive compounds and are designed to meet the biological needs. The products appearance, texture or flavour will very often guide the consumer to his/her final choice. This is why the preservation of food products requires the maintenance of their initial qualities by protecting them from the external environment and by limiting transfers and material losses. Optimizing the conservation of the organoleptic qualities of food products, and increasing their shelf life are two major challenges for the food industrial sectors. The answer of a packaging industry is very often development of new materials and processing technologies. These challenges are looking forward to improve customer satisfaction with better quality products, and the possibility to meet increasing free service market dominance.

To involve all the links in the food supply chain, the special strategy under the research and development of project named EMAC (EMballage ACTif) was established. This project has brought together the packaging material producers and the food industries as users of these packaging materials through the research institutes.

The project consortium, led by the industrial group Lactalis, involves the participation of four SMEs (AFT Plastics: compounder specialized in the development of composite materials with natural fibres; Chazal groupe and Salaisons Dijonnaises: delicatessen meat product producers; Plasti-lax: packager specializing in thermoforming and moulding/injection for rigid packaging), two major industrial groups (Lactalis: 1<sup>st</sup> European dairy group; Wipak: packager specialized in flexible film extrusion), four laboratories and technical centres (ICMUB-UMR 5260: specialist laboratory of synthesis and characterization of polymeric materials; ESIREM: engineering school materials; ESIEC: Engineering school for packaging of the University of Reims; Welience: food and bio-industrial technology transfer centre; UMR PAM: joint research Unit of the University of Burgundy/AgroSup Dijon, including PAPC



laboratory (activity and transfer of molecules) and PAM-PMB (microbiological and food process engineering); CVG: Centre de Valorisation des Glucides et produits naturels). EMAC project involves a lot of partners and two PhD, one post-doc, one engineer and several trainees have been recruited to target all aspects, phases and challenges of the research project.

The EMAC project is mainly based in terms of innovation on the development of active packaging systems that can interact intelligently with food contents. The new packaging systems should improve the organoleptic characteristics and nutritional properties of meat and dairy products through control of different volatile elements and physicochemical parameters composing the protective atmosphere. The control of these characteristics will result in extended product shelf life.

This doctoral thesis was a part of the EMAC project and has two main objectives:

- **the better understanding of the impact of formulation, process and storage parameters on the physico-chemical properties, on the structure and on the antimicrobial efficiency of bio-based active films.**

This allows optimising

- **the development of an active packaging film to preserve the best qualities and organoleptic properties of sliced dairy and meat products.**

The conventional principle of inertia of the package has been repealed by new European Union regulations in 2009. This reinforces the safety principles by opening up new fields of applications such as active packaging. The **second chapter** will present a literature review on the traditional and modern active packaging systems. Since their introduction in 1840, plastics have revolutionized human's everyday life and environment. The emerging sector of bio-based materials is also experiencing a strong growth. In this chapter, the accent is made on the chitosan, as the principle bio-based polymer used in this study. Furthermore, the impact of incorporated active volatile compound on the properties of polymer matrices, and *vice versa*, the importance of polymer system in the retention and preservation of compound efficiency and activity, are fully described.

The **third chapter** will be devoted to the description of materials and methods used for film preparation, its characterization and these assessments of application.

In the design of antimicrobial films, active compound must be in one way or another incorporated in the packaging system. Very few studies concern the importance of the processing parameters on the retention and on the preservation of active volatile compound. Therefore, in the **fourth chapter**, the influence of formulation and processing parameters on the properties of the film forming solution and retention of active volatile compound will be presented. Formulation and drying are defined as two main parameters featuring active film making.

Chitosan offers a great potential as active compound retender and active releaser. Still, there are some constraints that are limiting its use on the industrial level. Thus to improve processability, mechanical and water vapour barrier properties of chitosan films, associating chitosan with polyethylene will be proposed in the **Chapters five and six**. In the **Chapter five**, the water vapour and gas barrier properties of chitosan self standing films and chitosan coatings on polyethylene are presented. To better understand the barrier behaviour, in the **Chapter six**, structural and thermal properties of developed materials will be assessed.

The incorporation of carvacrol as the model of active antimicrobial volatile compound might change the chitosan film forming properties and its adhesion on the supporting material. Thus in the **Chapter seven**, the influence of carvacrol incorporation on the interfacial, structural and transfer properties of chitosan based self standing films and coatings will be studied.

As chitosan is a water sensitive polymer, water vapour can strongly influence film structure and functional properties. Most of the packaged fresh food products have high water content, so they will immediately change the vapour composition in the packaging. Then the influence of both relative humidity and temperature as mostly controlled parameters during storage of a food product must be focused on. The **Chapter eight** will present the results of the effect of hydration level and the presence of liquid water on the surface, thermal and barrier properties of hydrated chitosan based films and coatings. These results allow to better understand the transfer mechanism of desorption and diffusion of active carvacrol from chitosan films that are also given in the chapter eight.

In **Chapter nine**, the influence of water vapour on the structural changes in chitosan network and water vapour diffusion in the film will be explained by water

vapour sorption isotherms analysis. In this chapter, the influence of hydration level and film composition on the mechanical properties will also be given.

Results from chapter's three to eight are very important for the determination and the understanding of antimicrobial efficiency and organoleptic impact of activated chitosan films. The next two chapters are the validation of the studied systems. Antimicrobial efficiency in the vapour phase of chitosan films activated with carvacrol will be presented in **Chapter ten**. *Bacillus subtilis*, *Escherichia coli*, *Listeria monocytogenes*, *Lactobacillus plantarum*, *Salmonella Enteritidis* and *Penicillium camemberti* will be used as model microorganisms for their relevance as contaminants or industrial strains in the food industry.

After laboratory evaluation and understanding of the transfer mechanism of activated chitosan coatings, first prototype of active packaging will be validated. Industrial validation that includes production of packaging material and evaluation of organoleptic impact on the real food products will be described in **Chapter eleven**.

Finally, conclusions on the main results in relationship to the observed phenomena will be discussed in **Chapter twelve**. This chapter will end with perspectives.

*Chapter 2*  
*Bibliographic review*

---



## 2.1. Conventional packaging *versus* modern technologies

Packaging is the science, art, and technology of enclosing or protecting products for distribution, storage, sale, and use. From processing and manufacturing through handling, design and storage all the way to the consumer, almost all foods, whether fresh or processed, are enclosed in some form of packaging (Anker, 2000). Although it is not known when humans first made containers for storing food, it is supposed that various types of food containers made of organic, light-weight materials such as shells, animal organs, woven grasses, gourds, parts of trees including hollowed logs and leaves have been used from the ancient times (Hook and Heimlich, 2007). Listed materials are easily compostable in the environment; therefore little evidence of their use was preserved.

The main function of packaging is protection and preservation from external contamination. In doing so, packaging provides protection from three major classes of external influences: chemical, biological and physical, thus heat, light, moisture, oxygen, pressure, enzymes, spurious odours, microorganisms, insects, dirt and dust particles, gaseous emissions, and so on (Robertson, 2006) (Fig. 2.1.) Moreover its purpose is to preserve freshness of the content inside the barrier, to maintain and to extend the quality throughout the product's shelf-life (Miller and Krochta, 1997).

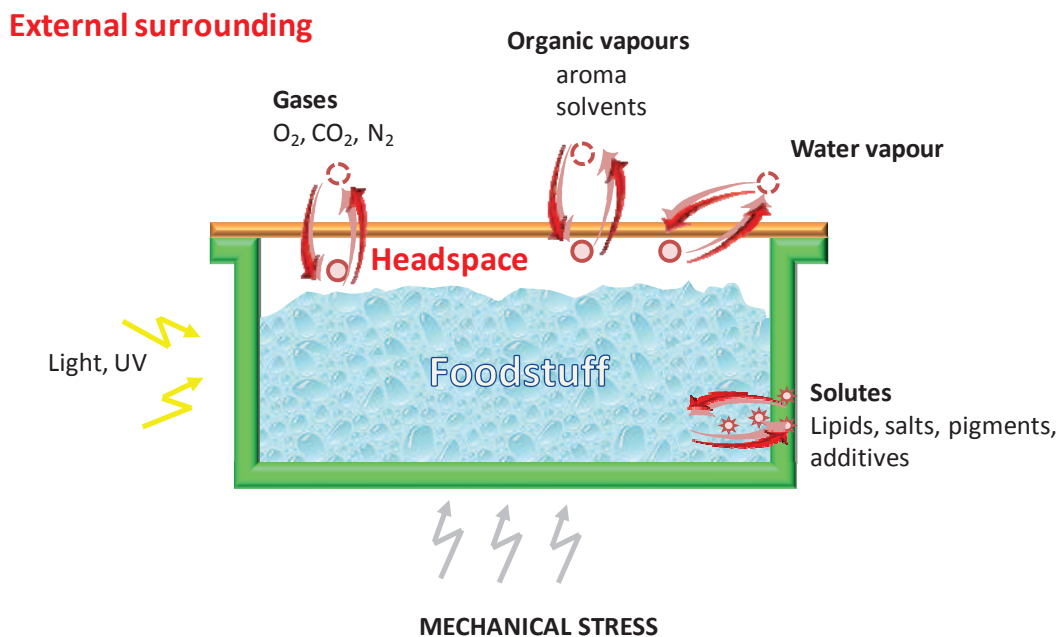


**Figure 2.1.** Protective function of food packaging.

Increase in shelf life involves retardation of enzymatic, microbial, and biochemical reactions through various strategies such as temperature control, moisture control, addition of salt, sugar, carbon dioxide, or natural acids, removal of oxygen, or a combination of these (Robertson, 2006). Conventionally, the ideal packaging material should be inert and resistant to hazards and should not allow molecular transfer from or to packaging materials (Robertson, 2006). Thus, it presents passive barriers designed to delay the adverse effects of the environment on the food product. However, in the past decade, in order to answer increasing needs and demands from consumers, research and development crops up new and modern food packaging systems. In retails, general trends involve centralization of activities and ways to reduce costs, while maintaining food safety and quality by hurdle technology. The way foods are produced, distributed, stored and retailed, reflects the continuing increase in consumer demands for improved quality and extended shelf-life for packaged foods. These changes are placing ever-greater demands on the performance of food packaging (Kruijf et al., 2002).

According to Ahvenainen (2003) the novel trend of packaging technology includes “smart packaging” / “interactive packaging” / “active packaging” / “clever packaging” or “intelligent packaging”. The addition of an active substance in the material can improve packaging functionality (Appendini and Hotchkiss, 2002). These systems consider the packaging as a delivery system to release the antimicrobial into food in an effective manner, via interactions between products, packaging and surrounding environment. Thereby, the product’s quality, safety and shelf life are extended (Suppakul et al., 2003).

Intelligent packaging is “packaging which senses and informs” and aims to monitor the quality of the food product or its surrounding environment to predict or measure the safe shelf life. The package function switches on and off in response to changing external/internal conditions and can include a communication to customer or end user as to the status of the product.

Certain packaging technologies include additives that are intended to change the quality of the food itself. For example, some enzymes can be added to the inside of juice packaging in order to degrade the bitter compounds in the juice (Keller et al., 2002). These systems stay under a question: should they be evaluated as packaging or as direct food additives?

## **2.2. Consumer's requirements and safety considerations**

### **2.2.1. Consumer requirements**

Rapid way of life, globalization and modernization, are some of the reasons for changes in the way of groceries purchases and food storage. Our eating habits have changed dramatically during the 20<sup>th</sup> century. Food service has grown to become a major part of consumer spending. Furthermore, our today's meals have to be quick and convenient to prepare, healthy and tasty. Also, we often tend to buy food once a week and we eat ready to eat meals. Two major convenience trends—meals eaten in transit and multi-component meals—have also advanced the food service packaging industry. Finally, we expect our food not to be too expensive and in short, to be tasty, safe, cheap, healthy, available all year round, "as natural as possible", varied, and sometimes elegant or exotic (Balasubramanian et al., 2009). To answer all this requirements, polymer industries have begun exploring alternatives to presently used chemicals and synthetic materials. In addition to the desire for natural compounds that enhance quality, there is also a need for an efficient method for their delivery into foods. Addition of compounds directly into food is an established practice with some disadvantages. Active food packaging can concentrate its action both directly on the food surface and through the headspace. Then, it allows reducing the use of preservatives into food formulation (Quintavalla and Vicini, 2002). The latter is an important factor for foodstuffs where the absence of preservatives is preferred with the aim of both satisfy a consumer request and to respect the traditional food formulation (Davidson and Juneja, 1990).

### **2.2.2. Safety considerations**

National regulatory bodies specify safe levels of the substances that could be added into food. Safety requirements are of global significance along the whole food production chain. From harvest of the raw materials to storage of processed food products in the home, a key concern is suppressing the growth of unwanted organisms that may spoil food. Addition of antimicrobials in formulation often results in instant inhibition of non-desired microorganisms. However, there is a great risk of development of mutant organisms that are later on hard to handle (Balasubramanian et al., 2009). Moreover, preservatives are an everyday topic in public discussions, and whenever it comes up, many consumers associate them with harmful, modern chemicals in foodstuffs. Thus consumers demand natural and preservative free products, as well as providing enjoyment. Consumers now want food to enhance our



health and wellbeing. In order to meet safety standards and at the same time to maintain organoleptic quality, active and intelligent packaging systems have gained great interest of scientific world and food industry.

What all packaging have in common is to protect what they contain and to help to maintain health (active protection function). The term “safety” sums up a number of regulatory requirements which are demanded upon packaging. In practice, a package is regarded “safe” if it has successfully passed relevant tests to prove that it meets with all of these requirements (Galić et al., 2011).

Since the first commercial active packaging materials have been produced, they have been widely used in the Japanese, Canadian, Australian and United States markets. Because of the safety regulations, the use of these materials has been restricted in the European marketplace until 2004.

In the European Union (EU), regulation constraints such as the overall migration limit (OML) resulted in a different set of regulatory hurdles for the clearance of active packaging materials. Recognizing the benefits of bringing safe, new materials entering into European markets, the EU has currently developed a new regulatory standard. Until 2004, the European Legislation has protected the health of consumers both ensuring that no material in contact with foodstuffs can change their organoleptic properties and permitting only a minimum interaction between foods and packaging. However modern packaging aspects, already present on the other continents, have forced the European Legislation bodies to regulate lack of penetration of these materials. Thus, in 2004, the Regulation 1935/2004 has derogated the old legislation with the purpose to assure a high level of human health protection. It deals with materials and articles intended to come into contact with food and already contain general provisions on the safety of active and intelligent packaging. Furthermore, by the date, the framework for the European Food Safety Agency (EFSA) evaluation process started (Dainelli et al., 2010). In this regulation, it is claimed that materials have not to transfer their constituents to food in any quality that could endanger human health or bring about any organoleptic change of the food. Releasing systems are allowed to change the composition of the food without masking spoilage, providing that the released substance should not mislead the consumer.

The latest act adopted on 29 May 2009, opens the door of the European continent to the use of active packaging materials. The Regulation (EC) No 450/2009

lays down specific rules for active and intelligent materials and articles intended to be used in contact with foodstuffs to be applied in addition to the general requirements established in Regulation (EC) No 1935/2004 for their safe use.

EC No 450/2009 introduces the concept of functional barrier. By a definition, it consists of one or more layers of food-contact material and prevents the migration of substances in amounts which could endanger human health. Consequently, these active substances do not need a safety evaluation. Furthermore it opens the door to use of nanoparticles, which should be assessed on a case-by-case basis as regards their risk until more information is known about such new technology.

EC No 450/2009 establishes that the substances responsible for the active functions can either be contained in separate containers such as small sachets or directly be incorporated into the packaging material. They may release or absorb substances and they must not be cancerogenic, mutagenic, toxic to reproduction nor in nanoform. Moreover, they have to be listed into the community list of authorised substances established by EFSA and must comply with the food additives regulation (EC No 1333/2008) and food flavourings regulation (EC No 1334/2008).

It also deals with any kind of releasing systems. Notwithstanding the environmental and antimicrobial value of essential oils, their use might be affected by safety issues and unsatisfactory organoleptic impact. When it comes to the question of their use in the active packaging materials, by the EC 450/2009 regulation they have been positively listed. Extracts having an antimicrobial or preservative effect on the food or any other technological function, extracts from plants, micro-organisms or animal origin can be incorporated into the food packaging to exert a function in the food and are covered by the food additives regulation. These extracts are then considered as releasing active substances. As active substances are not part of the passive material, their transfer does not need to be included in the calculation of the overall migration limit. Consequently, the overall migration from active releasing materials can exceed the OML described in EU or national legislation, provided the levels transferred to the food comply with the restrictions in relevant food law such as food additives regulation. Any decision, which packaging shall be used, should be proceed by specific laboratory tests. A well known procedure is the test concerning migration, including qualitative and quantitative (overall/specific migration) analysis.

Thanks to the above regulations, European markets are now opened to the use of new technologies of active packaging. The intensive accent to realization of this regulation was actually a result of pressure from the US market. Namely, these systems have been used in food preservation in the US since mid 80's of the past century. It is mainly due to the fact that marketing requirements for new active and intelligent packaging technologies in the United States are not very different from the requirements for conventional packaging materials. The only additional necessity for manufacturers is to take care to the formation of any by-products or degradation products that may be formed during the functionalisation of the material. Antimicrobials in food packaging are regulated by Food and Drug Administration (FDA) as food additives under Section 409. However, they also require registration with Environmental Protection Agency (EPA) under Federal Insecticide, Fungicide and Rodenticide Act (FIFRA). In the United States, the term "active packaging" generally describes any packaging system that protects food from contamination or degradation by creating a barrier to outside conditions while interacting with the internal environment to control the atmosphere within the package. These substances also improve the packaging material's ability to extend the shelf life of the food contained inside (Keller et al., 2002).

Above mentioned facts import new opportunities to both food and material industries to place new products on the European market. In parallel, the production of authentic products and traditional specialities poses some qualities related to the natural origin of typical ingredients and the additives absence, which can influence sensory properties and consumer's expectations (Cayot, 2007). The definition of authentic products has been recently promoted by the European Union through EuroFIR (European Food Information Resource) project and two directives, the Council Regulations EC No 509/06 and No 510/060 of 20 March 2006. Many food products have been registered by EU as „Protected Designation of Origin“ or „Protected Geographical Indication“. Consequently, these regulations have increased the attention of food companies towards new products that can evoke traditional taste and flavour (Kuhne et al., 2010). However, the introduction of active systems into the European marketplace in the recent future requires support with a substantial information campaign identifying benefits and how they function. It is clear that the innovation becomes a strategic tool to achieve competitive advantage but because of the high costs, evaluation of the economic consequences and environmental implications for active systems must be performed (Kruijf et al., 2002).

### 2.3. Active packaging – basic concept

Three broad considerations must be taken into account when choosing the appropriate packaging concept: requirement of food, followed by the packaging format and the requirements of active agent (Han, 2005). Creation of activity in packaging materials frequently involves the introduction of additional components into otherwise inactive materials. Active packaging can be classified into two main types: non-migratory active packaging and active releasing packaging. While the first type acts without intentional migration, in the second one a controlled migration of agents is allowed and targeted. This includes both non-volatile agents and emission of volatile compounds in the atmosphere surrounding the food (Dainelli et al., 2008) (Fig. 2.2.). Due to great innovation potential and big accent in active packaging development, there is a huge palette of active compounds that can be added inside the packaging.

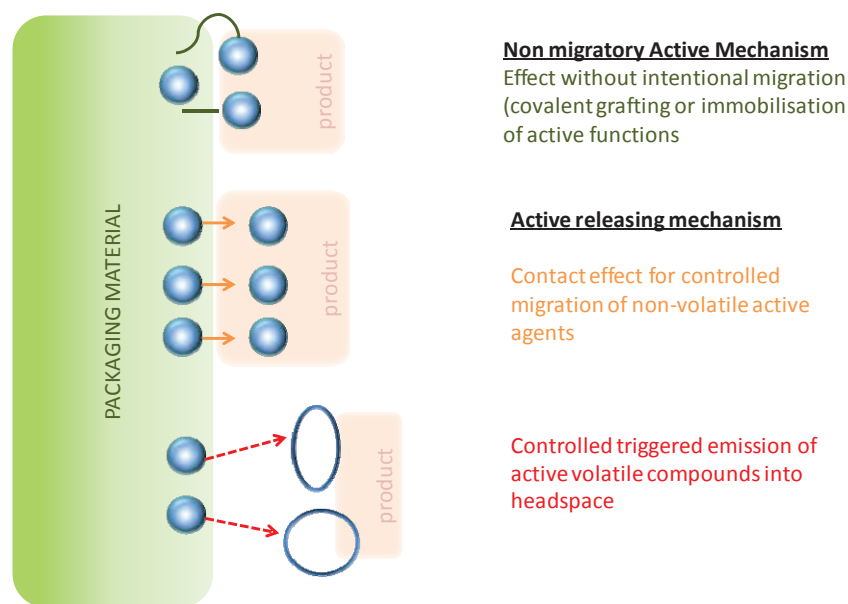


**Figure 2.2.** Different modes of active releasing mechanisms (Dainelli et al., 2008).

The nature of support material is very diverse including papers, plastics, biopolymers, metals or combinations of these materials. While in conventional packaging, all mass transfers such as permeation, migration, sorption between material and food product must be minimized, active packaging systems employ materials that are sufficiently permeable to provide controlled release or absorption and migration of active compounds (e.g. preventing increased carbon dioxide concentrations in the package, or protecting the food from degradation due to light or

water vapour exposure). Active packaging systems are, in fact, not one technology but a collection of technologies in response to specific problems. In the literature, active packaging systems are classified to:

- ↪ Addition of sachets or pads containing volatile agents into packages;
- ↪ Incorporation of volatile and non-volatile agents directly to polymer;
- ↪ Coating or adsorbing agents on the polymer surfaces;
- ↪ Immobilization of agents to polymer by ion or covalent linkages;
- ↪ Use of polymers with particular properties (Appendini and Hotchkiss, 2002; Gutierrez et al., 2009).

Active compound might be released by diffusion, by matrix degradation, by swelling or by melting (Desobry and Debeaufort, 2011). In the first one, the principal steps in the release of a compound from a matrix system are diffusion of the active agent to matrix surface; partition of the component between matrix and food; and finally, transport away from the matrix surface. The second one is driven by erosion. Release by swelling includes mainly systems where molecule in a polymeric matrix is unable to diffuse to any significant extent within the matrix. Then in a swollen film the entrapped molecule is able to diffuse due to higher intermolecular spaces. The final one, release by melting is obtained when the matrix wall is melt and then the active compound is released (Desobry and Debeaufort, 2011).

Well studied and already applied systems may be designed to:

- ↪ release ethanol (e.g. Lichter, 2002), carbon dioxide, sulphur dioxide (e.g. Cantin et al., 2011), antioxidants (e.g. López-de-Dicastillo et al., 2012; Contini et al., 2012; Gemili et al., 2010) or antimicrobial agents (e.g. Imran et al., 2012; Kanatt et al., 2012; Sanchez Gonzales et al., 2011a,b) in the package.
- ↪ Contrarily, systems may absorb: excessive moisture (e.g. Azevedo et al., 2011), unwanted odours (e.g. López-de-Dicastillo et al., 2011), flavours (e.g. Ahvenainen, 2003) or gases like oxygen (e.g. Busolo and Lagaron, 2012; Aday and Caner, 2012) and ethylene from the package (Picon et al., 1993).
- ↪ Moreover, they may be able to improve the quality of the food by for example removing allergens like lactose, or fats like cholesterol from dairy products (e.g. Ahvenainen, 2003).

## **2.4. Antimicrobial food packaging**

The quality of foods has been defined as their degree of excellence and includes factors of taste, appearance, nutritional content and microbial safety. In 1997, Floros and co-workers (Floros et al., 1997) identified antimicrobial packaging as one of the most promising versions of an active packaging system. Microorganisms, temperature, sunlight, oxygen, humidity etc. may induce microbial proliferation in the food, degradation of food components and alterations in the organoleptic properties with consequent consumer's rejection. Despite increase in awareness of importance of high level hygiene in food supply chain, foodborne illnesses caused by microorganisms are still large public health problem. Recent food-borne microbial outbreaks are driving force for innovative ways to inhibit microbial growth in the foods while maintaining quality, freshness and safety. Besides, due to consumer's demands for both minimally processed and preservative-free products, and due to concerns related to the use of chemical additives, use of natural additives with antimicrobial properties, seems to be a promising alternative for food industry. By a definition, antimicrobial food packaging materials have to extend the lag phase and reduce the growth rate of microorganisms in order to extend shelf-life and to maintain product quality and safety (Han, 2000). A number of review articles have described the nature of antimicrobial films and their antimicrobial constituents, their construction and general effectiveness (Rojas Grau et al., 2009; Dutta et al., 2009; Appendini and Hotchkins, 2002; Suppakul et al., 2003; Ozdemir et al., 2004; Han, 2005; Joerger, 2007). The most investigated compounds include organic acids, enzymes, metal ions, fungicides, ethanol, and natural extracts. Different antimicrobial bio-based films with incorporated essential oils are listed in Table 2.1.

Table 2.1. Antimicrobial biopolymer based films with essential oils

Film forming polymer	Essential oil component	Tested microorganism	Reference
<b>Alginate</b>	Oregano essential oil	<i>S. aureus</i> , <i>L. monocytogenes</i> , <i>E. coli</i> , <i>S. Enteritidis</i> , <i>S. Typhimurium</i>	Benavides et al., 2012; Oussalah et al., 2006
	Chinese cinnamon	<i>E. coli</i> O157:H7, <i>S. Typhimurium</i>	Oussalah et al., 2006
	Garlic oil	<i>E. coli</i> , <i>S. Typhimurium</i> , <i>S. aureus</i> , <i>B. cereus</i>	Pranoto et al., 2005a
	Savory	<i>E. coli</i> O157:H7, <i>S. Typhimurium</i>	Oussalah et al., 2006
	Oregano oil/carvacrol	<i>E. coli</i> O157:H7	Rojas Grau et al., 2007
<b>Alginat-apple puree</b>	Cinamon oil/cinnamaldehyde		
	Lemongrass oil/citral		
	Mexican oregano	<i>A. niger</i> , <i>P. digitatum</i>	Avila-Sosa et al., 2012
<b>Amaranth</b>	Cinnamon		
	Lemongrass		
<b>Chitosan</b>	Rosemary		Abdollahi et al., 2012
	Lemon	<i>Botrytis cinerea</i> , <i>L. monocytogenes</i> , <i>E. coli</i> , <i>S. aureus</i>	Perdones et al., 2012
	Limonene		Sanchez Gonzales et al., 2011
	1,8-cineole	<i>Salmonella</i> Anatum	Thangvaravut et al., 2012
	Cinnamon essential oil	<i>L. monocytogenes</i> , <i>E.coli</i> , <i>L. plantarum</i> , <i>L. sakei</i> , <i>Pseudomonas fluorescens</i>	Mahdi Ojagh et al., 2010
	Mexican oregano	<i>Aspergillus niger</i> , <i>P. digitatum</i>	Avila-Sosa et al., 2012
	<i>Zataria multiflora</i> Boiss	<i>L. monocytogenes</i>	Avila-Sosa et al., 2012
	Grape seed extract	<i>L. monocytogenes</i>	Avila-Sosa et al., 2012
	Cinnamon	<i>L. monocytogenes</i> , <i>E. coli</i>	Zivanovic et al., 2005
	Lemongrass	<i>L. monocytogenes</i> , <i>E. coli</i> , <i>S. aureus</i>	Sanchez Gonzales et al., 2011a
	Bergamote	<i>P. italicum</i>	Sanchez Gonzales et al., 2011a
	Tea tree	<i>L. monocytogenes</i> , <i>E. coli</i> and <i>S. aureus</i>	Sanchez Gonzales et al., 2011a

Gelatine film	Bergamot	<i>E. coli</i> , <i>L. monocytogenes</i> , <i>S. aureus</i> , <i>S. Typhimurium</i>	Avila-Sosa et al., 2012
	Lemongrass essential oil	lactic acid bacteria (LAB), H <sub>2</sub> S-producing bacteria, Enterobacteriaceae, <i>E. coli</i> , <i>L. monocytogenes</i> , <i>S. aureus</i> , <i>S. Typhimurium</i>	Ahmad et al., 2012a
	Citrus	<i>L. innocua</i>	Iturriaga et al., 2010
	Thyme	<i>L. innocua</i>	
	Oregano	<i>L. innocua</i>	
Gelatine/chitosan	Clove	<i>Pseudomonas fluorescens</i> , <i>Shewanella putrefaciens</i> , <i>Photobacterium phosphoreum</i> , <i>L. innocua</i> , <i>E. coli</i> , <i>L. acidophilus</i>	Gómez-Estaca et al., 2010
	Fennel		
	Cypress		
	Lavender		
	Thyme		
	Herb-of-the-cross		
	Pine		
	Rosemary		
	Oregano	<i>E. coli</i> O157:H7, <i>Pseudomonas</i> spp	Oussalah et al., 2004
	Pimento	<i>E. coli</i> O157:H7, <i>Pseudomonas</i> spp	Oussalah et al., 2004
Methyl cellulose	Oregano	<i>L. innocua</i>	Iturriaga et al., 2010
	Mexican oregano	<i>Aspergillus niger</i> , <i>Penicillium digitatum</i>	Avila-Sosa et al., 2012
Starch	Cinnamon	<i>Aspergillus niger</i> , <i>Penicillium digitatum</i>	Kechichian et al., 2010, Avila-Sosa et al., 2012
	Lemongrass	<i>Aspergillus niger</i> , <i>Penicillium digitatum</i>	Avila-Sosa et al., 2012
	Clove	Molds, yeasts	Kechichian et al., 2010
Starch/chitosan	Thyme	<i>B. cereus</i> , <i>E. coli</i> , <i>S. Enteritidis</i> , <i>S. aureus</i>	Pellisari et al., 2009
	Oregano	<i>E. coli</i> O157:H7, <i>S. aureus</i> , <i>Pseudomonas aeruginosa</i> , <i>L. plantarum</i>	Emiroglu et al., 2010
Soy protein	Oregano	<i>E. coli</i> O157:H7, <i>S. aureus</i> , <i>S. Enteritidis</i> , <i>L. monocytogenes</i> , <i>L. plantarum</i> , lactic acid bacteria, <i>Pseudomonas</i> spp.	Seydim and Sirakus, 2006
	Rosemary		Zinovadou et al., 2009
Whey protein	Garlic		



It is generally considered that packaging system consists of a three different parts including material, food product and the environment (external-surrounding and internal-headspace). If the incorporated antimicrobial compounds are non-volatile, packaging materials must contact the surface of the food so that the antimicrobial compound can diffuse to the surface (Fig. 2.2.). Moreover, its concentration on the surface might be minimized because of its diffusion to the inner part of a product and consequently antimicrobial effect will be also minimized (Min and Krochta, 2005). Its interaction with a food material might also cause loss of the antimicrobial property. Aseptically packed sausages or wrapped cheese are some of examples of these systems where the diffusion between packaging and the food, and the partitioning at the interface is the main migration phenomenon involved (Han, 2003). The industrial advantage of the non-volatile migrating systems is simplicity of the system design. They could be applied in currently existing packaging processes without high investment and easy maintenance.

On the contrary, if the incorporated antimicrobials are volatile compounds they do not need to contact the surface of the foodstuff (Appendini and Hotchkiss, 2002; Suppakul et al., 2003). Then, we are speaking about package/headspace/food systems. These include modified atmosphere packed (MAP) products, flexible packages, bottles and cups. Evaporation or equilibrated distribution of substance between material, headspace and foodstuff is the main migration mechanism (Han, 2003). After incorporation of a volatile substance in the material and packing of the food, compound is vaporized into the headspace, reaches the surface of the food and after all, it is absorbed by the food. Mass transfer in this system is dynamically balanced, thus the release of the volatile compound is dependent on the volatility and chemical interactions between compound and the system. Furthermore, the absorption rate of headspace volatiles into the food is related to food composition (proteins, lipids).

Commonly used compounds are plant extracts. From consumers' point of view, they have been generally accepted in pharmaceutical and nutraceutical applications. Thus it seems that their implantation on the packaging marketplace should not pose any problem. This is very important when commercialization, validation and the industrial application are envisaged.

In the antimicrobial compound selection process, the effectiveness against the targeted microorganisms must be taken into account as well as the possible interactions between the antimicrobial compound, the film-forming polymer and the food components. These interactions can modify both antimicrobial activity and film

characteristics. So, it is important to select the right packaging material for particular antimicrobial and environmental conditions; as well as the right antimicrobial for a specific food product and packaging process. Environmental conditions have to be considered because release rate kinetic could be influenced by temperature and moisture content in the packaging. Moreover, in most cases, the release of the active substance is not governed only by diffusion, but it is also due to swelling and water uptake of the film (Ouattara et al., 2000). Furthermore, slow release from packages prevents large amounts of antimicrobials in the food at the time of consumption, while still maintaining the desired activity. The continuous slow release should also be advantageous for re-sealable packages as they may be opened and closed numerous times (Chung et al., 2001). The release of antimicrobial compounds from polymeric packaging materials is claimed to be systematically controllable (Sebti et al., 2003). By releasing preservatives from the package (rather than mixing preservatives into the bulk of the food), a smaller amount of antimicrobial agent is needed to prevent the surface growth of microorganisms (Yalpani et al., 1992). Furthermore, the concentration of antimicrobial in the packaging must be calculated based upon the amount needed and precisely classified for the final product (Nerin et al., 2006). A number of mathematical models have been described by Brody et al. (2001). A multi-layer design is favoured because by selecting appropriate materials and its thicknesses, it allows to control the diffusion of antimicrobial compounds into food.

Above mentioned factors are keys for development of successful antimicrobial films and coatings. Important problems in evaluation of the „real“ antimicrobial efficiency is the extrapolation of results obtained on the model systems in the researching laboratories and the reality. Real food product has more nutrients, fat, proteins, salts etc., that might interact with the antimicrobial and thus it is different than the laboratory food simulants.

## **2.5. Essential oils as antimicrobial agents for active packaging systems**

To date, it has been demonstrated that essential oils, that are Generally Recognized As Safe (GRAS) for food application, effectively inhibit microbial growth and thus could be used to control foodborne pathogenic bacteria (Burt, 2004).

Essential oils have been already consumed by ancient Greeks and Romans that were using them as preservatives, perfumes and flavourings. In the 13<sup>th</sup> century they were being made by pharmacies and their pharmacological effects were described in

pharmacopoeias (Bauer et al., 2001). With the development of new techniques in food preservation in the last decade of 20<sup>th</sup> century, there is a great expansion of use of essential oils and their constituents in the field of food packaging. Numerous publications have presented data on the composition of the various oils. The major components of the economically interesting ones are summarised by Bauer et al. (2001). Spices and herbal plant species are known to contain a wide range of compounds capable of exhibiting antimicrobial activity. These compounds are produced as secondary metabolites associated with the volatile essential oil fraction of these plants.

The chemical structure of the individual essential oil components affects their precise mode of action and antibacterial activity (Dorman and Deans, 2000). Moreover, the activity of essential oils depends on the test conditions, microorganisms, and source of the antimicrobial compound (Roller, 2003). Essential oils are active against Gram negative and Gram positive bacteria at a wide range of pHs and salt concentrations. High degree of inhibition by volatile components of essential oils in the vapour phase has been demonstrated in the literature (Inouye et al., 2001; Goñi et al., 2009; Nedorostova et al., 2009; Kloucek et al., 2011). Since they are volatile, application as a vapour instead of as a liquid may be a feasible method of use with food products. Lower concentrations are also required if the vapour is aimed to act on bacteria grown on the food surface, without first coming into contact with the food itself. Thus flavour impact of essential oils on the food may be reduced (Burt, 2004). Sometimes, pleasant herbal aroma and flavour of the oils makes them favourable in many food and drink applications. Moreover, they are approved food flavourings in Europe. Still, great attention and more knowledge is required as tests using real foods often reveal that the developed antimicrobial packaging system is less effective than in previously performed laboratory conditions (Duan et al., 2007). Some of explanations can be the greater availability of nutrients for microbial cellular repair, higher organic acid and trace metal contents, interactions with compounds in the food that may interact with/or inactivate the active substance (Burt, 2004). Lack of good experimental design, discrepancies and error in a judgment, lack of studies on resistance development of organisms, lack of multi-disciplinary approach are some of the reasons why there are difficulties to make these antimicrobial systems more applicative in reality (Balasubramanian et al., 2009).

To be used in active packaging films, essential oils must be retained/entrapped in the polymer matrix. Today's trends in this domain are towards bio-sourced materials, namely bio-based polymers.

---

---

## 2.6. Biopolymers in food packaging

In the late 50's of the past century, food packaging is one application area that was revolutionised by oil-based polymers such as polyethylene (PE), polypropylene (PP), polystyrene (PS) and poly(ethylene terephthalate) (PET). These polymers quickly found wide acceptance in different packaging applications, due to their attractive properties such as flexibility, toughness, low weight, processability, desirable physical and mechanical properties with a favourable cost both for food industry and consumers. Durability, which makes these materials so useful, also ensures their persistence in the environment and complicates their disposal. This has become an ever growing problem for many of the plastics now in use. Awareness and consumer power, coupled with the inexorable rise in pre-packaged disposable meals, forces food manufacturers and packagers to improve environmental performances of their products (Jansen and Moscicki, 2009). Most plastic materials are not biodegradable, and they are derived from non-renewable resources. Newly discovered characteristics of natural biopolymers makes them the great choice for different types of wrappings and films (Krochta and De Mulder-Johnston, 1997). Based on their origin and production, bio-based polymers may be divided into three main categories including polymers directly extracted/removed from biomass (e.g. starch, cellulose, proteins, casein, gluten), polymers produced by classical chemical synthesis using renewable bio-based monomers (e.g. polylactic acid) and polymers produced by microorganisms or genetically modified bacteria (e.g. polyhydroxyalkanoates) (Chandra and Rustgi, 1998). In general, compared to conventional plastics derived from mineral oil, bio-based polymers have more diverse chemistry and architecture of the side chains. This gives those materials unique possibility to tailor the properties of the final package (Weber, 2000).

Use of edible and biodegradable films can reduce the number of disposable packaging and can reduce environmental pollution. To increase product shelf-life and to improve quality they may be used in a multi-layer packaging, they can enhance the organoleptic properties of packaged foodstuff, they can supplement the nutritional value, they can serve as carriers for antimicrobial and antioxidant agents and they can regulate transfer of moisture, oxygen, carbon dioxide, lipid, and aroma and flavour compounds in food systems (Anker, 1996).

Due to the big dominancy of synthetic plastics, biopolymers still haven't reached commercial competitiveness (Scott et al., 1999). Apart from not yet competitive mechanical properties, some restrictions and drawbacks, biopolymer films are still difficult and expensive to be processed in the large scale in comparison with synthetic

polymers. Thus, combination of two is a new approach that gains attention of packaging industry. In multi-layered systems, common polyolefin such as polyethylene may provide good chemical, mechanical and water vapour resistance. Biopolymer coating may serve as a carrier of active substances and for improving gas barrier properties. They could also be easily separated from the oil-based polymer and then they could be recycled.

The most commonly available biopolymers are those extracted from marine and agricultural animals and plants. Generally, they are based on proteins, polysaccharides and lipids. Starch, chitosan and cellulose can be potential candidates since they are not only biodegradable and edible, but also widely available, easy to handle and inexpensive (Rodríguez et al., 2006; Bertuzzi et al., 2007). The interest in these materials and the development of their applications in food packaging has increased. It is due to large surpluses of the raw materials, which are produced in large amounts as by-products of agro-industrial processes. Even if they have been used in several applications, there is still a great disposal of these by-products.

## **2.7. Chitosan**

Among all biomolecules naturally present and commercially available, those in carbohydrate groups have been extensively researched and commercialized. One of the most promising polymers, chitosan, offers real potential for broad spectrum of applications in the food and pharmaceutical industry. It is mainly due to its particular physico-chemical properties, short time biodegradability, biocompatibility, antimicrobial and antifungal activities, non-toxicity, toughness, durability, moderate values of water and oxygen permeability (Dutta et al., 2009; Elsabee et al., 2009; Aider et al., 2010; Kong et al., 2010; Chen et al., 2011; Muzzarelli et al., 2012).

### **2.7.1. Deacetylation, crystallinity and molecular weight**

Chitosan is a linear polysaccharide consisting of  $\beta$ -(1 $\rightarrow$ 4)-linked 2-amino-2-deoxy- $\beta$ -D-glucopyranose and 2-acetamido-2-deoxy- $\beta$ -D-glucopyranose residues (Fig. 2.3.) (Kumirska et al., 2011). Next to cellulose, it is the second most abundant natural biopolymer. It is found predominantly in the shells of crustaceans such as crabs and shrimps, in the cuticles of insects and in the cell walls of fungi. Its biosynthesis by living organisms in the lower plant and animal kingdoms has been estimated at  $10^{10}$ – $10^{12}$

tons/year (Percot et al., 2003). Commercial chitosan samples are typically prepared by chemical de-N-acetylation of chitin under alkaline conditions. Final chitosan samples can differ in size (average molecular weight), deacetylation degree (DA), polydispersity or crystallinity (Aranaz et al., 2009). DA represents the molar fraction of 2-amino-2-deoxy-D-glucopyranose units in the chitosan macromolecule and shows the percentage of free amino groups in the polymer chain. The process of deacetylation involves the removal of acetyl groups from the molecular chain of chitin, leaving behind a complete amino group (-NH<sub>2</sub>). Chitosan versatility depends mainly on the high degree of chemical reactive amino groups. The degree of deacetylation of commercial chitosan usually varies from 75% to 95%, depending on the production method. When preparing chitosan samples, reaction conditions must be controlled (Aranaz et al., 2009). During deacetylation process, crystallinity of chitosan can be damaged, because of degradation of polymeric chain and because of harsh conditions. Precise determination of its average molecular weight is difficult (Rinaudo and Domard, 1988). The usual average molecular weight reported in the literature is of the order of 10<sup>5</sup> g/mol. The influence of average M<sub>w</sub> on the viscosity in aqueous solutions plays an important role in the biochemical and bio-pharmacological significance of chitosan (Taranathan, 2003).

### 2.7.2. Chitosan solubility

In crystalline form, chitosan is normally insoluble in aqueous solutions. However, in dilute acids, the protonated free amino groups facilitate the solubility of the molecule. The pK<sub>a</sub> of primary amino groups depends closely on DA, so solubility of chitosan is also dependent on DA (Pillai et al., 2009).

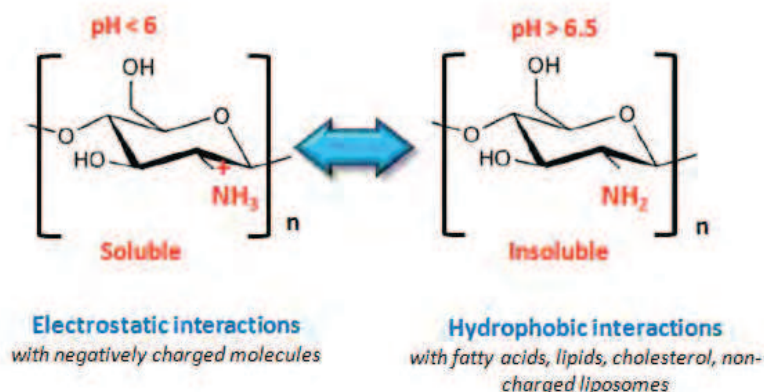


**Figure 2.3.** Soluble and insoluble structure of chitosan monomer (Kumirska et al., 2011).

---

Technologically, this determines its processing in form of films, microspheres/capsules, fibres, gels, powders, granules, tablets, microporous sponges, etc. At pH >6.5 chitosan solutions exhibit phase separation. At pH <6.5 chitosan is positively charged because of the presence of protonated amino groups (Elsabee et al., 2009). This makes chitosan an effective binder to negatively charged metals, biochemicals, macromolecules and cells (Fig. 2.3.). In solution, at pH between 6.0 and 6.5, free amino groups of chitosan molecules become less protonated and hydrophobicity along chitosan chain increases. Therefore, by hydrophobic/hydrophobic repulsions, in acetate buffer solutions, chitosan self aggregates can be formed (Kumirska et al., 2011).

Solubility of chitosan in organic solvents is limited. Aqueous solutions of acetic acid can tolerate the addition of great volumes of polar solvents without occurrence of polymer precipitation. It has been found that up to 70% (v/w) of alcohols (from methanol to butanol), ethylene glycol, diethyleneglycol, acetone and dimethylformamide, up to 40% of 2-propanol and up to 80% of glycerol can be added without chitosan precipitation.

### **2.7.3. Chitosan crystals diversity**

The knowledge of structural differences among chitosan products is very important in determining its properties. So, it is essential for the structure-activity-analysis of applied systems.

Biological and chemical reactivity of chitosan is strongly dependent on the extent of hydration and crystallinity (Ogawa et al., 1993). Chitosan crystal has two polymorphs, hydrated (tendon) and annealed (anhydrous) polymorph. The tendon chitosan shows a hydrated crystalline form which can be converted to an anhydrous form (Ogawa et al., 1993). Changes between different polymorphs are given in Fig. 2.4. (Okuyama et al., 1997; Okuyama et al., 1999).



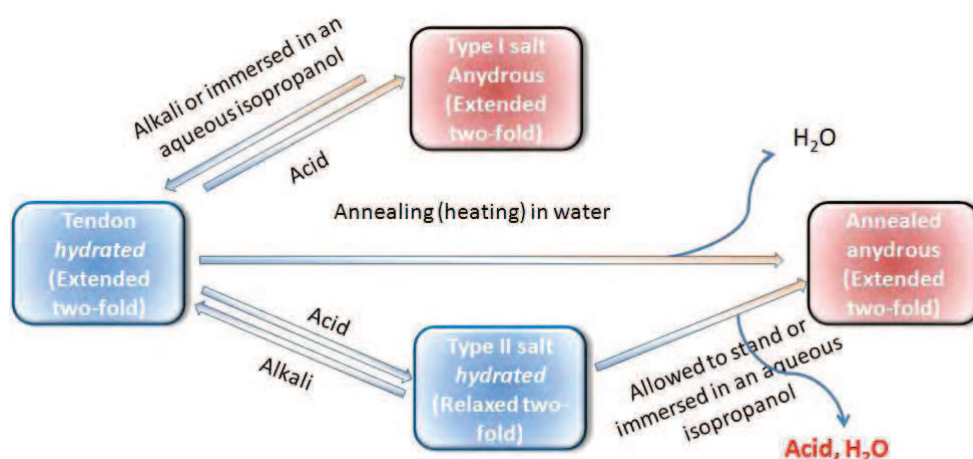


**Figure 2.4.** Crystalline transformation of chitosan (Ogawa et al., 2000).

Since chitosan is a polymer of D-glucosamine that has free amino group, it has a cationic character and it makes salt with an acid. There are four possible chitosan-acid salt types. In Type I salts, chitosan is in an extended two-fold helix (e.g. when formed with  $\text{HNO}_3$ ,  $\text{HBr}$ , L-ascorbic acid). In Type II salts, chitosan molecules takes up relaxed two-fold helix composed of asymmetric unit of tetrasaccharide (Fig. 2.5.) This form seems to be unstable, because no strong intramolecular bonds exist like in Type I form. The space between chitosan chains is filled with water and carboxylic acid, which account for more than 33% by weight according to thermo-gravimetric measurement and the observed density (measured in ambient conditions) (Okuyama et al., 2000). In its hydrogen iodide salts prepared at low temperatures, chitosan takes a 4/1 helix with asymmetric unit of disaccharide. In the fourth conformation, prepared with medical organic acids that have phenyl group, such as salicylic or genitistic acid, it was found to be in a form of 5/3 helix.



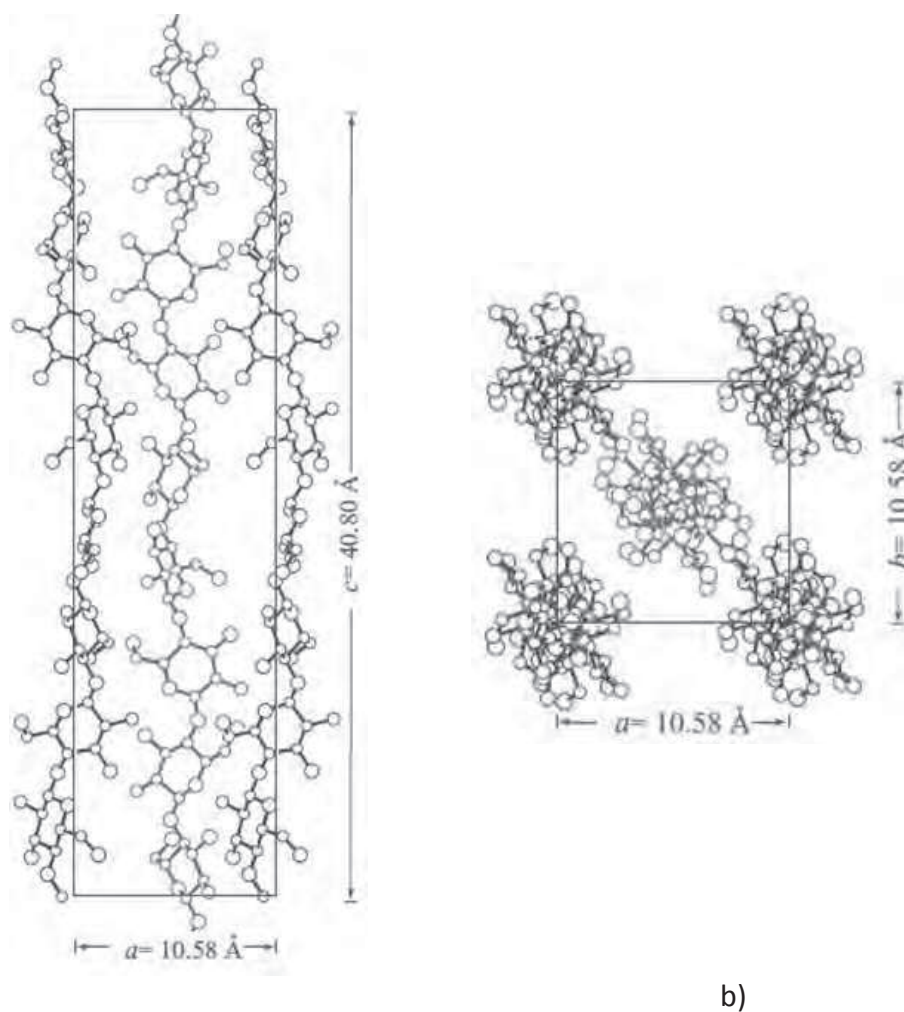


**Figure 2.5.** Plausible parallel packing structure of chitosan molecules in the Type II form projected (a) along the  $b$ -axis and (b) along the  $c$ -axis (Okuyama et al., 2000).

In a hydrated crystal, each chitosan chain takes an extended two-fold helix (a zigzag structure) (Fig. 2.6.). This helical symmetry is reinforced by the  $O_3 \cdots O_5$  hydrogen bond with a repeating period of  $10.34 \text{ \AA}$  (Fig. 2.7.)

Chitosan chains on  $c$ -axis are up chain, whereas, those in the unit cell are down chain. So, in this crystal, chitosan chains are packed in an anti-parallel fashion. Along  $b$ -axis, up chain and down chain make hydrogen bonds and form a sheet like structure. These sheets are stacked along  $a$ -axis (Fig. 2.6.a). Water molecules are present between these sheets and stabilize the crystal structure (Okuyama et al., 1999). Hydrated polymorph is the most abundant in chitosan samples. Commercially available chitosan samples have this crystal although their crystallinity is different.

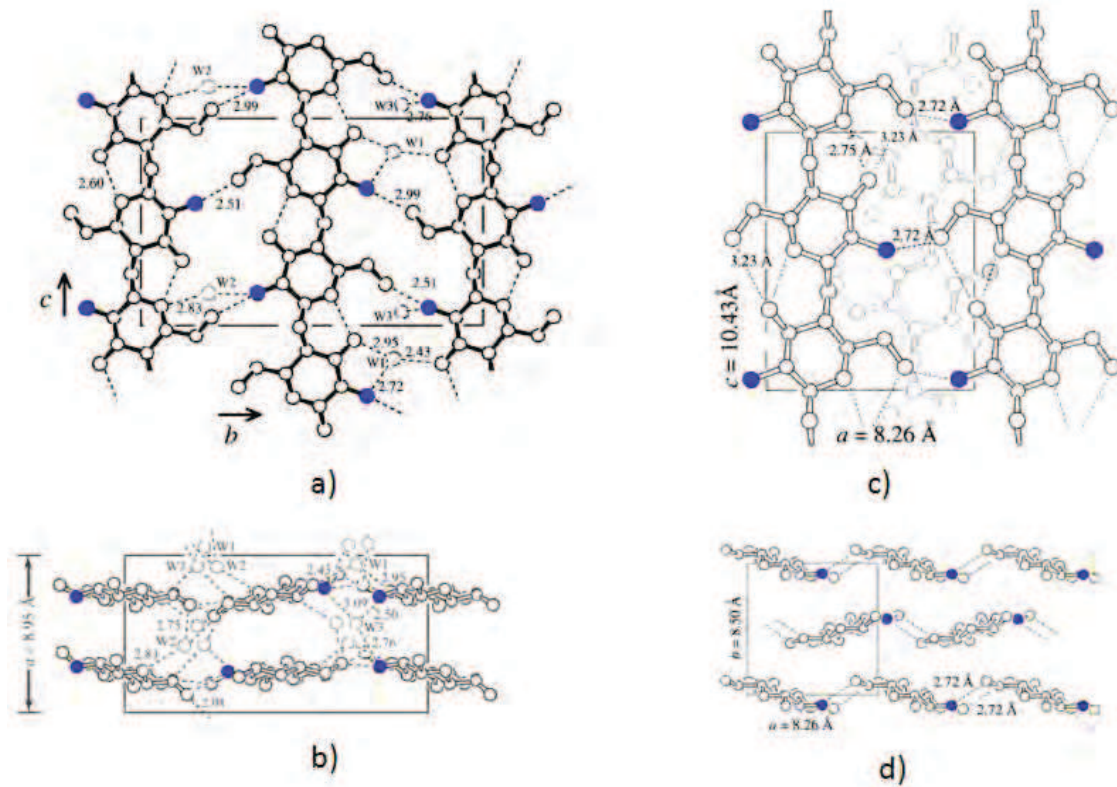


**Figure 2.6.** Molecular structure of hydrated (a, b) and anhydrous chitosan (c, d). Blue circles denote nitrogen atoms (Okuyama et al., 2000).

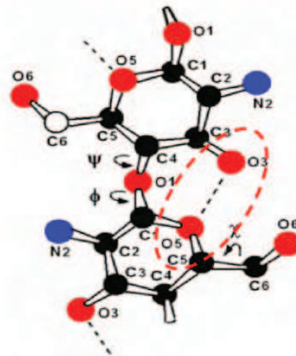


**Figure 2.7.** Bonding sites in chitosan crystal (Okuyama et al., 1997).

When dehydration occurs, to fill the space where two water molecules exist, there is a shift in the chain by breaking the hydrogen bonds between neighbouring polymer chains, shrinkage along  $b$  chain and enlargement along  $a$  (Fig. 2.8.). During this transformation, two independent neighbouring molecules along  $a$  in the hydrated form must become equivalent in the anhydrous form. The acid permeates into the specimen through water columns along the  $c$ -axis in hydrated chitosan unit cell. Then,

the interactions between the polymer chain and the acid force hydrogen bond network among polymer chains and water molecules to break, thereby facilitating the conformational change from the extended two-fold helix to the less-extended relaxed two-fold helix. Transformations from tendon to annealed polymorph occur irreversibly and involve a drastic change in the chain arrangement of chitosan (Ogawa, 1991; Muzzarelli, 1977). The anhydrous chitosan may be considered to be inert material.

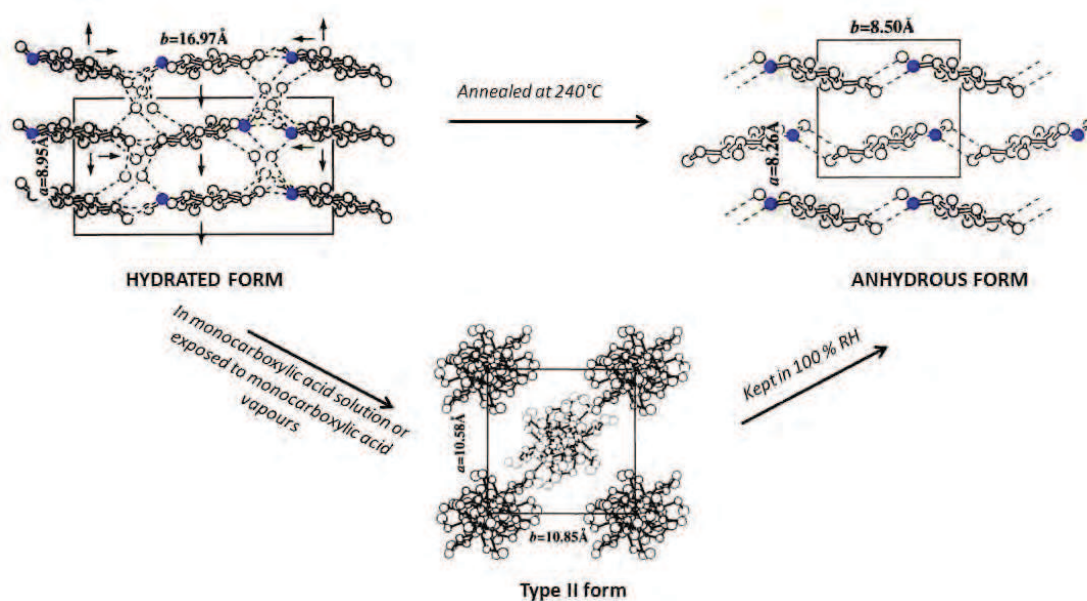


**Figure 2.8.** Schematic representation of dehydration of chitosan crystal (Okuyama et al., 2000).

Demarger-Andre and Domard (1994) reported that anhydrous (annealed) chitosan crystal can be obtained at room temperature from chitosan salts of several monocarboxylic acids (e.g. acetic). This is due to the removal of the acids accompanied by dehydration. Even if authors reported this phenomenon spontaneous, we could consider that a certain hydration level for this removal is required, and thus spontaneous is not really appropriate term to use. When stored at 100% RH, three months, one month and three weeks were required to produce the anhydrous chitosan polymorph from formic, acetic and propionic acid salts of chitosan, respectively. The water-removing action of only monocarboxylic acid is accelerated by relative humidity, hydrophobicity, pKa, solubility and boiling point of acid as speculated by Demarger-Andre and Domard (1994). Even that the water-removing

action of monocarboxylic acid has not been well defined yet, the most probable explanation is the conformational stability of chitosan molecule as described earlier.

Changes in structure properties are very important when film processing is envisaged. Then all above mentioned phenomena must be considered when producing and using chitosan systems. The knowledge of the structural differences among chitosan products is very important in determining the properties of these biopolymers and is essential for the structure/activity/analysis of packaging and biological systems.

#### **2.7.4. Chitosan films and their application**

Chitosan can form transparent films to enhance quality and extend storage life of food products (Aider et al., 2010). They might be formed as self-standing films, blended with other polymers, coated on both synthetic and bio-based polymers or used in multilayered packaging systems. Coating process is simple and allows accurate control of the film thickness on smooth, flat surfaces. Casting can be accomplished by controlled thickness spreading or by pouring. In solvent casting, which is the most common procedure, chitosan is firstly solubilised in a solvent medium. Then film forming solution is casted and dried either at ambient temperature (Caner et al., 1998; Chen and Hwa, 1996; Wiles et al., 2000), in oven (Butler et al., 1996) or in infrared drying systems (Srinivasa et al., 2004). Another possible processing method is hot melting. Still, there is no literature evident data describing extruded chitosan films. This is due to processing problems that are mainly attributed to reduced chitosan plastic flow properties, intrinsically difficult reproducibility, non controlled molecular architecture and spatial conformation of natural macromolecule (Mensitieri et al., 2011).

The functional properties of final film are dependent on a number of parameters including (Gontard and Guilbert, 1992):

- formulation (characteristics and concentration of the basic and secondary components, pH, molecular weight, degree of deacetylation, a suitable solvent (Park et al., 2002));
- film-forming conditions (type of surface upon which the film-forming solution is spread, drying conditions);
- conditions in which film is used (temperature, relative humidity);

- addition of plasticizers, dispersants and compatibilizers, emulsifiants, nanocomposites, etc. (Chillo et al., 2008; Fernández-Cervera et al., 2004; Suyatma et al., 2005).

Chitosan film itself can be used as antibacterial compound. Furthermore, it has been widely employed as a vehicle for incorporating functional ingredients such as: flavours and antioxidants (Martins et al., 2012; Moradi et al., 2012), colours, antimicrobials (Chafer et al., 2012; Abdollahi et al., 2012; Siripatrawan and Noipha, 2012), nutraceuticals (Mengato et al., 2012; Kester and Fennema, 1986), vitamins (Cho et al., 2012; Luo et al., 2012) and fatty acids (Srinivasa et al., 2007; Varags et al., 2006). Besides increasing product shelf life, these substances act as enhancers of the product nutritional value. There is evidence that chitosan antimicrobial films and coatings can increase storage life, retard weight loss, decline sensory quality and suppress the increase in activities of enzymes. For example, recently they were used to cover fresh fruits and vegetables (Talens et al., 2012; Perdones et al., 2012; Garrido Assis and Britto, 2011), in preservation of meat products (Vargas et al., 2011a; Petrou et al., 2012; Siripatrawan et al., 2012), fish (Gomez-Estaca et al., 2010; Fernandez Saiz et al., 2010) and cheese (Fajardo et al., 2010; Di Pierro et al., 2011; Moreira et al., 2011).

Potential implementation of chitosan in medicine is mainly due to its mechanical strength and rather slow biodegradation. It is very important material for biotech companies and it has been used as an excipient, for controlled drug release, in the preparation of tablets, beads, microspheres, gels, films, different carboxymethyl and succinyl derivatives used for tissue engineering and drug delivery (Bernkop-Schnürch and Dunhaupt, 2012). Due to its charged character, chitosan coatings are found to be ubiquitous in design of bio lubricated surfaces in artificial implants and frictional process in biological systems (Raviv et al., 2003). Moreover, chitosan based hydrogels can be formed from polyelectrolyte solutions involving a variety of molecular interactions. Polymer chain reorganisation in these systems might be obtained by solvent exchange. Gelation mechanism includes physico-chemical events and the molecular reorganisation that might result in special “onion like” membranes. These systems were recently used for tissue engineering (Ladet et al., 2008).

Features that packaging materials should display as far as mass transport properties are concerned, include control of food products respiration; supply of a selective barrier to gases and water vapour; capability of maintaining, as long as



possible, a modified atmosphere in the package headspace; reduction of the migration of lipids; and possible release of food additives such as flavour, colours, antioxidants and antimicrobial agents (Tharanathan, 2003).

Most of mechanical properties of chitosan films are comparable to those of cellulose or other polymers of medium strength (Jeon et al., 2002). They are flexible, durable, strong, tough and hard to break. Due to its good plasticization efficiency, large availability and low exudation, glycerol is the most used plasticizer for chitosan films. Plasticized chitosan has improved elasticity, so plasticizers allow overcoming chitosan films brittleness (Suyatma, et al., 2005; Ziani et al., 2008).

In fact, barrier properties of chitosan, mainly with reference to moisture, are inferior to existing packaging materials. Gas and aroma permeability are unpaired by the presence of adsorbed moisture. Chitosan is not very permeable in dry state, but likewise other hydrophilic polymers, the permeability increases significantly with an increase in water content.

With the respect to above mentioned problems, to improve physical, functional and barrier properties of chitosan films, blending it with both biodegradable and synthetic materials has been proposed. Moreover, chitosan blends could replace synthetic polymers in many applications. Thickness of plastic components can be reduced with attaining the same overall performances and also reducing the problems of disposability of traditional plastics (Farris et al., 2009; Vermeiren et al., 2003; Tharanathan, 2003). Recently, different blends were studied, such as starch-chitosan (Li et al., 2011), quinoa protein/chitosan (Abugoch et al., 2011), HDPE/chitosan (Mir et al., 2011) and ethylene methyl acrylate/ethylene vinyl acetate copolymer/chitosan (Massouda et al., 2011).

Under special conditions, chitosan can be coated on polyolefins. In these systems, polyolefin could add hydrophobicity to the packaging and thus decrease the impact of hydrophilic/water sensitive chitosan layer. Still, up to date there are few publications concerning surface modification or adhesion of chitosan on the synthetic polymers.

---

---

## **2.8. Efficacy, structure and distribution of active compound in the polymer matrix**

Active compounds can be incorporated directly into the packaging material or they can be put in patches, sachets etc. (Gutierrez et al., 2009b). The number of recently published articles and patents in the last 10 years suggests rapid expansion in interests of both scientific and large public audience. Intensive research in this field has been performed using both plastics and/or biopolymers.

### **2.8.1. Influence of antimicrobial compound on the structure of polymer/biopolymer matrices**

Although many studies have demonstrated the antimicrobial effect of essential oils and their active compounds against a broad spectrum of pathogenic bacteria in food, there are very few publications that discuss their incorporation as additives in polymeric plastic films (Ha et al., 2001; Suppakul et al., 2006, 2008; López et al., 2007a). When using conventional materials, antimicrobials can be put into the film by adding it directly during the extrusion process. Some examples are dehydroacetic acid sodium salt incorporated in high-density polyethylene (HDPE) film (Zema et al., 2010), nisin containing low-density polyethylene (LDPE) and LLDPE (Richard and Cooksey, 2012), mono and multilayer polyvinyl alcohol (PVAL) films containing lysozyme (Buonocore et al., 2005), polypropylene (PP) and polyethylene/ethylene vinyl alcohol copolymer (PE/EVAL) films containing different essential oils (Lopez et al., 2007a) etc.

Even that usually small amount of antimicrobial compound are incorporated, it is interesting how these substances can change pretty stable structure of plastic materials. Valderrama Solano et al. (2011) produced antimicrobial packaging materials by incorporating oregano and thyme essential oils into LDPE (via two different methods: ionizing treatment and directly by extrusion). No significant differences were observed in thicknesses of films with and without oil and they did not affect its mechanical properties. However, when essential oils were incorporated during extrusion, plasticizing effect was observed. Moreover, oxygen transmission rate and water vapour permeability were reduced. Similarly, Nostro et al. (2012) observed plasticizing effect of carvacrol and cinnamaldehyde (3.5% wt and 7% wt respectively) incorporated in polyethylene-co-vinylacetate (Nostro et al., 2012). These compounds reduced the intermolecular forces of polymer chains, and thus improved film's flexibility and extensibility. The analysis of the surface characteristics demonstrated that active compound lowered the contact angle values without causing any

remarkable variation in the surface roughness (Nostro et al., 2012). The same substances in polypropylene did not affect its thermal stability, but they decreased crystallinity, increased oxygen permeability and increased thermo-oxidative stability. Furthermore, an increase in the porosity can occur, thus reducing elastic modulus (Ramos et al., 2012).

In the peculiar cases of biopolymers or edible polymers, as already mentioned for chitosan, films are usually produced by solvent casting. Film drying is generally accompanied by the loss of volatiles. Process conditions influence the final film structure and performances. Furthermore, incorporating essential oils may significantly affect the structural organization of the film-forming substance and biopolymer network. Desobry and Debeaufort (2011) precisely classified their impact on the film physico-chemical properties. A cross-linking effect in the film can influence film microstructure, mechanical behaviour and barrier properties to oxygen and water vapour.

Because during drying, an “emulsion type” structure is formed, incorporation of essential oils generally decreases the transparency and gloss of bio-based polymer films. This phenomenon has been observed regardless the matrix nature or volatile compound (Desobry and Debeaufort, 2011). According to Du et al. (2009), colour of biopolymer films is directly influenced by type and concentration of added essential oil. In chitosan based films their incorporation generally increased yellowness or brownish colour of the plain film (Moradi et al., 2012). On the contrary, it was determined that rosemary essential oil improved the transparency of the chitosan films and it reduced films’ light transmission in UV more than 25% (Abdollahi et al., 2012). However, essential oils or their constituents generally increase the heterogeneity of polymer matrix.

Oil droplets create discontinuities that usually induce a loss of mechanical properties. Decrease of the tensile strength and Young (elastic) modulus was also observed (Pranoto et al., 2005a,b; Zivanovic et al., 2005). Bergamot oil (0.5%) added to chitosan films reduced tensile strength and elongation, two and three times, respectively (Sanchez Gonzalez et al., 2010a). On the contrary, Abdollahi et al. (2012), showed that rosemary essential oil in combination with nanoclays significantly improved the tensile strength and elongation of chitosan. In active chitosan and polyvinyl alcohol films tensile strength was improved with the addition of mint and pomegranate peel extract (Kanatt et al., 2012).



---

Changes in microstructure and mechanical properties indicate changes in the organisation of macromolecules that form film network. So, it also affects permeability of films to water vapour, oxygen, and/or aroma compounds. Decrease in water vapour permeability of generally hydrophilic biopolymers, can be due to the interactions of oil components with macromolecular chains. This can promote a decrease in the hydrophilic character of the film matrix. Citrus and lemon grass essential oils decreased water permeability of gelatin films (Tongnuanchan et al., 2012; Ahmad et al., 2012b). *Zataria multiflora* boiss extract decreased water vapour permeability of sodium caseinate film (Broumand et al., 2011). Citronella, coriander, tarragon and thyme reduced water vapour permeability of hake protein films (Pires et al., 2013). Atarés et al. (2010) showed that the addition of small proportions of ginger and cinnamon essential oils resulted in a reduction in water vapour barrier properties of soy protein isolate films. Contrarily, the addition of bergamot oil increased the water vapour permeability of gelatine films (Ahmad et al., 2012b). Rojas-Grau et al. (2007a) did not show any change in the oxygen permeability of alginate-apple puree film when oregano, carvacrol, lemongrass oil, citral, cinnamon oil, or cinnamaldehyde were added in a range of 0.1% to 0.5%. It was attributed to the low content of encapsulated volatile compounds that did not disturb the network structure.

From above mentioned examples on active antimicrobial compounds, gas transfers through films are influenced by several other parameters. Thus in the next subsection, parameters having a great impact on film gas permeability will be described.

### **2.8.2. Parameters influencing gas transfers through biopolymer films**

#### **Influence of film structure and film forming components**

The design and the optimization of the composition of biopolymer film are very important especially for controlling their barrier and mechanical properties. There are several variables that affect permeation and diffusion of molecules through polymers. The permeability coefficient is not only a function of chemical structure; it also depends on many physical factors such as density, crystallinity, orientation, cross-linking, plasticizers, moisture sensitivity and temperature. In the Fig. 2.9., O<sub>2</sub>, CO<sub>2</sub> and water vapour permeabilities of petrochemical-based plastics (referred to as common polymeric packaging materials) are compared to those of selected biopolymers.

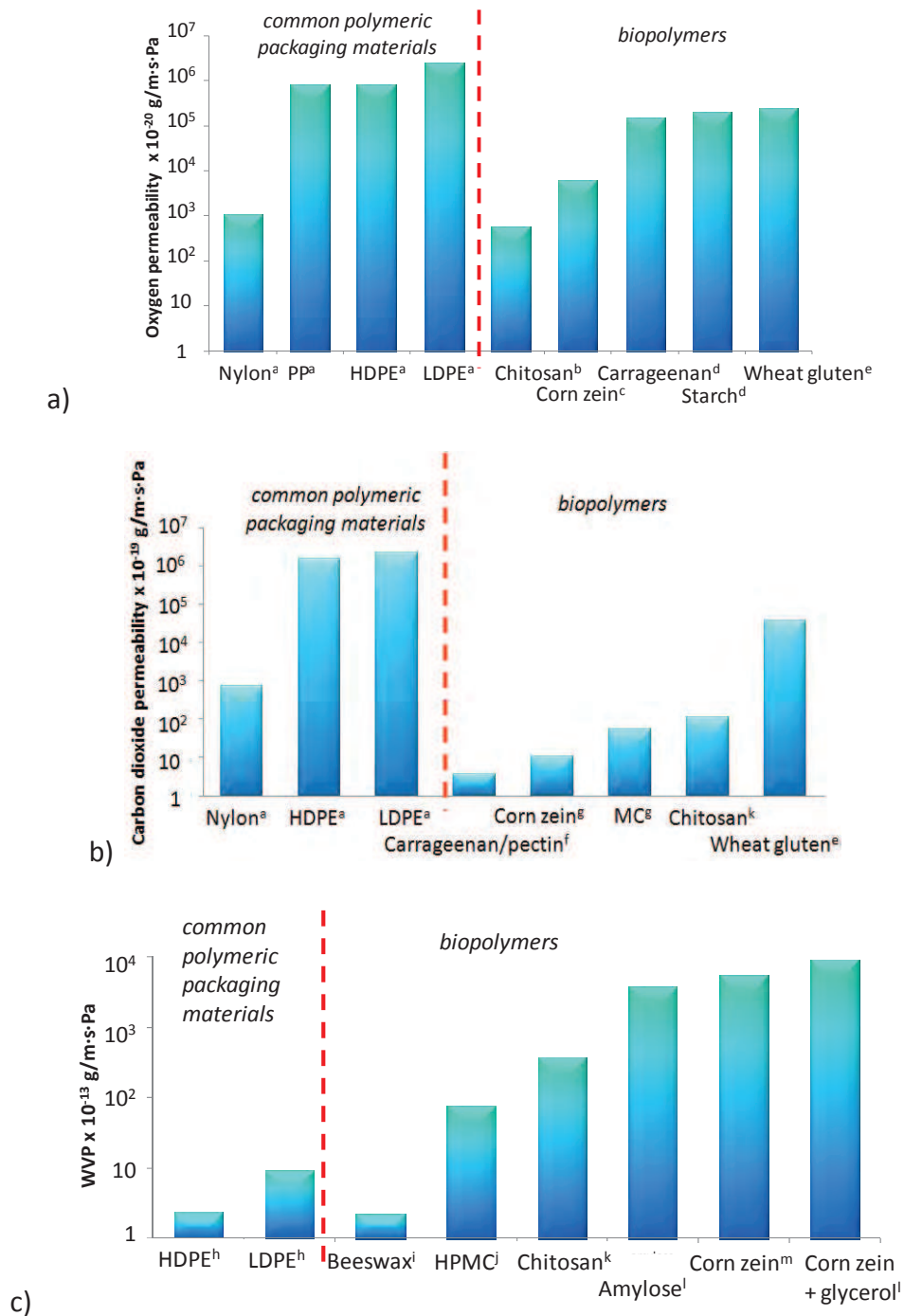


**Figure 2.9.** Oxygen (a), carbon dioxide (b) and water vapour (c) permeability for several biopolymers and synthetic polymers as evaluated at 25°C and in dry environment (for PO<sub>2</sub> and PCO<sub>2</sub>).

<sup>a</sup>Galić et al., 2009; <sup>b</sup>Park et al., 2002; <sup>c</sup>Gennadios et al., 1993; <sup>d</sup>Ribeiro et al., 2007; <sup>e</sup>Mujica Paz and Gontard, 1997; <sup>f</sup>Castelló et al., 2010; <sup>g</sup>MC (methylcellulose) Park and Chinan, 2012; <sup>k</sup>Wong et al., 1992; <sup>l</sup>Gennadios et al., 1994; <sup>m</sup>Ghanbarzadeh et al., 2007.

Another important parameter is chain packing. Simple linear polymer chains, such as in high-density polyethylene, pack tightly, thereby lowering film permeability.

---

Polymer chains with bulky side groups pack poorly, resulting in increased permeabilities (Ashley, 1985). Thus, as the conditions at which the analysis is carried out affect the results, film properties should be compared at, as much as possible identical testing conditions.

Due to their hydrophilic nature, polysaccharide films are generally rather poor water vapour barriers. However, they are less permeable to water vapour than most protein films (Fig. 2.9.c). Pure lipid films have extremely low WVP. Differences in the nature, the structure and the film processing conditions were thought to be responsible for changes in oxygen permeability (Maté and Krochta, 1996). Changes in solvent polarity may change structure and final film properties. Caner et al. (1998) studied the effects of different types of acids (acetic, formic, lactic, propionic), their concentrations, plasticizer concentrations, and storage time (up to 9 weeks) on water vapour and oxygen permeability of solution-cast chitosan films. Among the acids used for preparing chitosan solutions, chitosan films prepared with acetic and formic acid showed the lowest and highest water vapour permeability,  $9.49 \times 10^{-11}$  g/m·s·Pa and  $12.1 \times 10^{-11}$  g/m·s·Pa, respectively. Moreover, the oxygen permeability was the lowest when lactic acid was used in film preparation ( $7.41 \times 10^{-16}$  g/m·s·Pa), while the films prepared with formic acid had the highest oxygen permeability ( $22.8 \times 10^{-16}$  g/m·s·Pa). Chitosan films prepared with acetic acid showed the second lowest oxygen permeability ( $28.6 \times 10^{-16}$  g/m·s·Pa). In the work of Park et al. (2002), water vapour permeability in chitosan films ranged from 0.3 to  $0.7 \times 10^{-9}$  g/m·s·Pa and oxygen permeability from 0.47 to  $9.72 \times 10^{-21}$  g/m·s·Pa. Differences were attributed to molecular weight and type of organic acid solvent used. For chitosan films prepared with aqueous formic acid and different lipids, Wong et al. (1992) determined oxygen transmission of  $1.84 \times 10^{-12}$  g/m<sup>2</sup>·s·Pa, while Muzarrelli et al. (1974) have reported an oxygen permeability coefficient of  $1.27 \times 10^{-17}$  g/m·s·Pa.

In general, the incorporation of plasticizers in polymers has a relatively complex influence on permeability (Stannett, 1968). The presence of plasticizer in the film formulation decreases the intermolecular forces and increases both free space and chain mobility, thus modifying the stiffness and barrier properties (i.e. Fig. 2.9., corn zein). Plasticization of matrix leads to widening of bonds and then gas permeability normally increases with the plasticizer content (Arvanitoyannis et al., 1998). By inserting between the macromolecular chains, these additives also lower the glass transition temperature of a given polymer. By modifying the local segmental motions they have an indirect effect on the transport parameters. These plasticizing molecules

---

also possess their own diffusion coefficient that depends on their physical state (solid or liquid). Butler et al. (1996) found that glycerol-plasticized chitosan films (glycerin as plasticizer, 0.25 mL/g and 0.50 mL/g chitosan) had extremely low oxygen permeability ( $7.71 \times 10^{-18}$  g/m·s·Pa) at 0% relative humidity. Increasing the plasticizer content increased the oxygen permeability.

Incorporation of fat alters the barrier efficiency. It is attributed to the length of lipid carbon chain and to oxygen solubility in fats (Kester and Fennema, 1986). However, the effect of fat incorporation strongly depends on the film structure (emulsions, micro/nano-emulsion, multilayer...), on the physical state of fat (solid fat content), on the fat chain length, on the saturation of fatty acids, on the hydrogenation degree of oils, on the crystalline form of the fats, etc. So the real impact of fat incorporation in biopolymer matrices remains difficult to interpret (Morillon et al., 2002).

The glass transition temperature of the film is also important parameter to take into account. Depending upon processing conditions, crystallinity can vary even for a particular polymer. Above glass transition temperature, polymers exist in a rubbery or plastic amorphous state where chain mobility lessens barrier properties. Macromolecular fragments are more mobile and there is an appreciable “free volume” between them. At temperatures below the glass transition temperature, polymers exist in a “glassy” form. Crystalline polymers are characterized by a high degree of molecular mass, which provides them impermeability. So, diffusion can only occur in amorphous domains or through structural imperfections (Weinkauff and Paul, 1990). The crystalline zones act as excluded volumes for the sorption process and are impermeable barriers for the diffusion process. On one hand, they increase the effective path length of diffusion, and, on the other hand, they seem to reduce the polymer chains mobility in the amorphous phase (Klopfer and Flaconnèche, 2001). Therefore, the permeability of films below their glass transition tends to be extremely low.

The film thickness also affects transfers in edible films. In dry conditions it is assumable that transfer coefficients will linearly decrease when the thickness increases. On the contrary, thickness can have inverse impact in humid environment, leading to a permeability increase. This is probably due to a swelling process of the films which is not proportional of the initial thickness (Debeaufort et al., 1993; Cuq et al., 1996).

### Influence of the diffusing molecule properties

Molecular size and shape of the transfer molecule affect diffusivity and solubility. Small molecules generally diffuse faster than longer ones. Polar molecules diffuse faster than non polar molecules, especially through polar films. Solubility of gases can influence the permeability in the moist conditions. The solubility of the permeant depends in large part on its compatibility with the polymer. Generally, more easily condensed gases are more soluble in polymer. For example CO<sub>2</sub> is more condensable than O<sub>2</sub> and N<sub>2</sub> and it has a much higher solubility in water ( $7.5 \times 10^{-4} \text{ cm}^3_{\text{STP of CO}_2} / \text{g}_{\text{water}} \cdot \text{Pa}$ ) than O<sub>2</sub> ( $2.8 \times 10^{-7}$ ) and N<sub>2</sub> ( $1.45 \times 10^{-7}$ ). The solubility and diffusivity of O<sub>2</sub> ( $2.42 \times 10^{-5} \text{ cm}^2/\text{s}$ ) are larger than N<sub>2</sub> ( $2 \times 10^{-5} \text{ cm}^2/\text{s}$ ). Then the permeability of gases in polymer systems usually follows order CO<sub>2</sub> > O<sub>2</sub> > N<sub>2</sub> (Salamone, 1996). Properties of diffusing molecule can also influence the permselectivity of films and membranes. Permselectivity of CO<sub>2</sub> to O<sub>2</sub> is described by the Eq. 2.1.:

$$\alpha = \frac{PCO_2}{PO_2} \quad (\text{Eq. 2.1.})$$

From the application point of view, in a preservation of fresh products with high water content, low PO<sub>2</sub> and high PCO<sub>2</sub> inhibits growth of aerobic microorganisms, thus increasing the product shelf life. The degree to which atmospheric modification takes place in the packages depends on the film permeability, on the product respiration and on the influence of temperature on both of these processes (Beaudry et al., 1999; Cameron et al., 1994; Gennadios et al., 1993). Then the knowledge of permselectivity helps in design suitable packaging systems for high respiration products.

### External parameters

Temperature and humidity parameters are of crucial importance for food quality preservation, especially in real life situations, like in food market or in households for a long-term use.

Barrer (1937) was the first one who showed that the diffusion of small-size molecules in rubbery polymers is a thermally activated process. Temperature affects kinetic and thermodynamic phenomena, particularly sorption and diffusion. The thermal effects on solubility and diffusion show opposite trends. Generally, for gas adsorption, solubility decreases with increasing temperature. It is due to the lower condensability of the penetrant at higher temperatures. On the contrary, the effect of temperature on the diffusion is always positive (Rogers, 1985). When no structure change occurs in the temperature range considered, for all three physical quantities P,

S, and D, the temperature dependence can be described by a Van't Hoff–Arrhenius equation:

$$S = S_0 \cdot \exp\left(-\frac{\Delta H_S}{R \cdot T}\right) \text{ (Eq. 2.2.)}$$

$$D = D_0 \cdot \exp\left(-\frac{E_D}{R \cdot T}\right) \text{ (Eq. 2.3.)}$$

$$P = P_0 \cdot \exp\left(-\frac{E_P}{R \cdot T}\right) \text{ (Eq. 2.4.)}$$

where  $S_0$  is a constant and  $\Delta H_S$  is the partial molar enthalpy of sorption,  $D_0$  and  $P_0$  are pre-exponential factors and  $E_D$  and  $E_P$  are the activation energy of diffusion and permeation. Energy parameters depend on the morphology of the polymer matrix, crystallinity, phase transitions etc. (Meares, 1954). Physically, the activation energy represents the energy level that a molecule should reach to make a jump between one position and another one. It is always a positive quantity.

Liu (2008) measured the permeabilities of  $N_2$ , He,  $H_2$  and  $CO_2$  in water-swollen chitosan membranes at temperatures from 23°C to 60°C. The gas permeability was shown to increase with an increase in temperature. These results are similar to those obtained with dry chitosan membranes (El-Azzami and Grulke, 2007). Accordingly, the activation energy of permeation was lower for the water-swollen chitosan membrane than for dry chitosan.

As previously mentioned, bio-based polymers have impressive gas barrier properties in dry conditions (Fig. 2.9.). It is noteworthy that when relative humidity increases, gas permeability increases too and, then, better performance is given by plastic materials (Fig. 2.10.). When relative humidity increased from 0% to 96%, permeability of oxygen increased 3.5 and 28.3 times, respectively (Despond et al., 2001). Oxygen permeability in starch films was increased by 6.5 times and 48.1 times when the relative humidity increased from 60% to 80% and from 60% to 90%, respectively (Gaudin et al., 2000). Moreover, in wheat gluten films oxygen and carbon dioxide permeabilities were increased by 25 and 632 times when relative humidity increased from 0% to 100% (Mujica-Paz and Gontard, 1997) etc.

Moisture transport mechanism through a composite film depends upon the material and environmental conditions. Composition of film forming materials (hydrophilic and hydrophobic character), temperature and relative humidity of the environment influence water vapour permeability of the biopolymer edible films

(Ayranci and Tunc, 2003; Anker et al., 2002). Consequently, the water vapour permeability is the most extensively studied property of biopolymer and edible films. Water acts as a solvent and causes texture degradation, chemical and enzymatic reactions. Water activity of foodstuff is also an important parameter in relation with the product shelf-life. In low-moisture foods, low levels of water activity must be maintained to minimize the deteriorative chemical and enzymatic reactions and to prevent the texture degradation.

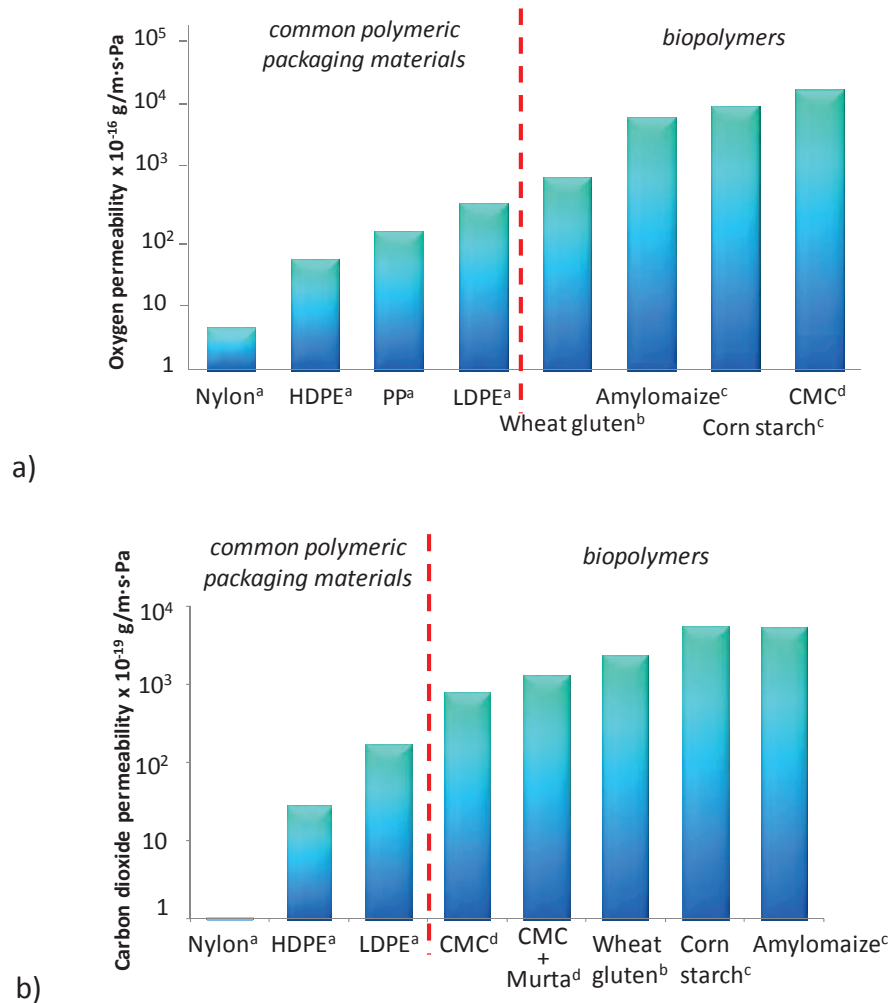


**Figure 2.10.** Oxygen (a) and carbon dioxide (b) permeability for several biopolymers and synthetic polymers as evaluated at 25°C and in humid environment.

<sup>a</sup>Galić et al., 2009; <sup>b</sup>Mujica Paz and Gontard, 1997; <sup>c</sup>Garcia et al., 2000a; <sup>d</sup> CMC (carboxymethyl cellulose) Bifani et al., 2007.

Changes in barrier properties indicate changes in a matrix structure. During processing and storage, solvent evaporation and matrix formation occur. Then, the active volatile compound is unavoidably lost. Thus it is very important to find a suitable



---

---

polymer system for incorporation and preservation of active compound if target is the antimicrobial activity of produced films.

### **2.8.3. Influence of polymer matrix on the retention and antimicrobial activity of incorporated compound**

At the different stages of processing, active packaging may require some level of adaptation. When materials are aimed to be used as antimicrobial films, it is very important to check the quantity of active compound and its antimicrobial efficiency. The effectiveness of antimicrobial films is determined by the release rate of the antimicrobial compounds, either directly to food or via air. The retention of active volatile by bio-polymer based layer during oven drying is affected by the nature of the matrix, the volatile concentration and the experimental conditions (e.g. drying rate, sample thickness, humidity) (Cha et al., 2003; Cagri et al., 2004; Rico-Pena and Torres, 1991). Because most of the reported data give the initial amount of the volatile active substance added in the antimicrobial film formulation and not the real final value, it is very difficult to compare literature results. Very few reports gave the real amounts of active compound in obtained films after film making processes. First of all, some examples of synthetic polymer systems will be given.

Ha et al. (2001) studied multilayered co-extruded and solution-coated polyethylene films with grapefruit seed extract. The results showed that co-extruded films had lower antimicrobial activity than the coated ones. As extrusion was performed at 160 – 190°C this was mainly due to low thermal stability of extract used (120°C). In the coated films, polyamide was used as a binder. This did not require heating. So, higher antimicrobial retention was obtained. High temperatures and shearing associated with the extrusion process can deteriorate the antimicrobial compounds. Then lower efficiency will be obtained. An alternative is to apply them as a coating. A thin layer of bacteriocin solution onto polyethylene/oriented polyamide film had good inhibitory effectiveness against *Listeria monocytogenes* on hamburger meat (Mauriello et al., 2004). Good efficiency was also found in solvent casted Saran® F-310 resin (a copolymer of vinylidene chloride) and poly(vinyl alcohol) (PVAL) with nisin, lactoferrin, sodium diacetate, sorbic acid or potassium sorbate (Limjaroen et al., 2003; Buonocore et al., 2003).

In bio-based polymer systems, retention of aroma compounds can be caused either by molecular interaction with specific molecules or by an increase in viscosity of the matrix (Guichard, 2002). According to Seuvre et al. (2006), polysaccharides



---

influence the volatility of the aroma compounds molecules and their partitioning between different phases mainly by two mechanisms. The first one, diffusion decrease, is predicted by the Stokes – Einstein equation stating that diffusion is inversely proportional to local viscosity (Baines and Morris, 1987; Wilke and Chang, 1955). The second mechanism involves specific molecular interactions of aroma compounds with macromolecule due to adsorption, entrapment in microregions, complexation, encapsulation, hydrogen bonding, hydrophobic interactions, etc. (Godshall, 1997; Kinsella, 1989). Sanchez Gonzales et al. (2011a) showed that limonene loss during drying ranged from 39 to 99% when added from 0.5 to 3% (w/w) in chitosan films. Generally, when loss during drying is greater, the release in the vapour phase is faster.

Drying methods, conditions and matrix formulation (e.g. polymer concentration, suitable solvent system, addition of plasticizers, dispersants, emulsifiers, etc.) have to be set up to engineer films, to monitor the retention and thus the release of the active compound (Park et al., 2002, Chillo et al., 2008; Suyatma, et al., 2005). The choice of the solvent in the preparation of a film forming solution is of key importance because it affects the solubility, dispersion of hydrophobic volatile molecules, as well as the physicochemical properties of the final products.

Changes in polymer concentration or mixing polymers may meet above mentioned requirements. Arabic gum (AG) is a biocompatible and biodegradable polymer with more interaction sites and negative charges for interaction with polycationic polymers such as chitosan (Wareing, 1999). Because of its unique properties (e.g. emulsification, acid stability, low viscosity at high concentrations, etc.), it is used in many food applications (in beverages, emulsions, flavour encapsulation, as an agent that protects from oxidation and volatilization). The recovery and the oxidation stability of orange oil encapsulated in AG has been reported (Qi and Xu, 1999). Up to date, not a lot of work has been done to understand the aroma compound retention capacity of the chitosan blends with AG. Ionic and non-ionic surfactants, have been studied in different film productions (Bravin et al., 2004; Morillon et al., 2002; Rodríguez et al., 2006; Villalobos et al., 2006; Andreuccetti et al., 2011). Functional film properties can also be improved by adding emulsifiers that interact simultaneously with polar and hydrophobic sites in the casting matrix (di Gioia and Guilbert, 1999). Another example is incorporation of nanocomposites that can potentially be used to control the release of antimicrobial agents from film materials (Tunc and Duman, 2010). Moreover, reinforcement of the polymer matrix with layered

silicates can improve functional film properties (Park et al., 2004a; Sothornwit et al., 2009; Tunc et al., 2007).

In summary, a hot topic in food and pharmaceutical industry concern the efficiency of the incorporation of active compounds that provides better functionalities and increases product shelf-life. Advances in the development of new bio-based materials and active packaging methods have brought out higher quality materials with enhanced performance and good price/quality ratio. Natural and bio-sourced attributes, associated together with good performance *in vivo*, paved the way for essential oils and chitosan to the first place on the list of “new” active food packaging materials. In design of “the best material”, essential oils could bring the antimicrobial efficiency. However, this effect will be maintained only if antimicrobial is well retained and protected during processing. Aiming to this goal, chitosan can be used as film forming polymer. Due to its biocompatibility, it can be applied in food contact packaging and bio-products. On one hand, its swelling property and hydrophilic character can be used in controlled releasing systems. On the other hand, because of its sensitivity to water vapour, it can hardly be applied on industrial level. Coating chitosan on polyolefins can add some recyclable/biodegradable value to synthetic polymers, while polyolefins can improve the water vapour barrier properties. All together, essential oils, chitosan and its coating on basic plastic film seem to show one of the best potential systems for active bio-based packaging film.



*Chapter 3*  
*Materials and Methods*

---



Materials and Methods chapter is extracted from various publications in the thesis. Further details are amended and reorganized for easier reading.

### **3.1. Materials and reagents**

#### **3.1.1. Film forming materials**

Commercial grade chitosan (CS) (France Chitine, Marseille, France, powder 652, having a molecular mass of 165 kDa, viscosity 43 cps, food grade, degree of deacetylation of >85%) was used as main film forming polymer.

Arabic gum (AG) (Spraygum, CNI, France) was used as volatile „retentor“ and to constitute the blended biopolymer film matrix.

Anhydrous glycerol (Fluka, 98% purity, Fluka Chemical, Germany), Tween 20 (Sigma-Aldrich), lecithin (Sigma-Aldrich), nanoclays (montmorillonite, synthesis and characterization is detailed elsewhere (Reinholdt et al., 2005), polyethylene glycol (PEG 750, Aldrich Chemicals) and glycerol monostearate (Sigma-Aldrich) were used in order to improve aroma compound retention and mechanical properties.

Acetic acid (glacial 100%, Merck, Darmstadt, Germany) and pure ethanol (absolute, Sigma-Aldrich) were used as solvents in the preparation of the film forming solutions (FFS).

All the chemicals were used without further purification and freshly prepared solutions were used in all experiments.

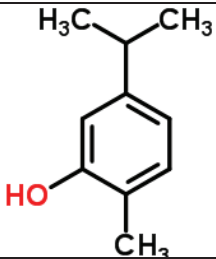
A commercial, low density polyethylene film (LDPE) (Wipak, Bousbecque, thickness of 45-50  $\mu\text{m}$ , density of 0.924  $\text{g}/\text{cm}^3$ , melting index 190°C/2.16 kg, 0.75 g/10 min) was used as a polyolefin material.

A prototype BIAKER 65 XX HFP Std (Polyester/Polyethylene/Ethylene vinyl-alcohol/ Polyethylene (PET/PE/EVAL/PE) was used for industrial trials and validation.

### 3.1.1.1. Antimicrobial compound

Carvacrol with a purity of about 97% (Fluka) was used as the antimicrobial volatile compound. Carvacrol characteristics are given in Table 3.1.

**Table 3.1.** Structure and physic-chemical characteristics of carvacrol

Molecular Formula	C <sub>10</sub> H <sub>14</sub> O
Average mass	150.22 Da
Boiling Point	234 – 236°C <sup>a</sup>
Structure formula	
Flash Point	107°C <sup>a</sup>
Specific Gravity	0.974-0.979 <sup>b</sup>
Appearance	Colourless to pale yellow liquid, pungent, spicy odour <sup>b</sup>
Solubility	In water: insoluble soluble in ethanol, diethyl ether, carbon tetrachloride, acetone <sup>c</sup>
log P <sub>o/w</sub> <sup>e</sup>	3.64 <sup>d</sup>

<sup>a</sup> Oxford University Chemical Safety Data

<sup>b</sup> Food and Agriculture Organization of the United Nations

<sup>c</sup> Lide, 1998

<sup>d</sup> Griffin et al., 1999

<sup>e</sup> logP is the logarithm of the ratio of concentrations of the un-ionized solute in the solvents. The log P value is also known as a measure of lipophilicity.

### 3.1.1.2. Other compounds

Different salts used to control water activity with aqueous saturated salt solutions are listed in the Table 3.2. All the salts were provided by Sigma Aldrich (France).

For a laser light scattering measurements 0.1 M sodium hydroxide (NaOH, Sigma Aldrich, France) and 10% (v/v) hydrochloric acid (HCl, Sigma Aldrich, France) were used.

n-hexane (Chromasolv, purity of >97%, Sigma-Aldrich) was used as the extraction solvent.

**Table 3.2.** Saturated salt solutions used to control water activity (Bell and Labuza, 2000).

Salt	Chemical formula	Water activity of the saturated salt solution (at 20°C)
Lithium chloride	LiCl	0.113
Potassium acetate	CH <sub>3</sub> COOK	0.231
Magnesium chloride	MgCl <sub>2</sub>	0.331
Potassium carbonate	K <sub>2</sub> CO <sub>3</sub>	0.432
Magnesium nitrate	Mg(NO <sub>3</sub> ) <sub>2</sub>	0.544
Sodium bromide	NaBr	0.591
Tin (II) chloride	SnCl <sub>2</sub>	0.725
Sodium chloride	NaCl	0.75
Potassium chloride	KCl	0.851
Barium chloride	BaCl	0.900
Potassium dichromate	K <sub>2</sub> Cr <sub>2</sub> O <sub>7</sub>	0.980

For microbiology experiments different culture media were used as given in the Table 3.3.

**Table 3.3.** Culture media used in microbiology experiments.

Culture Media	State: Microorganism
<b>Luria Broth Agar</b> (LB, Sigma Aldrich)	Liquid and solid: <i>Bacillus subtilis</i> , <i>Escherichia coli</i> and <i>Salmonella Enteritidis</i>
<b>Columbia Agar</b> (GC, Biokar Diagnostic)	Solid: <i>Bacillus subtilis</i>
<b>Brain Heart Infusion Broth</b> (BHI Broth, Sigma Aldrich)	Solid: <i>Listeria innocua</i>
<b>Brain Heart Infusion Agar</b> (BHI Agar, Sigma Aldrich)	Liquid: <i>Listeria innocua</i>
<b>Potato Dextrose Agar</b> (PDA, Sigma Aldrich)	Solid: <i>Penicillium camemberti</i>
<b>Man Rogosa Sharpe</b> (MRS, Sigma Aldrich)	Liquid and solid: <i>Lactobacillus plantarum</i>



## 3.2. Film formation

In this work, more than 200 different combinations for obtaining chitosan based films and coatings were prepared. That's why principal steps in film formation will be described.

### 3.2.1. Self standing chitosan films

A chitosan solution was prepared by dissolving the chitosan powder in the 1% (v/v) aqueous acetic acid solvent, to obtain 1, 2 or 3% (w/v) film forming solutions. To achieve the complete dispersion of chitosan, the solution was stirred for 2 h at room temperature. To prepare aqueous hydroalcoholic acid media, ethanol was mixed in ratio ethanol:aqueous acetic acid 30:70.

In order to improve physico-chemical, functional and barrier properties of chitosan films, different compounds were added to film forming solutions (FFS). The codification of different film forming solutions and dry films used in all experiment is given in the Table 3.4.

Carvacrol (CVC) (from 0.01 to 3%, w/v) was dispersed in the film forming solution (FFS) and the mixture was homogenized at 24000 rpm for 10 minutes with an Ultra Turrax (T25 IKA).

Different amounts of glycerol (GLY) (up to 50% w/polymer dry matter (p.d.m.)) were added to the chitosan solution under stirring.

Polyethylene glycol (PEG) (up to 30% w/p.d.m.), lecithine (from 0.5 to 30% w/p.d.m.), Tween 20 (from 2.5 to 30% w/p.d.m.) and glycerol monostearate (up to 5% w/p.d.m.) were added in some film formulations after solubilisation of chitosan powder.

In order to study whether the addition of nanoclays (NC) has an impact on the aroma compound retention and on the release properties of dried films, CS/NC films were prepared. First, CS was dispersed in the 1% (v/v) acetic acid in aqueous solution, to obtain 1, 2, or 3% of chitosan (w/v) solutions. Meanwhile, an exact amount of NC powder (to obtain 10% w/w dry polymer) was dispersed into 30 mL of distilled water under magnetic stirring at 500 rpm for 2 h. In a second step, NC suspension was added to the film forming solution under mixing at 5000 rpm for 15 minutes. In the last step, carvacrol was added, and the mixture was homogenized for 10 minutes at 24000 rpm (rotation per minute) with an Ultra Turrax (T25 IKA). As nanoclays are aimed to induce

the brittleness of dry films, glycerol was added in order to improve the film mechanical properties. Actually, two different sequences, differing in order of addition of the NC were prepared. In the first sequence, named A, after dissolution of chitosan, glycerol was added (30, 40 or 50 w/dry polymer matter) and FFS was mixed next 15 minutes. Meanwhile, carvacrol was mixed with NC dispersion. For the second sequence, named B, glycerol was added to clay suspension under mixing for 10 minutes. Then, two suspensions were mixed together for 15 minutes at 5000 rpm. In the last step carvacrol was added to the mixture and following procedure was the same as the one used for all other films.

To achieve chitosan/arabic gum blends (CS/AG), AG was added in the FFS of CS (50% w/w) and mixed under magnetically stirring for 2 h. The next steps were the same as for other chitosan films.

After preparation, FFS were poured into a glass Petri dish. In order to obtain films, solvents were removed by drying in a ventilated climatic chamber (KBF 240 Binder, ODIL, France) at fixed temperatures ranging from 20°C to 100°C and RH ranging from 10 to 80%. After drying, the films were peeled off the surface and stored in a ventilated climatic chamber (KBF 240 Binder, ODIL, France) before measurements.

**Table 3.4.** Composition of film forming solutions/dry films and their abbreviations.

Abbreviation	Film composition
CSA	Chitosan solubilised in the aqueous acetic acid
CSACVC	Chitosan solubilised in the aqueous acetic acid and activated with carvacrol
CSAGLY	Chitosan solubilised in the aqueous acetic acid and plasticized with glycerol
CSAGLYCVC	Chitosan solubilised in the aqueous acetic acid and both activated with carvacrol and plasticized with glycerol
CSE	Chitosan solubilised in the hydroalcoholic acetic acid
CSECVC	Chitosan solubilised in the hydroalcoholic acetic acid and activated with carvacrol
CSEGLY	Chitosan solubilised in the hydroalcoholic acetic acid and plasticized with glycerol
CSEGLYCVC	Chitosan solubilised in the hydroalcoholic acetic acid and both activated with carvacrol and plasticized with glycerol
PE	Polyethylene
PECSE	Polyethylene coated with chitosan solubilised in the hydroalcoholic acetic acid
PECSECVC	Polyethylene coated with chitosan solubilised in the hydroalcoholic acetic acid and activated with carvacrol

Schematic presentation of preparation of chitosan based films is given in Fig. 3.1.

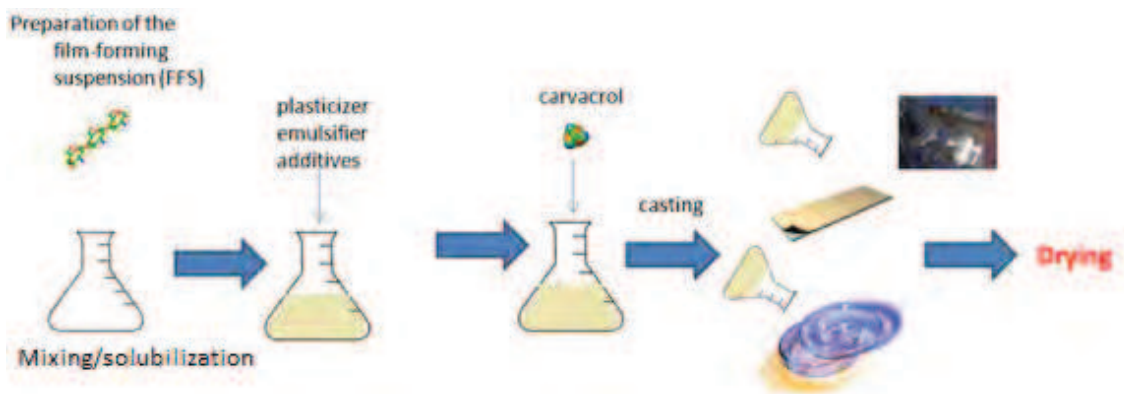


**Figure 3.1.** Chitosan based films preparation.

### 3.2.2. Chitosan coated polyethylene films

A hydroalcoholic acid chitosan solution was prepared as described in the section 3.2.1. Chitosan coated polyethylene films were fabricated in the Laboratory CNAM-PIMM Paris, France according to Sollogoub et al. (2009). The system design is given in the Fig. 3.2., and schema of produced films in the Fig. 3.3. The coating was carried out at room temperature, using a Nordson slot die (Chameleon™), appropriate to fluids of viscosity ranging between 0.5 and 2 Pa/s. The die is fed continuously by a gear pump, the flow rate of which is adjustable from 5 to 500 mL/min. A roll winding device creates movement of the support material at a speed ranging between 0.2 and 4 m/min. The deposit width is set to 100 mm and the die opening to 150 μm. Films were dried in a flow of a dry air at 50°C. After drying, they were stored in a ventilated climatic chamber (KBF 240 Binder, ODIL, France) before measurements.

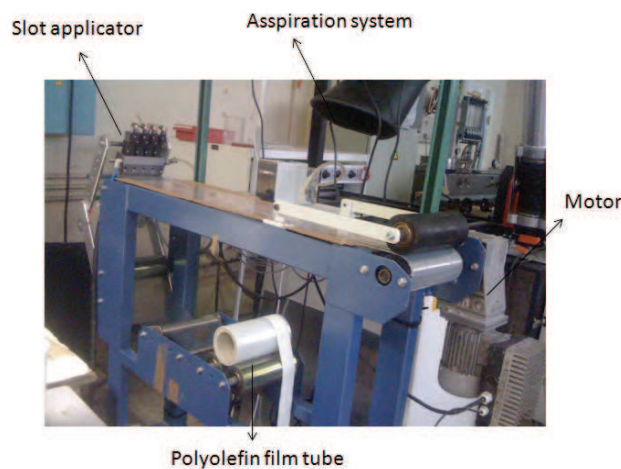


**Figure 3.2.** Coating system for obtaining chitosan coated polyolefin films.



**Figure 3.3.** Schema of (a) chitosan coated and (b) activated chitosan coated polyethylene.

For the industrial scale production, samples were prepared and dried in the Wipak, Gryspeert S.A.S., Bousbecque, France. These samples were used for industrial trials, packaging of real food products (Welience, Lactalis, Salaison Dijonaise and Chazal) and sensorial evaluation of these products. A hydroalcoholic acid chitosan solution was prepared as previously described. The prototype material named BIAKER 65 XX HFP was used as coating support material. Coating solutions were either cast on the BIAKER 65 XX HFP or activated BIAKER 65 XX HFP. Activated BIAKER 65 XX HFP corresponds to film obtained after extrusion of polymer compounds mixed with carvacrol. Two experimental designs were used (Fig. 3.4.).

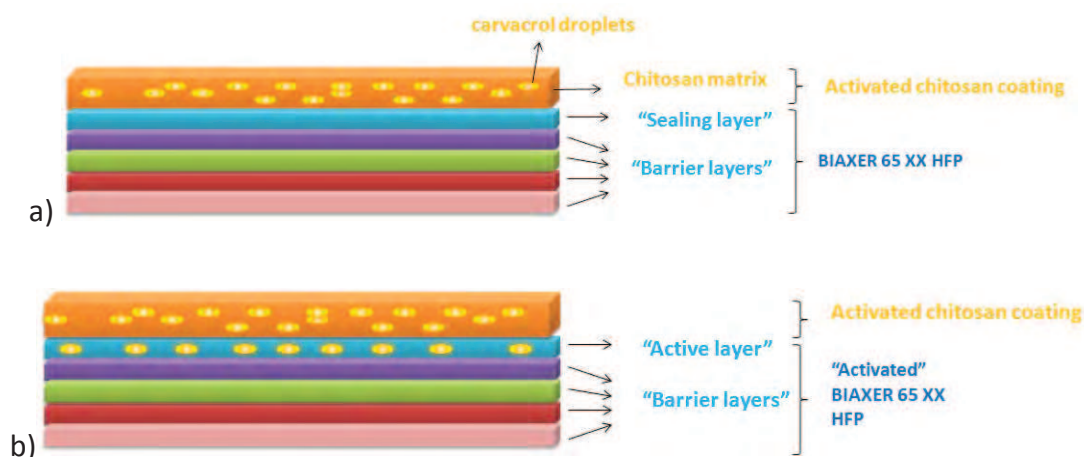


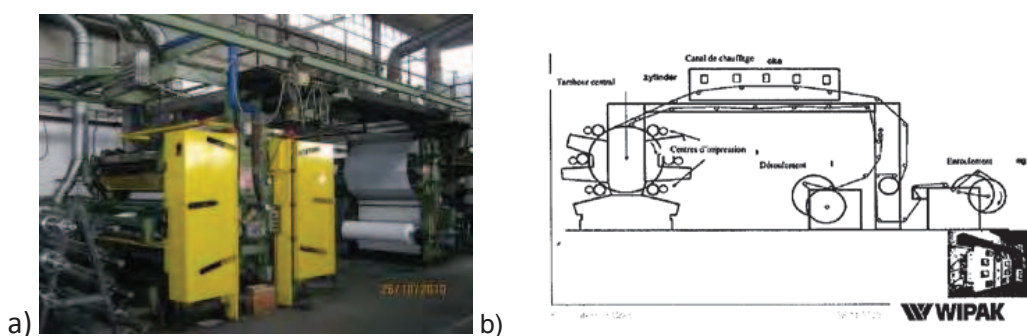
**Figure 3.4.** Schema of chitosan coatings on BIAKER 65 XX HFP.

In the first one (a), coating was applied on the reference material. In the second one (b), it was applied on the already modified material that had active compound (carvacrol and/or thymol) incorporated in its mass. The experimental design was made to apply 0.2 g of a coating per m<sup>2</sup> of film with dry mass based of 0.06% carvacrol and 1% chitosan (before drying). These modified materials were also produced in the Wipak factory by the extrusion process followed by flexography to apply the coating. The codification and possible variations of films is given in the Table 3.5.

**Table 3.5.** Composition and codification of multilayer packaging films.

Abbreviation	Film composition
<b>BIAXER 65 XX HFP AP8</b>	Carvacrol containing chitosan coating on the BIAXER 65 XX HFP AP1 (that contains 0.1% of thymol in synthetic polymer mass)
<b>BIAXER 65 XX HFP AP9</b>	Carvacrol containing chitosan coating on the BIAXER 65 XX HFP AP2 (that contains 1% of thymol in synthetic polymer mass)
<b>BIAXER 65 XX HFP AP10</b>	Carvacrol containing chitosan coating on the BIAXER 65 XX HFP AP3 (that contains 0.1% of carvacrol in synthetic polymer mass)
<b>BIAXER 65 XX HFP AP11</b>	Carvacrol containing chitosan coating on the BIAXER 65 XX HFP AP4 (that contains 1% of carvacrol in synthetic polymer mass)

Printing machine Carint, type Flexo 6 groups, was used to produce coated films (Fig. 3.5.). Following parameters were used: temperature of a tunnel: 70°C, width: 950 mm, speed: 100 m/min. After drying, all samples were packed in the aluminium foils and stored in the factory stock.

**Figure 3.5.** Flexoprinter Carint (a) Anonymous; b) Wipak, Bousbecque

### 3.3. Characterization of film forming solutions

#### 3.3.1. Rheological behaviour of film forming solutions

The rheological behaviour of film forming solution (FFS) was analysed at  $20 \pm 1^\circ\text{C}$  by means of a viscosimeter (HAAKE RotoVisco 1, Thermo Electron Corporation, Karlsruhe, Germany). Rheological curves were obtained after a stabilization time of 3 min. The shear stress  $\tau$  was measured as a function of shear rate  $\dot{\gamma}$  ( $\text{s}^{-1}$ ) from 0 to  $250 \text{ s}^{-1}$ . The power law model:

$$\tau = K \cdot \dot{\gamma}^n \quad (\text{Eq. 3.1.})$$

was applied to determine the consistency index ( $K$ , Pa/s) and the flow behaviour index ( $n$ , dimensionless).

### 3.3.2. Structure and dispersion of film forming solutions

The structure of the film forming solutions as well as that of resulting film was studied by laser light scattering. The instrument Malvern Mastersizer Hydro 2000 SM (Malvern Instruments Ltd, Worcestershire, UK) was used. It uses the principle of measuring an optical model, where the incident laser beam is diffracted by the sample (Fig. 3.6.). This technique is based on measuring the intensity of diffraction of an incident radiation by the particles present in the sample. A light beam penetrates circulating sample and comes to the particles which deflect light as they pass in front of the light beam (Fig. 3.6.a). Finally, the signal is detected (Fig. 3.6.). The light ray encountering a particle can be absorbed or transmitted. Because the particles are completely opaque at the temperature of analysis (20°C), the light does not penetrate. Particle size distribution of dispersed particles is actually a list of values or a mathematical function that defines the relative amount of particles present, sorted by their size. Particle size distribution is calculated by comparing a sample's scattering pattern with an appropriate optical model using a mathematical inversion process.

Two different models are used, the Fraunhofer approximation and Mie Theory. While Mie theory describes scattering in all directions in space related to meeting the obstacle, the Fraunhofer theory of diffraction of light is applied if particle size significantly exceeds the wavelength used (>1mm). The principle of Fraunhofer therefore applies to all steps to convert the angular profile in particle size, by avoiding the need to introduce the refractive index of the dispersed phase. The diffraction angle depends on both the particle size, shape and the wavelength of the incident light and is inversely proportional to the particle size. The particle diameter is thus determined on the assumption of spherical particles. The intensity of the diffracted radiation is a function of radius of the particle. The angle of diffraction is larger for smaller particles (Fig. 3.6.a). Analysis of the particles as a whole provides the distribution of their dimensions, with the number of particles of each size, by measuring an "equivalent diameter of diffraction". Moreover, this type of analysis provides a mathematical distribution of particle size at which an average diameter can be deduced. The size distribution is usually in the form of histograms, the relative proportion, expressed as frequency of different size classes of the population. The instrumentation used allows measurements from 0.1 to 2000 microns. In this distribution, two averages are determined: the surface-average diameter ( $d_{3,2}$ ) and volume mean diameter ( $d_{4,3}$ ):



$$d_{3,2} = \frac{\sum n_i d_i^3}{\sum n_i d_i^2} \quad (\text{Eq. 3.2.})$$

$$d_{4,3} = \frac{\sum n_i d_i^4}{\sum n_i d_i^3} \quad (\text{Eq. 3.3.})$$

where,  $n_i$  indicates the number of particles of diameter  $d_i$ .

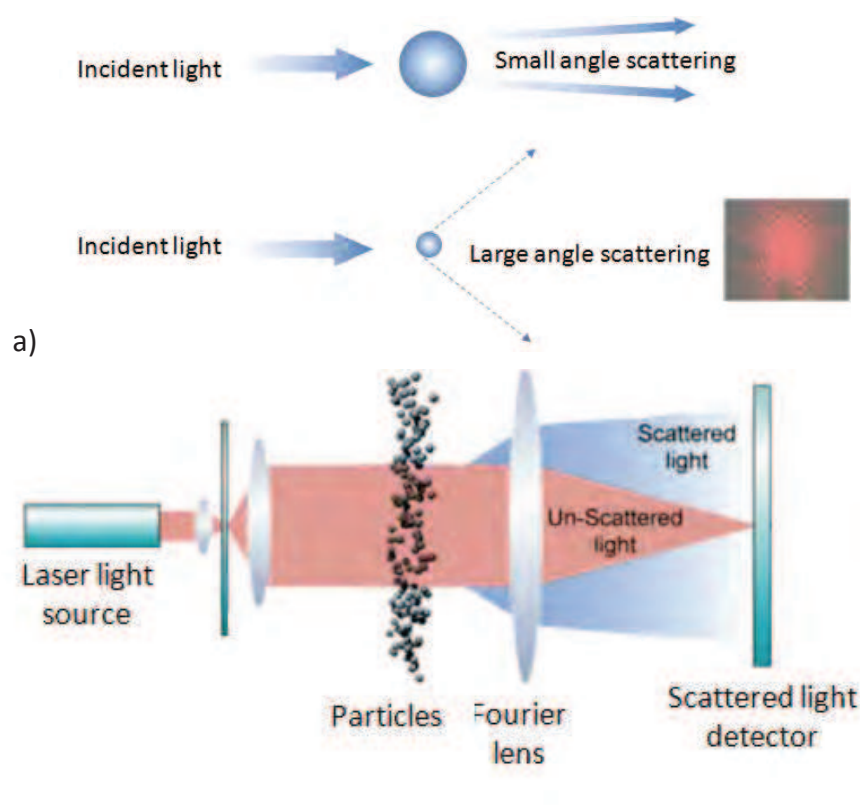


**Figure 3.6.** a) Diffraction of a laser beam by small and large particles and b) laser scattering measurement principle.

The average diameter  $d_{3,2}$  (Sauter's diameter) represents the fineness of the solution in terms of area ratio. It corresponds to the diameter of a sphere with the same volume to surface area ration as the particle. Equivalent volume/mass diameter,  $d_{4,3}$ , is a diameter of a sphere with the same volume (mass) as the particle.

To analyze the sample, few drops of film-forming solution were dispersed in the dispersion module containing appropriate solvent (aqueous acetic acid or hydroalcoholic acetic acid). Dispersion was stirred at 2020 rpm in order to dilute

sample and to allow the passage of liquid in the optical cell. To verify the particles distribution after film drying, samples were prepared by dispersing 1 g of dried film in 50 mL of appropriate solvent at room temperature with moderate magnetic stirring. To identify the incidence of particles aggregation (chitosan and/or carvacrol and/or glycerol), samples were also dispersed under moderate magnetic stirring in 50 mL of a 0.1% (w/w) Triton X-100 solution at room temperature according to Karbowski et al. (2007). Reproducibility was tested by carrying out nine measurements of each replicate.

### **3.4. Physico-chemical characterization of chitosan based films and coatings**

#### **3.4.1. Aroma compound retention and release**

##### 3.4.1.1. Aroma compound retention in biopolymer matrix

In order to follow the aroma compound release/retention, solvent extraction technique and a gas chromatography analysis were performed. N-hexane was used as the extraction solvent (due to high affinity of carvacrol for n-hexane). Pieces of dry film were put in the glass vial and a known amount of n-hexane was added at ratio 0.2:1.5 (m/v), followed by stirring till the entire aroma compound was extracted. The aroma compound extraction yield was taken into account for the final calculation. The extraction yield was measured by successive extractions till the sample was exhausted.

The aroma compound was quantified by injecting the extract into a gas chromatograph and calculated from an external calibration curve. For each sample three repetitions were performed.

##### 3.4.1.2. Measuring of the aroma compound in gas phase

In order to measure the carvacrol release from the film (solid phase) into a headspace (gas phase), a static headspace method was used. The film was put into a headspace vial (40 mL Supelco) and then sealed immediately with Mininert Valves (Supelco). Each measurement was carried out at the equilibrium and the time determined to reach equilibrium was 4 h at 25°C. After equilibration, a volume of 1 mL of headspace air was taken out using a gastight syringe (Hamilton, Switzerland) and injected in the gas chromatograph. Two headspace injections were made per vial. The amount of carvacrol released in the gas phase was calculated from the external calibration curve.



#### 3.4.1.3. Gas chromatography analysis

The volatile flavour compounds in the film extracts and in the headspace above the film were analyzed by a Shimadzu GC 14B gas chromatograph, equipped with a flame ionization detector (GC-FID) and 30 m length DB-Wax column (J&W) with 0.53 mm i.d. and 1.0  $\mu\text{m}$  film thickness and nitrogen as carrier gas (60 kPa). Hydrogen and air were used as ignition gases. The oven temperature programme was set at 210°C, isothermal. The injector and detector temperature were at 240°C, isotherm.

#### 3.4.1.4. Calculation of partition coefficient

The partition coefficient is defined as the mass concentration ratio of the molecule between two phases (gas phase above and in the film). After drying, the obtained antimicrobial film is a solid matrix. The partition coefficient studied in this work can be defined as follows:

$$K = \frac{C_g}{C_f} \quad (\text{Eq. 3.4.})$$

with  $C_g$ , concentration of the volatile compound in the gas phase ( $g_{\text{aroma}}/g_{\text{air}}$ ) above the  $C_f$ , concentration of the volatile compound in the film ( $g_{\text{aroma}}/g_{\text{film}}$ ).

#### 3.4.1.5. Determination of drying curves

Drying curves were obtained by plotting a graph of moisture ratio versus time. The moisture content at each time interval (once per hour) was calculated from the weight loss data and the dry solid weight of the sample, till no further weight loss was observed. Aroma compound concentration in solution/gel/film at a given time was determined as described in section 3.4.1.1.

#### 3.4.1.6. Release kinetics of carvacrol

In order to follow the carvacrol release, an extraction technique and a gas chromatography analysis were performed. Samples were conditioned at <2%, 75% and >96% RH and 4, 20 and 37°C for more than 60 days. At each sampling time, the dosage of the carvacrol residues was tested as described in 3.4.1.1. For each sample three repetitions were performed. To determine diffusion coefficient of carvacrol, Fick's second law was used which describes the change in the concentration of diffusing molecules in the films with respect to time and position. To be able to use Fick's second law, it was assumed that there is no chemical reaction between carvacrol and film matrix. Thus the mass transfer in the film takes place only by diffusion coefficient

of carvacrol in the film,  $D$ , considered as constant. A solution of Fick's second law is given by Crank (1975). Carvacrol apparent diffusivity was estimated by fitting Eq. 3.5. to the experimental kinetic data using a pre-estimation of  $D$  using Microsoft Excel.

$$\frac{M_t}{M_0} = \sum_{n=0}^{\infty} \frac{8}{(2n+1)^2\pi^2} \exp\left(-\frac{(2n+1)^2\pi^2}{4L^2}Dt\right) \quad (\text{Eq. 3.5.})$$

where  $t$  is the time (s),  $M_t$  the amount of carvacrol released (g/g) from the film at time  $t$  (s) and  $L$  the film thickness (mm). The equation was fit with  $n=6$ .

### 3.4.2. Structure properties of chitosan films and coatings

#### 3.4.2.1. Thickness measurement

Film thickness was measured with an electronic gauge (PosiTector 6000, DeFelsko Corporation, USA). The final values were reported as the mean of 5 measurements at 5 different locations of the film surface.

#### 3.4.2.2. Colour measurements

The colour of the film was determined using a colorimeter (Minolta, CM-3600d, Tokyo, Japan). Hunter  $L^*$ ,  $a^*$ , and  $b^*$  values were averaged from three readings across for each sample, and then the total colour difference ( $\Delta E$ ) was calculated according to Ghorpade et al. (1995).

#### 3.4.2.3. Film microstructure

The film microstructure was examined using Environmental Scanning Electron Microscopy (ESEM, Philips XL 30 ESEM, Japan).

ESEM allows the examination of practically any specimen under any gaseous conditions, unlike conventional SEM (Scanning Electron Microscopy) which operates in vacuum. Then as chitosan films had certain amount of water and aroma compounds, to avoid the evaporation of those, ESEM was used. Samples do not need to be desiccated and coated with gold-palladium, so their original characteristics may be preserved for further testing or manipulation.

An ESEM employs a scanned electron beam and electromagnetic lenses to focus and direct the beam on the specimen surface in an identical way as a conventional SEM. A very small focused electron spot (probe) is scanned in a raster form over a small specimen area. The beam electrons interact with the specimen surface layer and produce various signals (information) that are collected with appropriate detectors.

The output of these detectors modulates, via appropriate electronics, the screen of a monitor to form an image that corresponds to the small raster and information, pixel by pixel, emanating from the specimen surface.

A  $5 \times 10 \text{ mm}^2$  film was fixed on the support using a double side adhesive tape with an angle of  $90^\circ$  to the surface to allow the observation of the film cross section and film surface. The surface in contact with the glass support during drying will be referred to as the “support side” and the other surface in contact with the air during drying will be referred to as the “air side”. All the films were cut with a new razor blade to prevent as much as possible any morphological damage. The films were observed at different magnifications up to  $\times 15000$  for focusing and images were taken at magnification from  $\times 800$  to  $\times 2500$  with an intensity of 8 kV and absolute pressure of 230 Pa.

### 3.4.3. Mechanical properties

To determine mechanical film properties, universal test Machine (TA.XT plus model, Stable MicroSystems, Haslemere, England) was used according to ASTM standard method D882 (ASTM, 1992). Tensile strength (TS), film elastic modulus (EM) and elongation (E) properties were determined from stress–strain curves, estimated from force deformation data. Equilibrated film samples were mounted in the film extension-grips of the testing machine and stretched at a rate of 50 mm/min until breaking (Fig. 3.7.).

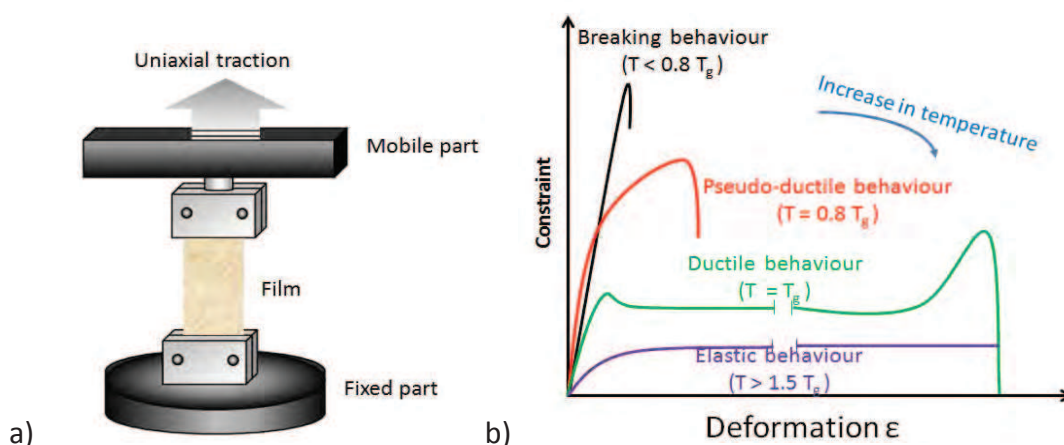


**Figure 3.7.** a) Schema of a module used for testing mechanical properties and b) evolution of constraint/deformation curves in function of polymer glass transition temperature ( $T_g$ ) (adapted from Gibson and Ashby, 1988).

At least eight replicates of each type of film formulation were tested. Samples were cut in a rectangular section of 1 cm wide and 10 cm long. Before testing, all samples were equilibrated for 7 days at <2, 30, 52 and 75% RH in a cabinet using adequate saturated salt solutions at 25°C.

#### **3.4.4. Thermal properties**

##### 3.4.4.1. Thermal gravimetric analysis

A thermal gravimetric analysis (TGA) was used to evaluate the thermal stability of the samples. TGA is a type of testing performed on samples that determines changes in weight in relation to a temperature program in a controlled atmosphere. Analysis is carried out by raising the temperature of the sample gradually and plotting weight (percentage) against temperature.

Thermogravimetric measurements were made using a TGA Q500-O574 (TA Instruments). The samples were heated from 25°C to 700°C at a heating rate of 10°C/min under a nitrogen atmosphere. Films were stored at 25°C and 0, 30, 75 and ~100% RH at least 7 days prior to measurements.

##### 3.4.4.2. Differential scanning calorimetry

Differential scanning calorimetry (DSC) monitors heat effects associated with phase transitions and chemical reactions as a function of temperature. The differential heat flow required to maintain the same temperature in the testing sample and in thermally neutral sample, used as a reference, is measured. The sample and reference are heated by independent elements. A signal proportional to the difference of heat supplied to the sample and to reference is obtained. The curve  $\Delta H/\Delta t$  (t=time) depending on the temperature (T) is recorded.

A differential scanning calorimetry was performed using a DSC Q1000-O506 (TA Instruments). An empty capsule was used as an inert reference and the calibration was performed using the indium standard. The accuracy of the measurements was estimated at  $\pm 0.1^\circ\text{C}$ . The heating and the cooling rates under nitrogen atmosphere were fixed at 10°C/min. Since chitosan is a hydrophilic polymer which tends to retain moisture, the experiment consisted in the 2 runs in order to eliminate the moisture effect. The following temperature program that ranged between 80°C and 350°C was used for all the samples:

- a) equilibrating at 25°C, cooling from 25°C to -80°C at a rate of 10°C/min, isothermal for 10 minutes and heating to 220°C, isothermal for 5 minutes ;
- b) cooling down to -80°C at a rate of 10°C/min, isothermal for 10 minutes;

- c) reheating to 350°C at a rate of 10°C/min, isothermal for 5 minutes;  
 d) and finally cooling down to 25°C at a rate of 10°C/min.

Prior to the experiments samples were conditioned at 25°C and 0, 30, 75 and ~100% of relative humidity (RH) for at least 7 days. Reproducibility was tested by carrying out the two measurements for each sample. The mass of all the samples was around 10 mg.

### 3.4.5. Surface properties

#### 3.4.5.1. Fourier Transform Infrared Spectroscopy - Attenuated Total Reflectance

The infrared spectroscopy gives a data about the interactions between the atoms and their vibrations. The vibrational frequencies are determined by the shape, the mass of the atoms and eventually by the associated vibronic coupling. The changes on film's surfaces were assessed by FTIR-ATR spectroscopy (Brucker, IFS 28, equipped with zinc selenide (ZnSe) crystal). Data treatment was done using a Software OPUS. All spectra were an average of 64 scans at a resolution of 4 cm<sup>-1</sup>, from 650 to 4000 cm<sup>-1</sup> and determined at 25°C. Samples were previously conditioned at 25°C and 30% of relative humidity (RH) for at least 7 days prior to the experiments.

#### 3.4.5.2. Contact angle and wettability

##### Mathematical definition of the contact angle

The first definition of the contact angle goes back to the Greek mathematician Euclid in Euclid's Elements: the angle between the tangent and the circumference. Then, with the birth of calculus, Newton, in a manuscript from 1664, stated that: "The contact angle is compared to another angle as a point vis-à-vis a line, because the curvature of a circle equals four right angles, and this curvature can be conceived as consisting of an infinite number of contact angles, as a line consists of an infinite number of points" (Loget, 2002). Now it is defined as: "the dihedral angle formed by two contiguous interfaces to their apparent intersection" (B.O., 2003).

##### Determination of a contact angle

Contact angle ( $\theta$ ) is described as a relationship between the surface tension at a point of the three phase contact line (Fig. 3.8.) between a solid phase S, a liquid L and its vapour V given by:

$$\gamma_{L_V} \cdot \cos\theta = \gamma_{S_V} - \gamma_{S_L} \quad (\text{Eq. 3.6.})$$

where  $\gamma_{LV}$ ,  $\gamma_{SV}$  and  $\gamma_{SL}$  are the surface tensions of the liquid-vapour, solid-vapour and solid-liquid, respectively (Young, 1805).

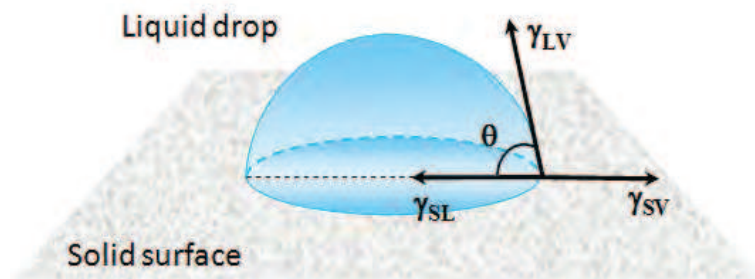


**Figure 3.8.** Contact angle of a drop of liquid deposited on a solid surface and the surface tension at the contact point of three phases.

The Young equation, based on a thermodynamic equilibrium can be applied to isotropic solids, smooth, and rigid surfaces, free of chemical reaction/dissolution in the presence of liquid. Still, in many ways, most solid surfaces deviate from perfection (smooth, chemically homogeneous, rigid, insoluble and non-reactive). In reality these surfaces are often heterogeneous, deformable, rough, etc. The contact angle value is dependent on surface heterogeneity, but as Drelich (1997) pointed out, there is no universal theoretical model for this phenomenon with all the possible cases that could exist.

The contact angle was measured by the sessile drop method, in which a droplet of the tested liquid was placed on a horizontal film surface. Measurement was done using a DGD-DX goniometer (GBX, Romans-sur-Isere, France), equipped with the DIGIDROP image analysis software (GBX, Romans-sur-Isere, France) according to Karbowiak et al. (2006) (Fig. 3.9.). The sessile drop method is basically an optical contact angle method, which is the most frequently used to estimate wetting properties of a solid surface. A droplet of a testing solution ( $\sim 1.5 \mu\text{L}$ ) was deposited on the film surface with a precision syringe. The method is based on image processing and curve fitting for a contact angle measurement. This is made from a theoretical meridian drop profile, measuring contact angle between the baseline of the drop and the tangent at the drop boundary. Video acquisition of a magnified image of the drop profile is conveyed to a computer via a CCD camera, which enables to quantify changes in the droplet shape recorded as digital images over the time. The contact angles were measured on both sides of the drop and averaged. The measurement was carried on over 120 s. The effect of evaporation was assessed on the aluminium foil considered as

an impermeable reference surface. All measurements were done on both sides of the films. For chitosan self supported films, the surface in contact with the glass support during drying will be referred to as the “support side”. The other surface in contact with the air during drying will be referred to as the “air side”.

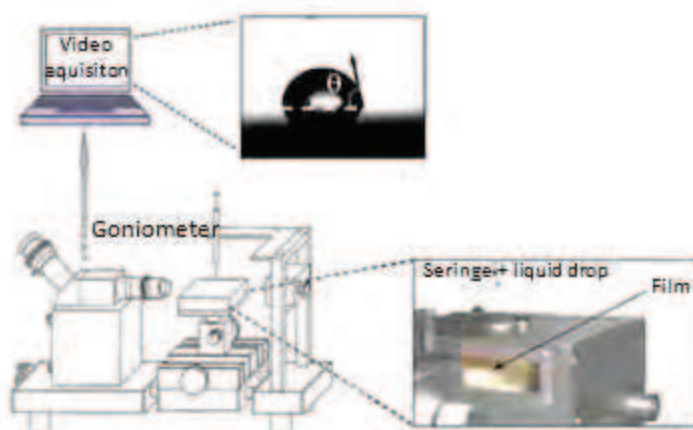


**Figure 3.9.** Schema of the experimental system used for contact angle measurements.

#### Determination of surface tension and critical surface tension

The surface tension of the film forming (coating) solutions ( $\gamma_L$ ) was measured by the sessile drop method and Laplace-Young approximation (Song and Springer, 1996a, 1996b). In order to determine the drop shape, using the image analysing software, solutions were taken with a 1 mL syringe (Hamilton, Switzerland). The estimation of the critical surface tension ( $\gamma_C$ ) of the PE, the coated PE and the self-standing chitosan films was obtained by extrapolation from the Zisman plot (Zisman, 1964). Zisman plots were obtained by plotting the cosine of the contact angles ( $\cos\theta$ ) of a series of standard liquids (Chapter 7, Table 7.1.) on the film surface versus the surface tension of the same liquids (Fig. 3.10.). The critical surface tension values of films are the mean of the extrapolation of  $\cos\theta$  for the liquids that form approximately a straight line. Extrapolation of this line to the point of  $\cos\theta=1$ , yields the value of the critical surface energy equal to liquid surface tension ( $\gamma_L$ ) at this point.

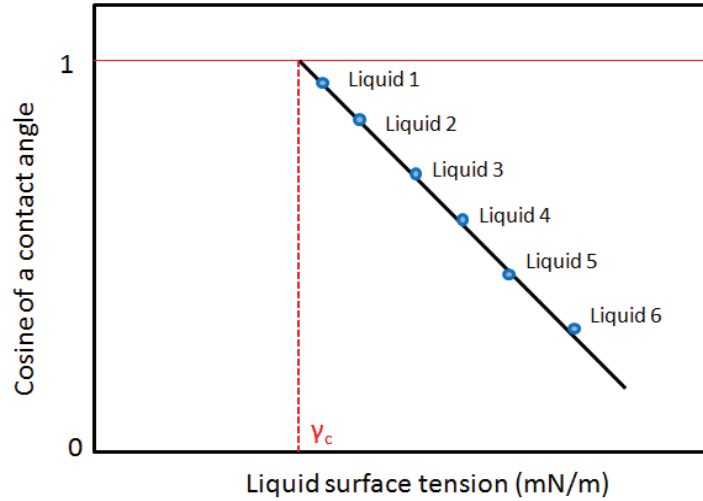


**Figure 3.10.** The Zisman plot design.

### Absorption flux

Absorption flux ( $F_{abs}$ ) was obtained from the drop volume kinetics taking into account the evaporation flux ( $F_{eva}$ ), according to Karbowski et al. (2006). When a water drop is deposited onto a solid surface a decrease of volume and contact angle occur. To explain this decrease over a time, two mechanisms are suggested: evaporation that results due to the pressure difference between the water drop and the surrounding atmosphere, and absorption inside the film.

$$V(t) = V(0) - V_{eva}(t) - V_{abs}(t) \quad (Eq. 3.7.)$$

where  $V_{eva}$  is the evaporated volume ( $\mu\text{L}$ ) and  $V_{abs}$  is the absorbed volume ( $\mu\text{L}$ ).

Considering that absorption is negligible in aluminium foil, it was used as reference to estimate the evaporation flux  $F_{eva}$  as follows:

$$F_{eva} = \frac{V_{eva}(t) - V_{eva}(t + dt)}{A_S(t) \cdot dt} = \frac{dV_{eva}}{A_S(t) \cdot dt} \quad (Eq. 3.8.)$$

where  $A_S$  is the surface area of the water droplet on this reference material.

The volume absorbed by a hydrophilic material can therefore be calculated after the subtraction of the evaporated volume. The initial volume of the droplet as well as the contact area is dependent upon the measurement as they are controlled manually



by accurate syringe. The absorbed volume at time  $t$  can be determined from the reference evaporation flux and the surface area of the droplet on the tested surface:

$$dV_{abs}(t) = V(t) - V(t + dt) - dV_{eva}(t) = dV(t) - dV_{eva}(t) \quad (Eq. 3.9.)$$

$$dV_{abs}(t) = dV(t) - F_{eva} \cdot dt \cdot A_S(t) \quad (Eq. 3.10.)$$

where  $A_S$  is the surface area of the water drop on the tested surface.

The absorption flux  $F_{abs}$  is thus the absorbed volume per base area unit (that corresponds to the interface liquid/solid) and per time unit:

$$F_{abs} = \frac{dV_{abs}}{A_B(t) \cdot dt} \quad (Eq. 3.11.)$$

where  $A_B$  is the base area of the water drop on the tested surface.

When swelling occurs, the droplet volume increases so  $F_{abs}$  cannot be estimated. The swelling index was obtained from the drop volume kinetics using the following equation:

$$SW_{index} = \frac{\Delta V}{V_0} \cdot 100 = \frac{V_2 - V_1}{V_0} \cdot 100 \quad (Eq. 3.12.)$$

where  $\Delta V$  is the droplet volume variation ( $\mu\text{L}$ ) during  $dt$  time (s) measured on the film sample.  $V_2$  is the maximal volume ( $\mu\text{L}$ ) of the droplet,  $V_1$  is the minimal volume ( $\mu\text{L}$ ) of the droplet and  $V_0$  is the initial volume ( $\mu\text{L}$ ) of the droplet.

### Surface free energy and wettability

Surface free energy and its polar ( $\gamma_{SP}$ ) and dispersive ( $\gamma_{SD}$ ) components were calculated by the Owens–Wendt method (Owens and Wendt, 1969):

$$\gamma_S = \gamma_{SD} + \gamma_{SP} \quad (Eq. 3.13.)$$

$$\gamma_L(1 + \cos\theta) = 2((\gamma_{SD} \cdot \gamma_{LD})^{0.5} + (\gamma_{SP} \cdot \gamma_{LP})^{0.5}) \quad (Eq. 3.14.)$$

Because two unknowns,  $\gamma_{SD}$  and  $\gamma_{SP}$  appear in Eq. 3.14., it is insufficient to determine the SFE of a polymer. Thus, the contact angle has to be measured using two measuring liquids of known surface tension and their polar ( $\gamma_{LP}$ ) and dispersive ( $\gamma_{LD}$ ) component (deionised water as the liquid with the dominant polar component and diodomethane with the dominant dispersive component). That yields to the two

equations in the form of Eq. 3.14., with different values of the constant coefficients. As a result, a system of two linear equations is obtained:

$$\begin{aligned} (\gamma_{SD})^{0.5} + a(\gamma_{SP})^{0.5} &= b(1 + \cos\theta_1) \\ (\gamma_{SD})^{0.5} + c(\gamma_{SP})^{0.5} &= d(1 + \cos\theta_2) \end{aligned} \quad (\text{Eq. 3.15.})$$

where a, b, c, d are the coefficients dependent on the types of these liquids and  $\theta_1$  and  $\theta_2$  are contact angles of water and diodomethane over a tested film.

The Young's equation, which describes the contact angle with interfacial tensions of solid and liquid, clearly shows that the wetting is favoured by a low  $\gamma_{SL}$ , a high  $\gamma_{SV}$  and a low  $\gamma_{LV}$ , and that spreading occurs when  $\gamma_{SV} - \gamma_{SL} > \gamma_{LV}$  (Fig. 3.8.). If spreading does not occur, the drop is finite as dimensional, and then, at equilibrium, it leads to the existence of a contact angle. In theory, the value of the contact angle can vary from  $0^\circ$  to  $180^\circ$ . A contact angle of  $0^\circ$  implies a full spreading of the liquid to the solid surface, while a value of  $180^\circ$  corresponds to a surface absolutely non-wettable, which represents the limit of a system without unreal interactions (Fig. 3.11.).

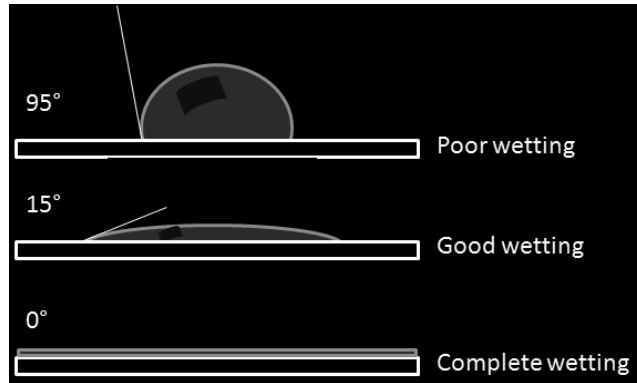


**Figure 3.11.** Wetting of a solid surface.

When considering the attractive forces at a given interface, it has been suggested that the liquid-vapour interfacial tension is the sum of contributions from the different intermolecular forces (Kaelble, 1970; Rabel, 1971; Dupre, 1869). For a pure liquid, if polar and dispersive interactions are known, and if the contact angle between that liquid and a solid is obtained, the interaction can be described by the adhesion coefficient (work of adhesion per unit area,  $W_a$ ), given by Dupre equation (Dupre, 1869):

$$W_a = \gamma_{SV} + \gamma_{LV} - \gamma_{LS} \quad (\text{Eq. 3.16.})$$

where  $W_a$  is the work of adhesion between the liquid drop and the solid (the work necessary to separate the liquid from the solid to give both solid and liquid phases in equilibrium with the vapour phase) to obtain:

$$W_a = \gamma_{Lv}(1 + \cos\theta) \text{ (Eq. 3.17.)}$$

Cohesion coefficient (work of cohesion per unit area,  $W_c$ ) is given by:

$$W_c = 2\gamma_{LV} \text{ (Eq. 3.18.)}$$

Then, spreading coefficient ( $W_s$ ) for a liquid over a solid is calculated as:

$$W_s = W_a - W_c = \gamma_{SV} - \gamma_{LV} - \gamma_{LS} \text{ (Eq. 3.19.)}$$

The physical significance of this energy change is the work needed to separate the solid and liquid from the solid/liquid interface. The equilibrium spreading coefficient can only be negative or equal to zero.

## 3.5. Transfer measurements

### 3.5.1. Theoretical background

Key characteristics of packaging materials are their barrier properties to gases and vapours. Gas permeation has been studied for over 150 years. However, significant advances in the understanding the gas permeation have been made only in the last three decades. The interest in the field was generated from developments of new synthetic polymeric materials. The permeation is affected in a complex way by a number of parameters within the material, like flexibility of the polymer chains, morphology, orientation, crystallinity, interaction between the permeant molecules and the polymer, and interaction with eventual filler (Chapter 2). The first study of gas permeation through a polymer was conducted by Thomas Graham in 1829 (Stannet, 1978). He observed a loss in volume of a wet pig bladder inflated with  $\text{CO}_2$ . In 1866, Graham gave the solution to diffusion process, where he postulated that the permeation process involves the dissolution of penetrant, followed by transmission of the dissolved species through the membrane.

The transfer of a molecule through the polymer film is governed by the concentration gradient, from the highest concentration to the lowest concentration. The permeability of a polymer film is often described in three stages:

- 1) the solution or sorption of the diffusate into the surface of the polymer exposed to higher concentration;
- 2) migration or diffusion of the dissolved solute through the polymer according to the concentration gradient towards the opposite surface; and
- 3) desorption on the opposite side of the film (Fig. 3.12.).

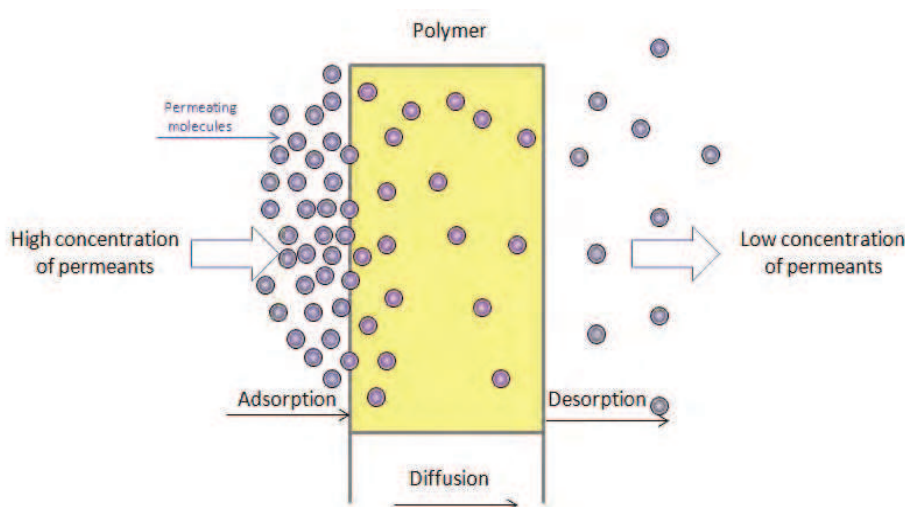


**Figure 3.12.** Transfer mechanism through polymer film.

Sorption involves the take-up of molecules from environment into package, but not through it. Diffusion refers to the transport of molecules through the polymer. Desorption is the opposite of sorption. Migration is the passage of molecules originally contained in the packaging material to a food product. Finally, permeability includes the transfer of molecules through the package, from inside of the packaging to the external environment or vice versa.

The solubility, diffusion, and permeability coefficients are key parameters that affect a polymer's barrier performance.

#### 3.5.1.1. Diffusion process

Diffusion represents the kinetic property of the polymer-permeant system. It occurs as a result of natural processes, which tend to equal out the concentration of a given species of molecules in a given environment. According to Crank (1975), the diffusion coefficient describes the mechanism by which molecules move in a material

under the effect of a potential gradient, following a succession of random molecular motions in all directions in a space. The model proposed by DiBenedetto and Paul describes the transport of gas molecules parallel to the polymer chains (DiBenedetto, 1964). The gas molecule is assumed to be trapped in the bundle under equilibrium. During a thermal fluctuation, the expansion of chains near the molecule creates a cylindrical passage, thereby allowing the gas molecule to make a diffusional jump to the other end of this passage. With the closing of the passage, the gas molecule is at a new position under thermal equilibrium. On the macroscopic scale, this movement coincides with a small displacement of gas molecule along the chain. These random displacements result in the diffusion of the gas molecule through the membrane.

The diffusion coefficient is defined by Fick's first law:

$$J = -D \frac{\partial c}{\partial x} \quad (\text{Eq. 3.20.})$$

where  $J$  ( $\text{g/m}^2\cdot\text{s}$ ) is the transfer rate, in other words, the quantity transferred per unit time and per unit area,  $C$  ( $\text{g/m}^3$ ) is the concentration of permeant,  $x$  (m) is the thickness of the films and  $D$  ( $\text{m}^2/\text{s}$ ) is the diffusion coefficient.

There are two types of diffusion behaviour in the polymer:

- Fickian behaviour which is characterized by diffusion coefficients independent of concentration. This behaviour is often observed in the diffusion of gases such as oxygen in synthetic polymers.
- Non-Fickian behaviour which is characterized by diffusion coefficients dependent on the concentration or time. This behaviour is observed for water vapour and organic vapours in organic polymers (Neogi, 1996).

#### 3.5.1.2. Sorption process

The sorption process is described as the distribution of penetrating molecule between two or more phases. It includes adsorption, desorption and incorporation into the gaps, but also the formation of aggregates, "clusters" and other phenomena (Rogers, 1985). Sorption is governed by the strength of interactions between permeant/permeant, permeant/polymer and polymer/polymer. „Ideal“ sorption is the most easily expressed by Henry's Law:

$$C = S \cdot p \quad (\text{Eq. 3.21.})$$

where  $p$  (Pa) is the partial vapour pressure of the permeant,  $C$  ( $\text{g}/\text{m}^3$ ) is the concentration of the permeant and  $S$  ( $\text{g}/\text{m}^3 \cdot \text{Pa}$ ) is the solubility coefficient.  $S$  depends on the temperature and varies with the vapour pressure of the solute.

### 3.5.1.3. Permeability

The permeability is selective process and is characteristic of the polymer-diffusate interaction when the latter is an organic liquid in which the macromolecular films swell. The permeability coefficient includes both kinetic and thermodynamic properties of polymer-permeant system and involves three steps as previously mentioned.

The balance of compounds around a thin polymer membrane can be described by the Fig. 3.13.

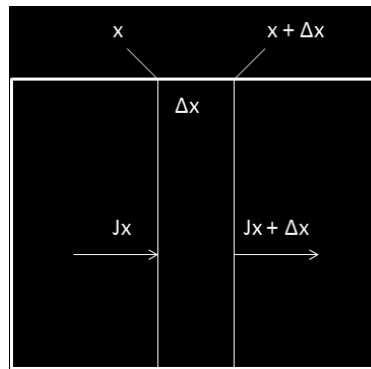


**Figure 3.13.** Diffusion flow around a thin polymer membrane.

The rate of diffusion (or flow) of the permeant on the distance interval,  $\Delta x$ , is equal to the cumulative rate of permeant in the membrane according to Eq. 3.22.:

$$J_x - J_{x+\Delta x} = \frac{d(C \cdot \Delta x)}{A \cdot dt} \quad (\text{Eq. 3.22.})$$

where  $C$  is the concentration of permeant,  $A$  the film surface,  $C \cdot \Delta x$  is the amount of permeant in the membrane depending on the distance  $\Delta x$  at any time. The expression on the right side of Eq. 3.22. represents the exchange rate of the permeant in the interior of the membrane. Dividing Eq. 3.22. by  $A \cdot \Delta x$  and by taking the limit of  $\Delta x$  close to zero, gives:

$$\lim_{\Delta x \rightarrow 0} = \frac{J_x - J_{x+\Delta x}}{\Delta x} = -\frac{\partial J}{\partial x} = \frac{\partial C}{\partial t} \quad (\text{Eq. 3.23.})$$

If the sorption equilibrium is quickly established, the rate of passage of the gas through the polymer film depends mainly on the rate of diffusion. In this case, assuming that  $D$  is constant and the substitution of  $J$  with  $D$  in the Eq. 3.23., gives the second Fick's law that describes the non stationary state of the film:

$$D \frac{\partial^2 C}{\partial x^2} = \frac{\partial C}{\partial t} \quad (\text{Eq. 3.24.})$$

Permeation of small molecules in polymer depends on their solubility and diffusivity. The mass transfer of simple gases such as hydrogen, air, oxygen, carbon dioxide, and nitrogen through polymer films is described by the Eq. 3.25. that relates solubility ( $S$ ), diffusion ( $D$ ), and permeability coefficients ( $P$ ):

$$P = f(D, S) \quad (\text{Eq. 3.25.})$$

If  $D$  and  $S$  are independent on the concentration,  $P$  can be expressed as:

$$J = P \frac{\partial p}{\partial x} \quad (\text{Eq. 3.26.})$$

In practice, the permeability is defined as a steady state for  $D$  and  $S$ . Integrating the equations 3.20., 3.21. and 3.22., following relation is obtained:

$$P = \frac{(dM/dt) \cdot e}{A \cdot \Delta p} \quad (\text{Eq. 3.27.})$$

where,  $M$  is the amount of permeant (g) over time  $t$  (s),  $A$  ( $\text{m}^2$ ) the exchange surface of the exposed film transfer,  $\Delta p$  (Pa) the partial pressure difference and  $e$  (m) is the film thickness.

### 3.5.2. Gas permeability measurements

The gas permeability determination was performed using a manometric method, on a permeability testing appliance, Brugger, Type GDP-C (Brugger Feinmechanik GmbH, Germany) according to ISO/DIS 15 105 1.

The sample is put between the top and bottom part of the permeation cell. The volume of the bottom part is as small as possible and known. Prior to each test the bottom part of the permeation cell is evacuated. During testing the top part is filled with the test gas. In the other chamber the pressure increases because of the

transmission through the specimen. The permeation rate is calculated than based on the pressure increase.

The increase in pressure during the test period was evaluated and displayed by an external computer. Data were recorded and permeance was calculated by a GDP-C Software. The sample temperatures (4 and 25°C) were adjusted using an external Thermostat (HAAKE F3 with Waterbath K). The desired relative humidities ranging from 0 to ~96% were regulated in the top part of the permeation cell. For a first series of measurement a glass fibre disc was humidified with a saturated salt to set up the desired humidity. In the second experimental series, the relative humidities were regulated using external saturation systems with different salt solutions for each relative humidity differential. Relative humidity in the chamber was checked during the whole experimental period using Optic USB Base Station HOBO Pro v2 temperature/relative humidity data logger (Onset®HOBO®DataLoggers, U23 Pro v2, France) and the data were recorded on the PC and transferred using a special software HOBOWare Pro 3.0. Three repetitions were made for each sample.

### 3.5.3. Water vapour permeability measurement

The water vapour permeability (WVP) of films was determined gravimetrically using a modified ASTM E96-80 (1980) standard method, adapted to edible materials by Debeaufort et al. (1993).

The driving force of water vapour diffusion through a film is the difference between the partial pressures of water vapour in air on both film sides. In a stationary state, equilibrium is established on both film sides between the water concentration on the membrane surface and the water vapour concentration in air that is dependent on the temperature at the film surface and its surroundings. If the partial water vapour pressures on both sides are different, a gradient of water concentration is established in the film and the permeation occurs.

In this work, three relative humidity differentials of  $\Delta$  33-0%,  $\Delta$  75-30% and  $\Delta$  100-30% and the temperature of  $25\pm 1^\circ\text{C}$  were used. Prior to the WVP measurements, all the film samples were equilibrated at  $25\pm 1^\circ\text{C}$  and 30% relative humidity for at least 72 h. The film samples were then placed between two Teflon rings on the top of the glass cell (Fig. 3.14.) containing different salt solutions. These permeation cells were introduced into a ventilated chamber (KBF 240 Binder, ODIL, France), maintained at 30% RH and  $25\pm 1^\circ\text{C}$ . WVP ( $\text{g}/\text{m}\cdot\text{s Pa}$ ) was calculated from the change in the cell weight versus time at the steady state, using the following equation:



$$WVP = \frac{\Delta m}{\Delta t \cdot \Delta p \cdot A} \cdot e \quad (\text{Eq. 3.28.})$$

where  $\Delta m/\Delta t$  is the weight of moisture loss per unit of time (g/s),  $A$  is the film area exposed to the moisture transfer ( $9.08 \times 10^{-4} \text{ m}^2$ ),  $e$  is the film thickness (m), and  $\Delta p$  is the water vapour pressure difference between the two sides of the film (Pa). Three replicates for each film type and RH gradient were made.

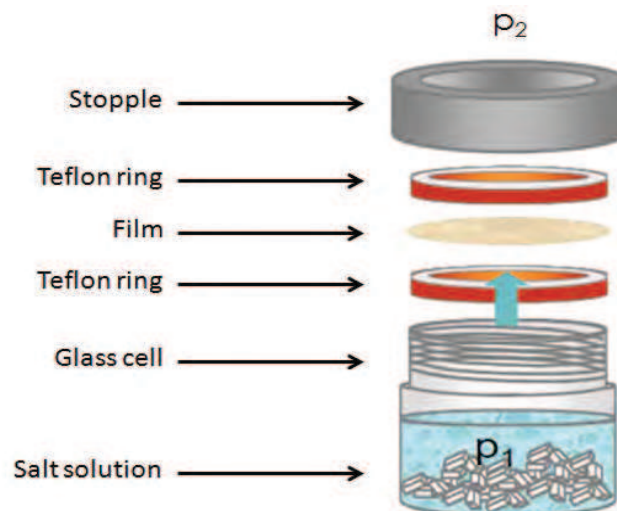


**Figure 3.14.** Water vapour permeation cell.

### 3.5.4. Moisture sorption isotherms

#### 3.5.4.1. Theoretical background

The sorption isotherm allows estimating the water content at equilibrium of a solid material exposed to the surrounding moisture. This measure is widely used in the field of bio-based materials and foods. It allows determination of ideal conditions for storage of these materials to prevent microbiological spoilage and preserve their mechanical strength. The sorption isotherm of a product is the graphical relationship between water content and water activity at equilibrium for a given temperature. This relationship is complex. An increase in  $a_w$  is usually accompanied by an increase in water content, but in a non-linear fashion.

Considered as the "fingerprint" of a food product, this isotherm curve (usually S-shaped) shows how water content changes as water activity is increased or decreased (Roudaut and Debeaufort, 2010). If the composition or quality of the material changes,

then its sorption behaviour might also change. The International Union of Pure and Applied Chemistry (IUPAC, 1985) classified adsorption isotherms into six general types (Fig. 3.15.). Depending on the nature of material (crystalline or amorphous), the shape of isotherm is different and corresponds to different types of interactions between adsorbed substances and adsorbent and/or its porosity.

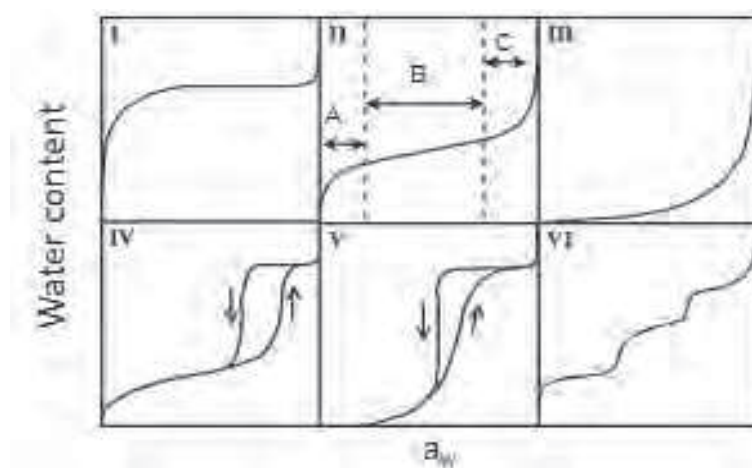


**Figure 3.15.** Types of water vapour sorption isotherms (IUPAC, 1985).

The Type I isotherm, called Langmuir isotherm, is typical of microporous solids and chemisorption isotherms. Type II is the sigmoid shaped isotherm, shown by finely divided non-porous solids. If, however, the solid is porous and has a significant internal surface, then the thickness of the adsorbed layer on the walls of the pores is necessarily limited by the width (diameter and length) of the pores. The form of the isotherm is modified correspondingly; instead of type II and III, type IV, V and VI exist (Roudaut and Debeaufort, 2010).

Different mathematical models have been developed for description of sorption isotherm, for evaluation of specific surface area, of number of a sorbing sites etc. (i.e. GAB, BET, Langmuir, etc.).

Sorption isotherms can be generated from an adsorption process or a desorption process. The difference between these curves is defined as hysteresis. This phenomenon has come from a change of state of the material or conformational changes of molecules during dehydration (Simatos, 2002).

The moisture sorption isotherms of most foods are non-linear, generally sigmoidal in shape, and have been classified as type II isotherms. This type II isotherm is usually divided in three zones corresponding to different ways of moisture fixation on the solid substrate as shown on Fig 3.15. The zone A ( $a_w < 0.2$ ) presents the

---

adsorption of a monomolecular layer of water. This corresponds to the van der Waals interactions between hydrophilic parts of the matrix and water molecules. Water adsorption occurs progressively until it creates a continuous monolayer of water molecules at both the external surface of the product and on the surface of infractuositities and pores of the product. Water is considered as strongly fixed and in a "semi-rigid" state, because of the great importance of interactions between water molecules and the surface. When the whole surface is saturated, the second zone B starts (Van den Berg, 1991). Then, it corresponds to the adsorption of successive layers of water to the monolayer by hydrogen bonds ( $0.2 < a_w < 0.7$ ). Finally, the third zone C ( $a_w > 0.7$ ) results from an excess water present in macro-capillaries or as part of the liquid phase in high moisture materials. Herewith, the water is in a liquid state and it exhibits nearly all the properties of bulk water, and thus is able to act as a solvent (Al Muhtaseb et al., 2002).

#### 3.5.4.2. Experimental part

An Autosorp (Biosystems, Couternon, France) apparatus was used to determine the moisture sorption isotherms. To control humidity; HPLC grade water (Prolabo, France) was used. The desired RH conditions varied step by step from 0 to 85%. Samples were weighed periodically (0.01 mg/h variability for 500 mg of a sample) with a time interval of 6 hours. To assure reaching the equilibrium, long periods were chosen. If the samples did not attain constant weight after 7 days, the next RH was preceded.

Analysis of the water vapour sorption was carried out at 25°C. Duplicate film samples, accurately weighed, were placed into proper cells. Prior to measurements, the tested samples were dried over P<sub>2</sub>O<sub>5</sub> for 10 days. Then they were additionally dried in the Autosorp apparatus under the dry air flow (having dew point at -60°C that corresponds to RH < 0.046%). This value was considered as the initial zero value or polymer dry basis for water vapour sorption isotherm calculation.

For determination of water vapour desorption isotherms, the polymer dry basis was considered as the value obtained after desorption process under the dry air flow. Moreover, samples were additionally dried at 105°C for 48 h at the end of both sorption-desorption-sorption processes. During this drying the degradation and reorganisation of chitosan polymorph might occur. Moreover, when films were dried by this method, colour modification occurred. This denoted some chemical reactions and possible structure change. Then for the further desorption calculations, the

polymer dry weight was considered as the final value obtained after the equilibration of the desorption process at 0% RH.

To describe water vapour sorption isotherms, the semi-theoretical multilayer sorption model Guggenheim-Anderson-de Boer (GAB) (Anderson, 1946) was used as follows equation 3.29.:

$$m_a = \frac{m_m \cdot C_{GAB} \cdot K_{GAB} \cdot a_w}{(1 - K_{GAB} \cdot a_w) \cdot [1 + (C_{GAB} - 1) \cdot K_{GAB} \cdot a_w]} \quad (Eq. 3.29.)$$

where  $m_a$  is the equilibrium moisture content on dry basis (g water/g dry matter).  $m_m$  is the monolayer moisture value (e.g., it indicates the maximum amount of water that can be adsorbed in a single layer of dry film, and is a measure of the number of sorbing sites). This model is the most accepted model for foods or edible materials. The parameters of the model were determined by adjustment between the GAB equation and the experimental results, using a regression analysis carried out by Microsoft Excel and Matlab software (version 7.01, The Mathworks, Natick, MA). The water molecules are adsorbed by the polar groups on the polymer chains and the next  $n$ -th layer corresponds to the water molecules successively condensed on the first layer. In the above equation,  $a_w$  is water activity, and  $C_{GAB}$  and  $K_{GAB}$  are the equation parameters. In this model, the subsequent layers properties are discriminated from those of the pure liquid bulk. The  $C_{GAB}$  constant is related to adsorption energies of first and second layers whereas the  $K_{GAB}$  constant is related to the adsorption energies of second and subsequent layers which lie somewhere between the monolayer adsorption energy and the pure adsorptive liquefaction energy. These constants are defined by the relations (Quirijns et al., 2005):

$$C_{GAB} = C_{0GAB}^e \cdot \left( -\frac{\Delta H_{GAB1} - \Delta H_{GABn}}{RT} \right) \quad (Eq. 3.30.)$$

$$K_{GAB} = C_{0GAB}^e \cdot \left( -\frac{\Delta H_{GAB1n} - \Delta H_{liq}}{RT} \right) \quad (Eq. 3.31.)$$

with  $\Delta H_{GAB1}$  the adsorption enthalpy of the first layer and  $\Delta H_{GABn}$  that one of the subsequent layers.  $C_{0GAB}$  is Arrhenius type constant to express temperature dependence of  $C_{GAB}$ .

### 3.5.5. Calculation of water vapour diffusion coefficient in film

Taking into account water vapour sorption isotherms and assuming a Fick's law, it is possible to determine an apparent diffusion coefficient of water in the film. The observed phenomenon can be described as the mass transfer through a membrane of constant thickness (L). Initial conditions are a uniform initial distribution and different water surface concentrations, zero on one side and infinite for the other side. Mass transfer problem can be solved using an analytic solution to the Fick's law applied to transient state:

$$\frac{M_t}{M_\infty} = 1 - \sum_{n=0}^{\infty} \frac{8}{(2n+1)^2 \pi^2} \exp\left[\frac{-D(2n+1)^2 \pi^2 t}{4L^2}\right] \quad (\text{Eq. 3.32.})$$

where  $M_t$  denotes the total amount of diffusing substance which has enter the film at time t and  $M_\infty$  the corresponding quantity after time.

This model was applied to experimental values in order to determine the apparent diffusion coefficient of water in the film, by minimising the sum of the square of the differences between measured and predicted values, using Levenberg-Marquardt algorithm, and taking D as adjustable parameter. Two repetitions were performed for each studied sample.

Modeling and data analyses were performed using Matlab software (version 7.01, The Mathworks, Natick, MA). The determination coefficient was first calculated to check the adjustment of the model to experimental data according to Karbowiak et al. (2011) (see Fig. 9.3. for example). This was done for each individual data series.

## 3.6. Antimicrobial properties of chitosan films and coatings

Evaluation of antimicrobial efficiency was performed in collaboration and partially realised by Ms. Sylvie Moundanga from Laboratory PAM-PMB.

### 3.6.1. Microbial cultures

The following microbial strains were selected as non pathogenic models of undesirable microbial contaminants in the food industry: Gram positive bacteria *Bacillus subtilis* 168 BGSC 1A (Ohio, USA), *Listeria innocua* DSM 20649 (Germany) and *Lactobacillus plantarum* (UMR PAM, Dijon, France); Gram negative bacteria *Escherichia*

*coli* TG1 K12 from the microbiology laboratory culture collection (UMR PAM, Dijon, France) and *Salmonella Enteritidis* CIP 81.3 (France) and fungi *Penicillium camemberti* DSM 1233 (Germany).

Bacterial cultures were regenerated from cryopreserved strains by plating and isolating individual colonies on Petri dishes containing LB Agar, for *L. innocua*, *E. coli* and *S. Enteritidis*, Columbia Agar for *B. subtilis* or MRS agar for *Lactobacillus plantarum*. Pre-cultures were prepared by transferring a single colony into a 250 mL conical flask containing 50 mL (for *E. coli*) or 150 mL (for *S. enteritidis* and *B. subtilis*) of LB broth, 150 mL of BHI broth (for *L. innocua*) or 10 mL of MRS (for *L. plantarum*). The bacteria were then cultured overnight (12 h) in optimal temperature conditions (37°C) and orbital agitation (without agitation for *L. innocua* and *L. plantarum*). Then an aliquot of the pre-culture was used to inoculate an adequate volume of a similar growth liquid medium (0.5 mL in 50 mL of LB broth for *E. coli*; 1 mL in 50 mL of LB broth for *S. enteritidis* and *B. subtilis*; 0.5 mL in 100 mL of BHI broth for *L. innocua*, 10 mL of MRS for *L. plantarum*) (Fig. 3.16.). Bacterial cells were incubated in the same optimal conditions of culture as previously described, up to late exponential phase. Subsequently, these appropriate liquid cultures were then used for inoculation of nutrient agar plates in order to obtain target bacterial cells.

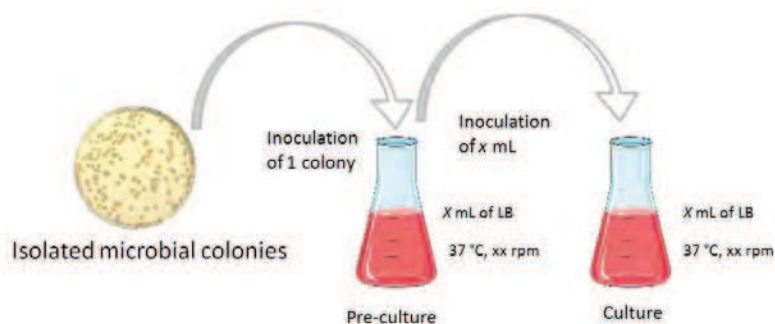


**Figure 3.16.** Schema of isolation procedure and preparation of a culture.

### 3.6.2. Inoculation

For *P. camemberti*, a loopful of mycelium with fungal spores was transferred to a PDA agar plate. For all bacterial strains, inoculation was carried out with a 48 circular prongs (8x6 arrays) replica platter (Sigma-Aldrich) suitable for 96 wells microplate. Only one well out of two of the eight lines and of the first six columns of a sterile 96 wells (8x12 array) microplate (Nunc Brand, USA, Fig. 3.17.) was filled with 200  $\mu$ L of the cell suspension obtained as previously described. The replica platter allowed

performing an efficient and repeatable transfer of bacterial colonies from the microplate to the agar plate. Therefore 24 drops of equal and always similar volume (1.5  $\mu\text{L}$  per drop) were regularly dispensed in a 90 mm diameter Petri dish containing LB agar (for all bacterial strains except *L. innocua* and *L. plantarum*), BHI agar (for *L. innocua*) or MRS agar (for *L. plantarum*).

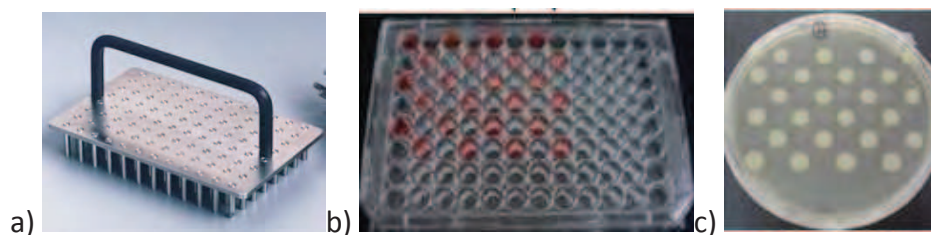


**Figure 3.17.** Photos of a) replica platter, b) microplate, c) inoculated Petri dish.

In this study, the cluster of cells formed on the agar surface from the whole cellular population initially contained in a drop of bacteria suspension was called “colony”. Since only one well out of two of the microplate was filled, drops on the nutrient agar plate did not touch each other even when colonies grew. Thus 24 distinct inocula of known and repeatable initial cellular concentration (10 cells per inoculum) were obtained. The inoculum size had to be high enough to permit the count of cells stemming from an inoculated drop by classical methods (enumeration with a Malassez haemocytometer and count of colonies forming units (CFU)) as soon as the exponential phase of growth. Easy estimation of bacterial growth was achieved by macroscopic observations and cell diameter measurement of the colonies formed.

### 3.6.3. Experimental design

The pure aroma compound or the chitosan-based films were laid down on the lid of the Petri dish and the inoculated agar plate was put in an inverted position above this lid. In the case of pure aroma compound, a drop of solution was deposited on the centre of the cover, whereas the film covered the surface of the lid (Fig. 3.18.). To prevent leakage of vapours, all the plates were sealed with Parafilm<sup>®</sup> immediately after laying of the antimicrobial material. Then, the Petri Dishes were incubated, still in the inverted position, in optimal conditions of growth depending on the strain tested, as described previously.



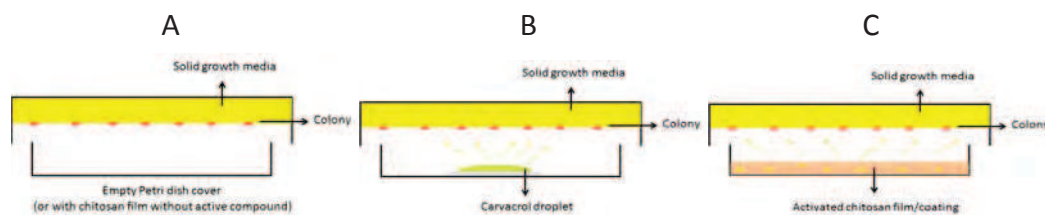


**Figure 3.18.** Schema of Petri dishes used in the experiments. A control test; B test with pure aroma compound; C test with activated chitosan films/coatings.

Two experimental procedures were applied. The first one was developed to check if the antimicrobial compound in the vapour phase prevents the microbial growth just after inoculation. Therefore, the pure aroma compound, control film and films containing carvacrol were deposited in the Petri dish lid at the same time it was inoculated ( $t_0$ ). For the second experimental series, film or aroma compound was deposited in the Petri dish lid after a previous incubation phase. The length of this initial incubation phase ( $t_1$ ) was defined as the time needed to obtain macroscopically visible colonies. In work performed by Moundanga (2012) it was determined as 4 h for *E. coli* and *B. subtilis*, 6 h for *S. Enteritidis* and *L. innocua*, 12 h for *L. plantarum* and 24 h for *P. camemberti*. This period corresponds approximately to the early exponential phase and it was chosen to obtain colonies which had not yet reach their final size. Indeed, it was necessary that after  $t_1$  bacterial colonies were still able to grow over time when placed in favourable conditions (control without film neither antimicrobial compound) to easily underscore a possible inhibition of growth due to the compounds tested. This experimental design allowed checking if the concentration of the antimicrobial compound in the vapour phase was high enough to inhibit the growth of already formed colonies. Two inoculated controls, one sealed with Parafilm<sup>®</sup> and the other one without Parafilm<sup>®</sup>, and both, with neither carvacrol nor film, were prepared. This was done to ensure that airtighting of Petri dish does not influence the growth of the inoculated strains (possible anoxia). The control with Parafilm<sup>®</sup> was used as reference for the microbial growth. Besides, film without aroma compound was used to exclude the potential activity of other volatile ingredients from the film such as acetic acid or water. Furthermore a non inoculated control was prepared to exclude any contamination in the experimental system. Every test was replicated at least twice.



### 3.6.3.1. Size of colonies

To estimate the relative growth of cells in presence of the antimicrobial compound compared to the control, the radial diameter (cm) of colonies was followed. Measurements were carried out during seven days of incubation. Plates were photographed to determine the evolution of colony size over time and pictures were analysed using Photoshop® software. The average diameter of 20 colonies was used as a mean result. For the second experimental series (exposure to antimicrobial vapours after an incubation phase), colony size diameter ratio  $d_x/d_1$  was calculated where  $d_x$  is the average colony size diameter and  $d_1$  the initial colony size diameter at the time of colony film exposure.

### 3.6.3.2. Cellular counts

A whole colony was harvested from the nutrient agar plate with a sterile inoculating loop and cells were re-suspended in 1 mL of physiological saline solution (0.9% w/w). In the case of the pure aroma compound, harvested colonies were those closest to the centre of the plate and all at equal distance from the aroma drop. Counts were then performed using a Malassez counting chamber to determine the total number (N) of cells in the colony. Colony-forming unit (CFU) were also counted to estimate the number of cultivable cells in the same colony. Cultivability (C) was calculated as follows:

$$C(\%) = \frac{CFU}{N} \cdot 100 \quad (Eq. 3.33.)$$

## **3.7. Sensory evaluation**

Evaluation of sensory impact was performed in collaboration and partially realised by Ms. Karen Joly, Mr. Jean-Marie Delaitre and Ms. Anne Endrizzi from Welience.

### Food samples

Jambon blanc (Chazal), Pâté en croûte (Chazal), Terrine (Salaisons Dijonnaises), Jambon persillé (Salaisons Dijonnaises) and Feta (Lactalis) were directly supplied from factory (Fig. 3.19.).



**Figure 3.19.** Five food products used in this study.

Freshly delivered products were repackaged under the sterile conditions with three different chitosan/carvacrol coated polyethylene films (Fig. 3.20.a). 150-200 g of each product was placed in the previously sterilized container (with  $H_2O_2$  and dried prior conditioning) and closed with the active film. This allowed controlling the sample mass and free volume in container to assure that all samples were conditioned in a same manner.

Samples were grouped by two, placed in a bigger container (Fig. 3.20.b) and packed under controlled atmosphere. The packing conditions were as following: ratio  $CO_2/N_2$  50/50, pre-vacuum of 20 mbar and re-injection of gases at 600 mbar. During the conditioning, a great attention was given that no direct contact between food and film occurred. This way we were sure that the antimicrobial action was through the headspace only. Moreover, the sensory impact could only be due to exposure to carvacrol vapours released from active films. Two control tests for each product were made. The first one was the originally supplied packed food, while the second one, food re-packed with non active film (Wipak, BIAXER 65 XX PEEL) served as a control of eventual microbial contamination during reconditioning. All samples were kept at 4°C before tasting (Fig. 3.20.c). All conditioning was performed in Welience, Dijon.

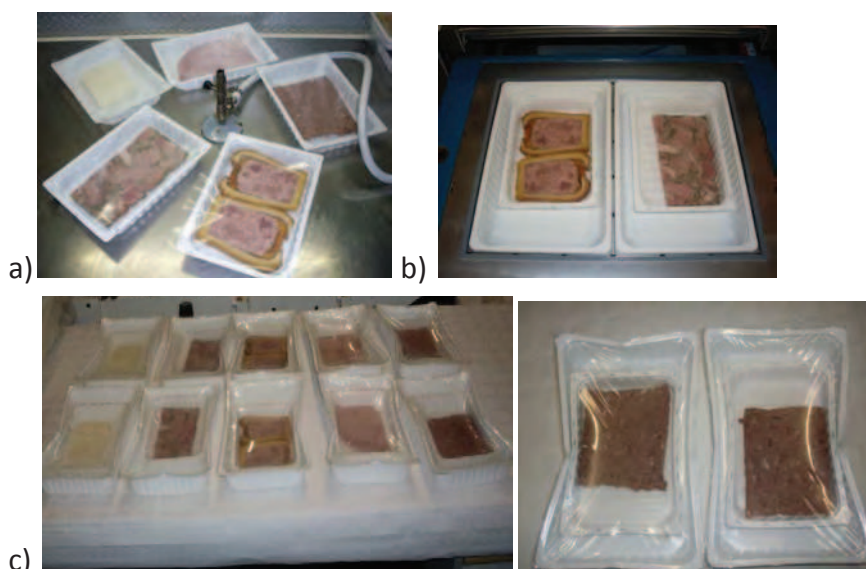


**Figure 3.20.** Re-packaging of food products under sterile conditions and using active or control films.

#### Triangle test-theoretical background

The triangle test is one of the commonest tests used in the sensory analysis. The basic procedure is that each panellist is presented with three samples – two packed under one film and one under another film – and is asked “Which one is the odd sample?”. If sample A is being tested against sample B, there are six possible permutations for the order in which the samples may be presented. These are:

AAB ABA BAA ABB BAB BBA

As far as possible, one-sixth of the panel should be presented with each permutation to avoid bias. Their response will either be correct or incorrect. In order to analyse the data statistically the number of correct responses is compared with the number which would theoretically be expected to have occurred by chance. This method is effective for determining that either a perceptible difference results (triangle test for difference) or that a perceptible difference does not result (triangle test for similarity) when for example, a change is made in ingredients, processing, packaging, handling or storage. In accordance, the difference is defined as a situation in which samples can be distinguished on their sensory properties, while the similarity is a situation in which any perceptible differences between the samples are so small that products can be used interchangeably.  $\alpha$  risk applies to a probability of concluding that a perceptible difference exists when one does not.  $\beta$  risk is probability of concluding that no perceptible difference exists when one does.

### Sensory evaluation

A group of 11-15 panellists, consumers (men and women) of typical burgundy products with small previous experience, evaluated the smell, visual appearance, taste and general acceptability of the samples. The purpose of sensory evaluation was to check that there are no visual difference between the standard products and repackaged products under classic film and to assess the presence or absence of a significant difference between the standard products repackaged in classic film and standard products repackaged under active film. The former was done to assure the absence of contamination during repackaging.

In evaluation of odour and taste differences triangular tests were conducted in specially equipped room (Welience, Dijon). For each treatment and sampling date, the five products were evaluated by each judge. At each storage time, samples were freshly opened before the degustation and each product was subjected to a panel of testers to assess the sensory quality. The coded samples were presented and they were tasted in a different order for each subject. Each person had to rinse their mouths between each test with water and bread. Furthermore, a sensory evaluation based on descriptive analysis was carried out in order to better understand how the panellists perceive odours and/or differences between the samples.

### **3.8. Statistical analysis**

The statistical analysis of data was performed through variance analysis (ANOVA) using Xlstat-Pro (win) 7.5.3. (Addinsoft, New York). The data were ranked and statistical differences were evaluated on the ranks with a one-way analysis of variance (ANOVA) and Tukey's multiple comparison tests. The principal component analysis (PCA) was used for detailed examination of the data. In all cases, a value of  $p < 0.05$  was considered to be significant.



*Chapter 4*

*How composition and process parameters affect  
volatile active compounds in biopolymer films*

---

Publication: **Mia Kurek**, Emilie Descours, Kata Galić, Andrée Voilley, & Frédéric Debeaufort (2012).

Carbohydrate Polymers, 88, 646-656.

Unpublished part of this chapter:

4.1.2. Particle size distribution



Active packaging film is one of the top subjects in today's food processing industry. The activity of the active film depends on the quantity and availability of the active compound. When we are speaking about the volatile compounds such as essential oils or their components, we must consider that some of these will be lost during film processing. While there is a lot of a research done in verifying the antimicrobial activity of essential oils incorporated in the bio-based polymers, very little published data exist on the influence of processing parameters, especially on the stability and retention of plant essential oils into bio-based/edible films and coatings. Authors mostly report the initial amount of antimicrobial volatile substances added in the film-forming solution instead of the real concentration in the films. Quantifying compounds mobility is a crucial element in understanding the mechanisms of release in the headspace or in contact with food. Therefore, the retention of the active/antimicrobial compound is one of the most important features of active biopolymer film processing.

Essential oils are regarded as alternatives to chemical preservatives, and their use in foods meets the demands of consumers for minimally processed natural products. Depending on the nature and strength of the binding, release of aroma compounds in the gas phase will be more or less decreased (Desobry and Debeaufort, 2011).

One way of investigating the retention (or release) of aroma compounds by polysaccharide-based matrices is to measure the gas/matrix partition coefficient ( $K$ ). This parameter describes the distribution of volatile compounds between the gas phase and the solid matrix, after equilibrium is reached (Boland et al., 2004). So, knowledge of this property must be studied to allow the estimation of the volatile's concentration in the packaging headspace. Several parameters should be taken into account. These include the type and the concentration of components along with the nature and the physico-chemical properties of the aroma compounds e.g. volatility and hydrophobicity (Seuvre et al., 2006).

This chapter presents the influence of drying parameters (temperature and relative humidity) and film formulation (polymer, casting solvent and additives) on carvacrol retention and its mass partition coefficient. The drying kinetic, the properties of film forming solution, as well as physical film properties, were studied in order to develop chitosan films as vehicles for controlling aroma compound retention and release for further packaging applications.



## 4.1. Characterization of the film forming solutions

### 4.1.1. Rheological behaviour of film forming solutions

Viscosity can influence drying kinetics and aroma compound retention. The experimental flow curves of film forming solutions (FFS) between 0 and 250 s<sup>-1</sup> (Fig. 4.1.) have been very closely fitted by Ostwald de Waale model ( $r > 0.99$ ). The addition of ethanol changed the rheological properties of solution. Hydroalcoholic acid solutions showed more pronounced pseudoplastic behaviour ( $n$  value from 0.82 to 0.84), whereas a less shear thinning behaviour was observed for aqueous acidic media ( $n$  value from 0.93 to 0.95). A viscosity decrease, attributed to the conformational change of the macromolecular chains, was reported (Vargas et al., 2011; Kasaai et al., 2003; Bonilla et al., 2012). Higher alcohol and chitosan content resulted in greater viscosity. Solvent polarity changed the organisation of chitosan chains and therefore viscosity increased. In more concentrated hydroalcoholic acidic FFS, structuring degree was greater, so was dynamic viscosity. Those associated structures formed macro clusters in concentrated polymer solutions (Uspenskii et al., 2010).

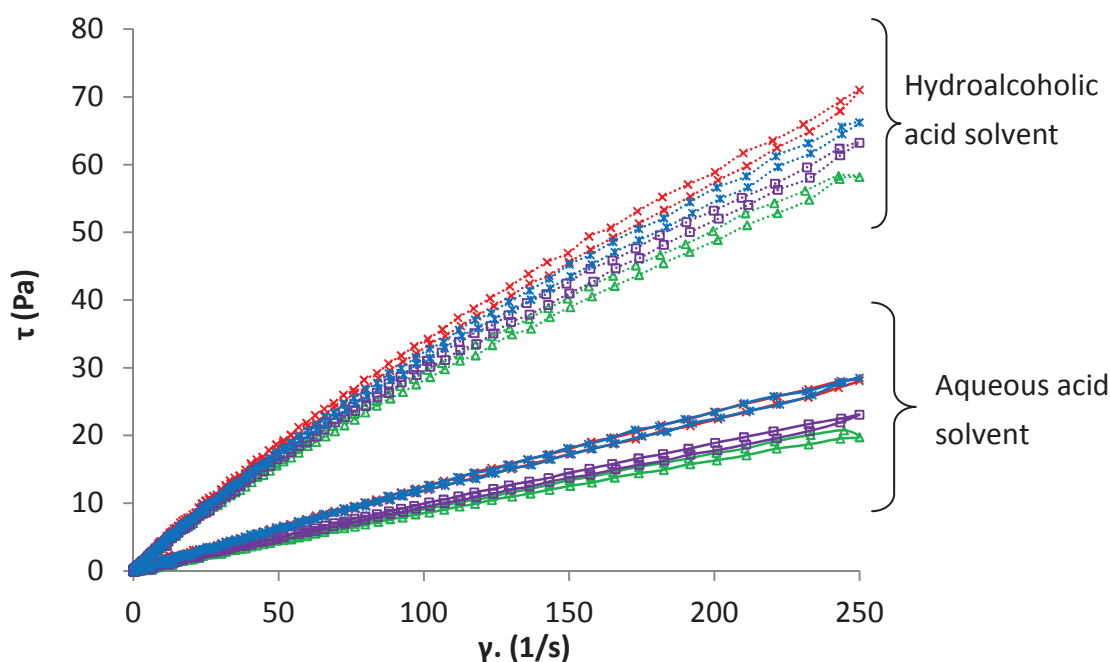


**Figure 4.1.** Typical flow curves, at 20°C, of the film forming solutions prepared in the aqueous acidic media (continuous lines) or in the hydroalcoholic acid media (dashed lines).

× chitosan, △ chitosan and carvacrol, □ chitosan, carvacrol and glycerol, \* chitosan and glycerol.

The incorporation of carvacrol, as a non miscible compound, significantly reduced viscosity in both systems: from 173 to 111 mPa/s and from 683 to 633 mPa/s for aqueous acidic and hydroalcoholic FFS, respectively. Indeed, the adsorption of polymer on the droplet surface favours a decrease of its effective thickening concentration in the aqueous media (Bonilla et al., 2012). In aqueous acid solutions glycerol interfered with the polymer chains, and provoked a decrease in chitosan viscosity. Therefore K values increased (from 0.11 to 0.13). This effect was not observed in the hydroalcoholic solutions. Different solvents probably affect the drying and the final chitosan film structure in the same way as FFS properties, which govern film functional properties.

#### 4.1.2. Particle size distribution

*(Unpublished part of this chapter)*

Stability of the film-forming solution greatly affects the final microstructure of film matrix, which might impact its functional properties. In this sense, characterization of some dispersion stability factors could help to better understand the differences in the physico-chemical characteristics of the final film. Scanning electron microscopy can be used to determine structure of suspensions/solutions/emulsions, but it does not quantify stability and dispersion of particles in the system. Instead, laser diffraction particle size analysis allows determining and quantifying the size and the distribution of particles in FFS, or after solubilisation/dispersion of films in FFS solvent.

This study aimed to verify the influence of two solvents (aqueous acetic acid and hydroalcoholic acetic acid), glycerol and carvacrol on the particle size distribution in different film formulations. Mean particle diameters ( $d_{3,2}$  for characterization of the fine and spherical particles, and  $d_{4,3}$  for larger particles with irregular form like aggregates) and type of distribution are given in Table 4.1.

Aqueous acetic acid favoured solubilisation of chitosan flakes and then no peaks were observed in CSA-FFS and CSA film granulograms. On the contrary, in the presence of ethanol, one part of chitosan particles were swollen and not completely solubilised. This means the film-forming “system” is probably a colloidal suspension instead of a solution as observed for CSA. Thus, chitosan self-aggregates could be formed by intra- and inter-molecular hydrophobic interactions (Kumirska et al., 2011). This behaviour depends mainly on the distribution of the particles in the FFS, its viscosity and rheological properties. Indeed, viscosity of FFS in hydroalcoholic acid solvent was significantly higher than those in aqueous acid solvent (Fig. 4.1.).

**Table 4.1.** Mean diameter ( $d_{3,2}$  and  $d_{4,3}$ ) and type of particle size distribution before (FFS) and after film drying (film).

Aqueous acid solvent				Hydroalcoholic acid solvent			
	$d_{3,2}$	$d_{4,3}$	Distribution		$d_{3,2}$	$d_{4,3}$	Distribution
CSA	FFS	nd	nd	CSE	FFS	141.5±5.7	419.9±76.1 multi
	film	nd	nd		film	602.7±9.1	752.1±21.8 mono
CSACVC	FFS	285.2±69.9	322.2±21.2 multi	CSECVC	FFS	365.9±52.5	392.1±32.2 mono
	film	36.5±19.1	343.4±257.8 multi		film	22.0±1.1	119.7±11.1 multi
CSAGLY	FFS	36.4±16.11	229.4±137.1 multi	CSEGLY	FFS	55.4±28.9	329.9±92.2 multi
	film	391.7±6.75	712.1±11.1 mono		film	513.6±26.4	780.0±23.7 mono
CSAGLYCVC	FFS	259.6±69.9	343.2±47.6 multi	CSEGLYCVC	FFS	259.4±98.8	655.9±92.5 multi
	film	379.2±20.5	552.6±21.7 mono		film	444.9±16.6	737.7±19.0 mono

nd=not detected; multi=multimodal; mono=monomodal

To confirm the formation of aggregates, samples were additionally solubilised in Triton X-100. By interfering between chitosan chains, this non ionic surfactant, contributed to the repulsions between chitosan chains and prevented the aggregation. Thus lower  $d_{3,2}$  and multimodal distribution corresponding to fragmented chitosan aggregates were observed (Fig. 4.2.a).

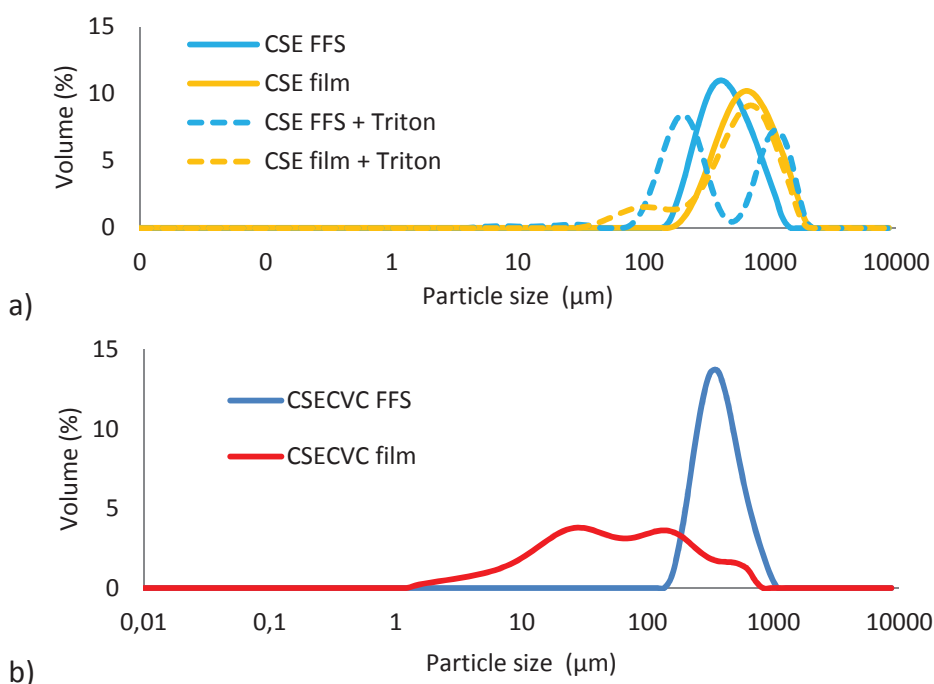


**Figure 4.2.** Particle size distribution of a) chitosan film forming solution and film before and after addition of Triton X-100<sup>1</sup>; b) chitosan/carvacrol film forming solution and film. <sup>1</sup>Triton X-100 polyethylene glycol p-(1,1,3,3-tetramethylbutyl)-phenyl ether

In glycerol containing FFS the size distributions were multimodal, probably due to droplet flocculation that occurred after the homogenization process. Unlike, after drying, in every case monomodal distribution was observed and the average size diameter was increased (Table 4.1.). This was attributed to the coalescence phenomenon.

When only carvacrol was added in the colloidal suspension, the average diameter was higher than in the simple FFS (CSE-FFS). It is likely that only a small portion of carvacrol molecules was well dispersed. It was probably due to the insufficient quantity of free chitosan chains to ensure the interfacial adhesion of particles (Bonilla et al., 2012). It seemed that carvacrol had a stabilizing role during drying and influenced the structuring of the chitosan matrix. Film drying led to a significant ( $p < 0.05$ ) reduction of the particle sizes, as compared to FFS, as can be seen in Table 4.1. and Fig. 4.2.b. In the literature, chitosan has been used to stabilize oil in water emulsions of food-grade sunflower oil (Rodriguez et al., 2002), film-forming dispersions containing oleic acid (Vargas et al., 2011) and essential oils such as bergamot oil (Sanchez-Gonzales et al., 2010). Droplet size is a determining factor for stability and in FFS it affects viscosity. In dry film it affects functional film properties. After re-solubilisation of dry films, carvacrol droplets diameter was found to be around 0.2 and 2  $\mu\text{m}$ . This was also confirmed by microscopic observations (Chapter 7, Fig. 7.3.).

However, in the presence of both glycerol and carvacrol, particle size distribution was the same as for films without carvacrol. Carvacrol seems to lose its stabilizing/structuration properties. This was attributed to its great affinity for (solubility in) glycerol and therefore it couldn't anymore stabilize the emulsion. Moreover, in dry films observed by ESEM, carvacrol droplets were hardly visible, which confirms our hypothesis (Chapter 8, Fig. 8.3.).

To conclude, ethanol allows faster drying and better solubilisation of carvacrol, while acetic acid brings the acidity which allows the better solubilisation of chitosan. The effect of drying of the film forming solution has favored, firstly, the aggregation (appearance of new populations of particles that disappear of big ones consecutively to the addition of Triton X-100) and, secondly coalescence of particles (changes from multimodal to monomodal distribution).

## **4.2. Drying process**

Drying is considered as one of the most important steps during biopolymer film preparation (Arvanitoyannis et al., 1998; Kaya and Kaya, 2000; Sothornvit and Krochta, 2005). During drying, all volatile agents, including solvents and aromas are progressively evaporated. Consequently, as solvent removal increases, the film dry matter increases too. Increasing drying temperature boosts the volatilization of the volatile compounds present in the film forming structure. Thus drying time was shorter (Tables 4.2. and 4.3.). Drying temperatures seemed to be an important factor influencing both physico-chemical film properties and carvacrol retention.

Hydrophobic carvacrol is naturally immiscible in hydrophilic biopolymer solutions. Ethanol was used to enhance carvacrol dissolution, to obtain better mixing with aqueous acetic acid and to decrease drying time. After ethanol is evaporated, the remaining system is a hydrophilic film containing hydrophobic substance. It is important to realize that, naturally, such a system has a limited uptake. Carvacrol was unavoidably evaporated with solvents. But, the overall mechanism of aroma compound loss is complex because there is simultaneously a change in the biopolymer viscosity, a change in the physical state from liquid to solid, a change in polarity due to the differential evaporation rate between volatiles, a probable change in the interaction nature and strength, and finally, a change in the macromolecular structure as here after suggested.

In the crystal, chitosan chains are packed in an antiparallel way. In the salt solutions with acetic acid, called Type II salts, the chitosan molecule takes up a relaxed two fold helix composed of asymmetric units of tetrasaccharide. Since water molecules are included in the crystal, they tend to enter between these sheets and stabilize the crystal structure. Type II crystals change to the annealed chitosan polymorph by spontaneous water-removing action of the acid (Ogawa et al., 2004). Amorphous structures that might be obtained by solvent casting greatly contributed to the matrix relaxation and carvacrol release. The polarity of hydrophobic carvacrol molecules was changed after solubilisation and dispersion in hydroalcoholic FFS. Thus, more molecules were locked in the chitosan network. Solute polarity is an important factor in transfer process (Arora et al., 1991; Matsui et al., 1992). Therefore, as ethanol evaporates faster than water, in the beginning of the drying, carvacrol losses were more pronounced.

Table 4.2. Colour parameters of chitosan films influenced by the composition. Samples were dried at 20°C and 30% RH.

Film	Chitosan dry matter (g)	Glycerol % (w/p.d.m.)	Nanoclays or arabic gum % (w/p.d.m.)	Drying time (h)	L*	a*	b*	ΔE
Chitosan film without carvacrol (CSA)	1	0	0	14	96.40 <sup>b</sup>	-0.97 <sup>c</sup>	4.40 <sup>g</sup>	2.64 <sup>h</sup>
	2	0	0	14	96.30 <sup>b</sup>	-1.23 <sup>c,d</sup>	5.00 <sup>g</sup>	3.29 <sup>h</sup>
	3	0	0	18	96.10 <sup>b,c</sup>	-1.37 <sup>c,d</sup>	5.23 <sup>g</sup>	3.55 <sup>h</sup>
Chitosan film with carvacrol (CSACVC)	1	0	0	14	97.57 <sup>a</sup>	-0.93 <sup>c,d,e</sup>	5.03 <sup>g</sup>	5.59 <sup>g</sup>
	2	0	0	14	96.33 <sup>b</sup>	-1.23 <sup>c,d</sup>	5.27 <sup>g</sup>	5.81 <sup>g</sup>
	3	0	0	18	94.90 <sup>d</sup>	-1.27 <sup>c,d</sup>	5.60 <sup>f,g</sup>	6.13 <sup>f,g</sup>
Chitosan film with carvacrol and glycerol (CSACVGLY)	1	30	0	14	94.07 <sup>d</sup>	-1.73 <sup>d,e,f</sup>	14.20 <sup>d</sup>	12.43 <sup>d</sup>
	2	30	0	14	88.37 <sup>g</sup>	-1.80 <sup>d,e,f</sup>	23.97 <sup>b</sup>	22.16 <sup>b</sup>
	3	30	0	18	94.43 <sup>d</sup>	-1.77 <sup>d,e,f</sup>	14.43 <sup>d</sup>	12.66 <sup>d</sup>
Chitosan film with carvacrol (CSACVC) and nanoclays	1	0	10	12	NA	NA	NA	NA
	2	0	10	12	90.37 <sup>f</sup>	-0.83 <sup>c</sup>	16.47 <sup>c</sup>	16.8 <sup>c</sup>
	3	0	10	13	NA	NA	NA	NA
Chitosan film with carvacrol, glycerol (CSACVGLY) and nanoclays	1	30	10	14	89.00 <sup>g</sup>	-2.17 <sup>f</sup>	26.53 <sup>a</sup>	26.83 <sup>a</sup>
	2	30	10	14	85.00 <sup>h</sup>	0.67 <sup>b</sup>	23.80 <sup>b</sup>	24.11 <sup>b</sup>
	3	30	10	16	85.37 <sup>h</sup>	0.43 <sup>b</sup>	23.57 <sup>b</sup>	23.87 <sup>b</sup>
Chitosan (CSA)/arabic gum blends	3	30	50	12	91.70 <sup>e</sup>	7.20 <sup>a</sup>	17.00 <sup>c</sup>	16.86 <sup>c</sup>
	3	40	50	12	95.07 <sup>c,d</sup>	-1.93 <sup>e,f</sup>	9.70 <sup>e</sup>	10.11 <sup>e</sup>
	3	50	50	13	96.63 <sup>a,b</sup>	-1.93 <sup>e,f</sup>	7.47 <sup>f</sup>	7.92 <sup>f</sup>

NA - not measured because produced films were too brittle <sup>a-h</sup>Different superscripts within a column indicate significant differences among formulations (p<0.05). p.d.m = polymer dry matter

**Table 4.3.** Influence of drying temperature on the colour parameters and the drying time of the chitosan based films. All films were plasticized with glycerol (30% w/p.d.m.) and dried at 30 % RH.

Film	Drying temperature (°C)	Drying time (h)	L*	a*	b*	ΔE
Chitosan (CSA) 1% (w/p.d.m.)	20	14	94.07 <sup>b</sup>	-1.73 <sup>f</sup>	14.20 <sup>g</sup>	12.42 <sup>h</sup>
	60	1.75	94.07 <sup>b</sup>	-1.50 <sup>f</sup>	13.30 <sup>g</sup>	11.50 <sup>h</sup>
	100	0.75	94.13 <sup>b</sup>	-1.53 <sup>f</sup>	13.20 <sup>g</sup>	11.41 <sup>h</sup>
Chitosan (CSA) 2% (w/p.d.m.)	20	14	88.37 <sup>d</sup>	-1.80 <sup>f</sup>	23.97 <sup>d</sup>	22.16 <sup>d,e</sup>
	60	4.5	86.33 <sup>e</sup>	-1.63 <sup>f</sup>	22.07 <sup>d,e</sup>	20.25 <sup>e,f</sup>
	100	0.75	84.37 <sup>f</sup>	-1.33 <sup>f</sup>	20.13 <sup>e</sup>	18.30 <sup>f,g</sup>
Chitosan (CSA) 3% (w/p.d.m.)	20	18	94.43 <sup>a,b</sup>	-1.77 <sup>f</sup>	14.43 <sup>g</sup>	12.66 <sup>h</sup>
	60	1.75	96.30 <sup>a</sup>	-1.33 <sup>f</sup>	7.23 <sup>h</sup>	5.48 <sup>i</sup>
	80	1.5	96.17 <sup>a</sup>	-1.33 <sup>f</sup>	6.83 <sup>h</sup>	7.31 <sup>i</sup>
	100	0.75	96.23 <sup>a</sup>	-1.40 <sup>f</sup>	6.50 <sup>h</sup>	4.78 <sup>j</sup>
Chitosan (CSA)/Arabic gum blends (50:50 w/w)	20	12	91.70 <sup>c</sup>	7.20 <sup>d</sup>	17.00 <sup>f</sup>	23.09 <sup>d</sup>
	60	3.5	75.27 <sup>g</sup>	7.60 <sup>d</sup>	49.07 <sup>b</sup>	47.85 <sup>b</sup>
	80	1	71.40 <sup>h</sup>	10.67 <sup>c</sup>	57.50 <sup>a</sup>	56.69 <sup>a</sup>
	100	0.5	45.57 <sup>j</sup>	21.53 <sup>a</sup>	27.33 <sup>c</sup>	33.50 <sup>c</sup>
Chitosan (CSA) 3% (w/p.d.m.) with nanoclays (10% w/p.d.m.)	20	14	85.00 <sup>e,f</sup>	0.67 <sup>e</sup>	23.80 <sup>d</sup>	24.11 <sup>d</sup>
	60	3	85.37 <sup>e,f</sup>	0.43 <sup>e</sup>	23.57 <sup>d</sup>	23.87 <sup>d</sup>
	100	0.75	63.97 <sup>i</sup>	14.37 <sup>b</sup>	47.57 <sup>b</sup>	47.84 <sup>b</sup>

<sup>a-i</sup> Different superscripts within a column indicate significant differences among formulations (p<0.05)

Moisture and carvacrol content in the sample in different intervals were determined (Fig. 4.3.).

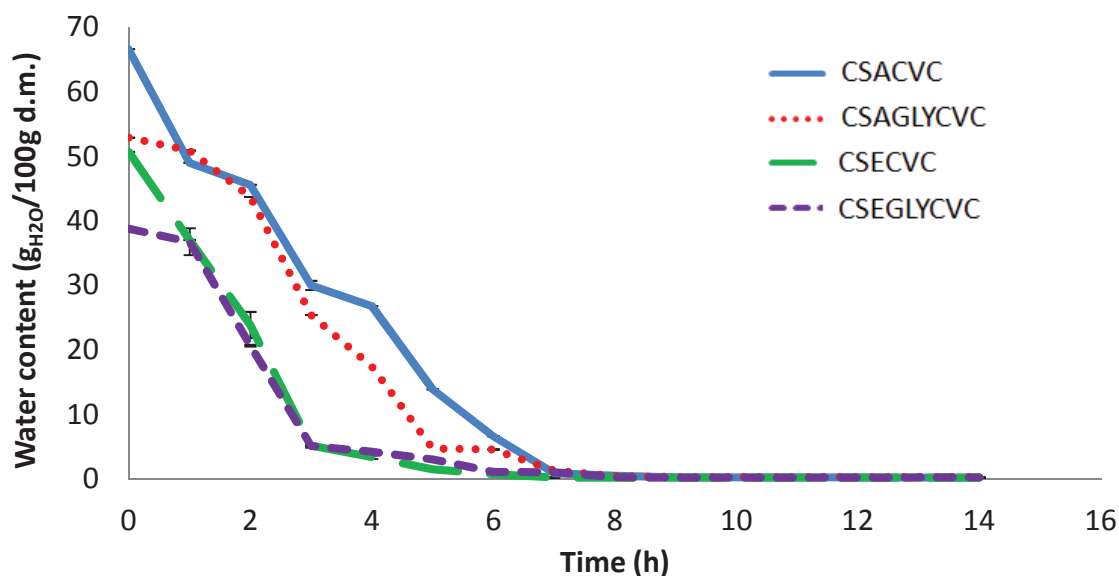
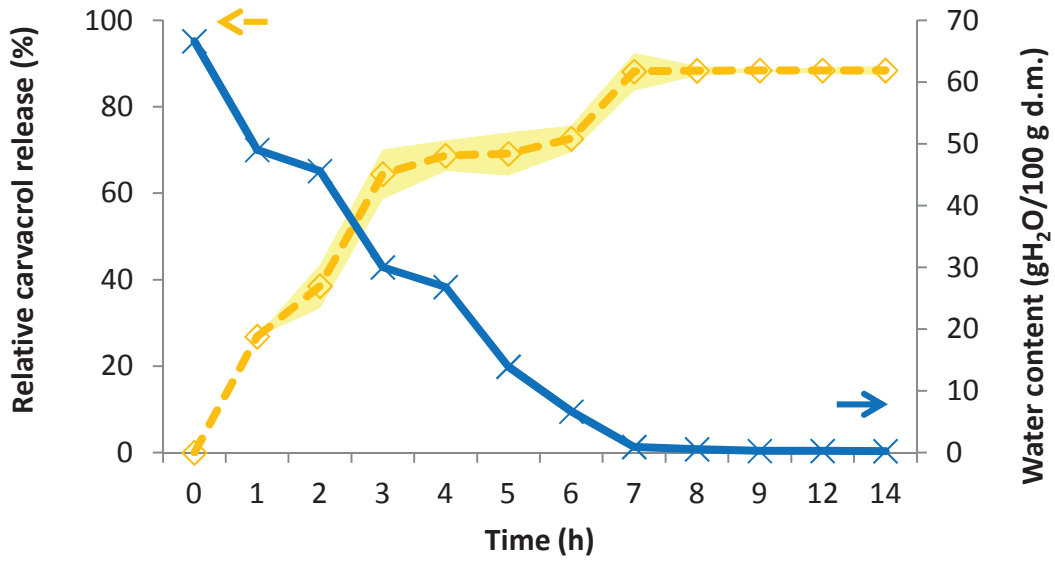


Figure 4.3. Drying curves of the chitosan solutions.

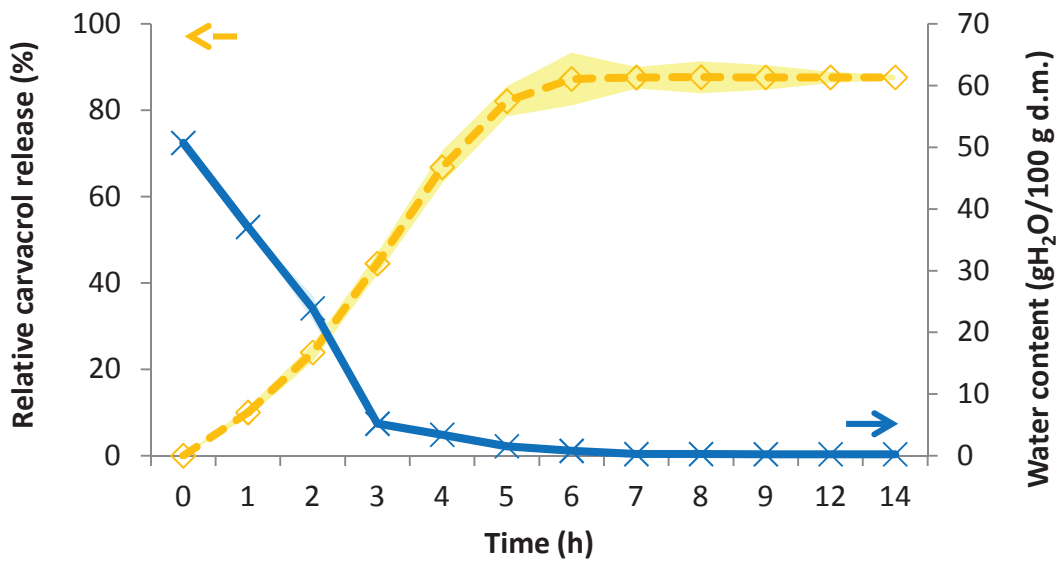
The time required to obtain constant film weight for hydroalcoholic and aqueous acidic solutions was 6 and 7 hours, respectively (Fig. 4.3). To ensure that weight changes were negligible, films were left in the drying chamber up to 14 h. Generally, the loss of volatiles was greatly influenced by the water content in drying film (Fig. 4.4.). Therefore, there was no significant change in carvacrol content when films were left up to 14 h. Mayachiev et al. (2010) reported that at ambient temperature it took 52, 50 and 47 h for 1, 2 or 3% Indian gooseberry extract to obtain dry films, respectively. Theoretically, mass transfers have a constant rate at the beginning and they slow down after reaching critical moisture content. At high moisture levels, the carvacrol rate loss from a drying solution is mainly dependent on its volatility. Higher water uptake resulted in matrix plasticization and then its release was facilitated. Soottitantawat et al. (2005) reported that the release rate of menthol increased, upon increasing water activity. Glycerol attracts and deters water molecules so the shape of the drying curves was changed. The evaporation rate is proportional to the saturated water vapour pressure above the solution surface. This pressure is considered as constant, throughout the drying process until the final stages, when the pressure is reduced. On the contrary, curves do not display a linear trend (Figs. 4.3. and 4.4.).



A)



B)



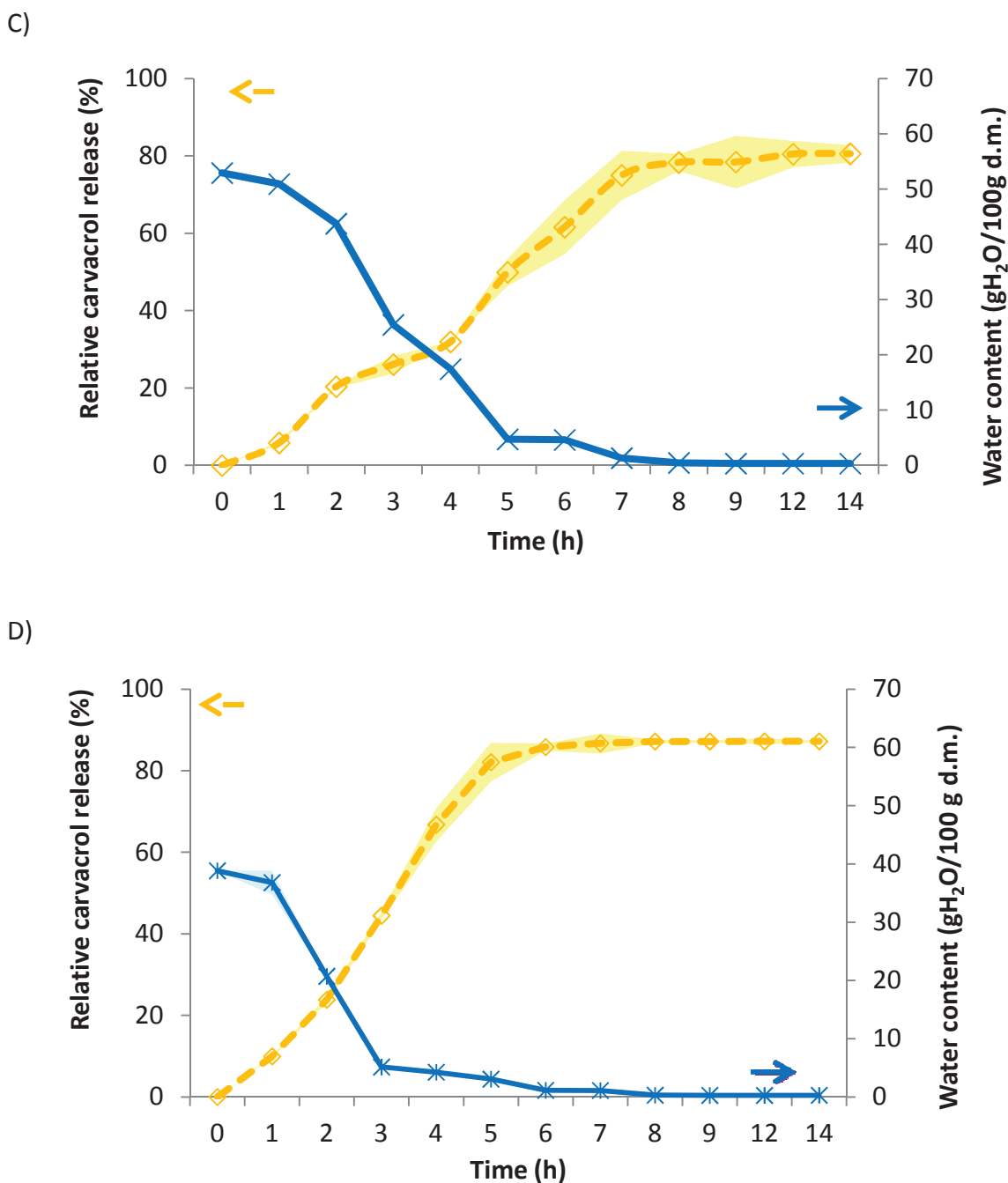


**Figure 4.4.** Water content (g<sub>H<sub>2</sub>O</sub>/100 g d.m.) and relative carvacrol release (% of initially added amount) from chitosan based films during drying. A) aqueous acidic media (CSA), B) hydroalcoholic media (CSE), C) aqueous acidic media with glycerol (CSAGLY), D) hydroalcoholic media with glycerol (CSEGLY). (The coloured zones correspond to standard deviation of the curves).

Due to the internal heating phenomenon, saturated pressures became larger and thus led to non-linear slopes of hydroalcoholic and aqueous acid FFS curves, respectively. Over the time, structural change in the thin layer of FFS modifies diffusion which disturbs the evaporation rate. According to Buonocore et al. (2003) the release of an active compound from the polymer network took place in several steps. Correspondingly, carvacrol loss depended on intermolecular migrations between chitosan chains, its solubility and its diffusion towards the matrix surface. During the first hour, less aroma compound was released from plasticized FFS. The water evaporation rapid rate was delayed for about 2 h (Fig. 4.4.C, D). At the end, glycerol didn't have any significant effect on the overall drying period. The gelatinization technique and the drying method influenced the tapioca starch/glycerol network characteristics and caused changes in physical film properties (Flores et al., 2007). Below gelation point, more than 50% of initially added carvacrol was lost (Fig. 4.4.). These values correspond to ~10% of water in sol/gel. Indeed the authors reported that at gel point, the water content was below 15% (Batista et al., 2007). Once dried, the plasticized chitosan films had more water than the unplasticized ones. Similar results were mentioned by Ziani et al. (2008). At low moisture contents the diffusion coefficient became a determining loss factor.

### **4.3. Film macroscopic appearance**

The film appearance was studied by colour measurement according to Ghorparde et al. (1995) and was done for the targeted application and not for the physico-chemical reactivity. Film transparency is a key to good film acceptance by users. Therefore, two different aspects of colour changes have been measured as a function of the composition and the drying temperature. Results are given in Tables 4.2. and 4.3.

CSA and CSACVC films presented good transparency. This was indicated by high lightness values ( $L^*$ ) that ranged from 94.9 to 96.4 (Tables 4.2. and 4.3.). A significant decrease in this parameter was found when both glycerol and NC were incorporated (85.4, 85.0 and 89.0 for CSA 3, 2, or 1 % (w/v) respectively).  $L^*$  was higher than that of chitosan-based nanocomposites reported in previous studies (66.8 and 85.8) (Rhim et al., 2006). It was probably because of different types of NC. Still, it was in the same range as obtained by Casariego et al. (2009). Martins et al. (2010) found that

incorporation of  $\alpha$ -tocopherol in chitosan based films led to a decrease in lightness (from 95.4 to 92.3) and an increase in greenness ( $a^*$  decreased from 3.54 to -1.42). The  $b^*$  value is the parameter describing the natural colour of chitosan, and it was the chromatic coordinate that influenced the total colour difference.  $b^*$  increased from 5.94 to 15.73 and it indicated the yellowness of the CSA films. The yellowness was intensified with chitosan concentration and addition both of glycerol and arabic gum.

As an indicator of global colour changes,  $\Delta E$  was calculated from other colour parameters. Increase of  $b^*$  and  $\Delta E$ , in the presence of NC was previously reported (Casariego et al., 2009; Park et al., 2002). Again, this value showed more changes with increasing temperature, especially when CSA was blended with AG. Srinivasa et al. (2004) observed an increase in yellowness in oven-dried chitosan films. Furthermore, when the casting temperature was increased, the films presented different yellow and green colour changes (lower  $b^*$  and  $a^*$ ). These changes may be attributed to oxidation, nonenzymatic browning or Maillard reaction between protein traces and reducing sugars from AG but no chemical analysis has been done to confirm this hypothesis. According to Deng et al. (2009) and Kanatt et al. (2008), glycerol incorporated in chitosan may be oxidized so the products could react with chitosan through the Maillard reaction. In Tables 4.2. and 4.3. decrease in  $L^*$  value at higher temperatures can be due to the presence of glycerol and not NC.  $L^*$  changed remarkably for CSA/AG blends (75.3, 71.4 and 45.6 for 60, 80 and 100°C respectively) and films with NC (85.4 and 63.9 for 60 and 100°C, respectively). Overall colour changes were more intense with higher amounts of acetic acid for chitosonium acetate films heated for 2 h at 120°C (Kam et al., 1999).

#### **4.4. Film properties as a function of composition and drying conditions**

##### **4.4.1. Influence on mass partition coefficient**

Usually, the mass partition coefficient  $K_{\text{mass}}$  (ratio between the aroma compound concentration in the air and the aroma compound concentration in the film) is inversely proportional to the retention capacity during processing.  $K_{\text{mass}}$  can be related to carvacrol retention by chitosan based films during film processing (casting plus drying) (Fig. 4.5.).

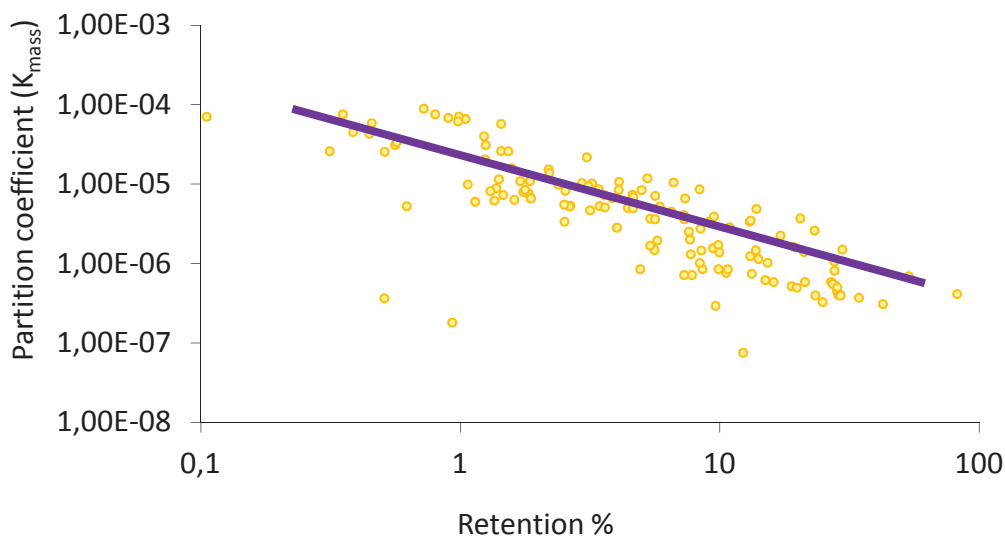
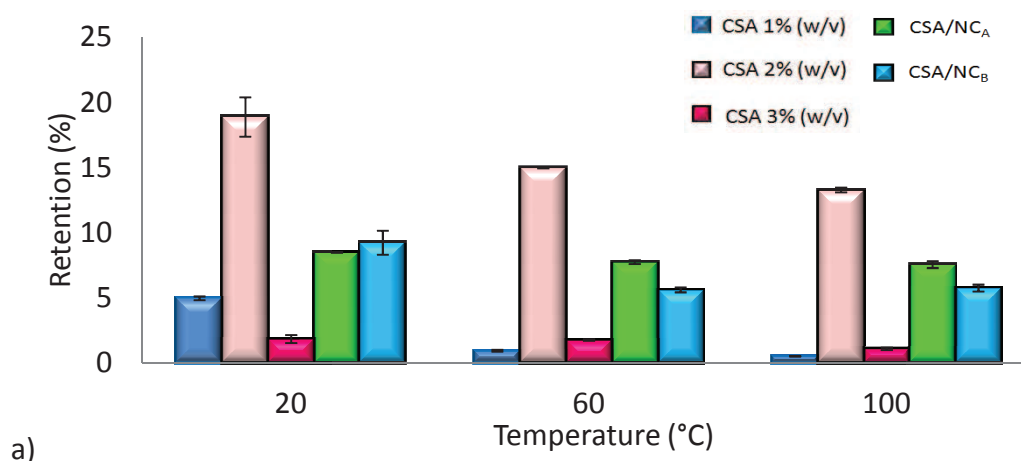


**Figure 4.5.** Relationship between the carvacrol retention during the film processing and the air/film partition coefficient during the film storage.

Actually, more than 200 formulations in drying temperature interval from 20 to 100°C and various humidities (from 10 to 80% RH) were tested. Formulations included two polymers (chitosan and arabic gum) and various additives (at various concentrations) as aroma compound retention enhancers such as glycerol, polyethylene glycol, Tween 20, lecithin and nanoclays. The partition coefficient of an aroma compound between the headspace and the film matrix is influenced by many factors (e.g. volatility, polarity, water solubility and temperature) (Bangs and Reineccius, 1982; Saravacos and Moyer, 1968). The composition, the physico-chemical properties of the matrix, as well as the intra-network interactions can change the thermodynamic behaviour of volatile molecule reflecting its ability to reach a gaseous phase. Only free dissolved molecules exert a vapour pressure and therefore, they can influence  $K_{mass}$  (de Roos, 2003). The principal component analysis (PCA) was done to better identify the main parameters of the composition/process which influenced carvacrol retention, drying time and  $K_{mass}$ . It appeared that carvacrol retention in chitosan based films increased with decreasing drying time, drying humidity and NC (axis representation and data of the PCA analysis not given). A negative correlation was found for chitosan, glycerol and AG addition, drying temperature and dry film thickness. The time required to obtain dry films depended mostly on film thickness, chitosan, AG and glycerol. With temperature increase, drying time was shorter.

Besides,  $K_{\text{mass}}$  increased with drying temperature and humidity increase, whereas it decreased when more chitosan, glycerol or AG were present in thicker films.

Higher chitosan concentrations did not show significant differences in  $K_{\text{mass}}$ , that was in order of magnitude of  $10^{-6}$  ( $3.88 \times 10^{-6} - 6.18 \times 10^{-6}$ ). The addition of glycerol lowered carvacrol release from dry CS films whereas  $K_{\text{mass}}$  was in order of  $10^{-7}$ . On the contrary, the rise in glycerol/polymer dry matter ratio in CSA/AG blends, facilitated carvacrol release, and therefore  $K_{\text{mass}}$  increased up to  $10^{-5}$ . The protective colloid functionality of AG led to lower partitioning of the aroma compound between films and surrounding atmosphere. Even though better protection with AG during drying was observed, in equilibrium, the amount of released carvacrol from dry film remained equal (data not shown). Consequently, no significant difference in  $K_{\text{mass}}$  was observed. The effect of temperature on the  $K$  was previously studied by Etre and Kolb (1991), Kolb et al. (1992) and Carelli et al. (1991). According to literature, the relationship between  $\log K$  and  $1/T$  may be considered as linear. Temperature increases the aroma compound volatility and the diffusivity according to Henry's law (Buttery et al., 1971). Therefore at higher temperatures the release of volatile is higher and  $K_{\text{mass}}$  lower. The final result is less aroma compound (Fig. 4.6.A). This behaviour was confirmed for CSA films, but not for CSA/AG blends. The possible explanation is better stability of AG/carvacrol complexes formed in CSA/AG blends at higher temperatures, as will be discussed further on.



a)

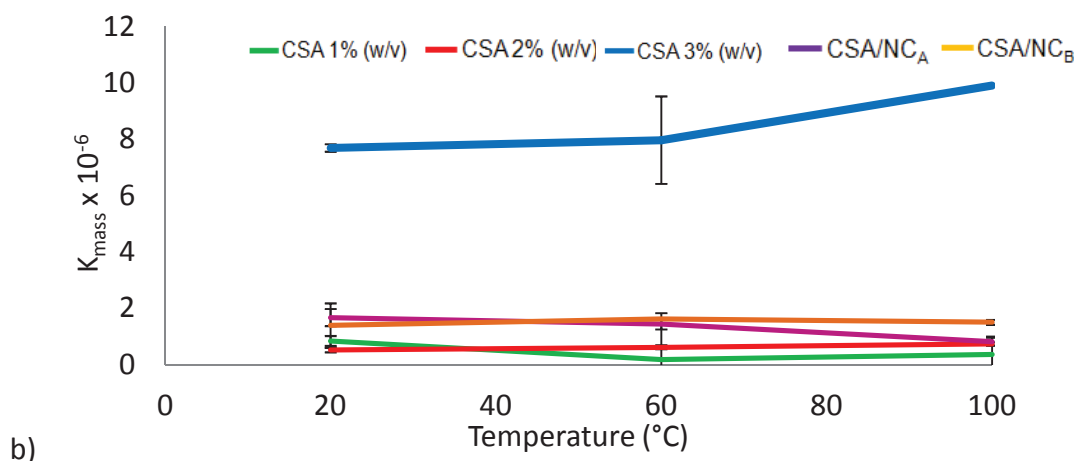


**Figure 4.6.** Carvacrol retention (a) and the air/biopolymer partition coefficient ( $K_{\text{mass}}$ ) (b) in the chitosan based films with or without the addition of nanoclays when dried at temperature scale from 20 to 100°C.

Finally, to better understand carvacrol retention behaviour, the most important parameters (chitosan dry matter, glycerol, NC and GA) were studied. Furthermore, the influence of the drying temperature was discussed.

#### 4.4.2. Influence of chitosan concentration

Different concentrations of chitosan in film forming solutions changed structure, thickness and carvacrol retention. Generally, a lower amount of polymer indicates a reduction in its retention capacity. It was attributed to the inclusion of carvacrol molecules within the matrix. This phenomenon was explained by Voilley and Simatos (1980). A sol/gel transition occurs faster when the chitosan solution is more concentrated (Montembault et al., 2005). Then again, 1% (w/v) chitosan FFS (CSA) remained aqueous for a longer period. Influenced by solvent evaporation, more carvacrol was lost. On the other hand Boland et al. (2004) reported a higher release with increased matrix rigidity. This might explain why films with the highest chitosan concentration entrapped a lesser quantity of aroma compound. At higher temperatures, polymer concentration plays an important role. Retention varied from 4.9 to 18.9, from 0.93 to 14.99 and from 0.51 to 13.29 for 1 and 2% CSA films dried at 20, 60 and 100°C, respectively. Several explanations can be made. First of all, it is to expect that higher carvacrol loss would occur at temperatures close to its flash point (106°C). Drying at lower temperatures does not only decrease aroma compound volatilization, but it might also influence polymer crystallinity. Srinivasa et al. (2004) stated out that ambient dried chitosan films had a lower crystallinity than those at 70,

80 or 90°C. There are two main explanations of interactions between polysaccharide and aroma molecules (viscosity modifications and molecular interactions (hydrophobic interactions, hydrogen and covalent bonding)) (Baines and Morris, 1987; Lubbers et al., 1998; Roberts et al., 1996; Secouard et al., 2003). In theory, hydrophobe/hydrophobe interactions are endothermic reactions, so an increase in temperature amplifies them. This explains why chitosan macromolecules were networked faster at higher temperatures, forming a denser structure and leaving fewer spaces for carvacrol.

Generally, the viscosity increased when the concentration of the dispersed phase increased. Increased temperature can increase flexibility of chitosan macromolecules, and as a result, viscosity decreases. Therefore, films cast from less dense chitosan solutions lost more volatiles. The authors reported that highly volatile aroma components are much better retained with an increase in the feed solid level (Charve and Reineccius, 2009). However, increasing the solid level too much may result in non dissolved material and increased viscosity, which may slow down the film formation. Therefore there must be an optimum solid concentration. High temperature exposure results in the build-up of a more porous crust that offers less resistance to carvacrol vapour diffusion during drying. The retention of aroma compounds is dependent on its diffusivity after the formation of a semi permeable surface. Diffusion and volatilization pathways are shorter; consequently more carvacrol is lost (Fig. 4.6. and Table 4.4.).



**Table 4.4.** Composition of the chitosan based films and its influence on the thickness, drying time, carvacrol retention and the air/biopolymer partition coefficient when dried at 20°C and 30% RH.

Film	Chitosan dry matter (g)	Glycerol % (w/p.d.m.)	Nanoclays or arabic gum % (w/p.d.m.)	Thickness (µm)	Drying time (h)	Carvacrol retention (%)	$K_{mass} \times 10^{-6}$
Chitosan film (CSA)	1	0	0	28±3	14	1.35±0.06 <sup>g</sup>	6.13±0.49 <sup>b,c,d</sup>
	2	0	0	50±5	14	9.45±0.15 <sup>c</sup>	3.88±0.19 <sup>e</sup>
	3	0	0	58±5	18	4.24±0.10 <sup>d,e</sup>	5.53±0.65 <sup>c,d,e</sup>
Chitosan film with glycerol (CSAGLY)	1	30	0	35±3	14	4.96±0.14 <sup>d</sup>	0.85±0.18 <sup>f</sup>
	2	30	0	55±5	14	18.90±1.51 <sup>b</sup>	0.52±0.08 <sup>f</sup>
	3	30	0	60±5	18	1.83±0.31 <sup>f,g</sup>	7.70±0.13 <sup>a,b</sup>
Chitosan film (CSA) with nanoclays	1	0	10	NA	12	NA	NA
	2	0	10	78±6	12	2.42±0.37 <sup>f,g</sup>	5.71±0.68 <sup>c,d,e</sup>
	3	0	10	NA	13	NA	NA
Chitosan film with glycerol (CSAGLY) and nanoclays	1	30	10	95±10	14	28.17±0.89 <sup>a</sup>	0.47±0.08 <sup>f</sup>
	2	30	10	110±10	14	21.31±0.22 <sup>a,b</sup>	0.59±0.01 <sup>f</sup>
	3A	30	10	110±10	16	8.49±0.03 <sup>c</sup>	1.68±0.30 <sup>f</sup>
	3B	30	10	110±10	16	9.23±0.93 <sup>c</sup>	1.40±0.78 <sup>f</sup>
Chitosan (CSA)/arabic gum blends with glycerol	3	30	3	95±10	12	4.63±0.09 <sup>d,e</sup>	4.98±0.98 <sup>d,e</sup>
	3	40	3	118±11	12	3.22±0.14 <sup>e,f</sup>	7.14±0.81 <sup>a,b</sup>
	3	50	3	138±13	13	1.78±0.15 <sup>f,g</sup>	8.48±1.92 <sup>a</sup>

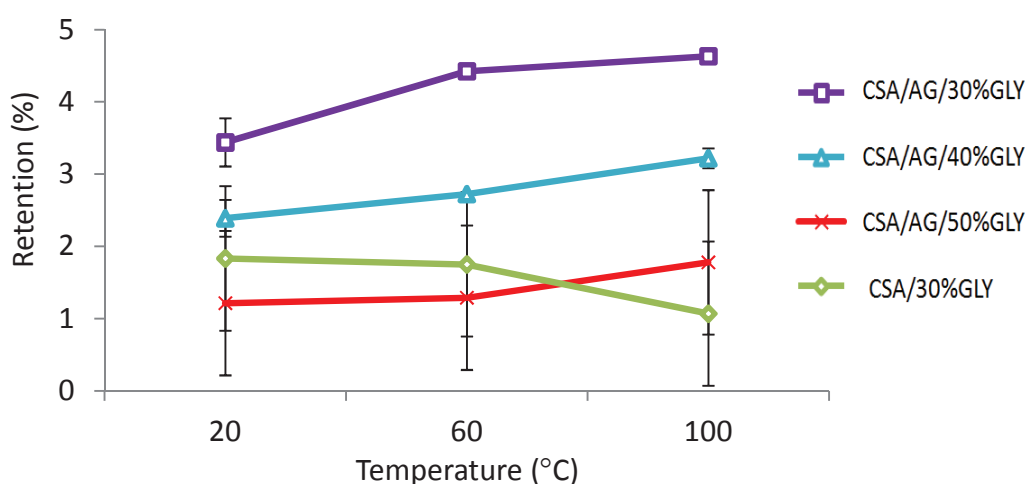
NA - not measured because produced films were too brittle

<sup>a-g</sup> Different superscripts within a column indicate significant differences among formulations (p<0.05)

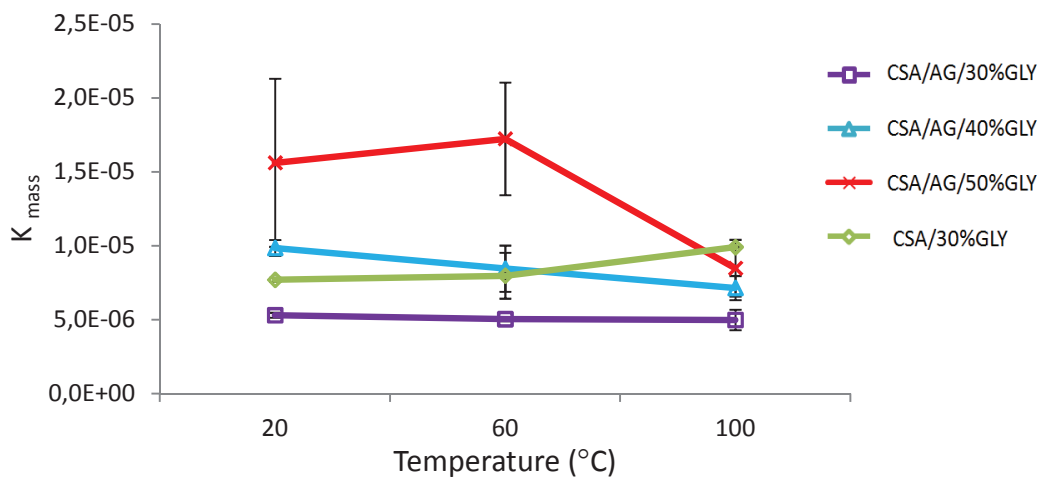
#### 4.4.3. Influence of additives

Drying time and thicknesses are mainly dependent on chitosan concentration and glycerol, whereas retention is directly glycerol and NC content dependent. An increased concentration of additives led to a greater molecular contact between the chitosan and the compounds. Therefore, forces between polymer chains were weakened and the matrix network was more opened. Chitosan films of high deacetylation degree, that have higher crystallinity, are more mobile (Chen et al., 1994). Increased macromolecular chain mobility facilitated carvacrol uptake (from 1.35 to 4.94 and from 9.46 to 18.90 for chitosan 1 and 2% (w/v) respectively). Glycerol displaced bound water and acetic acid. It resulted in an increased number of existing bonds and in the formation of new bonds (with chitosan–NH groups) (Park et al., 2001, Cerqueira et al., 2012). In this sense, glycerol was a competitive agent for carvacrol, as it occupied places where aroma compound could interact.

At higher concentrations (40 and 50% of polymer dry matter) glycerol facilitated the mobility of polymer chains, disturbed gelation and film formation. Thus, drying time was longer and more carvacrol was lost at all temperature ranges. Likely, it changed the film thickness and enhanced carvacrol diffusion into the atmosphere (Table 4.4.). Similar findings were reported by Sebti et al. (2007). Sanchez Gonzales et al. (2011) observed a reduction in the film thickness by means of essential oil evaporation. To sum up, both unplasticized and plasticized films had lower thickness as polymer dry matter decreased. It seems that temperature had no significant effect on these film formulations (Fig. 4.7.).



a)



b)

**Figure 4.7.** Retention (a) and partition coefficient ( $K_{mass}$ ) (b) of carvacrol as a function of the film composition and the drying temperature.

When nanoclays were mixed in FFS, only films with glycerol could be obtained. Lavorgna et al. (2010) stated that in films without glycerol, NC stacks lay with their platelet surface parallel to the casting surface. Brittleness is due to the complex/branched primary structure and weak intermolecular forces of natural polymers (Günister et al., 2007). These authors indicated interlayer distances of 16.34 Å, thereafter carvacrol (size 6.62 - 10.14 Å) could easily enter the free spaces of unfilled gaps. Perisco et al. (2009) reported that carvacrol is able to enter the clay galleries enhancing the lamellar distance up to 38.4 Å. Statistical analyses didn't show significant effects between A and B processing sequences of CSA/NC films. NC stacks were randomly orientated in the space. In a previous study, Wang et al. (2005) reported that the size of some stacks reached even up to 600 nm. That might be the reason why NC aggregates appeared in the tested samples. Mascheroni et al. (2010) suggested that increased carvacrol retention capacity exhibited by NC/wheat gluten was due to the entrapment of the carvacrol molecules in the aggregated structures, due to specific interactions between different components of the mixture. The interaction between solvents and clays controls the dispersion of the platelets and, as a consequence, it determines the resulting properties of nanocomposites (Burgentzlè et al., 2004). Glycerol enhanced the intercalation of chitosan in the silicate galleries and hindered flocculation. Moreover it reduced the surface energy of the aqueous solution and it extended the H-bonding between CSA-NC (Shanmugaraj et al., 2006). So, enough gaps were formed and better carvacrol dispersion was achieved (Darder et al., 2003). As a consequence, retention increased 21, 2.6 and 2.2 times in films (CSA) containing 1, 2 and 3% (w/v) chitosan, respectively. Even though the volatility and

consequently the carvacrol loss from CSA matrix were higher at higher temperatures, the addition of NC seemed to protect the carvacrol molecule. There are two possible explanations: a reduced drying time (at 100°C and 60°C drying time decreases 3 times) and the thermal stability of formed structures. Indeed, the authors pointed out that NC/carcacrol decomposed at higher temperatures (Keawchaoon and Yoksqn, 2011). Carvacrol losses from soy protein isolate coated papers were up to 37% when processed at 90°C, being higher than those prepared at 25°C and 50°C (12 – 14%, respectively).

Arabic gum and chitosan mainly form coacervates. They are liquid-like, mobile and reversible structures formed as a result of low charge density in systems where the ionic interaction of opposite polyelectrolyte is of moderate strength (Biesheuvel and Cohen Stuart, 2004). The formation of soluble complexes is attributed to a chitosan lower charge density and the presence of non-charged monomers (Coelho et al., 2011). Therefore, during the homogenization of carvacrol molecules, they can enter the coacervate CSA/AG globules which protected the aroma compound from evaporation. Differences in the nature of biopolymers increased the formation of a bubbled structure (Alcantara et al., 1998). This was not the case for pure chitosan films. In the presence of AG, the retention rate increased from 2.5 up to 3.2 folds, in a range from 20 to 100°C, respectively. Whereas the polymer dry matter increased by 50%, the incorporation of AG shortened the drying time 19 and 32 times in the interval from 20 to 100°C, respectively. Better film forming and emulsifying properties of AG increased essential oil retention from 45 to 63% with an AG concentration increase (Fernandes et al., 2008; Krishnan et al., 2005).

#### **4.5. Conclusions of Chapter 4**

This chapter brought attention to the complexity and the importance of controlling both composition and process parameters during the drying of biopolymer active films. In the Fig. 4.8. simplified and summarized view of main parameters influencing the active volatile compound retention and release from biopolymer films is given (adapted from Desobry and Debeaufort, 2011).

In relation to the effectiveness of potential antimicrobial packaging, it is very important to know the amount of active compound retained in the film matrix after processing. Volatile compound retention by biopolymer films is complex, and many

factors could affect it and interact. Moreover, the film structure, including additives, influences the aroma compound retention and the release from the films.

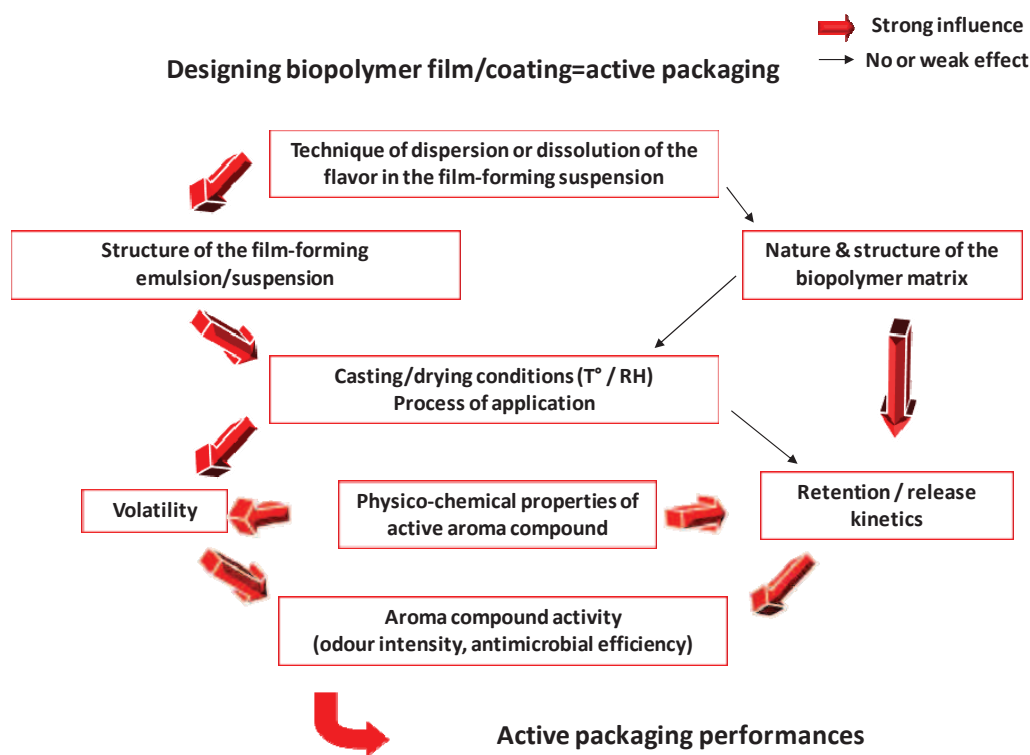


**Figure 4.8.** Overview of the mechanism and the main parameters influencing active packaging film performances.

An appropriate solvent that influenced FFS also affected film drying (kinetics and time) and therefore the structure which governs the film functional properties (aroma compound retention, release and film appearance) was also changed. Indeed, acetic acid aqueous media allow complete solubilisation of the chitosan. Consequently, more homogeneous structure is formed. On the contrary, hydroalcoholic acid media led to formation of colloidal suspension that induced structuration of different matrix network. Drying time is reduced when hydroalcoholic solutions are used for solubilization of a polymer powder. The partition coefficient can be related to carvacrol retention during film processing (casting plus drying) in chitosan based films. The glycerol-plasticized samples display higher water content due to the high hydrophilic character of glycerol. The loss of aroma compound is greatly influenced by the water content in the drying film. Drying curves did not display linear trend. It is due to the structural changes in the thin layer of FFS because the diffusion was modified according to the time. It seems that the drying time and thickness are mainly

dependent on the chitosan and glycerol content, whereas the retention is directly correlated to the glycerol and NC content. Disrupting intermolecular forces between polymer chains, plasticizers change the matrix structure that facilitates the carvacrol uptake. Moreover the addition of AG favoured carvacrol retention. Retention rate increased up to 3 folds in temperatures ranging from 20°C to 100°C. The presence of nanoclays in plasticized films promoted the aroma compound retention, which was more pronounced at lower drying temperatures.

In summary, in this chapter, the importance of processing parameters on the retention of active volatile compounds was highlighted. In the next two chapters the importance of composition of bio-based polymer films and coatings on their barrier and structural properties will be studied.



*Chapter 5*  
*Barrier properties of chitosan coated*  
*polyethylene*

---

Publication: **Mia Kurek**, Mario Ščetar, Andrée Voilley, Kata Galić, & Frédéric Debeaufort (2012).

Journal of Membrane Science, 404-405, 162-168.





In Chapter 4, it was demonstrated how film processing affects final composition of the dry film and thus influence its functional properties. The barrier to moisture, oxygen, carbon dioxide or combination of hereof in a packaging system can increase the food product shelf life and improve its quality (Srinivasa et al., 2002). Then for designing good food packaging film, it is very important to verify the gas permeability of barrier packaging materials.

In Chapter 2, the importance of the use of biopolymers in today's packaging industry is outlined. However, due to a good processability, a low energy processing demand and a good resistance to chemicals and harsh environments, polyolefins are still „the number one“ material in food packaging. Common polyolefin film that is non-polar hydrocarbon polymer with good water vapour barrier property is polyethylene (PE). However, due to their low gas barrier, different surface treatments can be used to improve their barrier performances against non condensable gases (Robertson, 1993). Moreover, polyolefins can be coated or laminated with gas barrier polymers like synthetic ethylene/vinyl alcohol (EVAL), copolymers, poly(vinylidene chloride) (PVDC), poly(ethylene terephthalate) (PET) or polyamide-6 (PA-6). Biopolymers such as chitosan are excellent gas barriers in dry conditions and even though they meet the gas permeability requirements, replacing food plastic packaging by self-standing biopolymers is a difficult task to achieve. So, the combination of chitosan with polyethylene can be a “winning” combination.

Still, several considerations, guidelines and parameters must be taken into account. When speaking about food storage, oxygen (O<sub>2</sub>) is the key factor that might cause oxidation, unwanted food changes and nutrient deterioration. In addition to the development of oxidative reactions where proteins and lipids degrade, when the oxygen permeability of the packaging material is too high, microorganisms present in the food can start to grow (Robertson, 1993; Sothornvit and Pitak, 2007). Carbon dioxide (CO<sub>2</sub>) is formed in some food due to the deterioration and respiration reactions (Vermeiren et al., 2003). On one hand, CO<sub>2</sub> may be added into a packaging to suppress microbial growth in some products (Lopez-Rubio et al., 2004). On the other hand, high levels of a carbon dioxide, resulting from food deterioration or oxidative reactions could cause adverse quality effects in the products. Some excess of carbon dioxide can be removed by using highly permeable plastics, whose permeability increases with higher temperatures (Brody et al., 2008).

Water vapour is a critical compound that can penetrate through the packaging materials. To avoid the moisture transfer that can affect food quality, control of water vapour permeability (WVP) is important to inhibit microbial growth, undesirable

textural changes and to ensure stability and safety during distribution and storage (Aloui et al., 2011). In the determination of permeability, the effects of both the temperature and the moisture content have to be taken into account to reflect as much as possible the conditions of intended use. Thus, measurements of permeabilities should be performed under the specific conditions that will be encountered by a packaged product. The transport properties of coated packaging materials are often influenced by coating composition. Due to their hydrophilic nature, polysaccharides are highly receptive to moisture and exhibit low water vapour barrier properties (Gennadios et al., 1994). Gas permeability of carbohydrate films and coatings depends on several factors such as film integrity, crystallinity, hydrophilic-hydrophobic ratio, the polymeric chain mobility, the interaction between the film-forming polymer and the presence of a plasticizer or other additives. The presence of plasticizers increases water vapour transmission of films regardless on the formulation (Rodriguez et al., 2006).

Therefore, the design and the optimization of the coating composition are very important for food packaging materials (Tihminlioglu et al., 2010). Differences in film forming conditions between cast films and coatings were thought to be responsible for changes in oxygen permeability (Maté and Krochta, 1998).

Detailed understanding of the characteristics of coated films is of a great practical and commercial importance. In this chapter, it is aimed to develop and study chitosan-based coatings applied on the LDPE films. Films and coatings will be analysed for their barrier properties against water vapour, oxygen, carbon dioxide and air. The effect of the temperature and the relative humidity on the barrier characteristics of the chitosan coated PE films will also be discussed.

## **5.1. Water vapour permeability**

### **5.1.1. Influence of coating process on the water vapour permeability of polyethylene**

Polyethylene films are known to be very hydrophobic and relatively not very permeable to water vapour. The WVP of PE film was similar (Table 5.1.) to those of the most commercial polymer films like polypropylene ( $6.5 \times 10^{-13}$  g/m·Pa·s) and polyvinyl chloride ( $7.1 \times 10^{-13}$  g/m·Pa·s) (Park, 1999). Therefore, it was interesting to verify if the deposit of a chitosan layer on the LDPE would alter its water vapour barrier properties. The water vapour permeability of uncoated PE was not sensitive to the relative

humidity increase. The WVP of untreated PE was  $5 \times 10^{-13}$  g/m·s·Pa. However, the water vapour transmission rate (WVTR) increased with the relative humidity (RH) gradient from  $0.55 \pm 0.05 \times 10^{-5}$  to  $1.84 \pm 0.08 \times 10^{-5}$  and  $2.55 \pm 0.39 \times 10^{-5}$  g/m<sup>2</sup>·s when the gradient varied, 0-33%, 30-75% and 30-100% RH, respectively. PE film is often considered as non water sensitive, so WVP remains not influenced by gradient. However, when it is coated by a biopolymer, this property seems to be lost. The presence of hygroscopic chitosan layer can act as a water reservoir on the PE surface, thus significantly promoting its water vapour permeability. Accordingly, chitosan interacts easily with the surroundings, absorbing water from the environmental humid air and therefore undergoing significant physical changes. In particular, the chitosan/water interaction leads both to an increased mobility in the hydrophilic macromolecule chains and to the swelling of the polysaccharide network. They are at the base of the gas diffusivity and gas solubility phenomena, respectively (Guilbert and Gontard, 2005). It is likely that high water sorption by chitosan induces surface water concentration much higher in the liquid state, and thus increases its permeability. Swelling also disrupted the structural integrity and barrier properties of the polymer network (Pushpadass et al., 2009). This hypothesis could be tested by determining the water content of the films in the steady state, but it is not precise enough to confirm it. To test this hypothesis, we exposed the coated side to lower humidity with the same gradients (Table 5.1., PECSE<sub>inv</sub>). Thus WVP decreased for at least 15% when the face of PE coated with chitosan is exposed to lower humidity (Table 5.1.), which tends to confirm mentioned above. Even though the presence of the bio-coating did not lead to any significant changes in WVP of the PE films; still, higher WVP of coated samples at higher  $\Delta$ RH was observed (Table 5.1.). This could explain that PE films are excellent water vapour barriers, and the addition of a thin layer coating was not enough to affect their initial performances at tested temperature (25°C). Similar observations were reported for PET and OPP fat/protein coated films (Farris et al., 2009). At  $\Delta$ RH 75%, higher WVP can be attributed to the very high increase in solubility. A decrease in the diffusivity appears to be accompanied by the formation of water clusters (Metz et al., 2005) thus increasing water vapour permeability at higher RH (Table 5.1.).

### 5.1.2. Influence of casting solvent and glycerol on WVP of self-standing chitosan films

Table 5.1. displays the WVP of all self-standing tested films, at 0-33%, 30-75%, 30-100% relative humidity differentials. The WVP of two films based on chitosan (CSA

and CSE) was tested at different RH gradients to highlight the effect of the solvent nature (acetic acid (A) or ethanol (E)) during the film preparation.

**Table 5.1.** Water vapour permeability ( $WVP \times 10^{-13}$  (g/m·s·Pa)) at 25°C of PE films coated with chitosan compared to chitosan self standing films prepared with different casting solvents and plasticizers.

Relative humidity differential	$\Delta RH$ 70%	$\Delta RH$ 45%	$\Delta RH$ 33%
PE	$4.62 \pm 0.73^f$	$5.55 \pm 0.23^f$	$7.72 \pm 2.58^f$
PECSE	$12.37 \pm 1.14^f$	$6.67 \pm 0.23^f$	$7.88 \pm 2.39^f$
PECSE <sub>inv</sub>	$9.14 \pm 1.09^f$	$6.41 \pm 3.28^f$	$2.85 \pm 0.34^f$
CSA	$4161.31 \pm 656.17^{a,b}$	$2199.80 \pm 1048.33^{d,e}$	$25.71 \pm 2.20^f$
CSE	$4100.77 \pm 588.88^{a,b}$	$2884.37 \pm 346.43^{b,c,d,e}$	$38.71 \pm 2.61^f$
CSAGLY	$5410.08 \pm 1543.67^a$	$1905.39 \pm 149.64^e$	$26.14 \pm 1.24^f$
CSEGLY	$3481.46 \pm 343.88^{b,c,d}$	$2635.38 \pm 414.28^{c,d,e}$	$105.17 \pm 6.57^f$

<sup>a-f</sup> Different superscripts indicate significant differences between formulations ( $p < 0.05$ )

When ethanol was used, the pH of the solution changed (from 4.5 to 5.2). This could modify the structure of the film due to variation in the polarity and thus of the solubility and the interfacial tension. Thus the obtained films were denser and their sensitivity to the plasticizing effect of water was reduced. In addition, ethanol concentration affected the solubility of chitosan and this resulted in different permeabilities of dry films. At water partial pressure between 0.40 and 0.54 the transport mechanism changed from a Fickian process to an anomalous process. A second important increase in water vapour flows was observed when partial pressure was above 0.95 (Despond et al., 2001).

Glycerol reduces the interactions between polymer chains and increases their mobility, so it was used as a plasticizer of chitosan films. Indeed, the obtained films were more flexible and less brittle. However, glycerol is also known for its antidepressant properties and therefore its strong hygroscopicity (Denavi et al., 2009). As a result, it promotes the sorption of water to relative humidities above 80%, and under these conditions the plasticizing effect of water is additional to that of glycerol, thus explaining higher WVP. At high hydration level, the water molecules partially dissolved chitosan to form a gel in which interactions among the polar groups of chitosan and additives were promoted. The mobility of the polymer chains increased and the packaging density was reduced. Thus, there was a significant increase in its

water sorption capacity (Vargas et al., 2009; Arvanitoyannis and Biliaderis, 1998). An increase in the interchain spacing caused by the inclusion of glycerol molecules between the polymer chains may promote water vapour diffusivity through the film and, hence, accelerate the water vapour transmission. The increases in WVP arising from plasticizer addition reported in this study are consistent with other works (Chillo et al., 2008; Pelissari et al., 2012).

Caner et al. (1998) reported that chitosan films had a WVP ranging from  $14.92 \times 10^{-13}$  to  $611.0 \times 10^{-13}$  g/m·s·Pa (at 25°C and from 50% to 100% RH). Changes were influenced by different acids and plasticizers. Water molecules play an important role in the packing and conformation of chitosan chains. Higher solubility of glycerol in hydroalcoholic medium may cause better distribution, therefore decreasing the number of the lattice between polymer chains and pathways for water permeation. Since WVTR through chitosan is a diffusion process, it is reasonable to expect that WVP is more strongly influenced by changes in the lattice volume fraction than by changes in the lattice dimensions. Therefore, permeability of CSEGLY was ten times lower at lower RH gradient, in comparison with higher RH gradient (Table 5.1.). Karbowski et al. (2008) showed that the increase in the diffusivity of water, or other small molecules in biopolymer films, is directly related to the water content and not that of the plasticizer added. The adsorbed water induces a plasticization of the chitosan network which increases the mobility of polymer chains. This could be attributed to the higher diffusivity due to weak intra- and intermolecular attractive forces in the polymer matrix. This phenomenon is favoured by the relative humidity increase.

Chitosan glycerol plasticized films had higher WVP values than PE (Table 5.1.), cast and extruded glycerol plasticized oat starch ( $0.042 \times 10^{-10}$  g/m·s·Pa and  $0.22 \times 10^{-10}$  g/m·s·Pa, respectively) (Galdeano and Sahbaz, 2009) and methylcellulose ( $0.50 \times 10^{-10}$  g/m·s·Pa) (Turhan et al., 2004). However, these values were lower than for glycerol plasticized wheat gluten ( $7.00 \times 10^{-10}$  g/m·s·Pa) and amylose films ( $3.80 \times 10^{-10}$  g/m·s·Pa) (Gennadios et al., 1994). The lowest values were obtained for CSE plasticized films ( $3.48 \times 10^{-10}$  g/m·s·Pa, Table 5.1.). Moreover, the authors reported that the WVTR of polysaccharide films were related to their thickness (Turhan et al., 2004; McHugh and Krochta, 1994; Myllarinen et al., 2002). During preparation, including film casting and drying, differences in film thicknesses due to edge effects are commonly observed. Therefore, it was expected to experience the difficulty of minimizing induced variations.

## 5.2. Oxygen, carbon dioxide and air permeability

### 5.2.1. Influence of coating process on gas permeability of coated PE

Biopolymer films are aimed to be good gas barriers. To investigate the ability of chitosan coating in enhancing barrier properties of traditional polyolefin films, polyethylene films were coated with thin chitosan layer (3 and 6  $\mu\text{m}$ ). For most plastic films,  $\text{CO}_2$  permeability is from 2 to 6 times greater than that of  $\text{O}_2$  and provides a range of selectivity. This allows a large selection of films of suitable ratios for specific food products (Ščetar et al., 2010).  $\text{PO}_2$  (Fig. 5.1.) was found to be two times lower than  $\text{PCO}_2$  (Fig. 5.2.) for tested PE film.

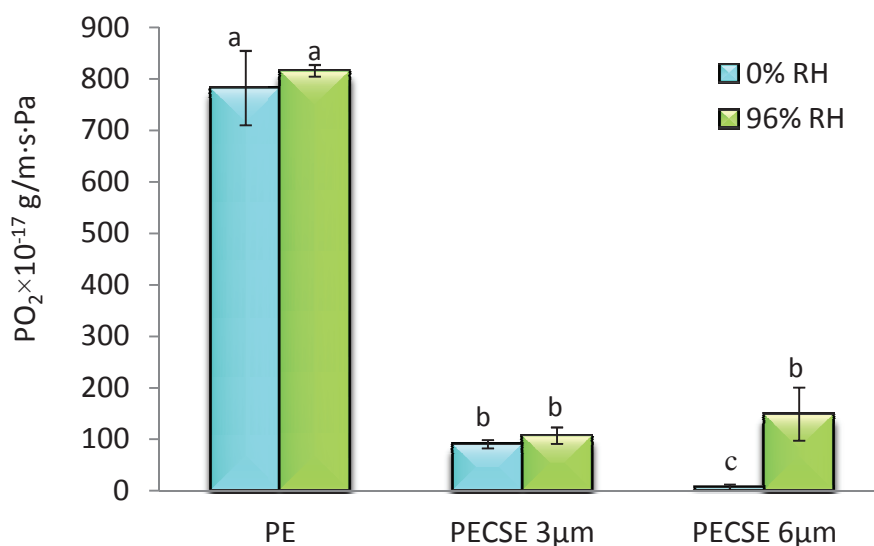


**Figure 5.1.** Oxygen permeability of polyethylene (PE) and PE chitosan coated samples (PECSE).

<sup>a-c</sup> Different superscripts indicate significant differences ( $p < 0.05$ ).

In dry conditions,  $\text{PCO}_2$  ( $1.02 \times 10^{-17} \text{ g/m}\cdot\text{s}\cdot\text{Pa}$ ) was lower (Fig. 5.2.) than  $\text{PO}_2$  ( $6.18 \times 10^{-17} \text{ g/m}\cdot\text{s}\cdot\text{Pa}$ ) for chitosan coated PE films (Figs. 5.1.). In comparison to the uncoated PE, the application of chitosan coatings on PE films showed more than two-order decrease in oxygen permeability (Fig. 5.1.) and three-order-decrease in carbon dioxide permeability (Fig. 5.2.).  $P_{\text{air}}$  (data not presented) was found to be lower than  $\text{PO}_2$  and  $\text{PCO}_2$  ( $2.66 \times 10^{-17}$  and  $2.08 \times 10^{-18} \text{ g/m}\cdot\text{s}\cdot\text{Pa}$ , for 3 and 6  $\mu\text{m}$  chitosan coated PE, respectively).

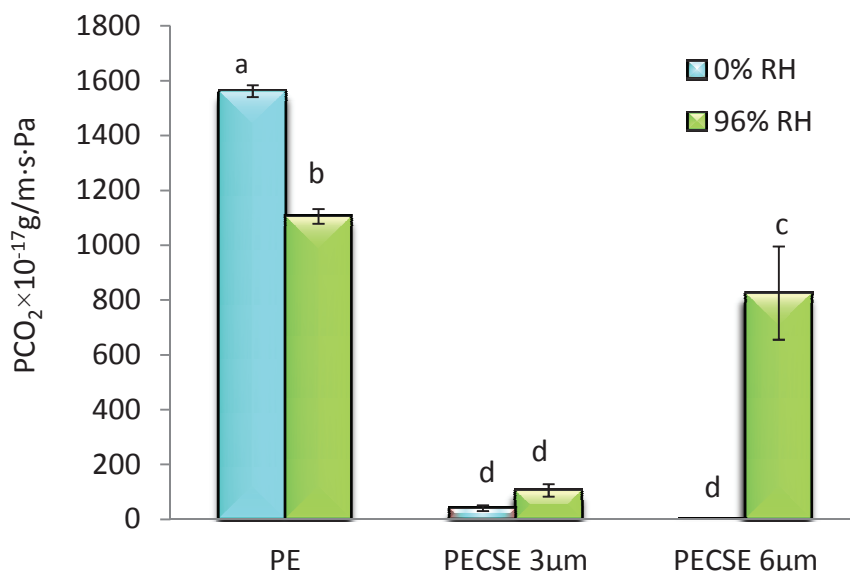


**Figure 5.2.** Carbon dioxide permeability of polyethylene (PE) and PE chitosan coated samples (PECSE).

<sup>a-d</sup> Different superscripts indicate significant differences ( $p < 0.05$ ).

Thermal analysis (Chapter 6, Kurek et al., 2012b) did not display changes in the PE structure after coating process. Therefore, the decrease in  $PO_2$  and  $PCO_2$  can only be attributed to the chitosan layer. Good barrier materials are considered if having  $PO_2$  less than  $2.44 \times 10^{-17}$  g/m·s·Pa at 23°C (Salame, 1986). According to this criterion, the chitosan coated PE was classified as excellent oxygen barrier. In a humidified environment, the  $CO_2/O_2$  ( $\alpha$ ) of coated samples increased (calculated from data given in Figs. 5.1. and 5.2.). Moreover, the  $\alpha$  increased with the coating thickness increase (from 2.2 to 33.6 for 3 and 6  $\mu$ m coatings, respectively). The high polarity of  $CO_2$  causes its better dissolution, condensability and higher solubility than  $O_2$  (Henry's law solubility constants for  $CO_2$  and  $O_2$  in water at 25°C indicates that  $CO_2$  ( $7.57 \times 10^{-6}$  cm<sup>3</sup><sub>STP</sub> of  $CO_2$ /g<sub>H<sub>2</sub>O</sub>·Pa) is 26 times more soluble than  $O_2$  ( $3.75 \times 10^{-7}$  cm<sup>3</sup><sub>STP</sub> of  $O_2$ /g<sub>H<sub>2</sub>O</sub>·Pa) (Lide, 2007), therefore  $PCO_2 > PO_2$ . The high permeability caused by higher diffusivity of  $CO_2$  could be due to the lower kinetic diameter, 3.3 Å and 3.46 Å for  $CO_2$  and  $O_2$ , respectively. The presence of the water vapour close to the hydrophilic polymer surface changed the structure of the thin chitosan coating and resulted in preferential permeation for acid gases such as  $CO_2$ . From the application point of view, in a preservation of fresh products with high water content, low  $PO_2$  and high  $PCO_2$  inhibits growth of aerobic microorganisms, thus increasing the product shelf life. The degree to which atmospheric modification takes place in the packages depends on the film permeability, product respiration and the influence of temperature on both of these



processes (Beaudry, 1999). Gases such as O<sub>2</sub>, CO<sub>2</sub> and water vapour exit or enter the package in a controlled manner and therefore, special films could be obtained by modifying the film manufacturing process. Also, they could meet aerobic respiration needs and maintain desirable CO<sub>2</sub> and moisture levels. It was found that PCO<sub>2</sub>/PO<sub>2</sub> of PE chitosan coated film was 5.5 at 25°C and 96% RH (from Figs. 5.1. and 5.2.).

The temperature increase from 4 to 25°C resulted in PO<sub>2</sub> rise for all tested films (Fig. 5.3.).

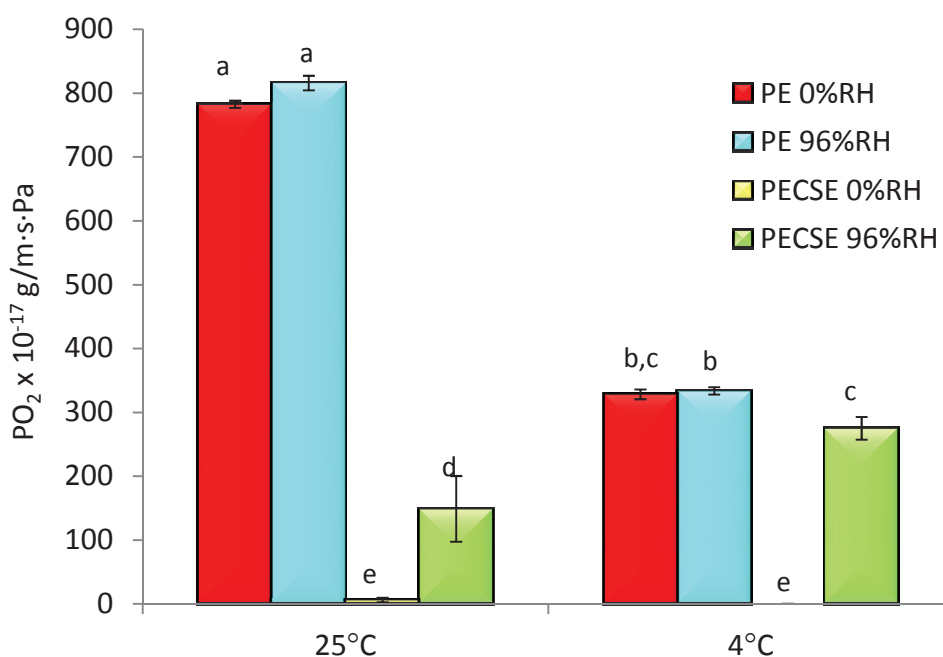


**Figure 5.3.** Changes in oxygen permeability of polyethylene and chitosan coated polyethylene films as a function of temperature and relative humidity.

<sup>a-e</sup> Different superscripts indicate significant differences ( $p < 0.05$ ).

As temperature increases, molecules have more energy and they can move much more easily through both PE part and chitosan coating. There is also a thermal expansion of the polymer material (Rogers, 1985). On the other hand when humidity increased, that effect was not so pronounced ( $PO_2 = 2.44, 0.54$  and  $6.40$  times higher for the PE, PE chitosan coated and chitosan films, respectively).  $PO_2$  generally follows Arrhenius behaviour, unless the polymer passes through a transition such as the glass transition temperature (Beaudry, 1999). The Arrhenius model applied to oxygen permeation has been confirmed both for some biosourced films (Ma et al., 2012) and polyolefins (Kurek et al., 2011). Lower difference observed for humidified samples was

due to the sorption of water molecules onto the coating surface that formed previously mentioned water reservoir. Therefore, it facilitated and increased oxygen permeation. There was no significant difference in activation energy between dry and humidified PE samples (36.62 and 37.69 kJ/mol, respectively). On the other hand, the activation energy values of the PE chitosan coated (113.26 kJ/mol) and the chitosan self-standing films (160.28 kJ/mol) were higher than those of the uncoated PE (36.62 kJ/mol). That indicates that the oxygen permeation through the PE coated films is more sensitive to temperature changes than that of commercial PE. Lower values at higher moisture rates (25.88 and 78.26 kJ/mol for coated PE and chitosan films, respectively) indicate that oxygen permeation depends more on humidity change than to temperature increase. Greater correlation of  $PO_2$  and RH than  $PO_2$  and temperature was also observed by Hong and Krochta (2006). These authors reported that the permeability of the whey-protein-coated films increased exponentially with RH (in the range from 30% to 85% at 25°C) and twofold increase for each 10°C was observed. The exponential effect of RH on oxygen permeability has been previously observed for other biopolymer films (McHugh and Krochta, 1994; Fabra et al., 2012).

### **5.2.2. Influence of casting solvent and glycerol on gas permeability of chitosan self-standing films**

In their dry state, all chitosan films had low  $PO_2$ ,  $PCO_2$  and  $P_{air}$  (Table 5.2.). The oxygen permeability of the CSA film was lower than previously reported ( $883 \times 10^{-17}$  g/m·s·Pa (Sathivel et al., 2007)). In Chapter 6, the influence of solvent nature and plasticizers on structural changes in chitosan films will be discussed (Kurek et al., 2012b). The general transport mechanism for a gas through polymeric material starts with a sorption of the gas molecules to the surface and then their dissolution in the polymer matrix. The next step is a diffusion step, described as a series of jumps from one cavity to another within the polymer matrix. At the final step gas molecules are desorbed from the other side of the material. From a kinetic point of view, in a layered chitosan structure pathways for gas permeation are much longer, so this results in lower gas permeabilities. Indeed, in dry conditions,  $PCO_2$  and  $PO_2$  were very close and fairly low (Table 5.2.).

**Table 5.2.** Oxygen, carbon dioxide, air permeability and CO<sub>2</sub>/O<sub>2</sub> permselectivity at 25°C and 0% (dry gas) and >96% (humid gas) of chitosan films influenced by casting solvent and glycerol addition in film formulation.

Chitosan Sample	Glycerol (% w/w dm)	PO <sub>2</sub> × 10 <sup>-17</sup> g/m·s·Pa		PCO <sub>2</sub> × 10 <sup>-17</sup> g/m·s·Pa		Pair × 10 <sup>-17</sup> g/m·s·Pa		Permselectivity CO <sub>2</sub> /O <sub>2</sub>	
		dry gas	humid gas	dry gas	humid gas	dry gas	humid gas	dry gas	humid gas
Aqueous acid solvent	0	1.04 ± 0.15 <sup>a</sup>	43.32 ± 6.70 <sup>b</sup>	6.98 ± 0.08 <sup>a</sup>	38.20 ± 3.18 <sup>c</sup>	3.79 ± 0.25 <sup>b</sup>		6.71	0.88
Aqueous acid solvent	30	8.76 ± 2.58 <sup>a</sup>	150.13 ± 0.18 <sup>a</sup>	7.80 ± 0.10 <sup>a</sup>	266.40 ± 9.93 <sup>b,c</sup>	34.27 ± 2.59 <sup>c</sup>		0.89	1.77
Hydroalcoholic acid solvent	0	2.22 ± 0.27 <sup>a</sup>	9.30 ± 3.28 <sup>a,b</sup>	1.49 ± 0.02 <sup>c</sup>	355.73 ± 187.22 <sup>b</sup>	0.22 ± 0.05 <sup>a</sup>		0.67	38.23
Hydroalcoholic acid solvent	30	4.98 ± 1.10 <sup>a</sup>	75.95 ± 3.28 <sup>b</sup>	3.80 ± 0.04 <sup>b</sup>	845.93 ± 12.73 <sup>a</sup>	1.23 ± 0.05 <sup>b,c</sup>		0.76	11.14

<sup>a-c</sup> Different superscripts within a column indicate significant differences among formulations ( $p < 0.05$ ).

Permeating humidified gas turns hydrophilic polymer chains into a swollen state and greatly increases gas permeability. This phenomenon was more pronounced for the CO<sub>2</sub> (from 5 to 238 times) than for the O<sub>2</sub> (from 4 to 42 times). So an increase in the selectivity was observed ( $\alpha$  was increased up to 56 times for CSE film, Table 5.2.). Actually, after drying there is always a trace of acetic acid left. High solubility of CO<sub>2</sub> in acids and its interaction with chitosan molecules makes CO<sub>2</sub> preferentially more permeable (Ito et al., 1997). Likewise, it may enhance the transport of the CO<sub>2</sub> through the chitosan films. Generally, the selectivity of CO<sub>2</sub>/O<sub>2</sub> found in this research was lower than that of Despond et al. (2001) ( $\alpha=16.7$ ).

The addition of ethanol during processing decreased PO<sub>2</sub>, PCO<sub>2</sub> and P<sub>air</sub>. During the film preparation several events may occur, such as structural orientation and conformation changes of chitosan matrix. It was attributed to the interactions between acetic acid and chitosan chains that strengthen the film network. Such events can facilitate diffusion of acetic acid through the expanded form of chitosan network in a manner that restricts the flow of gases (Srinivasa et al., 2007). Water molecules interact with polar groups in the matrix, gas molecules enter in micro-channels within film structure and material swells. This results in variations in gas permeability. Disturbing presence of water and molecular orientation of the polymeric chains may hinder the movement of gas molecules (Salame and Steingiser, 1977). The final reason could be increase in material polarity (Robertson, 1993).

The PO<sub>2</sub> of plasticized chitosan films was from 2.2 to 8.4 and from 3.5 to 8.2 times higher than unplasticized one (at 0% and 96% relative humidity, respectively, Table 5.2.). Since chitosan films had relatively high moisture contents (up to 20% for self-standing films) and water is itself an effective chitosan plasticizer, when adsorbed it influences the plasticizing ability of glycerol. So it can lower Tg and thus increase permeability (Robertson, 1993). The rupture of hydrogen bonds may create additional sites for the molecule dissolution and may increase mobility of the O<sub>2</sub> molecules within the amorphous phase (Gontard et al., 1996). The most important difference was observed for permeating air, being from 5.6 to 9 times higher for plasticized samples. Higher relative humidity increases the plasticizer effect on oxygen permeability of sorbitol plasticized starch films (from 3.5 to 718 times at a relative humidity from 57 to 90%) (Gaudin et al., 2000). The authors (Caner et al., 1998) found that the oxygen permeability of chitosan film ranged from 1.32 to 514 x 10<sup>-17</sup> g/m·s·Pa, according to type of acids and plasticizers.

### 5.3. Conclusions of Chapter 5

Generally, bio-based polymers are considered to be good barriers to gases. The casting of the chitosan coating onto the polyethylene films enhanced their gas barrier properties at low relative humidities. In dry conditions, the coated films were from 100 to 1000 times less permeable than the polyolefin film with the following permeation order  $PCO_2 > PO_2 > P_{air}$ . Even though polyolefins are expected not to be sensitive to water vapour gradient, WVP of coated films was increasing. Therefore, it was undoubtedly attributed to chitosan coating. Due to its hydrophilicity, the chitosan coating negatively influenced the water vapour barrier properties of the PE films. Still, statistically no significant difference was observed. A rise of the relative humidity decreased the barrier performances of the chitosan and probably changed its structure. Therefore, gas barrier properties at high humidity were also affected. Permeability at the higher moisture level rose up as the coating thickness increase. Polymer structure, physical properties (solubility and diffusivity of  $CO_2$  and plasticization effect of water molecules) and polymer/gas interactions influenced the permeation flow particularly in the humid environment, but still followed the same order  $PCO_2 > PO_2$ . Elsewhere, gas transfer through the self-standing chitosan film was influenced by the casting solvent and the plasticizers. Glycerol facilitated the mobility of the penetrant. Ethanol increased the polymer density and changed the network polarity. Therefore it decreased the permeation in dry state, but negatively affected it in wet state.

As shown in this chapter, all together, plasticizers and solvents as well as atmospheric conditions strongly influenced permeability performances of chitosan based films and coatings. To better understand the observed phenomena, in the following chapter, structural and thermal properties of chitosan based films and coatings on polyethylene will be studied.

*Chapter 6*  
*Structure and thermal properties of a chitosan  
coated polyethylene bilayer film*

---

Publication: **Mia Kurek**, Claire Hélène Brachais, Christelle Mary Nguimjeu, Aline Bonnotte, Andrée Voilley, Kata Galić & Frédéric Debeaufort (2012).  
Polymer Degradation and Stability, 97(8), 1232-1240.



In the previous chapter it was observed that coating polyethylene films with chitosan thin layer enhanced gas barrier properties of polyethylene. In dry conditions, the coated films (coating thickness 6  $\mu\text{m}$ ) were significantly less permeable than the polyethylene film with the following permeation order  $\text{PCO}_2 > \text{PO}_2 > \text{P}_{\text{air}}$  (Figs. 5.1. and 5.2.). The respective barrier properties of stand-alone chitosan or PE film can't explain this gain in barrier performances. Regarding the barrier properties, the critical compounds that can penetrate the packaging materials and degrade food quality are water vapour and oxygen of the surrounding atmosphere. The analysis of the structure and surface properties is important to better understand this performance.

Processing can cause serious damage of polymer material. Changes in solvent polarity may change structure and final film properties. Differences in polarity between PE support and chitosan coating may lead to decohesion between two layers. Moreover, plasticizers that are used to increase the flexibility or plasticity of polymers may cause significant changes in its structure and its functional properties. Migration of species such as plasticizers, from one layer to another, can also be a major drawback in multilayer films. Therefore, precise control of the processing and conditions of use, of any polymeric system is very important to get a material with good and desired properties, to avoid decomposition and undesired matrix degradation.

Thermal analysis such as thermogravimetry (TGA) and differential scanning calorimetry (DSC) have been widely employed for the characterization of polymeric materials. Moreover, these techniques are used to monitor physical modifications, changes in chemical structure and composition, or in molecular architecture of chitosan polymer matrix (El-Hefian et al., 2010; Appelqvist et al., 1993; Ratto et al., 1995). Furthermore, a kinetic study of thermal degradation can provide useful information for the optimization of the polymer processing (Navarro et al., 2003).

There are several reports about thermal decomposition and stability of chitosan (Zohuriaan et al., 2004; Pawlak and Mucha, 2003; Neto et al., 2005). Besides, thermal properties of low density polyethylene and its composites have been already well studied (Kurek et al., 2011; Murray et al., 2012; Weon, 2010). However, relatively few researches have been conducted on the influence of processing on the permeability properties, thermal and structural stability of polyethylene coated films (Farris et al., 2009; Hong et al., 2006; Ha et al., 2001; Shin et al., 2002).

In this chapter, thermal and surface structure characteristics of developed films and coatings were analysed. Moreover, in order to develop the performances of the coating layer, and to understand the influence of casting solvent and glycerol,



additional tests on chitosan self-standing films have been performed. Beside plasticizing properties, glycerol was also used as a model of small polar molecules that can be incorporated in the chitosan based bio-coatings. Therefore, the behaviour of this model could be extrapolated to that of small molecules such as flavourings, antioxidants or antibacterials.

## 6.1. Thermal properties

Thermal analyses were conducted to better understand the behaviour and barrier properties of dry films. Besides, the determination of the thermal properties of the PE and the chitosan coated PE samples was carried out to check if the coating material as well as the coating technique influenced the polyolefin film structure. Moreover, useful information on the hydration, crystallinity and the stability of the various chitosan coatings can be achieved. The thermal properties of the chitosan powder, PE films and all tested chitosan films are summarized in Table 6.1.

**Table 6.1.** Thermal properties of chitosan powder, chitosan based films, PE, and PE coated films obtained by DSC analysis.

SAMPLE	$T_d(^{\circ}\text{C})$	$\Delta H_d(\text{J/g})$	$T_{DS}(^{\circ}\text{C})$	$\Delta H_{DS}(\text{J/g})$	$T_D(^{\circ}\text{C})$	$\Delta H_D(\text{J/g})$
CS POWDER	43.2	0.2	201.7	101.0	300.1	64.8
CSA	72.9	11.5	215.8	193.9	318.9	24.2
CSAGLY	51.2 and 92.2	0.9 and 15.7	193.7	295.7	286.7	39.2
CSE	72.1	10.2	184.1	282.3	316.8	16.1
CSEGLY	52.1 and 90.2	1.3 and 9.4	168.4	290.9	284.7	12.7
	$T_d(^{\circ}\text{C})$	$\Delta H_d(\text{J/g})$	$T_m(^{\circ}\text{C})$	$\Delta H_m(\text{J/g})$	$T_D(^{\circ}\text{C})$	$\Delta H_D(\text{J/g})$
PE	/	/	112.9	90.7	/	/
PECSE	48.3	1.3	112.9	81.2	289.9	0.2

$T_d$ -dehydration temperature;  $T_{DS}$ -dissociation temperature;  $T_D$ -degradation temperature;  $T_m$ -melting temperature;  $\Delta H_d$ -enthalpy of dehydration;  $\Delta H_{DS}$ -enthalpy of dissociation,  $\Delta H_D$ -enthalpy of degradation,  $\Delta H_m$ -enthalpy of melting

### 6.1.1. Characterization of the chitosan coating

Chitosan is a partially crystalline polymer composed of rigid chains having a small specific volume (Sakurai et al., 2000). Changes in the inclination of the baseline in the DSC thermograms for the raw chitosan samples were very weak. Therefore no glass transition temperature ( $T_g$ ) could be detected and neither for other chitosan-based samples. The difficulty in  $T_g$  determination of chitosan-based materials was also pointed out by El-Hefian and co-workers (2010). Indeed, the  $T_g$  of chitosan is known to range between  $-23^\circ\text{C}$  and about  $220^\circ\text{C}$  according to moisture and/or plasticizer content. All samples containing chitosan displayed two/or three endothermic peaks in the first run and just one exothermic peak in the second run. The first endothermic peak was attributed to the loss of moisture and to solvent traces associated with the hydroxyl groups of the 85% deacetylated chitosan. This specific temperature detected at  $43.1^\circ\text{C}$  for the chitosan powder, is named as the dehydration temperature ( $T_d$ ) (Fernandez et al., 2004; Xu et al., 2006; Casariego et al., 2009). This peak did not appear in the second heating. For CSA and CSE films, the dehydration temperature was shifted around  $72^\circ\text{C}$  and reflected the strength of water/acetic acid/chitosan chains interactions (Table 6.1.). These interactions resulted from the film preparation step which requires the systematic use of acetic acid both for CSA and CSE films. In all CSE samples ethanol was completely evaporated during the processing. From the dehydration enthalpy ( $\Delta H_d$ ) it was also clear that these interactions were much more present in the CSA and CSE films than water/chitosan interaction in the pure chitosan powder.

In the glycerol plasticized films, CSAGLY and CSEGLY, the endothermic region for  $T_d$  consisted of two peaks that were detected around  $52^\circ\text{C}$  and around  $90^\circ\text{C}$  (Table 6.1.). This variation in the peaks position means that glycerol was also able to establish physical interactions with water, acetic acid and hydroxyl groups of chitosan chains. Endothermic peaks area is related to the relative amount of the interactive molecule in the film. There was a difference in the endothermic peak area for the plasticized samples, as they vary in their solvent-holding capacity. Considering that the acetic acid evaporated preferentially to glycerol, the relative amount of acetic acid in the films was lower than the glycerol amount. Therefore, the peaks around  $51^\circ\text{C}$  with  $\Delta H_d$  around  $1\text{ J/g}$  can be attributed to the interactions principally based on the acetic acid and the chitosan influenced by the glycerol (shift from  $72^\circ\text{C}$ ). As the new hydrophilic centres were formed, formation of the second peak around  $91^\circ\text{C}$  with  $\Delta H_d$  around

12 J/g can be attributed to the interactions principally based on the glycerol and the chitosan influenced by the acetic acid.

For the PECSE film, the thickness of the chitosan coating was about 6  $\mu\text{m}$  compared to 80  $\mu\text{m}$  for the self standing films. Therefore, the evaporation of acetic acid in the chitosan coating was more pronounced than in the films. Consequently, the lower  $T_d$  value detected at 48°C stands for the interactions between water/chitosan and small amount of the residual acetic acid ( $\Delta H_d$  around 1 J/g).

The second series of endothermic peaks displayed between 168°C and 215°C (called dissociation temperature,  $T_{DS}$ , values displayed in Table 6.1.) could not be attributed to a melting transition since a recrystallization peak was never detected by cooling the sample. Moreover as observed by Chuang and co-workers (1999), following the first heating, the characteristic peak could not be detected in the second heating (not shown in Table 6.1). The authors attributed the presence of this peak to the dissociation process of the interchain hydrogen bonding of the chitosan. This assignment was supported by the TGA results which showed that for the chitosan powder, no weight loss occurred in the  $T_{DS}$  region around 201°C (data not shown). However this dissociation temperature seemed to be influenced by the initial presence of the acetic acid and/or glycerol in the film. Indeed, except for the CSA film for which the  $T_{DS}$  can be detected at 215°C, the  $T_{DS}$  value of the films were systematically lower than the one of the pure chitosan powder. From the TGA analysis, it was interesting to note that the decomposition of glycerol (around 170°C) occurred in the  $T_{DS}$  area for the CSAGLY and the CSEGLY samples. Finally, for the PECSE film, due to the low amount of the chitosan when applied as a thin coating layer (6  $\mu\text{m}$ ), no  $T_{DS}$  could be detected.

At higher temperature, the exothermic peaks centred in the range from 284°C to 318°C appeared ( $T_D$  values in Table 6.1.). They were attributed to the thermal degradation as depolymerisation and pyrolytic decomposition of the polysaccharide backbone (Zohurian et al., 2004; Sakurai et al., 2000; Xiao et al., 2003).  $T_D$  was measured at 300°C for the pure chitosan powder whereas it was enhanced around 317°C when the acetic acid was incorporated in the film (CSA and CSE samples). On the contrary, the addition of a plasticizer in the chitosan films (CSAGLY and CSEGLY samples) is responsible for the decrease in the  $T_D$  values. The small exothermic peak in the PE coated sample that appeared around 289°C was attributed to the chitosan coating degradation. It can be observed that the degradation enthalpy of chitosan in

the coated sample was much lower than the one observed in the chitosan self standing films. It was due to the lower quantity of chitosan coating as already mentioned. Lower decomposition enthalpies obtained for dry films compared to chitosan powder can then be explained by formation of chitosonium acetate in the films using acetic aqueous solution as a solvent.

### 6.1.2. Comparative thermal stability of PE, coated PE and CSE film

The TGA thermograms of polyethylene, polyethylene coated and chitosan coating are illustrated in Fig. 6.1. As expected, under the nitrogen flow, the one step degradation of polyethylene occurred around 455°C. On the other hand, there were two main steps for the PE chitosan coated films degradation. The first one appeared as a broad change from 40°C to 270°C and the second one from 270°C to 483°C. When compared to the chitosan self standing CSE film weight loss curve, it is evident that the first degradation step of the coated PE is attributable to the chitosan coating and the second one to the additional degradation of both PE and chitosan. Concerning the amount of the residue after the degradation, the highest weight loss can be observed only for the PE films and light solid residues of 3% in the coated samples were attributed to the chitosan coating. From this comparison, we can also assume that the thermal stability of the PE layer was not affected by the chitosan-based coating.

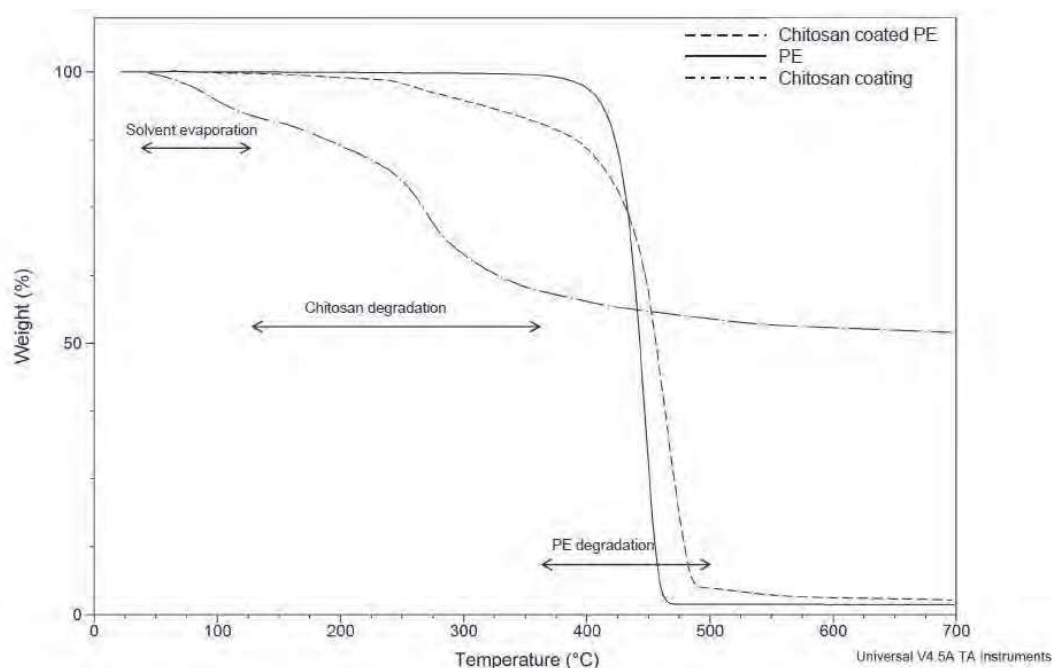


**Figure 6.1.** TGA thermograms of polyethylene (PE), chitosan coated polyethylene (PECSE) and chitosan coating (CSE).

### 6.1.3. Comparative thermal stability of glycerol plasticized and unplasticized samples

The TGA thermograms of chitosan powder and self-standing plasticized and not plasticized chitosan films are given in Fig. 6.2. For CSAGLY and CSEGLY samples, three steps of degradation were mainly observed (Lavorgna et al., 2010) instead of two for the unplasticized samples (CSA and CSE). The first one in the range from 30°C to 150°C results from the evaporation process related to the hydrophilic nature of the chitosan, with weight loss from 6% for the chitosan powder (corresponding to the residual water) to values up to 14% for the other films. For CSA and CSE samples, weight loss values were attributed to the evaporation of the residual water and the acetic acid. Higher weight loss observed for CSAGLY and CSEGLY were due to the evaporation of the residual water, of the acetic acid and of the glycerol. For the unplasticized samples, the second degradation step ranging from 150°C to 417°C, followed by the final mass loss up to 700°C was attributed to a complex process including the dehydration of the saccharide rings, depolymerisation and decomposition of the acetylated and deacetylated units of the polymers (Martins et al., 2012). It is important to note that this step was separated in the two stages for plasticized samples (from 120°C to 215°C and 215°C to 417°C) and was attributed to the glycerol degradation. This was clearly observed when comparing the derivative signal and the weight loss of the unplasticized and plasticized samples (data not shown) and coherent with the DSC thermograms.

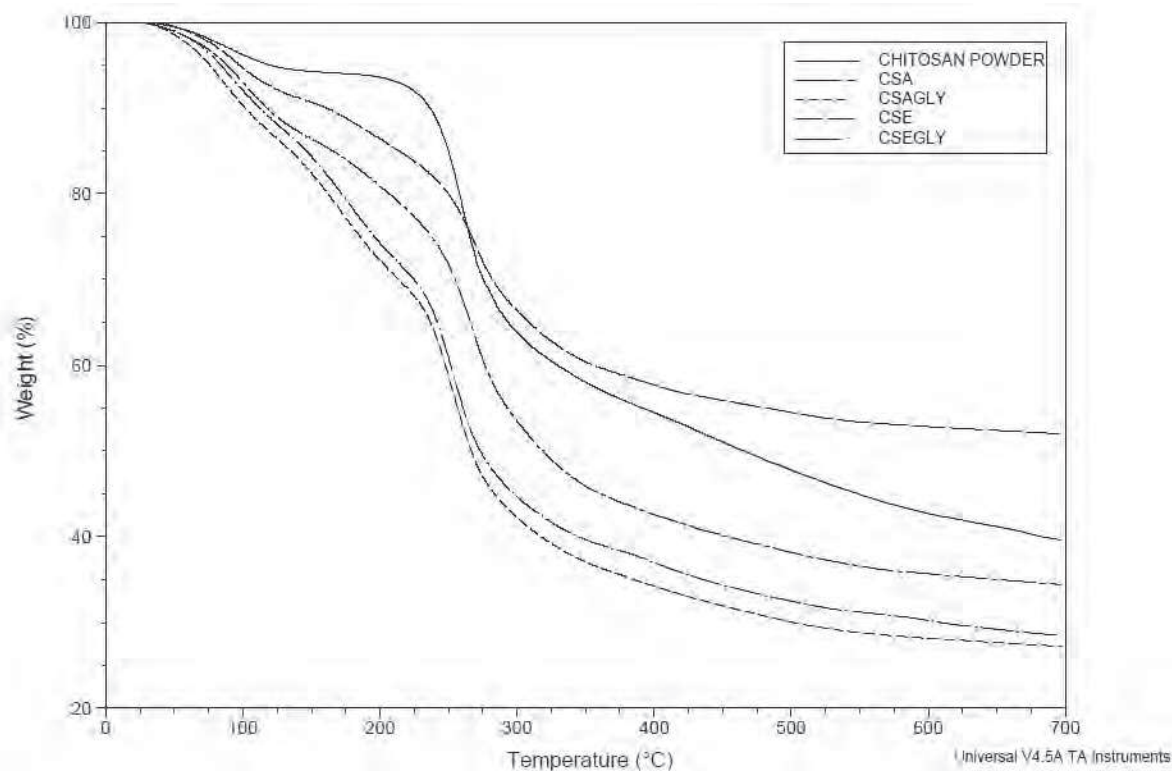
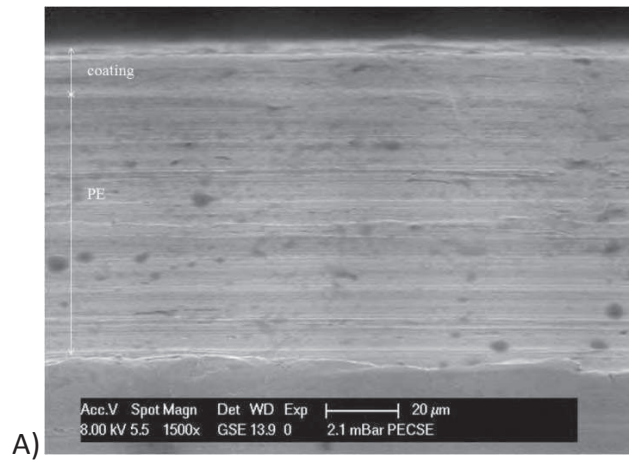


**Figure 6.2.** TGA thermograms of chitosan powder and chitosan films.

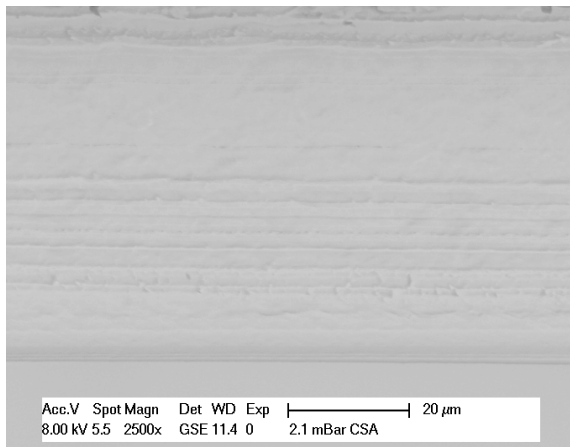
Moreover, closer examination of Fig. 6.2. indicates differences in the residual amounts of the chitosan powder, unplasticized and plasticized samples at 700°C. After degradation, the weight loss of the plasticized CSAGLY and CSEGLY film were the highest and equal to about 72%, in comparison with the unplasticized CSA (65%) and CSE (47%) samples. This low amount of residue for the plasticized samples can be related to the presence of glycerol that evaporates around 170°C. Surprisingly, an important gap between CSA and CSE weight loss is observed at 700°C that could only be related to the use of ethanol during the film fabrication process.

## 6.2. Film microstructure and surface analysis

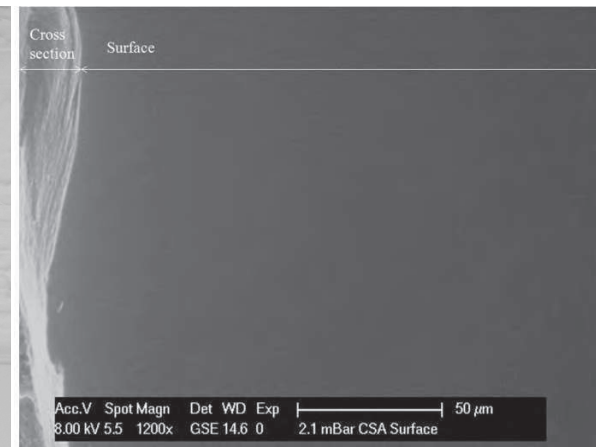
At a microscopic level, a good adhesion of the chitosan coatings on the polyethylene surface with the good integrity was observed (Fig. 6.3.A). Discontinuities in the polyethylene film are due to impurities and additives originally present in the PE. Micrographs indicated that the air side and the support side surfaces of pure chitosan films (CSE and CSA) were smooth, flat and without cracks (Figs. 6.3.C-G). After drying, the layered structure was observed (Figs. 6.3.B and 6.3.E).



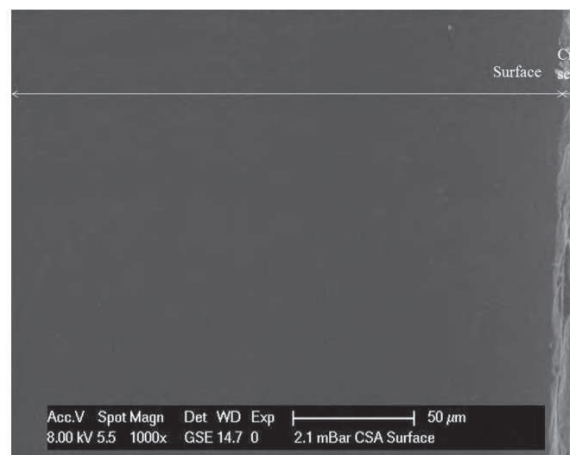
B)



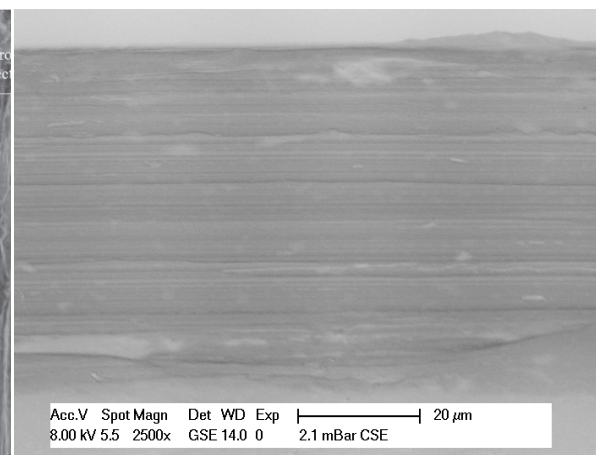
C)



D)



E)





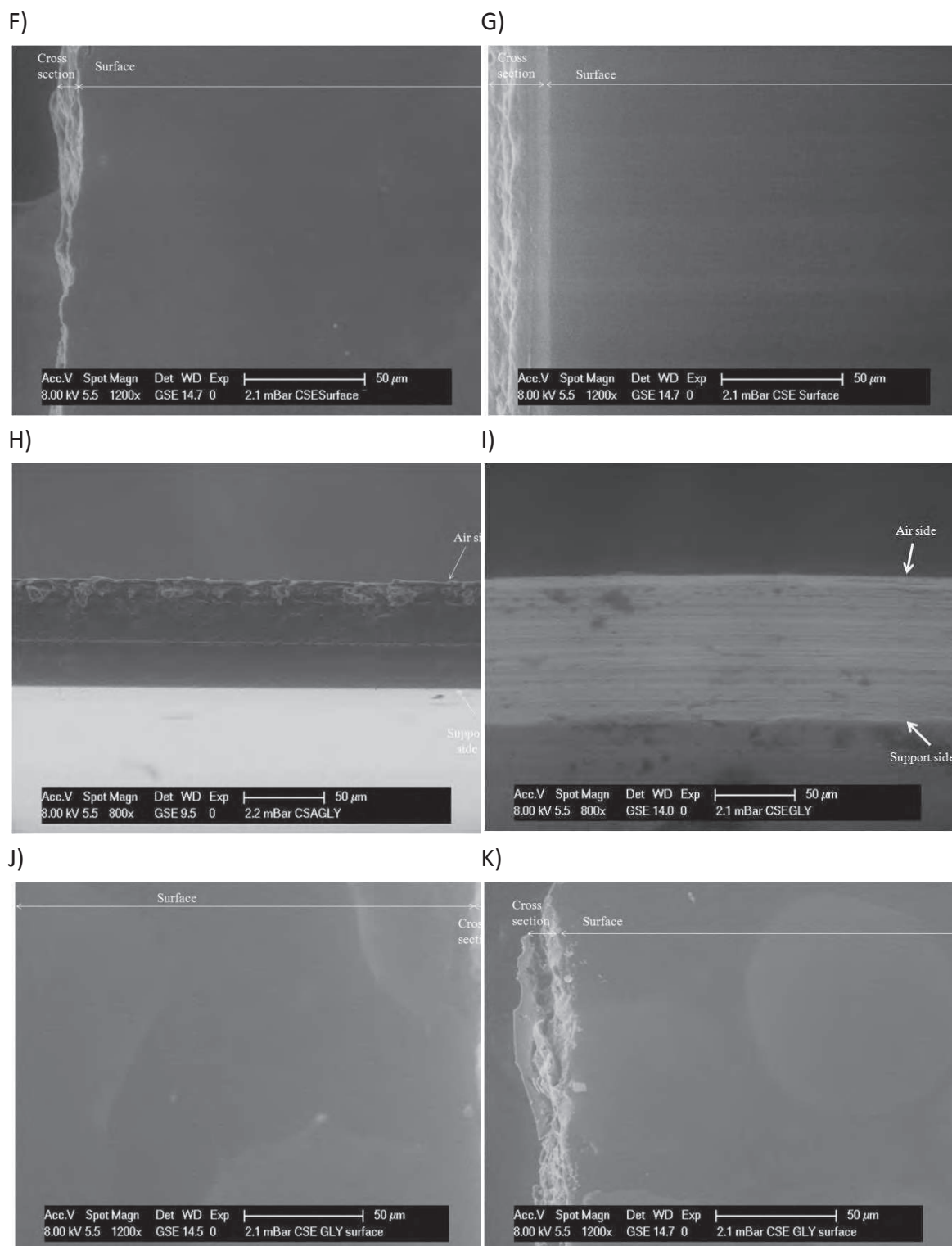


**Figure 6.3.** Micrograph of cross section of chitosan coated polyethylene (A); cross section (B), air side surface (C) and support side surface (D) of CSA film; cross section (E), air side surface (F) and support side surface (G) of CSE film; cross sections of glycerol plasticized samples-CSAGLY (H) and CSEGLY (I) and air side surface (J) and support side surface (K) of CSEGLY.



When a solution is cast, the solvent (mixture of water, acetic acid and ethanol) evaporates, and the interfacial concentration gradients are formed. Fluctuations of the concentration and the temperature between a Petri dish interface and a chitosan/air interface caused the formation of the layered structures (Torres et al., 2005). These changes in structure have also been confirmed by the DSC (Section 6.1.). In plasticized films, although there is a tendency of the film components to move from one side to the other, the structure all along the films is quite homogeneous. Fig. 6.3.I shows that CSEGLY has a much more homogeneous structure than film CSAGLY film (Fig. 6.3.F). This indicates that the repartition of glycerol was better in CSEGLY film. It was attributed to the hydrophilic character of glycerol that favours its solubility in ethanol and therefore a more homogeneous structure of the film prepared with hydroalcoholic acetic solvent was obtained. Nevertheless, there are some spots also distributed in a homogeneous way (Fig 6.3.K), that could be attributed to the plasticizer which goes up to the air side, probably because of a phase separation. However, phase separations were observed both on the air side and support side. Still, surfaces were flat and without pores and cracks (Figs. 6.3.J-K).

The molecular structure of the compounds and changes in the polymer matrix due to processing were verified with FTIR-ATR. The characteristic bands in all tested samples and FTIR-ATR spectra are given in Table 6.2. and Figs. 6.4. and 6.5.

**Table 6.2.** FTIR-ATR absorbance bands ( $\text{cm}^{-1}$ ) of raw chitosan powder and different chitosan films after processing.

SAMPLE	$\nu$ O-H, $\nu$ NH <sub>2</sub>	$\nu_{\text{as}}$ C-H	$\nu_s$ C-H	$\nu$ C=O (amide I)	$\delta$ NH (amide II)	$\delta$ CH	$\delta$ C-H	C-O group	$\nu_s$ C-O-C	$\nu$ C-O	$\rho$ CH <sub>2</sub>
CS POWDER	3100-3500	/	2875	1655	1598	1421	1383	1262	1156	900-1150	/
CSA	3100-3500	2926	2855	1630	1550	1406	/	1253	1152	900-1150	/
CSAGLY	3100-3500	2928	2870	1650	1536	1405	/	1255	1152	900-1150	/
CSE	3000-3500	2912	2845	1650	1549	1406	/	1254	1152	900-1150	/
CSEGLY	3000-3500	2962	2870	1650	1537	1405	/	1260	1151	900-1150	/
PE	/	2915	2847	/	/	/	/	/	/	/	719
PECSE (side PE)	/	2915	2847	/	/	/	/	/	/	/	719
PECSE (side CSE)	3100-3500	2915	2847	1650	1551	1407	/	1254	1152	900-1150	/

$\nu$ -stretching (as-asymmetrical, s-symmetrical);  $\delta$ -deformation;  $\rho$ -rocking.

The analysis of FTIR-ATR spectra indicated that no new chemical bonds were formed on the polymer surfaces. The PE side in the coated PECSE sample showed the same spectrum as the uncoated sample (Fig. 6.4.). This means that, despite the phase separation observed in the chitosan layer between glycerol and chitosan chains, no migration of glycerol into the PE could be detected. Bands at  $2915\text{ cm}^{-1}$  and  $2847\text{ cm}^{-1}$  were assigned to the asymmetrical and symmetrical C-H stretching, respectively. The peak at  $719\text{ cm}^{-1}$  corresponds to  $\text{CH}_2$  rocking in  $-(\text{CH}_2)_4-$  units (Zanetti et al., 2004). Similarly, the chitosan CSE side of the PECSE sample showed a similar spectrum to the one of the chitosan self standing film. The broad band between  $3100$  and  $3500\text{ cm}^{-1}$  were concerned as N-H and hydrogen bonded O-H stretch vibrations. Similarly to that of the PE, in the C-H stretch region, two peaks around  $2915\text{ cm}^{-1}$  and  $2847\text{ cm}^{-1}$  appeared (Dhanikula and Pachangula, 2004). Strong bands at  $1650\text{ cm}^{-1}$  and  $1551\text{ cm}^{-1}$  could be assigned to the vibration of C=O bond and the deformation of N-H bond (Abugoch et al., 2011; Martinez-Camacho et al., 2010). C-H deformation was observed at  $1407\text{ cm}^{-1}$  (Cardenas et al., 2008) and the band at  $1254\text{ cm}^{-1}$  was associated to the C-O bonds of ether or alcohol functions (Bettini et al., 2008). The band at  $1150\text{ cm}^{-1}$  corresponds to the symmetric stretching of C-O-C and the peaks from  $1150$  to  $900\text{ cm}^{-1}$  were assigned to the amino group on the C2 position of pyranose ring (Zhao et al., 2012; Pereda et al., 2012).

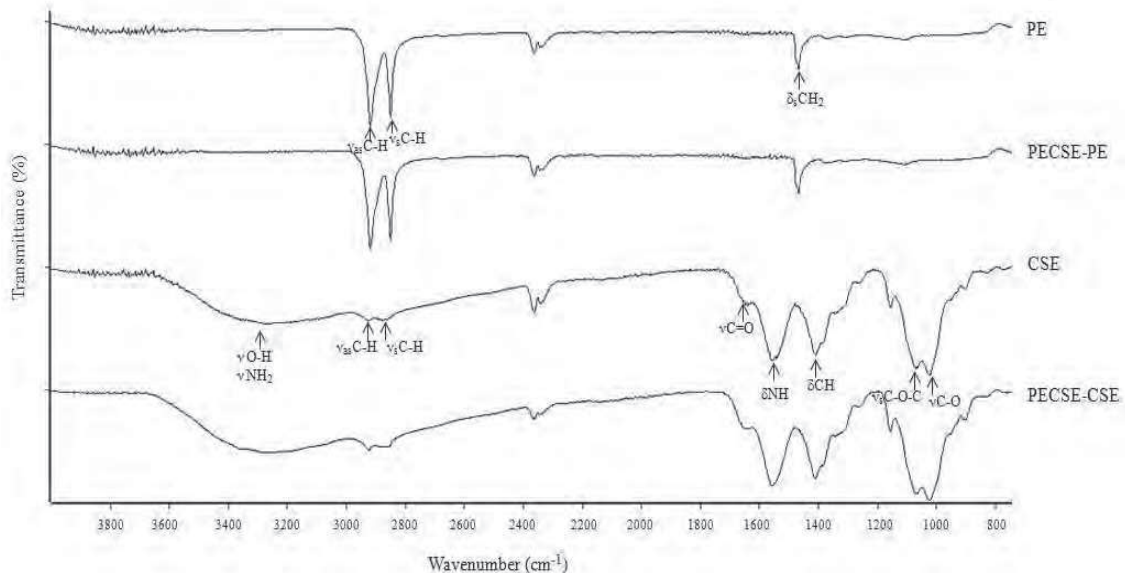


**Figure 6.4.** FTIR-ATR spectra of polyethylene (PE), chitosan film prepared with hydroalcoholic acid solvent (CSE), chitosan coated polyethylene - side polyethylene (PECSE - PE), chitosan coated polyethylene - side chitosan film (PECSE - CSE).

Moreover, some differences in the spectra of chitosan powder and dry films were observed. This was attributed to the film formation and increase in the order of the network structure (Fig. 6.5.).

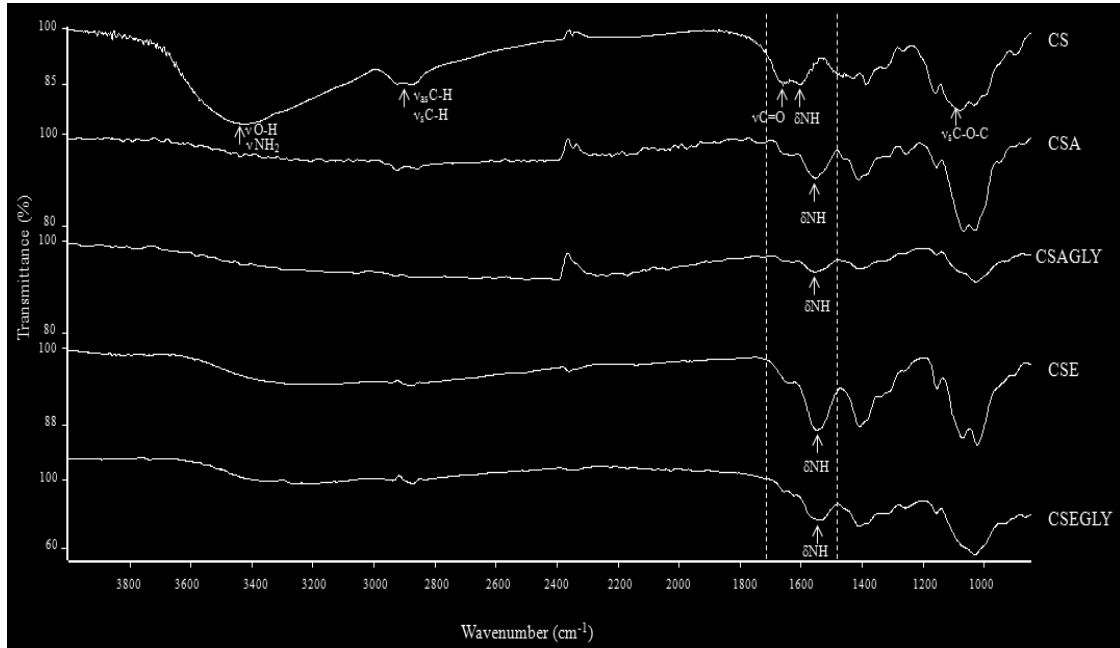


**Figure 6.5.** FTIR-ATR spectra of raw chitosan powder (CS), chitosan film prepared with aqueous acid solvent (CSA), chitosan film prepared with aqueous acid solvent and plasticized with glycerol (CSAGLY), chitosan film prepared with hydroalcoholic acid solvent (CSE) and chitosan film prepared with hydroalcoholic acid solvent and plasticized with glycerol (CSEGLY).

In the raw chitosan, O-H and N-H stretching bands were narrow and very intense whereas asymmetric and symmetric CH stretching peaks were in duplet. Overall observation was that in the region from 1700 to 1500  $\text{cm}^{-1}$  characteristic wave numbers for the dry films were systematically lower than the values of the chitosan powder. The shift of the 1598  $\text{cm}^{-1}$  peak suggests an increase in the number of the hydrogen bonds, interaction of primary amine groups of chitosan and acetic acid (presence of  $\text{NH}_3^+ \text{OOCCH}_3$  ionic bond) during the film drying. Moreover, these peaks were shifted to the lower values when glycerol was added. This was due to the interaction between glycerol and N-H groups in the chitosan. During the film drying glycerol displaced the acetic acid which was bound with chitosan macromolecules. Therefore shift in the N-H deformation was observed (from 1550 to 1536  $\text{cm}^{-1}$ ) (Brown et al., 2001). In addition, the band around 3200  $\text{cm}^{-1}$  became broader when ethanol was used as a solvent and glycerol was added as a plasticizer, probably due to the

polarity increase of the film forming solutions. In previous chapter it was reported that addition of the ethanol during processing decreased  $PO_2$ ,  $PCO_2$  and  $P_{air}$ . Observed behaviour was attributed to the structural orientation, conformation changes of chitosan matrix and increased crystalline spacing. Besides, micrographs (Fig. 6.3.) showed better dispersion of glycerol in CSEGLY films. Similar observations were previously reported (Lavorgna et al., 2010; Brown et al., 2001). The shift in the C-O group was probably the result of a lower mobility in the films due to its contribution to the formation of the solid structure, rearrangement of the hydroxyl bonds in the hydroalcoholic acid media and the interactions between the primary hydroxyl groups and the acetic acid. Indeed, Balau et al. (2004) confirmed by XRD analysis that differences in this range were related to the change of the amorphous material into a crystalline phase.

### **6.3. Conclusions of Chapter 6**

In summary, coated films showed a good visual and thermal stability, as well as a good adhesion between the synthetic surface and the biopolymer, as revealed by ESEM imaging. While the PE films showed one step in their degradation process, chitosan films followed three/or four steps for their degradation. Moreover, chitosan film degradation is influenced by solvents and plasticizers. Thermal studies revealed no significant changes in the structure of the PE film after the coating process. Still, it can affect the barrier properties that were therefore attributed to the chitosan layer. During the chitosan film formation some changes in the structural conformation occurred. In the aqueous acetate acid media, protonated chitosan molecules formed the chitosonium acetate. Glycerol established bonds with the amino groups of the chitosan and therefore displaced the acetic acid and strengthened the global structure of the film. Moreover, when PE was coated with chitosan, FTIR-ATR spectra showed a typical polyethylene spectrum on the support side, and the chitosan on the opposite surface confirming that coating process did not affect the polyolefin layer.

Given the points in the Chapters 5 and 6, one can conclude that chitosan based matrix showed great potential to be formed as self-standing film, or as coating on a polyethylene, with a good barrier performances and with no negative effects on support materials. Furthermore, in the Chapter four, chitosan films have shown a capacity to retain carvacrol as active volatile molecule and thus can be used in active packaging films development. However, the incorporation of carvacrol might affect the

structure and also final functional properties of chitosan films. Moreover, in design of good multilayer films, it is very important to check the wettability and the surface properties of polymers involved. Pursuing this further, in the following chapter, the influence of carvacrol on different physico-chemical properties of chitosan films and coatings will be studied.



*Chapter 7*

*Carvacrol affects interfacial, structural and  
transfer properties of chitosan coated  
polyethylene*

---

Publication: **Mia Kurek**, Claire-Helene Brachais, Mario Ščetar, Andrée Voilley, Kata Galić, Jean Pierre Couvercelle, & Frédéric Debeaufort  
Carbohydrate Polymers, submitted in March 2012.

Unpublished part of this chapter:

7.2. Effect of glycerol on the surface tension of chitosan film forming solutions and their spreadability/adhesivity on polyethylene





In Chapter two, it was pointed out that due to the health concerns and environmental problems; the current research on active packaging has focused on the use of natural preservatives or active compounds introduced in the biodegradable/bio-based packaging materials (Siripatrawan and Harte, 2010; Suppakul et al., 2003). Therefore, the incorporation of carvacrol as the main component from oregano essential oil, can improve both the antimicrobial and the functional film properties.

When designing the most suitable film for a determined use and functionality, it is important to understand the influence of physico-chemical factors on the functional properties of the film forming solutions and obtained films. The application target of this chapter is the development of the environmentally friendly, carvacrol activated chitosan-coated polyethylene film, with the potential of its use as an active food packaging material. Furthermore, it is aimed to assess the ability of the deposition of different compositions of chitosan coatings on the low density polyethylene. However, to better understand the possible changes in the chitosan matrix, chitosan self-standing films containing carvacrol have also been studied. Finally, surface modifications, changes in thermal and barrier properties after the coating processes, have been determined as a function of the coating composition.

### **7.1. Liquid surface tension of the film forming solutions and critical surface tension of polyethylene and chitosan films**

This work was designed to study the compatibility of the chitosan film forming solutions (FFS) and the PE film. PE was used as the support film coated by the FFS. To ensure adequate bonding, spreading and wetting, the film forming solution should have a liquid surface tension higher than the critical surface tension of the support material. Therefore, the surface tension of FFS is an essential factor for determining coating adhesion success. The phenomenon of spreading of the liquid over the surface, as measured by the contact angle, is dependent on the relative magnitude of cohesive and adhesive molecular forces that exist respectively within the liquid and between the liquid and the solid. Wetting is favoured by a low liquid-solid ( $\gamma_{LS}$ ) and liquid-vapour ( $\gamma_{LV}$ ) surface tensions, and a high solid-vapour surface tension ( $\gamma_{SV}$ ) (Eq. 3.6.). The first information given by the contact angle measurements can thus be exploited in a static manner with a comparative study at time 0 s when the drop is just deposited onto the tested surface, and time 30 s corresponding to a metastable equilibrium between the liquid droplet and the tested surface. In this static method, the sessile drop is assumed to be in the complete mechanical equilibrium, even if the value of the contact angle is

not the true equilibrium, due to the experimental conditions and tested surfaces that differ from the perfection (Karbowski et al., 2006). Initially, after the deposition of different FFS, a significant modification of the liquid/PE film contact angle occurred. Thus spreading was observed. The same trend was monitored during all the recorded period (120 s) (Fig. 7.1.). The obtained values were lower than 90°, hence denoting a spontaneous partial wetting of the PE surface with all the film forming solutions (Vargas et al., 2009; Hagenmaier and Baker, 1993).

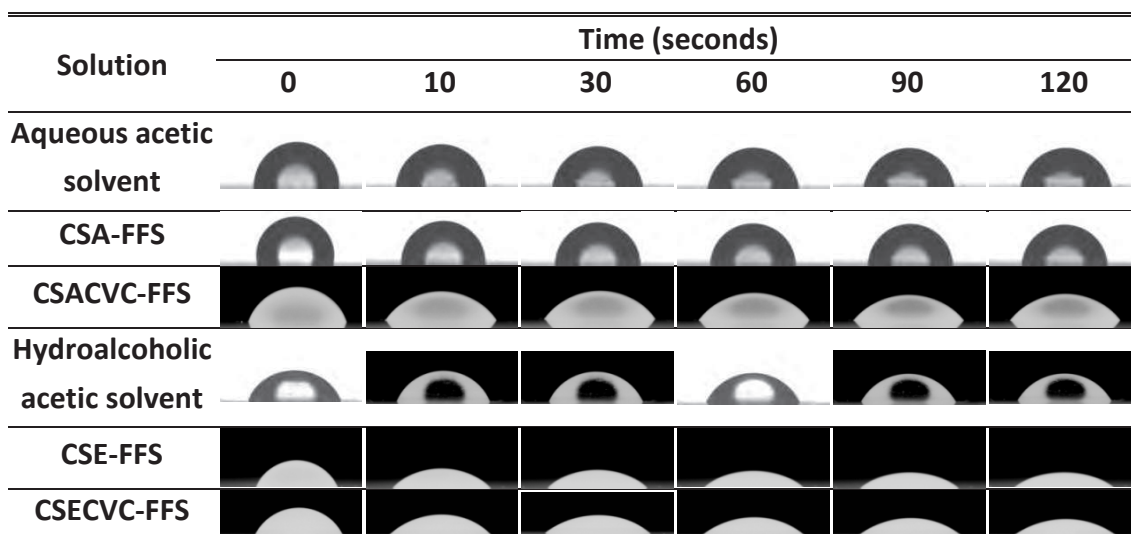


**Figure 7.1.** Pictures of solvents and chitosan film forming solutions when applied to polyethylene film.

CSA-FFS - chitosan in aqueous acid solution; CSE-FFS - chitosan in hydroalcoholic acid solution; CSACVC-FFS - chitosan and carvacrol in aqueous acid solution; CSECVC-FFS - chitosan and carvacrol in hydroalcoholic acid solution.

The coating solutions with ethanol (CSE and CSECVC) had a surface tension of 32.4 and 31.3 mN/m, respectively. These values were significantly lower than those of coatings based on chitosan solubilised in aqueous acetic acid (CSA and CSACVC), of 71.8 and 37.9 mN/m, respectively. The first two coating solutions, CSE and CSECVC, had a low surface tension due to the fact that the solvent was hydroalcoholic acid. Furthermore, the presence of carvacrol might act as a surface active ingredient (CSECVC). This fact is supported by the values for CSACVC-FFS where the surface tension was drastically decreased after the carvacrol incorporation. Moreover, results indicated that the CSE and the CSECVC coatings were more prone to spreading on the polyethylene film used in this study, since their liquid surface tension values were closer to  $\gamma_c$  (critical surface tension) of the PE film. This was determined from the Zisman's plot (Chapter 3, Section 3.4.5.). The lowest liquid surface tension value (31.3

mN/m) matched the lowest contact angle value (39°) and therefore, a better spreading and probably better adhesion followed.

### 7.1.1. Critical surface tension and surface free energy of PE films

The surface energy of the solid surface is related to the surface tension of the liquids and their contact angles. The determination of the critical surface tension ( $\gamma_C$ ) was done from the measurement of the contact angle of several standard liquids deposited on that surface. Young (1805) defined the contact angle as a wetting phenomenon for solid, non-porous and non-absorbent surfaces. The evaluation of  $\gamma_C$  and surface free energy through the surface forces measurement is an approach that quantifies the “surface affinity” for solutions. It was extrapolated from Zisman plot (as described in Chapter 3).

**Table 7.1.** Surface tension ( $\gamma_L$ ), dispersive ( $\gamma_L^D$ ) and polar ( $\gamma_L^P$ ) surface tension components, adhesion ( $W_A$ ), cohesion ( $W_C$ ) and spreading coefficient ( $W_S$ ) of standard liquids and chitosan film forming solutions (FFS) on the PE at equilibrium after 30 s ( $\Theta_{30s}$ ).

Compound	$\gamma_L$	$\gamma_L^D$	$\gamma_L^P$	$W_A$	$W_C$	$W_S$	$\Theta_{30s}$
	(mN/m)						
Water*	72.8	21.8	51.0	82.4 <sup>b</sup>	145.6 <sup>a</sup>	-63.2 <sup>g</sup>	82.4±4.8 <sup>a</sup>
Diodomethane*	50.8	50.8	0	79.7 <sup>b,c,d</sup>	101.6 <sup>f</sup>	-21.9 <sup>d</sup>	55.3±1.5 <sup>c</sup>
Glycerol*	64.0	34.0	30.0	86.4 <sup>a</sup>	128.0 <sup>d</sup>	-41.6 <sup>f</sup>	69.5±7.7 <sup>b</sup>
Tetradecane*	26.6	26.6	0	49.9 <sup>g</sup>	53.1 <sup>j</sup>	-3.2 <sup>a</sup>	28.6±2.5 <sup>e</sup>
Hydroalcoholic acid solution	55.0	ND	ND	76.4 <sup>d</sup>	110.0 <sup>e</sup>	-33.6 <sup>e</sup>	67.1±3.6 <sup>b</sup>
Aqueous acetic acid solution	70.0	ND	ND	78.2 <sup>c,d</sup>	140.0 <sup>c</sup>	-61.8 <sup>g</sup>	83.2±1.3 <sup>a</sup>
CSA-FFS	71.76	ND	ND	80.1 <sup>b,c</sup>	143.5 <sup>b</sup>	-63.4 <sup>a</sup>	83.3±3.5 <sup>a</sup>
CSE-FFS	32.41	ND	ND	57.4 <sup>e,f</sup>	64.8 <sup>h</sup>	-7.4 <sup>b</sup>	39.4±2.6 <sup>d</sup>
CSACVC-FFS	37.88	ND	ND	59.8 <sup>e</sup>	75.8 <sup>g</sup>	-15.9 <sup>c</sup>	54.6±0.2 <sup>c</sup>
CSECVC-FFS	31.3	ND	ND	55.6 <sup>f</sup>	62.6 <sup>i</sup>	-6.9 <sup>b</sup>	39.0±1.6 <sup>d,e</sup>

ND not detected; \* adapted from Van Oss (1994); <sup>a-h</sup> Different letters indicate a statistically significant difference within the column at  $p < 0.05$  level.

To verify the applicability of that method it was necessary to determine the surface free energy of polyethylene and chitosan films. Eq. 3.15. was used to calculate the values of the polar and dispersive film surface tension components. The surface free energy of the PE film was 35.7 mN/m. Thus PE film used in this study has a low-energy surface (<100 mN/m) (Owens and Wendt, 1996) with a higher dispersive (31.3 mN/m) and a lower polar (4.4 mN/m) component (Table 7.2.).

**Table 7.2.** Comparison of surface free energy and the dispersive ( $\gamma_s^D$ ) and polar ( $\gamma_s^P$ ) components of polyethylene film and chitosan self standing films. Measurement were done at air drying surface (air) and support drying surface (support).

FILM SAMPLE	Surface Free Energy (mN/m)	$\gamma_s^D$ (mN/m)	$\gamma_s^P$ (mN/m)	Critical surface tension (mN/m)
PE	35.76 <sup>f</sup>	31.29 <sup>g</sup>	4.47 <sup>c</sup>	17.36 <sup>h</sup>
CSE air	37.32 <sup>e</sup>	36.12 <sup>d</sup>	1.20 <sup>e</sup>	41.80 <sup>c</sup>
CSE support	32.76 <sup>h</sup>	31.90 <sup>f</sup>	0.85 <sup>f,g</sup>	38.55 <sup>g</sup>
CSECVC air	66.42 <sup>a</sup>	43.72 <sup>a</sup>	22.70 <sup>b</sup>	76.68 <sup>a</sup>
CSECVC support	32.68 <sup>h</sup>	31.90 <sup>f</sup>	0.78 <sup>g</sup>	38.74 <sup>f</sup>
CSA air	39.69 <sup>c</sup>	38.59 <sup>b</sup>	1.10 <sup>e,f</sup>	44.35 <sup>b</sup>
CSA support	34.30 <sup>g</sup>	33.44 <sup>e</sup>	0.86 <sup>f,g</sup>	39.34 <sup>e</sup>
CSACVC air	65.29 <sup>b</sup>	36.00 <sup>c</sup>	29.30 <sup>a</sup>	76.54 <sup>a</sup>
CSACVC support	37.68 <sup>d</sup>	35.79 <sup>c</sup>	1.88 <sup>d</sup>	40.02 <sup>d</sup>

<sup>a-h</sup> Different letters indicate a statistically significant difference within the column at  $p < 0.05$  level.

This denotes ability of PE to participate in non-polar interactions. Therefore, Zisman plot can be applied to estimate the critical surface tension, defined as the value of the superficial tension (liquid/vapour) at the intercept of the Zisman plot for  $\cos\theta=1$ . Table 7.1. shows the surface tensions of the four different film forming solutions, two solvents used to solubilise chitosan powder and four standard liquids applied on polyethylene film for the Zisman plots (Fig. 7.2.).

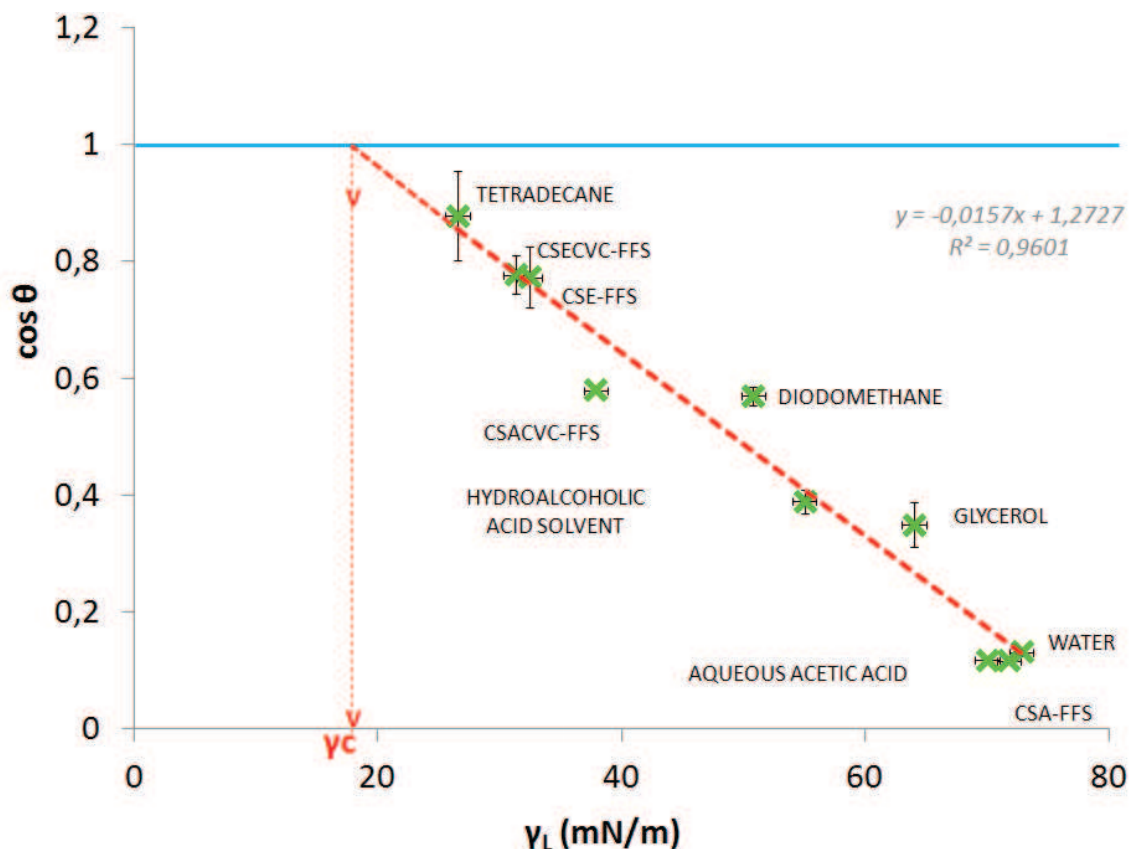


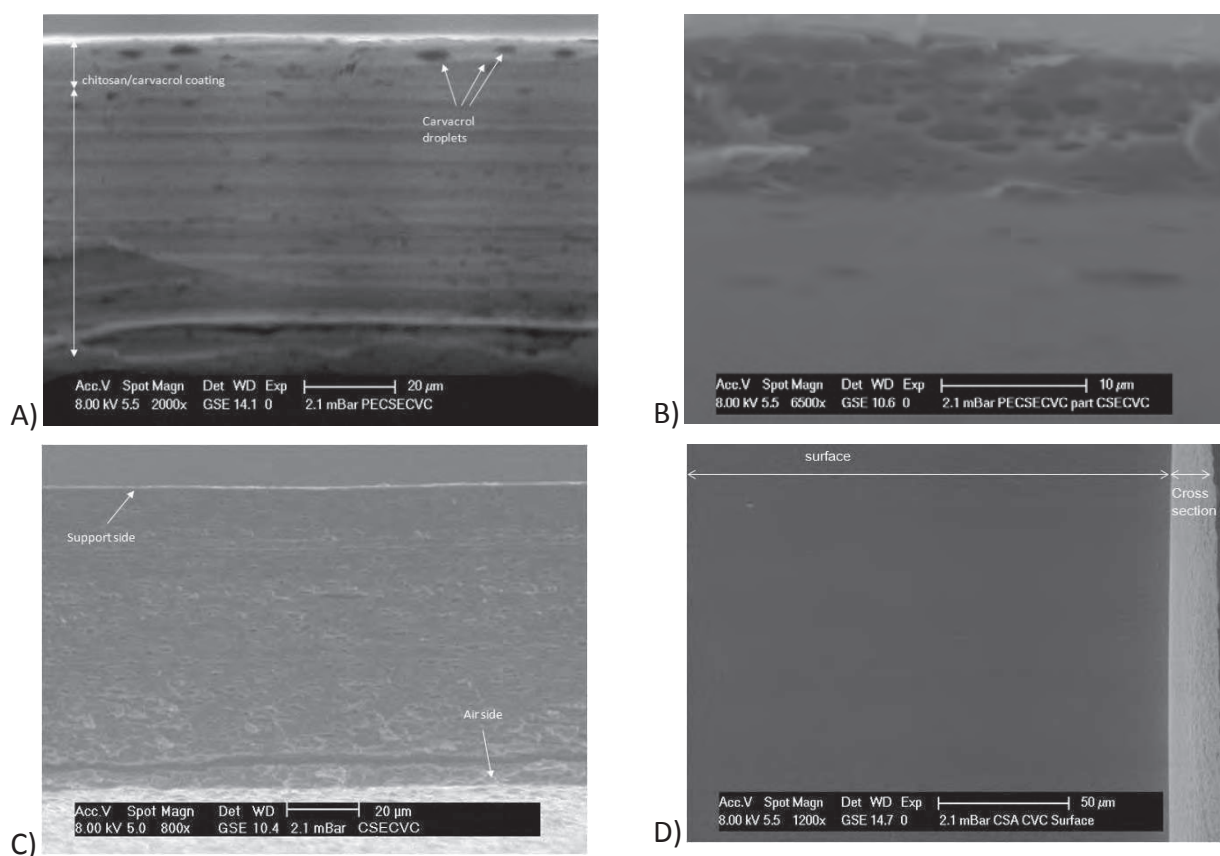
Figure 7.2. Zisman plot of polyethylene surface.

Elsewhere,  $\gamma_c$  values have been reported to be lower than the surface tension values of the same tested surfaces (Dan, 1970; Casareigo et al., 2008). A surface with these characteristics interacts with the liquid primarily by dispersion forces, thus influencing the effective spreading of the coating on the PE surface (Rulon and Robert, 1993). Therefore the compatibility of the surface polarity and FFS played an important role in the PE wettability. The PE, being very rich in apolar components features a significant apolar influence.

### 7.1.2. Wettability of polyethylene films by the coating solutions

Optimization of wettability ( $W_s$ ) includes optimisation of work of adhesion ( $W_A$ ) and work of cohesion ( $W_c$ ). Cohesion promotes contraction and adhesion promotes the spreading of a liquid. The obtained results are reported in Table 7.1. CSECV was considered as the most suitable solution to coat the PE surface as it had the highest  $W_s$  (the closest to zero) (Tzoumaki et al., 2009). The higher cohesive force of a coating solution caused the shrinkage of the CSA droplet. CSE and CSECV were more capable to spread on the PE. The higher surface tension (Table 7.1.) and contact angles of CSA-

FFS (83°) and CSACVC-FFS (54°), indicated that the forces between molecules were very strong. In addition to the reduced superficial tension of the FFS, the equilibrium-spreading coefficient ( $W_s$ ) was improved with ethanol and carvacrol (from -63.38 to -6.99). Moreover, smaller contact angle was observed over the whole tested period (Fig. 7.1.). Both good stability of coating/PE and lower free energy loss (Choi et al., 2002) increased the force required to separate the coating film from the PE. Thus the solution spread and good adhesion was obtained (Fig. 7.3.A). This phenomenon may be attributed to the adsorption of the surface active molecules at the liquid-vapour interface and its transfer to the solid-liquid interface during the coating process (Von Bahr et al., 1999). Surface active molecules in the FFS, which were adsorbed on the PE, caused increase of surface pressure of CSECVC-FFS that in turn increased its spreading and decreased the contact angle. Besides, wettability is influenced by viscosity. It must be low enough to allow the easy and homogeneous application of FFS onto the PE surface. In Chapter four, it was reported that the incorporation of carvacrol and ethanol significantly reduced the consistency index. Therefore a better wettability was obtained. For further application, CSE and CSECVC were chosen as the best coating formulations.





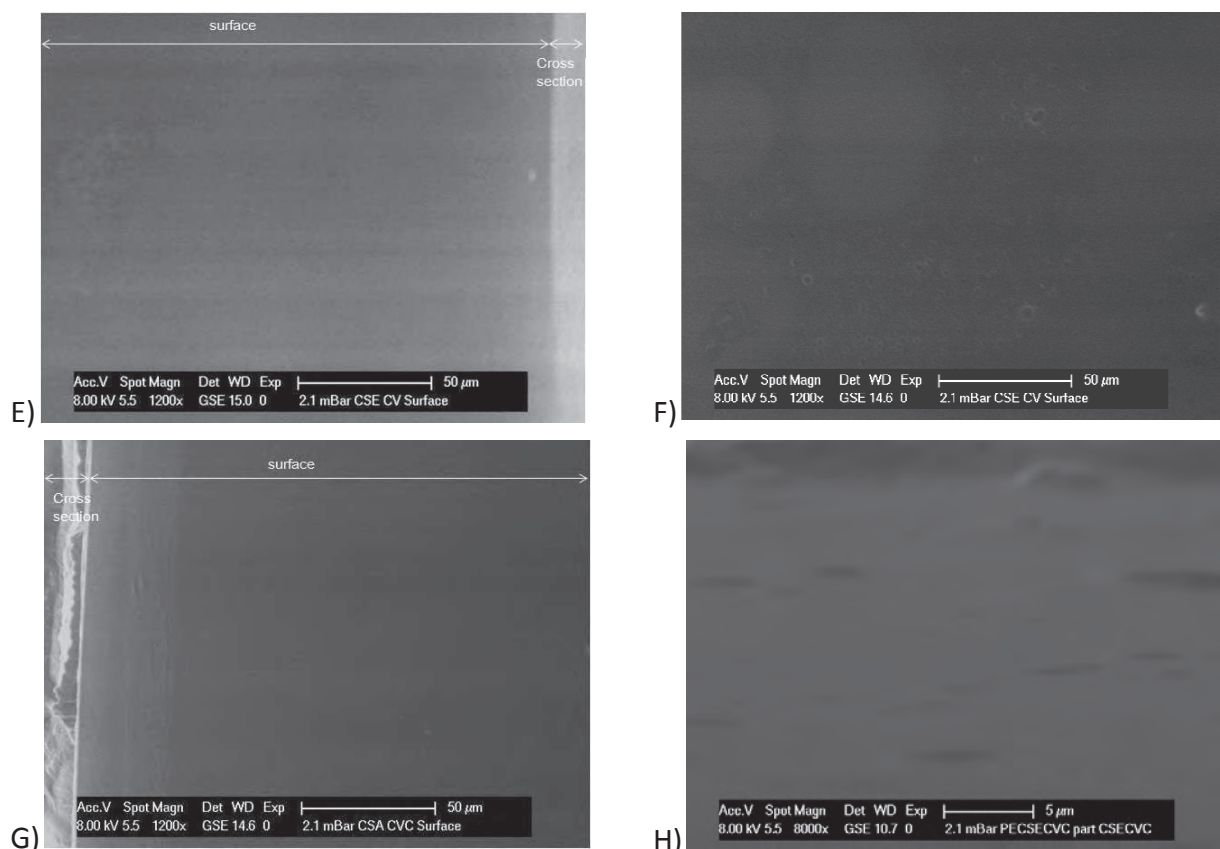


**Figure 7.3.** ESEM cross sections of PECSECVC film (A), CSECVC coating layer (B), CSECVC film (C) and surfaces of chitosan films – support side surface of CSACVC (D) and CSECVC (E) and air side surface of CSECVC (F,H) and CSACVC (G).

## 7.2. Effect of glycerol on the surface tension of film forming solutions and its spreadability/adhesivity on polyethylene

*(Unpublished part of this chapter)*

Generally, plasticizers like glycerol are used to improve mechanical properties of solid films. However, by interspersing themselves, incorporation of these agents as internal lubricants may reduce frictional forces between polymer chains. Thus they can change surface tension of film forming solution and its spreadability on support surface. The surface tension of tested film forming solutions is given in Table 7.3. Addition of glycerol had adverse effect on liquid surface tension ( $\gamma_L$ ) of CSA and CSE. While  $\gamma_L$  of CSAGLY-FFS was little bit lower than CSA-FFS,  $\gamma_L$  of CSEGLY-FFS was significantly higher than CSE-FFS. Plasticization with hydrophilic glycerol results in decreasing surface hydrophobicity. Then, it is to expect that higher repulsions between



hydrophobic PE and hydrophilic coating would take place that was not the case for CSA-FFS. However, addition of carvacrol both in hydroalcoholic aqueous solvent as well as in the acidic acid solvent decreased the surface tension of film forming solutions. Drop in the surface tension by the addition of carvacrol might be due to the interfacial adhesion between carvacrol and chitosan. However, as already observed in Chapter 4, in the presence of glycerol, carvacrol seems to lose its stabilizing/structuration properties. Then, the spreading was acerbated. Ziani et al. (2008) reported that the presence of glycerol was not significant in reducing surface tension since it is not a tensioactive molecule. Differences in this study obtained for CSEGLY sample might be because of the different solvent, amounts of glycerol and type of chitosan used.

**Table 7.3.** Surface tension of chitosan film forming solutions and their change with the addition of glycerol.

SAMPLE	$\gamma_L$	SAMPLE	$\gamma_L$
CSA-FFS	71.76±0.45 <sup>a</sup>	CSE-FFS	32.41±0.97 <sup>d</sup>
CSAGLY-FFS	67.22±0.10 <sup>b</sup>	CSEGLY-FFS	40.32±2.20 <sup>c</sup>
CSAGLYCVC-FFS	38.63±0.03 <sup>c</sup>	CSEGLYCVC-FFS	33.75±0.36 <sup>d</sup>

<sup>a-d</sup> Different letters indicate a statistically significant difference within the column at p<0.05 level.

Adhesion, cohesion and spreading coefficients of different film forming solutions on the polyethylene surface are given in Table 7.4. Photos of the film forming solutions on the polyethylene at different spreading times are given in Fig. 7.4.

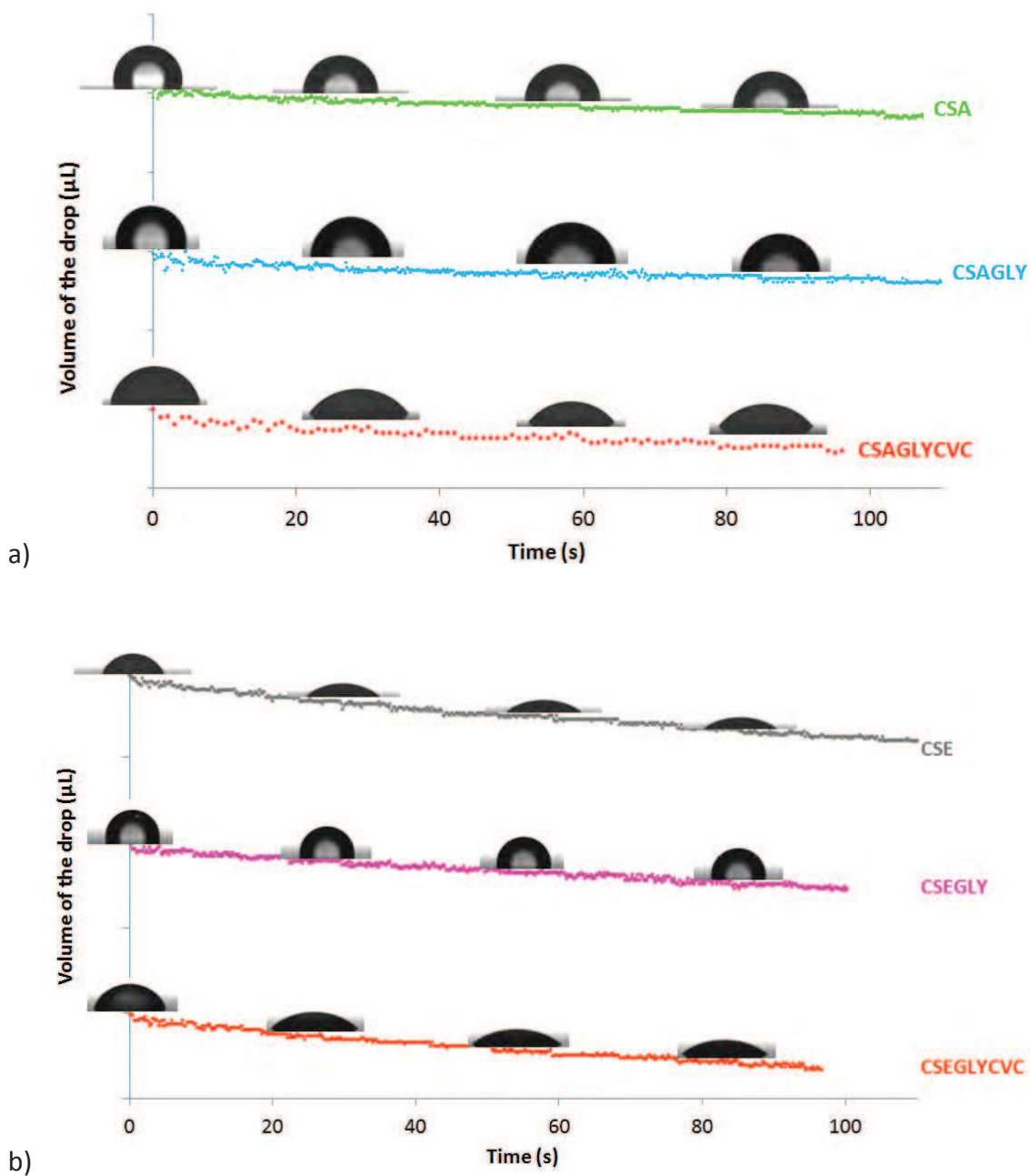


**Figure 7.4.** Changes in the drop volume of the film forming solution containing glycerol (GLY) and/or carvacrol (CVC) deposited onto the polyethylene as a function of the solvent nature (CSA=aqueous acetic acid solvent, or CSE=hydroalcoholic acid solvent).

**Table 7.4.** Adhesion ( $W_A$ ), cohesion ( $W_C$ ) and spreading ( $W_S$ ) coefficients of chitosan/glycerol film forming solutions onto polyethylene surface at equilibrium ( $\theta_{30s}$ ).

SAMPLE	$W_A$	$W_C$	$W_S$
CSA	80.14 <sup>a</sup>	143.52 <sup>a</sup>	-63.38 <sup>f</sup>
CSAGLY	75.54 <sup>b</sup>	134.44 <sup>b</sup>	-58.89 <sup>e</sup>
CSAGLYCVC	60.63 <sup>c</sup>	77.26 <sup>d</sup>	-16.63 <sup>c</sup>
CSE	57.45 <sup>d</sup>	64.82 <sup>f</sup>	-7.37 <sup>a</sup>
CSEGLY	45.6 <sup>e</sup>	80.64 <sup>c</sup>	-35.02 <sup>d</sup>
CSEGLYCVC	58.3 <sup>d</sup>	67.50 <sup>e</sup>	-9.16 <sup>b</sup>

<sup>a-f</sup> Different letters in the column indicate a statistically significant difference among the samples

The addition of glycerol decreased the adhesion coefficients in both solvents. Surprisingly it slightly improved the spreadability of the aqueous acetic acid film forming solution (Table 7.4.). However, in hydroalcoholic acid solution due to droplet flocculation after homogenization process (as described in Chapter 4) the cohesion forces were higher. So, the spreading was obstructed as the coefficient increased from -7 to -35. Nevertheless, regardless of glycerol, the spreading coefficient of all hydroalcoholic acid film forming solutions were fairly lower. In summary, spreading was favoured by both ethanol and carvacrol (Figs. 7.1. and 7.4.).

### 7.3. Surface free energy and critical surface tension of dry chitosan self standing films

To better understand the functional film properties, the hydrophilic/hydrophobic character of chitosan films, the surface free energy and the critical surface tension were determined. Results are given in Tables 7.1. and 7.2. The surface free energy controls the contact angle of the droplet with the film surface. On the film support side no significant changes occurred. The hydrophilic character was more pronounced on the air side (higher values of reported data) (Tables 7.1. and 7.2.). While a hydrophobic behaviour should be expected, significantly higher surface free energies were measured for CSECVC and CSACVC films (66.4 and 65.3 mN/m, respectively). The authors reported that the addition of hydrophobic agents, such as essential oils and lipids, could increase the surface hydrophobicity (Moradi et al., 2012;

Ojagh et al., 2010; Pereda et al., 2010). Opposite results in this study indicated that during drying process, some changes in the film structure occurred (Fig. 7.3.). Additionally high values of the water contact angles were reported for the support side (from 80-110°). From Table 7.1., it can be seen that the polar component ( $\gamma_s^p$ ) of chitosan surfaces were close to zero. Once again, when carvacrol was incorporated, this value changed up to 29 times (from 1.20 (CSE) to 22.70 mN/m (CSECVC) and from 1.10 (CSA) to 29.30 mN/m (CSACVC)). Farris and co-workers (2011) stated that this behaviour could be due to the non-polar impurities on the chitosan surface. On top of that, the possible orientation of the methyl moieties of the residual acetyl groups along the chitosan backbone may have become exposed at the solid/air interface for the thermodynamic reasons (Cunha et al., 2008). Higher dispersive components, ranging from 31.90 mN/m for CSE support side to 43.72 mN/m for CSECVC air side are coherent with the typical values found for the polysaccharide films.

#### **7.4. Molecular interactions in the films**

Molecular structure changes in polyethylene film, chitosan coatings and self-standing films were verified with the FTIR-ATR technique which allows a surface analysis of the samples. The characteristic bands in all tested samples are given in Table 7.5.

Table 7.5. FTIR-ATR absorbance bands ( $\text{cm}^{-1}$ ) of raw chitosan powder and different chitosan films after processing.

Vibration	Chitosan powder	CSA	CSACVC	CSE	CSEVCV	PE	PECSE (sidePE)	PECSE (sideCSE)	PECSECV (sidePE)	PECSECV (sideCSECV)
$\nu$ OH, $\nu$ NH <sub>2</sub>	3100-3500	3100-3500	3100-3500	3100-3500	3100-3500	/	/	3100-3500	/	3100-3500
$\nu_{\text{as}}$ C-H	/	2920-2940	2941	2912	2912-2929	2915	2915	2920	2915	2921
$\nu_{\text{s}}$ C-H	2875	2875	<b>2841-2875</b>	2845	<b>2850-2869</b>	2847	2847	2847	2847	<b>2850-2866</b>
$\nu$ C=O	1655	1644	<b>1644-1659</b>	1650	<b>1630</b>	/	/	1650	/	<b>1633</b>
$\delta$ NH	1598	1538;1555	1550;1538	1550;1538	<b>1538</b>	/	/	1551	/	<b>1538</b>
$\delta$ CH	1421	1403	1404	1404	1404	1462	1462	1404	1462	1404
$\delta$ C-H	1383	/	/	/	/	/	/	/	/	/
C-O group	1262	1260	1258	1254	1259	/	/	1254	/	1257
$\nu_{\text{s}}$ C-O-C	1156	1551	1151	1151	1151	/	/	1151	/	1151
$\nu$ C-O	900-1150	900-1150	900-1150	900-1150	900-1150	/	/	900-1150	/	900-1150
$\omega$ CH (phenyl ring)	/	/	<b>808-813</b>	/	<b>814-818</b>	/	/	/	/	<b>812-820</b>
$\rho$ CH <sub>2</sub>	/	/	/	/	/	719	719	/	719	/

$\nu$ -stretching (as-asymmetrical, s-symmetrical);  $\delta$ -deformation;  $\rho$ -rocking;  $\omega$ -wagging.

Bolded values assign differences after the incorporation of carvacrol.

FTIR-ATR analysis spectra indicated that no new chemical bonds were formed on the polyethylene surfaces. PE side in the coated PECSE and PECSECVC sample showed the same spectrum as the uncoated one. Bands at  $2915\text{ cm}^{-1}$  and  $2847\text{ cm}^{-1}$  were assigned to the asymmetrical and symmetrical C-H stretching, respectively. The peak at  $719\text{ cm}^{-1}$  corresponds to  $\text{CH}_2$  rocking in  $-(\text{CH}_2)_4-$  units (Zanetti et al., 2004). Chitosan used in this study was >85% deacetylated, therefore the typical C=O stretching peak at  $1655\text{ cm}^{-1}$  and N-H bending peak at  $1598\text{ cm}^{-1}$  were observed. These peaks represented the structure of N-acetylglucosamine, which could be found in chitosan with a lower degree of deacetylation (Balau et al., 2004; Martinez-Camacho et al., 2010). The chitosan sides of the coated samples showed a similar spectrum to the one of the chitosan self standing films (depending on the formulation). However, differences in the spectra of chitosan powder and dry films were observed. It was attributed to the film formation that increased structure order as well as to a number of hydrogen bonds, interaction of primary amine groups of chitosan and acetic acid (Kurek et al., 2012b). In the region from  $1700\text{ cm}^{-1}$  to  $1500\text{ cm}^{-1}$  characteristic for the C=O stretching and N-H bending bands, wave numbers for the dry films were systematically lower than the values of the chitosan powder. Other peaks were assigned as following: at  $1407\text{ cm}^{-1}$  to C-H deformation (Cardenas et al., 2008), at  $1254\text{ cm}^{-1}$  to C-O bonds of ether or alcohol functions (Bettini et al., 2008), at  $1150\text{ cm}^{-1}$  to the symmetric stretching of C-O-C and the peaks from  $1150\text{ cm}^{-1}$  to  $900\text{ cm}^{-1}$  to the amino group on the C2 position of pyranose ring (Pereda et al., 2012).

The spectrum of the raw carvacrol (not given in Table 7.5.) displays vibrations at  $1420\text{ cm}^{-1}$  assigned to C-H deformation, vibration at  $1250\text{ cm}^{-1}$  and  $1115\text{ cm}^{-1}$  assigned to C-O vibration and characteristic phenyl ring out-of-plane vibration at  $811\text{ cm}^{-1}$  (Schultz et al., 2005). This characteristic bond is observed in all samples containing carvacrol, confirming that some free carvacrol molecules are entrapped within the chitosan network. However, a new peak shifted to higher wavelength ( $820\text{ cm}^{-1}$  instead of  $811\text{ cm}^{-1}$ ) indicated the occurrence of carvacrol/chitosan interactions. New peaks also appeared after the carvacrol incorporation, in the symmetric C-H vibration region, at  $2850\text{ cm}^{-1}$  and  $2869\text{ cm}^{-1}$  for CSACVC and CSECVC samples respectively. Shift from  $1650\text{ cm}^{-1}$  to  $1630\text{ cm}^{-1}$  for the carbonyl bond and disappearance of N-H deformation at  $1550\text{ cm}^{-1}$  in CSECVC sample may be due to interactions between N-H groups in chitosan chain and OH group of the phenyl ring in the carvacrol molecule (5-isopropyl-2-methylphenol). In comparison to CSACVC films, carvacrol is more soluble in ethanol and thus better dispersed in FFS. Therefore during the film drying,

additional interactions might take place. Likewise, the band around  $3200\text{ cm}^{-1}$  became broader when ethanol was used as a solvent. It was probably due to the increase of polarity in the film forming solutions (Martinez-Camacho et al., 2010; Kurek et al., 2012b). The shift of the C-O bond was probably the result of a lower mobility in the films due to its contribution to the formation of the solid structure, rearrangement of the hydroxyl bonds in the hydroalcoholic acid media and the interactions between the primary hydroxyl groups and the acetic acid (Balau et al., 2004).

## **7.5. Film microstructure**

Environmental scanning electronic microscopy (ESEM) observations were carried out to contribute to a better insight in the homogeneity and in the microscopic structure of dried films. The final microstructure obtained by the different FFS after drying is influenced by the structural arrangement of chitosan and carvacrol before and after drying. A good adhesion was observed for the coated PE (Fig. 7.3.A). According to Sanchez-Gonzalez and co-workers (2010), droplet flocculation, coalescence and creaming can occur. Chitosan string arrangement as well as the evaporation front during drying caused a layered structure of carvacrol free films (Kurek et al., 2012b). Presence of carvacrol drives to heterogeneous structure (Fig. 7.3.B). Two phases in the film matrix were formed: carvacrol droplets embedded in a continuous chitosan polymer network. Besides, the heterogeneous structure could result in a lower stability of the FFS during drying. As the dry matter content increased, greater molecular contact between chitosan and carvacrol was obtained. Thus, formation of new interactions (as seen in FTIR-ATR spectrograms) might weaken the polymer chain aggregation forces. The formed matrix was more opened and the result was thicker films (thickness increased up to 15% for CSECVC films). Fig. 7.3.C shows that the upper part, corresponding to the evaporation surface during drying, exhibited a porous-like structure. This structure is also favoured by creaming of carvacrol droplet driven by solvent migration toward the evaporation surface. The lower part was more compact. The carvacrol oval droplet form (Figs. 7.3.A-C) was probably due to the deformation forces assigned to a polymer chain aggregation, network retraction and orientation due to the casting and the solvent evaporation. Surface micrographs indicated that the support side surfaces of chitosan films with carvacrol (CSECVC and CSACVC) were smooth and without cracks (Figs. 7.3.D and 7.3.E). Air side surface of CSACVC sample was smooth and homogeneous (Fig. 7.3.G), while air side surface of CSECVC sample showed discontinuities indicating phase separation and presence of

carvacrol droplets oriented to the evaporating surface (Fig. 7.3.F). Furthermore, surface convexity and presence of small holes, once again attributed to carvacrol were observed (Figs. 7.3.H and 7.3.G).

## **7.6. Thermal properties of coated PE and self standing carvacrol/chitosan films**

The determination of the thermal properties of the PE and the chitosan coated PE samples was carried out to verify whether processing or coating composition influenced the PE film structure. Moreover, useful information on the hydration, the degradation and the stability of the various chitosan coatings can be achieved. The thermal properties of the PE films and all tested chitosan films are given in Table 7.6. The DSC curve for the polyethylene film and chitosan coated PE film (PECSE samples) do not reveal any significant modification in the PE structure as reported in Chapter 6. For the chitosan/carcacrol coated PE films (PECSECVC), during the first heating, the melting point of the PE film at 113.5°C was observed. However, during the second heating, the melting point had shifted to 117.1°C (data not presented). This reorganization of the PE chains may be induced either by the presence of the chitosan film at the surface of the sample or by the cooling ramp of the DSC analysis itself.



Table 7.6. Thermal properties of chitosan coated PE, chitosan /carvacrol coated PE and chitosan self standing films.

FILM	Thermal properties obtained by DSC				Weight losses obtained by TGA						
	T <sub>d</sub> (°C)	T <sub>DS</sub> (°C)	T <sub>D</sub> (°C)	T (°C)	Weight loss (%)	T (°C)	Weight loss (%)	T (°C)	Weight loss (%)	T (°C)	Weight loss (%)
CSA	72.9	215.8	318.9	30-153	13.8	153-412	44.6	412-700	9.5		
CSACVC	51.2 and 90.7	186.3	285.5	35-150	13.4	150-200 and 200-405	7.6 and 35.3	405-700	9.0		
CSE	72.1	184.1	316.8	40-145	6.5	145-415	32.3	415-700	6.7		
CSECVC	52 and 90.3	168.4	284.7	35-135	8.4	135-200 and 200-413	6.9 and 29.8	413-700	7.1		
	T <sub>d</sub> (°C)	T <sub>m</sub> (°C)	T <sub>D</sub> (°C)	T <sub>D</sub> (°C)							
PE	/	112.9	/	455	98.0	/	/	/	/	/	/
PECSE	48.3	112.9	289.9	40-270	3.5	270-483	92	/	/	/	/
PECSECVC	49.6	113.5	273.3	35-270	4.4	270-485	91	/	/	/	/

T<sub>d</sub> - dehydration temperature; T<sub>DS</sub> - dissociation temperature; T<sub>D</sub> - degradation temperature, T<sub>m</sub> - melting temperature.

In previous chapter (Chapter 6) it was underlined that for the all chitosan self-standing films changes in the inclination of the baseline in the DSC thermograms were very weak and therefore no glass transition temperature ( $T_g$ ) could be easily detected. Moreover in this study, all chitosan films displayed two/or three endothermic peaks in the first run and only one exothermic peak in the second run. For CSA and CSE films, the first endothermic peak around 72°C fits the dehydration temperature ( $T_d$ ). The dehydration temperature is the temperature required to overcome interactions between the hydroxyl groups of the 85% deacetylated chitosan chains and water or acetic acid. For the raw chitosan, the dehydration temperature is much lower and detected around 43°C. In the films containing carvacrol, CSACVC and CSECVC, the endothermic region for  $T_d$  consisted of two peaks that were detected around 52°C and around 90°C. This variation in the peaks position means that a small amount of carvacrol was also able to establish physical interactions with water, acetic acid and hydroxyl groups of chitosan chains. These peaks do not appear in the second heating. For both coated samples, PECSE and PECSECVC,  $T_d$  values were detected at 48°C and 49°C, respectively. As coated layers were 10 times thinner than self-standing films, water and acetic acid were easily evaporated from the chitosan coating. Therefore the interactions between water/chitosan were less pronounced and  $\Delta H_d$  value was lowered.

The second endothermic peak at 215.8°C for CSA film and 184.1°C for CSE film was related to the dissociation process of the interchain hydrogen bonding of the chitosan as supported by no weight loss in TGA thermograms (Chuang et al., 1999). However, as described in previous chapter,  $T_{DS}$  values are influenced by the initial presence of plasticizers (glycerol and/or carvacrol for example) between the chitosan chains. For this reason, the carvacrol containing films show lower  $T_{DS}$  values (Table 7.6.), indicating structural changes in chitosan matrix, compared to CSA or CSE films. For the coated samples, no  $T_{DS}$  could be detected probably due to the low amount of the chitosan when applied as a thin coating layer (6  $\mu\text{m}$ ).

At higher temperatures, the exothermic peak appeared (degradation temperature,  $T_D$ , Table 7.6.). It was attributed to the thermal degradation, depolymerisation and pyrolytic decomposition of the polysaccharide backbone (Sakurai et al., 2000). This temperature corresponded to the maximum mass loss measured in TGA thermograms. Compared to raw chitosan for which  $T_D$  is around 300°C, the degradation temperature is higher with acetic acid containing samples (CSA and CSE) and lower in CSECVC and CSACVC samples. This was attributed to carvacrol that acts as plasticizer as already mentioned. The same behaviour and appearance of

small exothermic peak appearance in coated samples thermograms was attributed to the degradation of chitosan based coatings.

Thermal degradation temperatures and weight losses obtained from TGA analysis are reported in Table 7.6. As expected, under the nitrogen flow, polyethylene degrades in one step at around 455°C. Contrarily, coated samples show two steps of degradation. A broad change in weight loss from 40°C to 270°C appear as the first one and followed by the second degradation step from 270°C to 483°C. No significant changes are observed between coatings with and without carvacrol, probably due to the low amount of carvacrol present in the tested samples and detection limits of TGA apparatus.

For chitosan based films, two steps of degradation are observed.

The first weight loss, in the range from 30 to 150°C, is around 13% for CSA and CSACVC films and falls to 6-8% for CSE and CSECVC films. This step is attributed to the evaporation of the residual water (film equilibrated at 30% RH prior to TGA) and acetic acid used for the film preparation. The weight loss is only around 6% for raw chitosan powder.

The second degradation step ranges from 150°C to 415°C and is followed by the final weight loss up to 700°C. It is attributed to a complex process including the dehydration of the saccharide rings, depolymerisation and decomposition of the acetylated and deacetylated units of the polymers (Martins et al., 2012). Usually, films prepared with aqueous acetic acid solvent (CSA and CSACVC) have increased thermal stability compared to the CSE and CSECVC films, as evidenced by higher onset temperature of the second weight loss. Moreover, although authors have reported that incorporation of essential oils in chitosan and starch chitosan films increases the degradation temperature of tested films (Altiok et al., 2010; Pelissari et al., 2009), no significant changes in the thermal stability of the various chitosan films in our study is observed. However, closer examination of the curves shape between 150°C and 415°C reveals two stages (from 150°C to 200°C and 200°C to 415°C) for CSACVC and CSECVC samples (Table 7.6.). This may be attributed to the influence of carvacrol, introduced into the film matrix. The pure compound shows one-step weight loss in the range from 50°C to 185°C with a maximum weight loss at 169°C. This behaviour is also clearly observed when comparing the derivative signal and the weight loss of the carvacrol and non carvacrol samples (data not shown) and coherent with the DSC thermograms.

## 7.7. Water vapour permeability

Polyethylene films are hydrophobic materials known to be not very permeable to water vapour. Therefore, it was interesting to verify the effect of the coating composition (carvacrol and chitosan) and of the processing onto the water vapour permeability of coated PE films. In previous chapters, it was reported that the presence of hygroscopic chitosan layer, which interacts easily with the surroundings, can act as a water reservoir on the PE surface. Thus, it can significantly promote the water vapour permeability of the support layer as shown in Chapter 6 (Sebti et al., 2007). Therefore the aim of this experiment was to check the chitosan film behaviour, with incorporated carvacrol, when tested at low humidities. The water vapour permeability values (measured at relative humidity gradient from 0 to 33% RH) for polyethylene coated films are given in Fig. 7.5. and for self-standing chitosan films in Table 7.7.

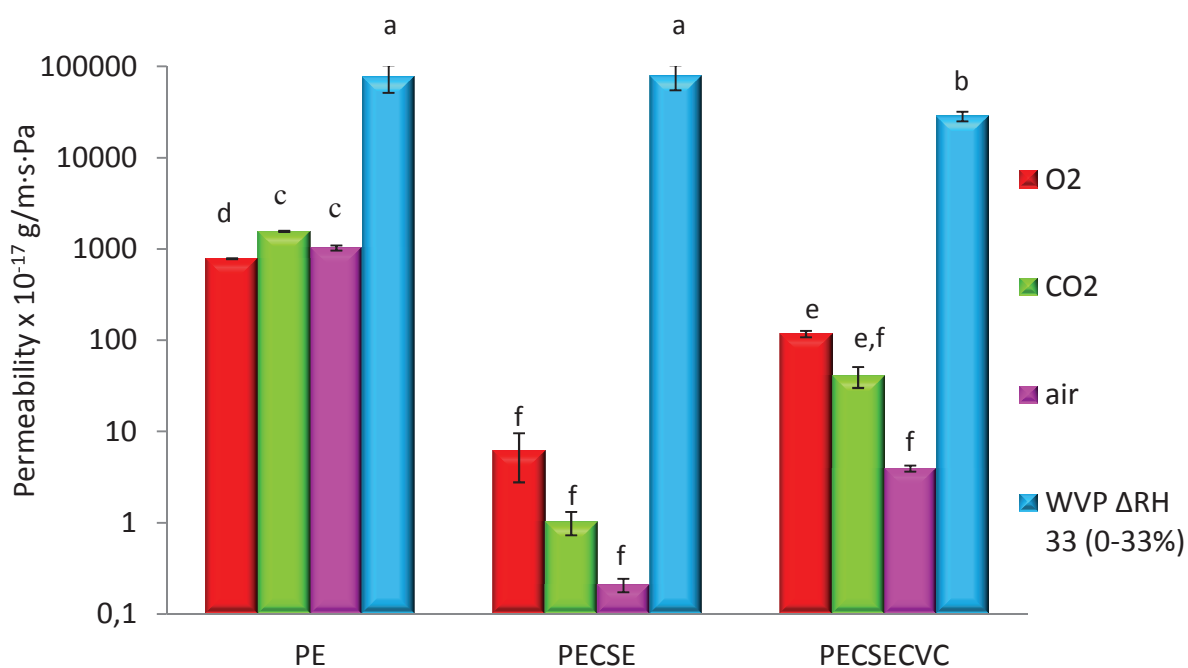


**Figure 7.5.** Water vapour (WVP), oxygen, carbon dioxide and air permeability of polyethylene (PE), chitosan coated (PECSE) and chitosan+carvacrol coated (PECSECVC) polyethylene film.

<sup>a-f</sup> Different superscripts indicate significant differences between formulations ( $p < 0.05$ ).

No significant differences were observed when thin chitosan coating (6  $\mu\text{m}$ ) without carvacrol was applied on polyethylene film ( $7.72 \times 10^{-13}$  and  $7.88 \times 10^{-13}$   $\text{g}/\text{m}\cdot\text{s}\cdot\text{Pa}$  for PE and PECSE, respectively). Moreover, the water vapour permeability was increased by incorporating carvacrol into the coating layer. Indeed, the addition of a hydrophobic material into a film does not guarantee reduced water vapour permeability, because the permeability of the films is influenced by the existence of the free channelling for the diffusion of water molecules (Pereda et al., 2012; Cheng et al., 2008). The water vapour permeability trend was similar to with that of the self-standing chitosan films. Opposite, the water vapour permeability in the samples with carvacrol increased for about five times. As supported by thermal analysis, carvacrol induced a plasticisation of the chitosan network. It is possible that it also decreased intermolecular attractions and increased molecular mobility which facilitated the migration of water vapour molecules. Moreover, the water vapour transfer in biopolymer films depends on the hydrophilic-hydrophobic ratio of the film constituents (Ahmad et al., 2012). Besides, this behaviour could be explained by the formation of porous structure with the addition of carvacrol that was supported by ESEM data (Fig. 7.3.). According to Bonilla et al. (2012) and Martins et al. (2012), the negative effect of the essential oil incorporation on the cohesion forces of the chitosan matrix could explain the phenomena of enhanced transport through the film despite the increased hydrophobic character of the matrix. The different effects of aroma compounds on the water vapour permeability were reported. The water vapour permeability of soy protein or alginate based films tends to be increased by the presence of ginger and cinnamon essential oils or their aroma compounds while carrageenan, chitosan or hydroxypropyl methylcellulose based films had lower water vapour permeability (Pranoto et al., 2005a; Atares et al., 2010; Hambleton et al., 2008; Rojas-Grau et al., 2007). At the same time, the difference between hydroalcoholic and aqueous acidic samples (CSE and CSA) was observed. Ethanol in FFS could modify the film structure as a result of the variation in the polarity and the interfacial tension. Thus, ethanol affected the solubility of chitosan powder and the water vapour permeability of dry films was increased.

**Table 7.7.** Water vapour (WVP), oxygen (PO<sub>2</sub>), carbon dioxide (PCO<sub>2</sub>) and air permeability (P<sub>air</sub>) and permselectivity (α) of chitosan self-standing films.

SAMPLE	WVP (10 <sup>-13</sup> g/m·s·Pa) ΔRH (0-33%)	PO <sub>2</sub> (10 <sup>-17</sup> g/m·s·Pa)	PCO <sub>2</sub> (10 <sup>-17</sup> g/m·s·Pa)	P <sub>air</sub> (10 <sup>-17</sup> g/m·s·Pa)	α CO <sub>2</sub> /O <sub>2</sub>
CSE	38.71±2.61 <sup>b</sup>	1.04±0.15 <sup>c</sup>	6.98±0.81 <sup>a</sup>	3.79±0.25 <sup>c</sup>	6.71
CSECVC	189.91±74.65 <sup>a</sup>	8.19±0.51 <sup>a</sup>	7.76±0.39 <sup>a</sup>	5.69±0.24 <sup>a</sup>	0.95
CSA	25.71±2.20 <sup>b</sup>	2.22±0.27 <sup>b</sup>	1.49±0.17 <sup>c</sup>	0.22±0.05 <sup>d</sup>	0.67
CSACVC	101.48±40.59 <sup>a,b</sup>	2.72±0.33 <sup>b</sup>	3.77±0.09 <sup>b</sup>	4.35±0.19 <sup>b</sup>	1.39

<sup>a-d</sup> Different superscripts within the columns indicate significant differences between formulations (p<0.05).

## 7.8. Oxygen, carbon dioxide and air permeability

One of the most interesting applications of chitosan based films is their high barrier that governs gas transfers between food products and their surroundings. Gas permeability properties could be changed by the addition of active compounds, which could act as structure enhancers. Oxygen, carbon dioxide and the air permeability of chitosan coated polyethylene films with or without incorporated carvacrol at 25°C in the dry state (to prevent moisture plasticization of the chitosan) are given in Fig. 7.4. The permeabilities of polyethylene films significantly decreased after the coating process. As the thermal and surface analysis did not display significant changes in the PE structure after coating, the decrease in gas permeability was undoubtedly due to the presence of the chitosan layer. The application of chitosan coating on the polyethylene surface decreased oxygen, carbon dioxide and air permeability from two to four orders of magnitude, respectively. This result agrees with earlier observations (Garcia et al., 2000). Elsewhere, the presence of carvacrol in the chitosan layer increased ten times the PO<sub>2</sub>, PCO<sub>2</sub> and P<sub>air</sub>. The gas permeability of biopolymer films depends on several factors such as the film integrity, the crystalline/amorphous phase ratio, the hydrophilic/hydrophobic ratio, the polymeric chain mobility and the interaction between film forming polymer chains and added molecules that all together might have changed the matrix structure (Garcia et al., 2000). Thus, the increase in the permeability with the addition of carvacrol may be associated to the breakdown of hydrogen bonds between the chitosan polymer chains (as seen in spectrograms) that opened additional sites for the dissolution of gases and increased

the mobility of oxygen molecules within the chitosan layer. Farris et al. (2009) reported that the addition of hydrophobic oil molecules decreased the cohesive energy density of the protein network. Additionally they acted as a plasticizer, increasing the free volume of the system. Therefore, the less tight lattices were formed and small gas molecules passed faster across the sample. Still, a significant difference ( $p < 0.05$ ) was observed reaching values of 117.5, 40.42 and  $3.94 \times 10^{-17}$  g/m·s·Pa compared to the controlled values (uncoated PE) of 782.5, 1562.23 and  $1025.9 \times 10^{-17}$  g/m·s·Pa for  $PO_2$ ,  $PCO_2$  and  $P_{air}$ , respectively. McHugh and Krochta (1994) indicated that whey protein films exhibit relatively poor oxygen barrier properties after lipid incorporation. The  $PCO_2$  of the PE film is 2 times higher than  $PO_2$  (Fig. 7.5.). Permeability of PECSE and PECSECVC followed the same permeability order:  $PO_2 > PCO_2 > P_{air}$ .

Furthermore, for all tested coatings,  $PO_2$  increased with the temperature increase. When temperature increased, molecules had more energy, so they could easily pass through both the PE film and the chitosan coating. Also it is possible that thermal expansion of the polymer material occurred (Rogers, 1985). Thus oxygen permeation through the chitosan coated PE films without carvacrol was more sensitive to temperature changes than that of commercial PE and chitosan coated PE with incorporated carvacrol (14 and 2 times higher at 25°C, respectively, data not shown). Hence, activation energies ( $E_a$ ) decreased in the following order:  $E_{aPECSE} > E_{aPE} > E_{aPECSECVC}$  (87.8, 28.4 and 27.2 kJ/mol respectively).

According to Gennadios et al. (2002) permeability is a steady state property that describes the extent to which a permeating substance dissolves and then the rate at which it diffuses through a film. During processing, the addition of ethanol as solvent decreased  $PO_2$ ,  $PCO_2$  and  $P_{air}$  of chitosan self standing film. It was attributed to the structural orientation and conformation changes of the chitosan matrix and probably to the densification of the chitosan network as previously described in chapter four. Better solubility of carvacrol in ethanol (that increased the bonding of carvacrol with the sites in the chitosan chains as supposed from FTIR-ATR spectra) might have decreased the matrix integrity and opened more channels for the diffusion of small molecules. Therefore, permeability was increased. The film structure as well as the distribution of carvacrol oil droplets might be associated with the gas and water vapour permeability of the resulting films (Fig. 7.3.). Even that, in Chapter four it was clearly pointed out that during the drying and storage period, an important volatile aroma compound loss occurred (up to 80%), the permeability increased 3, 2 and



1.3 times for CSECV and CSACVC films that were significantly different ( $p < 0.05$ ) from CSE and CSA (Table 7.7. and Fig. 7.6.). Nevertheless the permeabilities of all chitosan self-supported films remained weak and could be used as good barrier coating materials.

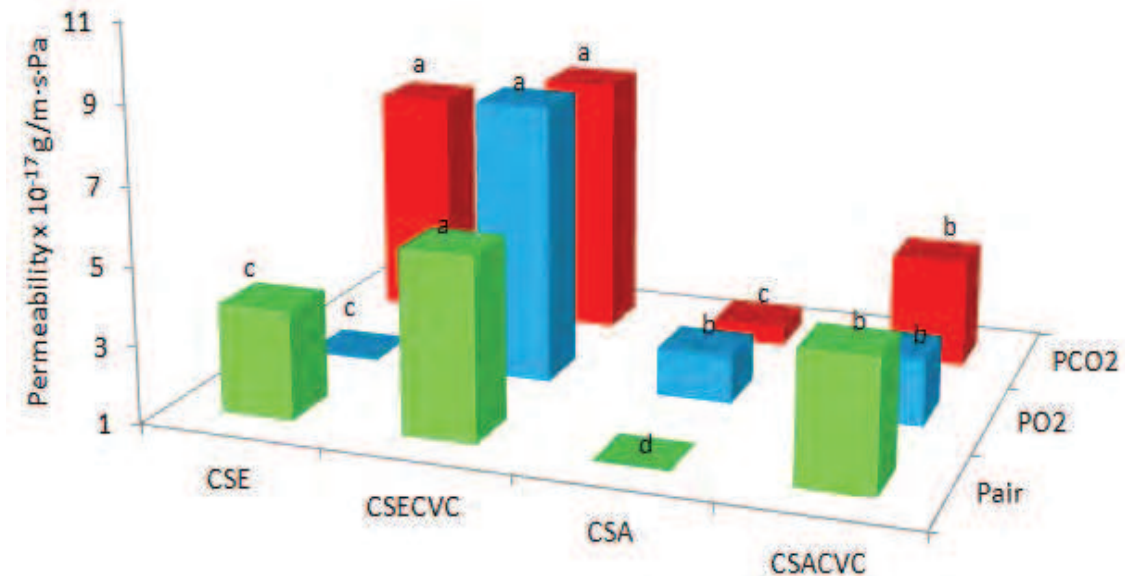


**Figure 7.6.** Changes in gas permeability of chitosan films in dry environment (0% RH) as influenced by the addition of carvacrol.

<sup>a-d</sup> Different superscripts within the columns indicate significant differences between formulations ( $p < 0.05$ ).

Permselectivity is the indication of the appropriateness of a given film for a specific food. It describes the ratio between CO<sub>2</sub> and O<sub>2</sub> permeabilities (Salame et al., 1986). Even though commercial packaging films have a typical permselectivity between 4 and 8 for highly respiring food products, lower values are required (Exama et al., 1993). Therefore chitosan films tested in this study could be used for similar food products applications (Table 7.7.). Selectivity allows balancing the pressure inside the packaging particularly for modified atmosphere packaging.

## 7.9. Conclusions of Chapter 7

For production of novel bilayer chitosan / PE films with better characteristics, the knowledge of wetting properties represents a key parameter in order to enhance their aptitude to adhere to plastic layer, while maintaining the integrity of packaging. Chitosan biopolymer film forming solutions spread and partially wet the polyethylene film surface. During the period of 120 s, measurements revealed contact angles lower



than 90°. In fact, these characteristics are primarily influenced by surface wettability of films, which is dependent upon the degree of contact achieved between plastic surfaces and wetting film forming solution. Furthermore, the magnitude of intermolecular forces involved has an important role. Keeping this in mind, hydroalcoholic acid solvent and carvacrol decreased the liquid surface tension of CSE and CSECVC film forming solutions, increased the solution surface tension and spreading, and decreased the contact angle. Then, the equilibrium-spreading coefficient was improved. Therefore, the chitosan film forming solution containing ethanol and carvacrol, as surface active components, was considered as the most suitable for polyethylene coating. FTIR-ATR analysis spectra indicated that no new chemical bonds were formed on the polyethylene surfaces. Carvacrol containing chitosan films had additional bonds at 811 cm<sup>-1</sup>, assigned to the out-of-plane vibration of phenyl ring in carvacrol molecule. Environmental scanning microscopy indicated that carvacrol containing films has a heterogeneous structure with two phases. Carvacrol droplets were embedded in the chitosan matrix. Thermal studies indicated that no significant structural changes in polyethylene film occurred after processing. The presence of carvacrol induced a plasticization of the chitosan network, thus lower dissociation temperatures were reported. Besides, it might have decreased intermolecular attractions and increased molecular mobility. Furthermore, the film structure as well as the distribution of carvacrol droplets was associated with facilitated migration of water vapour and gas molecules. Ethanol affected the chitosan powder solubility and the water vapour permeability of dry films was increased. Chitosan layer, as carbohydrate based polymer, significantly decreased the gas permeabilities of the polyethylene film. Carvacrol increased PO<sub>2</sub>, PCO<sub>2</sub> and P<sub>air</sub> of PE coated samples for ten times, following the order PO<sub>2</sub>>PCO<sub>2</sub>>P<sub>air</sub>.

To sum up, incorporation of carvacrol led to changes in the structure of chitosan matrix. Consequently, barrier properties of these materials were also influenced. In this chapter only dry environmental conditions were taken into account. However, the environmental conditions in food packaging are usually higher than 50% RH. This aspect was already assessed in Chapter 5. However, studied films did not contain carvacrol. So it is important to study the influence of relative humidity on the performances of carvacrol activated packaging films. For this purpose, the following two chapters will be focused on the influence of relative humidity on the physico-chemical and functional properties of different chitosan films.

*Chapter 8*

*Effect of relative humidity on carvacrol release  
and permeation properties of chitosan based films  
and coatings*

---

Publication: **Mia Kurek**, Alain Guinault, Andrée Voilley, Kata Galić, & Frédéric Debeaufort

Food Chemistry, accepted 2012.

Unpublished part of this chapter:

8.2. Influence of glycerol on surface properties of chitosan films

8.6. Influence of glycerol and relative humidity on the gas and water vapour permeability of chitosan films with carvacrol



Chitosan is a water sensible material that naturally interacts with water. Yakimets et al. (2007) determined the water content of biopolymer films as a critical variable that leads to water-induced transformations (for example, amorphous-crystalline transition) that have a strong impact on the molecular mobility and functional properties. In chapter two, it was underlined that hydrated chitosan exist in a twofold helix. This structure can be converted to a dehydrated form, very similar to the hydrated one, but with molecular packing and water content quite different (Ogawa et al., 2004). Moisture has a plasticizing or swelling effect on polymers, so it increases gas permeability (Ashley, 1985). Water increases the polymer-free volume, allowing the segments of polymeric chains to be mobile (McHugh et al., 1994). Moreover, in order to satisfy adequate functional properties, the film must be designed according to some surface properties. In previous chapter, it was shown how contact angle measurements enable investigation of the wetting behaviour of the biopolymer surface. It can be also a good indicator for the determination of their hydrophilic nature. In other words, it helps in understanding the mechanisms of polymer surface degradation and of active compound release, which have great importance both for food packaging and for pharmaceutical applications. However, poor water resistance and mechanical performance are limiting factors for the use of bio-based materials manufactured only from natural polymers. That is why there is growing demand in development and characterization of bio-based/synthetic polymer systems.

In previous chapter, changes of chitosan film properties after the incorporation of carvacrol were assessed. Similarly, during the storage and the use of packaging material, these properties will probably also change. The loss of active volatile compounds from bio-based matrix at specified temperature and relative humidity (RH) (that will simulate the timeline in the 'real food product' shelf life), requires the knowledge of the polymer water sensitivity, the diffusion coefficient of active compound, release rates and migration amounts according to moisture levels. Mass transfers through food packaging films exist whatever the type of material used, even if several of them are associated. Increased storage temperature and humidity can accelerate the migration of the active agents in the film. Thus, the protective action of antimicrobial films will be minimized, due to the high diffusion rates in the polymer and in the food.

The aim of this chapter was to investigate the influence of RH on the surface and thermal properties of bio-based self standing films and coatings applied onto polyethylene films. Once again, chitosan and carvacrol were used as models of biopolymer matrices and active compounds with an antimicrobial potential. The effect of incorporated carvacrol on the structure changes was studied. Water vapour, oxygen and carbon dioxide permeability has also been determined in order to monitor the film behaviour according to the temperature and RH. Furthermore, to better understand the influence of both temperature and RH on the carvacrol release, kinetics were studied at 4, 20 and 37°C and 0, 75 and >96% RH during more than 2 months. Chosen temperatures represent the storage conditions of most fresh food products, of ambient conditions or conditions of use, and those for optimal microbial growth.

### **8.1. Hydrophobicity and wettability of chitosan surfaces**

First of all, material wettability was tested in order to better understand how relative humidity (RH) influences the surface properties of chitosan/carcacrol based films and coatings. To estimate the resistance of films to liquid moisture, contact angle (that indicates surface hydrophobicity) at the time of deposit (0 s) and at metastable equilibrium (30 s), water absorption rate (wettability), swelling and delay of swelling of chitosan based films and chitosan coated polyethylene (PE) films were determined. Results are given in Table 8.1.

Practically, a large ( $\theta > 65^\circ$ ) and small ( $\theta < 65^\circ$ ) contact angles represent the quantitative definition of a hydrophobic and hydrophilic surfaces, respectively (Vogler, 1998). Moreover, in previous chapter surface free energy and critical surface tension were determined. These parameters allow the estimation of materials hydrophobicity. From Table 8.1. and Fig. 8.1., three types of behaviour can be observed. Changes in behaviour were depended on the polymer nature, the nature of the solvents used in chitosan film preparation and the addition of carvacrol.

**Table 8.1.** Contact angle at time 0 s ( $\theta_{t0}$ ), and at 30 s ( $\theta_{t30}$ ), absorption flux ( $F_{abs}$ ), time delay before swelling and swelling percentage data for the analysed films.

Film	Side	$\theta_{t0}$ (°)	$\theta_{t30}$ (°)	$F_{abs}$ ( $10^{-3}$ $\mu\text{L}/\text{mm}^2\cdot\text{s}$ )	Delay before swelling (s)	Swelling (%)
<b>CSA</b>	air	93.64±0.23 <sup>a,b,c</sup>	89.88±0.18 <sup>a,b,c</sup>	Direct swelling	/	53.51±5.46 <sup>a</sup>
	support	88.8±0.24 <sup>c</sup>	94.32±0.76 <sup>a</sup>	1.15±0.06 <sup>b,c</sup>	2.9±0.42 <sup>d</sup>	41.26±0.99 <sup>a,b</sup>
<b>CSACVC</b>	air	42.17±0.75 <sup>d</sup>	34.05±0.95 <sup>d</sup>	1.50±0.37 <sup>a,b</sup>	72.4±11.03 <sup>a</sup>	31.89±0.72 <sup>b,c</sup>
	support	98.71±1.78 <sup>a,b</sup>	91.33±1.11 <sup>a,b,c</sup>	1.65±0.12 <sup>a</sup>	/	/
<b>CSE</b>	air	87.26±0.51 <sup>c</sup>	89.90±1.57 <sup>a,b,c</sup>	0.32±0.02 <sup>d</sup>	10.8±1.13 <sup>c,d</sup>	22.89±1.79 <sup>c</sup>
	support	88.19±2.44 <sup>c</sup>	86.50±1.25 <sup>a</sup>	0.95±0.04 <sup>c</sup>	15.8±3.39 <sup>c</sup>	51.82±5.94 <sup>a</sup>
<b>CSECVC</b>	air	47.28±5.86 <sup>d</sup>	38.27±3.12 <sup>d</sup>	1.48±0.19 <sup>a,b</sup>	28.67±6.31 <sup>b</sup>	41.51±15.92 <sup>a,b</sup>
	support	100.64±9.52 <sup>a</sup>	92.27±10.39 <sup>a,b</sup>	1.40±0.26 <sup>a,b,c</sup>	/	/
<b>PE</b>		90.18±2.07 <sup>b,c</sup>	85.48±4.28 <sup>c</sup>	Evaporation	/	/
<b>PECSE</b>	PE	88.70±3.77 <sup>c</sup>	87.99±3.78 <sup>a</sup>	Evaporation	/	/
	CSE	93.58±0.52 <sup>a,b,c</sup>	90.70±0.59 <sup>a,b,c</sup>	0.40±0.03 <sup>d</sup>	/	/
<b>PECSECVC</b>	PE	93.26±1.04 <sup>a,b,c</sup>	91.95±1.46 <sup>a,b</sup>	Evaporation	/	/
	CSECVC	89.63±0.11 <sup>b,c</sup>	88.45±0.28 <sup>a,b,c</sup>	1.08±0.25 <sup>b,c</sup>	2.93±0.11 <sup>d</sup>	39.25±1.05 <sup>a,b</sup>

Mean of at least five measurements ± standard deviation.

<sup>a-e</sup> Different superscripts indicate significant differences between samples at  $p < 0.05$ .

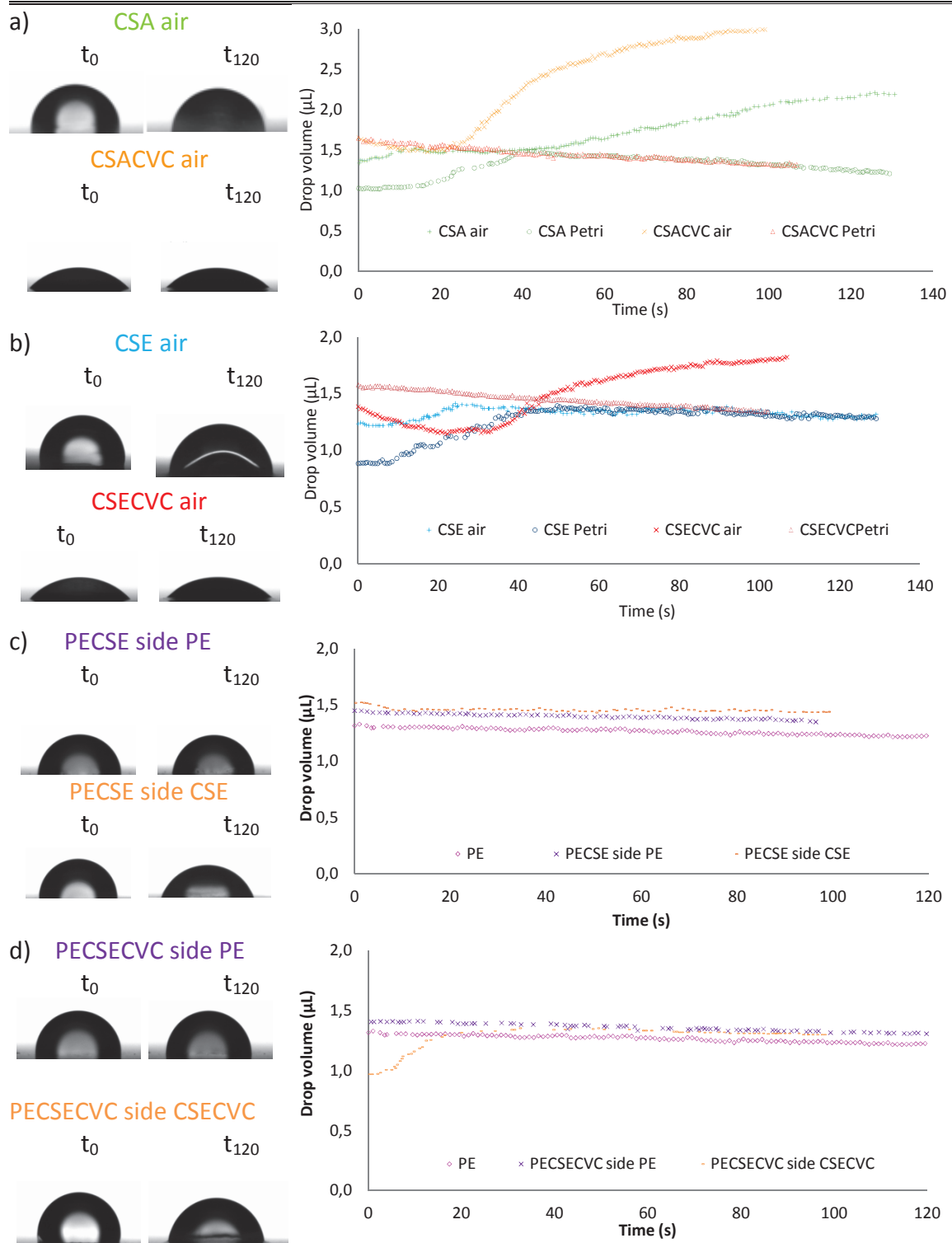


**Figure 8.1.** Shape and volume changes of water drop deposit on: (a) chitosan based films prepared with aqueous acetic solvent and (b) chitosan films prepared with hydroalcoholic acid solvent; (c) chitosan coated polyethylene; and (d) activated chitosan coated polyethylene.

First of all, during the experiment, the contact angle of a water droplet deposited on the PE film linearly decreased. This phenomenon was mainly due to evaporation and spreading. Indeed, the water cannot be absorbed on the PE, because it is a dense material with a maximum capacity of water absorption less than 0.2% of its mass. It can neither be spread because in this case, the volume of drop would be kept constant. The adsorption rate is affected when the excess water evaporates during the measurement. Thus, the “adsorption” rate on aluminium foil was determined to estimate the evaporation rate of the measurement, considering that aluminium does not significantly absorb water during the measurement. The data obtained on aluminium were similar to those on PE, confirming that evaporation is predominant. On the coated PE the water droplet profile began to change immediately upon deposition onto the chitosan-coated surface (Fig. 8.1.). Close values of surface free energies reported in Chapter 7 (35.76 and 37.32 mN/m for PE and coated PE, respectively), explain why no significant changes were observed in the contact angle values of PE and coated PE. Still, the presence of the thin chitosan layer (6  $\mu\text{m}$ ) caused the swelling of the coated side.

Contrarily, films based on chitosan have non-linear behaviour where changes such as solvation, hydration and/or swelling occurred (Fig. 8.1. and Table 8.1.). This behaviour differed depending on the solvent and the presence of carvacrol. Moreover, a different response was observed from the “air” to the “support” side. Thus, films prepared in the aqueous acidic solution (CSA) tend to be swollen (with a surface deformation) on the air side, since after submission an immediate increase in the drop volume was observed. Contrarily, films prepared in the hydroalcoholic acid solution (CSE) also swelled. The swelling occurred after the first absorption that was characterized by a decrease in both volume and angle of water droplet. The presence of water at the surface of chitosan results in low frictional surface forces, which is a desirable property in developing biocompatible materials. Moreover during contact angle measurement the swelling phenomenon was induced probably due to the plasticization by water and partial solubilisation of chitosan macromolecular chains. This behaviour seems to be contradictory to that observed for the water vapour permeability, which showed a lower resistance of CSE films to water transfer (results will be discussed later).

Farris and co-workers (2011) stated that reduction in the solid/liquid contact area is accompanied by a steep decrease in volume. Taking this into account, the sensitivity of films to the liquid moisture transfer was evaluated by the determination



of the water droplet adsorption rate. The water adsorption rate of the air side of CSA film was not determined, because the film started to swell immediately as the water droplet was deposited. This phenomenon was followed by a decreased hydrophobicity which favoured the wetting of the surface and thus the decrease of the contact angle. The absorption period before swelling was longer for air sides of CSACVC and CSECVC films (Table 8.1.). Moreover, for CSECVC  $F_{abs}$  was doubled (Table 8.1.). The support sides of carvacrol containing films were the most hydrophobic surface (highest contact angle). This might be explained by the different orientation of carvacrol droplets in the support side compared to the air side because of the evaporation phenomenon of carvacrol during film drying. Moreover, this was supported by the lower  $F_{abs}$  (0.32-1.15  $\mu\text{L}/\text{mm}^2\cdot\text{s}$ ) for air sides of CSA and CSE films than for CSACVC and CSECVC (1.40-1.65  $\mu\text{L}/\text{mm}^2\cdot\text{s}$ ).

To deepen analysis, the Owens and Wendt method was used to determine the film interfacial tension (Chapter 7). The addition of carvacrol led to a sharp increase of the interfacial tension which should result in a decrease in its wettability and thus its affinity for water. But this was not observed, then the films containing carvacrol absorbed water faster and swelled. That's why this behaviour could be explained by the film structure. In the previous chapter it was pointed out that carvacrol droplets caused irregularities in the polymer matrix. In this case, the surface roughness was increased due to evaporation of carvacrol during film drying. Thus, the side effect could be attributed to a reorientation of the molecules during the film drying (Karbowiak et al., 2006; Ogawa et al., 2004). Additionally, non-polar impurities in samples might increase surface heterogeneity (Cunha et al., 2008). Consequently, it favoured water penetration because of the capillary forces. Still, the PE coated samples did not exhibit these changes to a large extent, probably due to different drying procedures and lower coating thicknesses.

CSECVC film had higher contact angle values than CSACVC measured at time 0 s or 30 s. Hydroalcoholic solvent favoured the solubility of carvacrol and thus a more homogeneous droplet/matrix layer was formed. Here, the side effect was even more pronounced. This behaviour in the presence of carvacrol perfectly supports the results obtained for the water vapour permeability, in particular for the highest RH differential ( $\Delta\text{RH}$  100-30%). The swelling of material is desirable from an application point of view that might be the main guideline in the controlled release of active compounds. Moreover, it turns out that the surface phenomena play an important role in the mechanism of permeation.

## 8.2. Influence of glycerol on surface properties of chitosan films

(Unpublished part of this chapter)

Comparison of chitosan films with and without glycerol as plasticizer enables understanding the changes of surface properties. Indeed, it allows also correlating the nature of used additives (glycerol used as a plasticizer) and their influence on the orientation of polymer chains at the surface during film formation. Contact angles, absorption rates and percentage of swelling are given in the Table 8.2.

**Table 8.2.** Contact angle at time 0 s ( $\theta_{t0}$ ) and at 30 s ( $\theta_{t30}$ ), absorption flux ( $F_{abs}$ ), time delay before swelling and swelling percentage data for chitosan based films as influenced by the addition of carvacrol.

Film	Side	$\theta_{t0}$ (°)	$\theta_{t30}$ (°)	$F_{abs} \times 10^{-3}$ $\mu\text{L}/\text{mm}^2 \cdot \text{s}$	Delay (s)	Swelling (%)
CSA	air	93.64±0.23 <sup>a</sup>	89.88±0.18 <sup>a,b</sup>	IS	/	53.5±5.5 <sup>d,e,f</sup>
	support	88.8±0.24 <sup>a,b</sup>	94.32±0.76 <sup>a,b</sup>	1.15±0.01 <sup>b,c</sup>	2.9±0.4 <sup>c</sup>	41.3±0.9 <sup>e,f</sup>
CSAGLY	air	71.29±16.18 <sup>b,c</sup>	88.47±9.41 <sup>a,b</sup>	IS	/	237.6±41.9 <sup>a</sup>
	support	88.47±9.41 <sup>a,b</sup>	89.95±1.28 <sup>a,b</sup>	IS	/	83.9±37.6 <sup>d,e</sup>
CSAGLY	air	55.69±9.03 <sup>d,e</sup>	47.13±6.92 <sup>d</sup>	2.79±0.78 <sup>b</sup>	20.7±1.2 <sup>a</sup>	100.7±13.3 <sup>c,d</sup>
CVC	support	67.05±3.25 <sup>c,d</sup>	69.2±9.87 <sup>c</sup>	0.33±0.10 <sup>c</sup>	18.0±4.2 <sup>a</sup>	156.2±12.3 <sup>b,c</sup>
CSE	air	87.26±0.51 <sup>a,b</sup>	89.90±1.57 <sup>a,b</sup>	0.32±0.02 <sup>c</sup>	10.8±1.1 <sup>b</sup>	22.9±1.8 <sup>f</sup>
	support	88.19±2.44 <sup>a,b</sup>	86.50±1.25 <sup>b</sup>	0.95±0.04 <sup>b,c</sup>	15.8±3.4 <sup>a,b</sup>	51.8±5.9 <sup>d,e,f</sup>
CSEGLY	air	78.92±8.13 <sup>a,b,c</sup>	78.47±9.64 <sup>b,c</sup>	5.40±2.70 <sup>a</sup>	10.3±4.1 <sup>b</sup>	67.6±24.5 <sup>d,e,f</sup>
	support	90.34±0.16 <sup>a,b</sup>	102.97±3.28 <sup>a</sup>	IS	/	175.3±11.0 <sup>b</sup>
CSEGLY	air	43.22±1.39 <sup>e</sup>	87.58±2.18 <sup>a,b</sup>	IS	/	188.1±22.4 <sup>a,b</sup>
CVC	support	89.41±3.63 <sup>a,b</sup>	87.83±4.34 <sup>a,b</sup>	0.63±0.16 <sup>b,c</sup>	3.4±3.2 <sup>c</sup>	146.2±7.9 <sup>b,c</sup>

IS=immediate swelling

<sup>a-f</sup> Different superscript within the column indicates significant difference at a level  $p < 0.05$ .

Likewise for other chitosan film formulations, different behaviours were observed from one surface of the film (film-casting–support interface) to the other (film–air interface), which could be also attributed to the influence of the support on the polymer and to macromolecular orientation during drying. Table 8.2. shows that the contact angle of glycerol containing films was slightly decreased on the air film side. This was probably because of the presence of plasticizer. The effect was more pronounced in the CSAGLY sample, probable because the excess of the glycerol molecule moved to the surface of the air side as supposed from the ESEM micrographs

(Chapter 6, Fig. 6.4.). Then, glycerol increased the polar component of the film ( $\gamma_s^p$ ) and decreased its surface hydrophobicity (Fig. 8.2.). Addition of glycerol affected both structure and composition of the film surface: a reduction of polymer–polymer interactions with an increase of their chain mobility consequently to incorporation of glycerol within chitosan chains occurred. In addition, glycerol molecules were also present at the film surface. This behaviour was similar both for aqueous acid solvent and hydroalcoholic acid solvent. Contrarily to our results, Oh et al. (1999) observed a small decrease of the total surface free energy of the ethyl cellulose-based films with the addition of plasticizer. However, the addition of glycerol caused the substantial increase in moisture absorption and it caused changes in mechanical properties of the film (discussed in Chapter 10). In another words, at the same water activity, the water content was higher in film with glycerol than without glycerol. So the initial contact angle was expected to decrease as the water content increased.

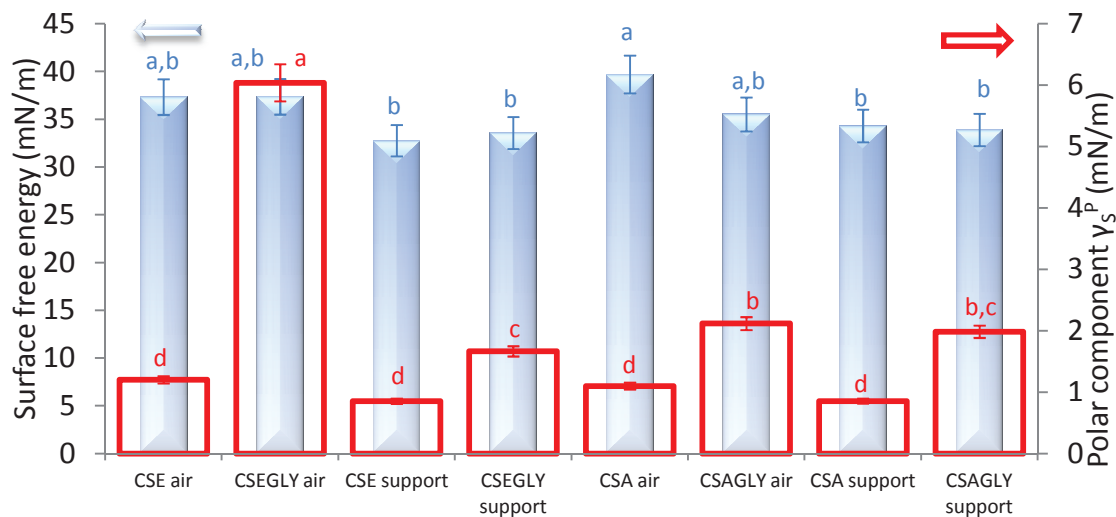


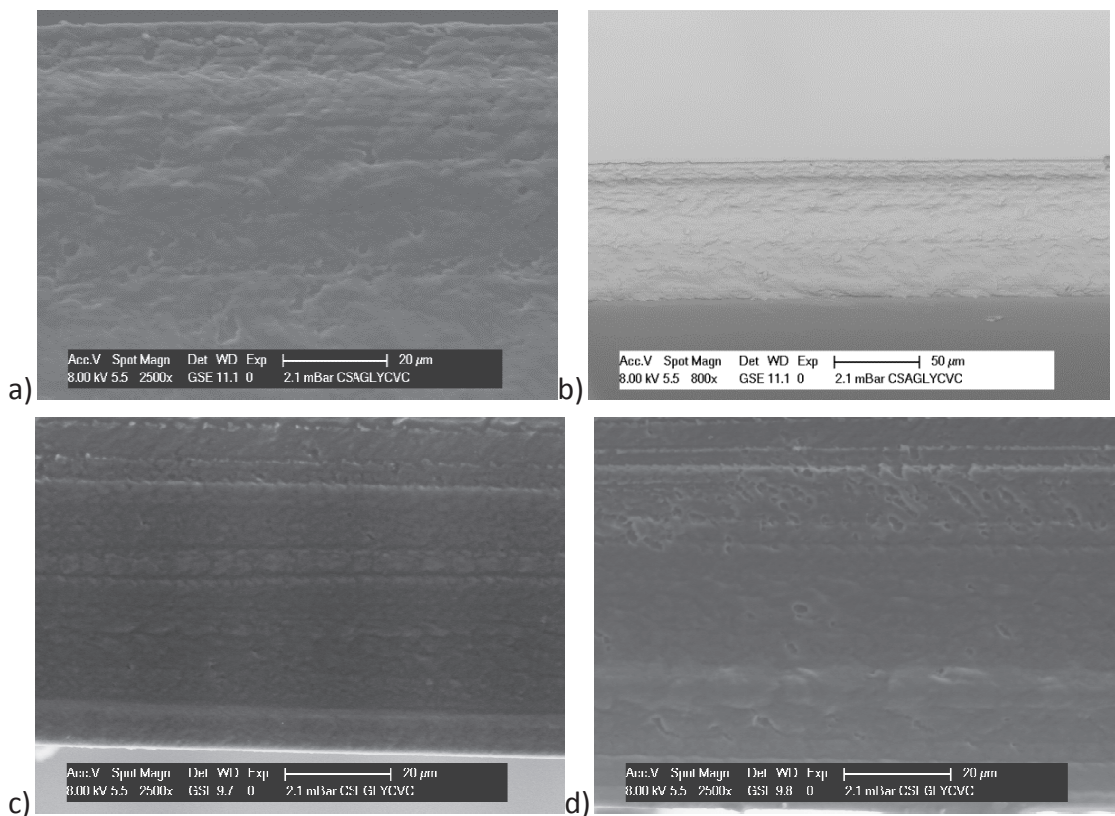
**Figure 8.2.** Comparison of the total surface free energy and its polar component in chitosan based films as influenced by glycerol addition.

<sup>a-d</sup> Different superscripts indicate significant differences between samples at  $p < 0.05$ .

Furthermore, the affinity of glycerol/chitosan films for water was clearly visible because its presence caused the swelling of the film matrix up to four times higher than in films without glycerol (Table 8.2.). This behaviour has been observed in several other bio-based films such as carrageenans (Hambleton et al., 2011), sodium alginate (Hambleton et al., 2011) and whey protein (Kokoszka et al., 2010). In addition, these authors have shown that when the glycerol content was high the period before swelling was shorter and that the swelling was increased. Similarly, in this study,

CSAGLY samples swelled immediately. However, 10 seconds delay before swelling was observed in CSEGLY samples. This was attributed to better repartition of glycerol in CSEGLY than in CSAGLY film (Chapter 6).

In the films that contained both glycerol and carvacrol, surface changes showed more complex phenomenon. The swelling was higher in CSEGLYCVC than in CSAGLYCVC samples. The most possible explanation is that glycerol was more soluble in ethanol and carvacrol was primarily dissolved in glycerol. These reduced the hydrophobicity effect of the carvacrol on the chitosan matrix. Then, the hydrophobic character of carvacrol was masked and then glycerol favoured the swelling. Better distribution of carvacrol in multi-component films and more complex matrix was confirmed by electron scanning microscopy (Fig. 8.3.). However it is interesting to note that support sides of both CSAGLYCVC and CSEGLYCVC had higher contact angles. This was probably due to the phase separation as observed at the film surface micrographs (Fig. 8.3).



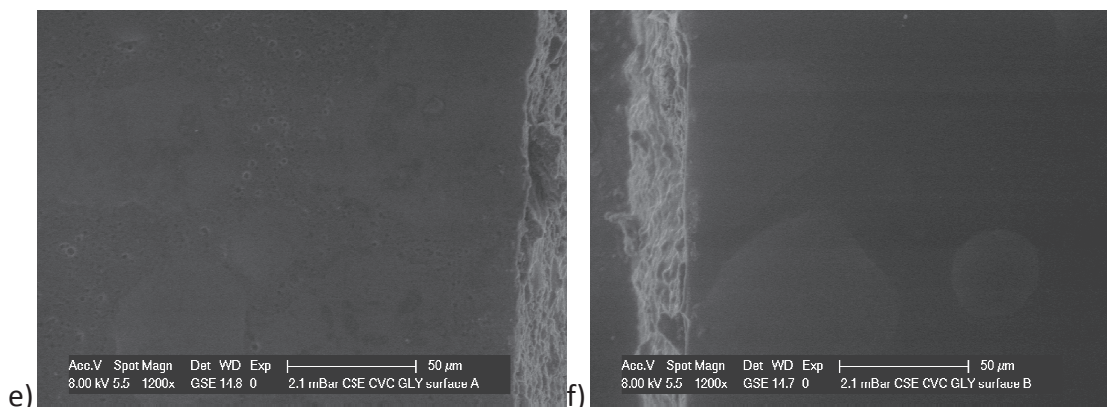


**Figure 8.3.** Micrographs of cross section of CSAGLYCVC (a) and (b); CSEGLYCVC (c) and (d); and (e) air and (f) support surface of CSEGLYCVC.

### 8.3. Thermal properties of chitosan based films influenced by relative humidity

A thermal analysis was performed in order to confirm the hypothesis about plasticization influenced by water and/or carvacrol. Before measurements, all the samples were conditioned to three RH (~0, 75 and ~100%).  $T_g$  is a value associated with the system mobility and is defined as a physical change from the glassy to the rubbery state in amorphous materials promoted by heat. The determination of  $T_g$  in chitosan based films was a difficult task because changes in the inclination of the baseline in the DSC thermograms were very weak. That is why we are generally speaking about the dehydration temperature ( $T_d$ ) related to with the evaporation process (characteristic phenomenon of hydrophilic polymers), the dissociation temperature related to the dissociation process of the interchain hydrogen bonding of the chitosan ( $T_{DS}$ ) and the degradation temperature related to the decomposition of the polysaccharide backbone ( $T_D$ ). Small endothermic dehydration peaks around 60°C and 96°C in dry (RH 0%) samples indicated that even after conditioning there was still a small quantity of water in the system, probably due to the solvent traces after drying. The observed  $T_{DS}$  values for chitosan films with and without carvacrol changed with RH. It was attributed to the different intensity of the plasticisation effect of water and carvacrol. When the RH was close to zero, the plasticisation effect of carvacrol was more pronounced. It was attributed to the fact that in the system, there was not enough of free water and then, carvacrol had the plasticizing role increasing the mobility of chitosan polymer chains. Thus, in dry system,  $T_{DS}$  values were consequently

lower for CSECVC (131°C) than for CSE samples (170°C). Additionally, less energy was needed to establish the film network. Furthermore,  $\Delta H_d$ ,  $\Delta H_{DS}$ ,  $\Delta H_D$  of CSECVC (around 0.7, 40 and 90 J/g respectively) were lower compared to CSE films (around 2, 70 and 112 J/g, respectively). When RH increased, the plasticization effect of water became more pronounced than that of carvacrol. Thus for 75% to 100% RH range the dissociation temperature were lower for samples without carvacrol (133°C for CSE and 159°C for CSECVC films). When increasing RH, the number of water molecules in the system increases. So the possibility for chitosan chains to interact with water molecules increases too. The hydrophilic character of chitosan and thus water binding capacity tends to draw additional water into the matrix limiting the interactions of carvacrol with the polymer chains and determine the final distribution of water in the system. The quantity of absorbed water increases and more energy was required (higher enthalpies at higher RH). The remarking effect was also in significant increase in carvacrol release at humidities above 75% that will be later discussed.

For the chitosan coated samples, only  $T_d$  and  $T_D$  temperatures were detected for chitosan part and  $T_m$  for PE. No significant changes were observed due to the low amount of the chitosan when applied as a thin coating layer (3-6  $\mu\text{m}$ ).

#### **8.4. Water vapour permeability of carvacrol/chitosan films and coatings at high RH differentials**

Water vapour permeability (WVP) is the most important and extensive properties of biopolymer films because of its direct influence on the deteriorative reactions in packed food. The permeability of films is not a constant (or intrinsic characteristic of the material) because it increases with RH gradient, contrary to the predicted sorption-diffusion model that describes permeability. This non-ideal behaviour is generally attributed to a structural modification of the film such as swelling, due to the sorption of water vapour. This swelling was also observed by others for biopolymers based materials (Karbowski et al., 2006; Kokoszka et al., 2010).

Polyethylene films are known to be very hydrophobic, low moisture sensitive and relatively not permeable to water vapour. Moreover, its WVP does not change with RH differential. In the chapter five and seven it was observed that the presence of the hydrophilic chitosan layer presented a reservoir of water on the PE surface (Kurek et al., 2012b). It is likely that high water sorption by chitosan resulted in a much higher concentration of water on the surface, even in a liquid state, which favoured the



sorption of water by PE, and therefore increased its permeability. At higher RH differentials, the addition of carvacrol in the coating layer decreased WVP, probably because of the hydrophobicity of the aroma compound while at lower RH the effect was opposite.

From Fig. 8.4. it is evident that all chitosan based films are not good water barrier materials compared to polyethylene. It is probably because of the inherent hygroscopic character of chitosan. Its WVP was nearly 2 to 3 orders of magnitude greater than that of PE film. Increased moisture pressure gradient significantly affected WVP.

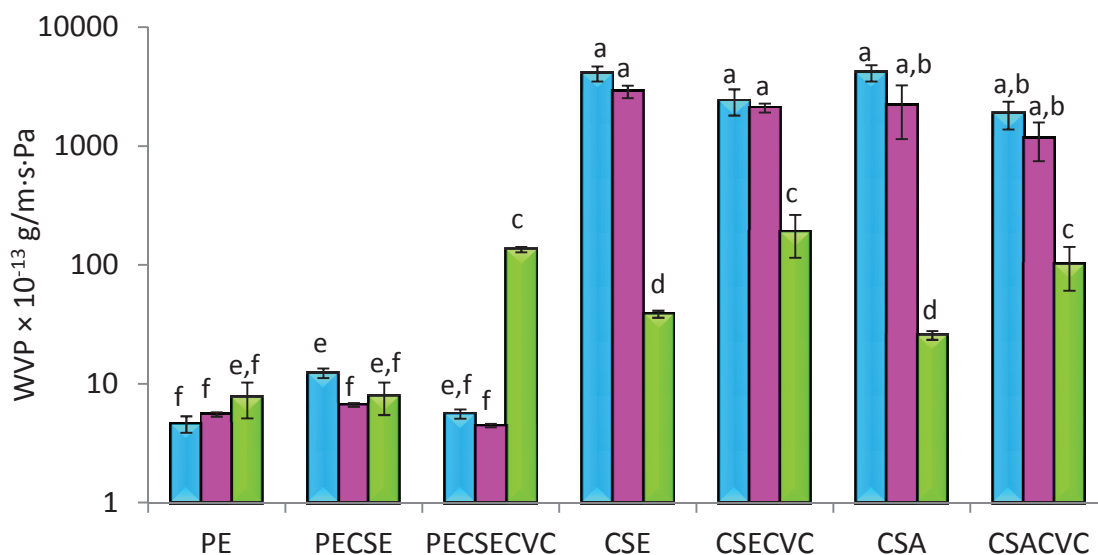


**Figure 8.4.** Water vapour permeability (WVP) at 20°C and three humidity differentials ■ 100-30% RH, ■ 75-30% RH and ■ 33-0% RH of chitosan films and carvacrol activated chitosan films compared to chitosan coated PE films.

<sup>a-f</sup> Different superscripts indicate significant differences between formulations ( $p < 0.05$ )

At lower RH differentials (33-0%), films without aroma compound (CSA and CSE) had lower permeability, from 10 to 15%, than that containing carvacrol (CSACVC and CSECVC) as shown in Fig 8.4. This, once again, suggests a plasticizing effect of carvacrol, only noticeable for the lowest RH and less marked plasticizing effect of water. Despite the increase in the hydrophobic character of the film when carvacrol was added, its incorporation might have negatively influenced the attractive forces between chitosan molecules and it might have increased segmental movements between them (Bonilla

et al., 2012). This hypothesis was reinforced with the DSC results that displayed a modification in  $T_{DS}$  and  $T_D$  (Section 8.3.).

The addition of hydrophobic substances could decrease the hydrophilic portion of the film decreasing its affinity for water at high RH (Hernandez-Munõz et al., 2004). But in our study, in self-supported chitosan films, the WVP tends to reach a plateau at high moisture environments (Fig. 8.4.). This is due to water impact on the molecular mobility that masked the hydrophobic effect of carvacrol. Then at 75-30% and at 100-30% RH differentials WVP were not significantly different. Indeed, adsorbed moisture has a plasticizing effect on the biopolymer network and leads to changes from glassy to rubbery material state (Phan et al., 2005). At higher RH film swelled and the swollen network of chitosan, together with the decreased density and the local viscosity, facilitated the diffusion of water molecules that was more rapid than through the glassy material.

### **8.5. Oxygen and carbon dioxide permeability**

When a chitosan film is applied with a food product, the gas concentration in the packaging may change during the storage. The chemical composition of the food surface is dynamic and biochemical changes in food, microbial respiration, gas solubility and permeability through packaging film will influence product quality. The efficiency of chitosan films and coatings strongly depends on its water vapour and gas barrier properties. These parameters are also depended on the chemical composition and the structure of the film forming polymers, the product characteristics and the storage conditions. To approach to the 'real' product conditions, influence of RH on the oxygen ( $PO_2$ ) and carbon dioxide ( $PCO_2$ ) barrier properties were examined (Fig. 8.5.). Generally, biopolymers are aimed to be a good barrier to gases at low RH. Thinking of chitosan as a new kind of oxygen-barrier coating material, it is possible to obtain a high oxygen barrier property on common plastic films and also to improve the biodegradability of the produced material.



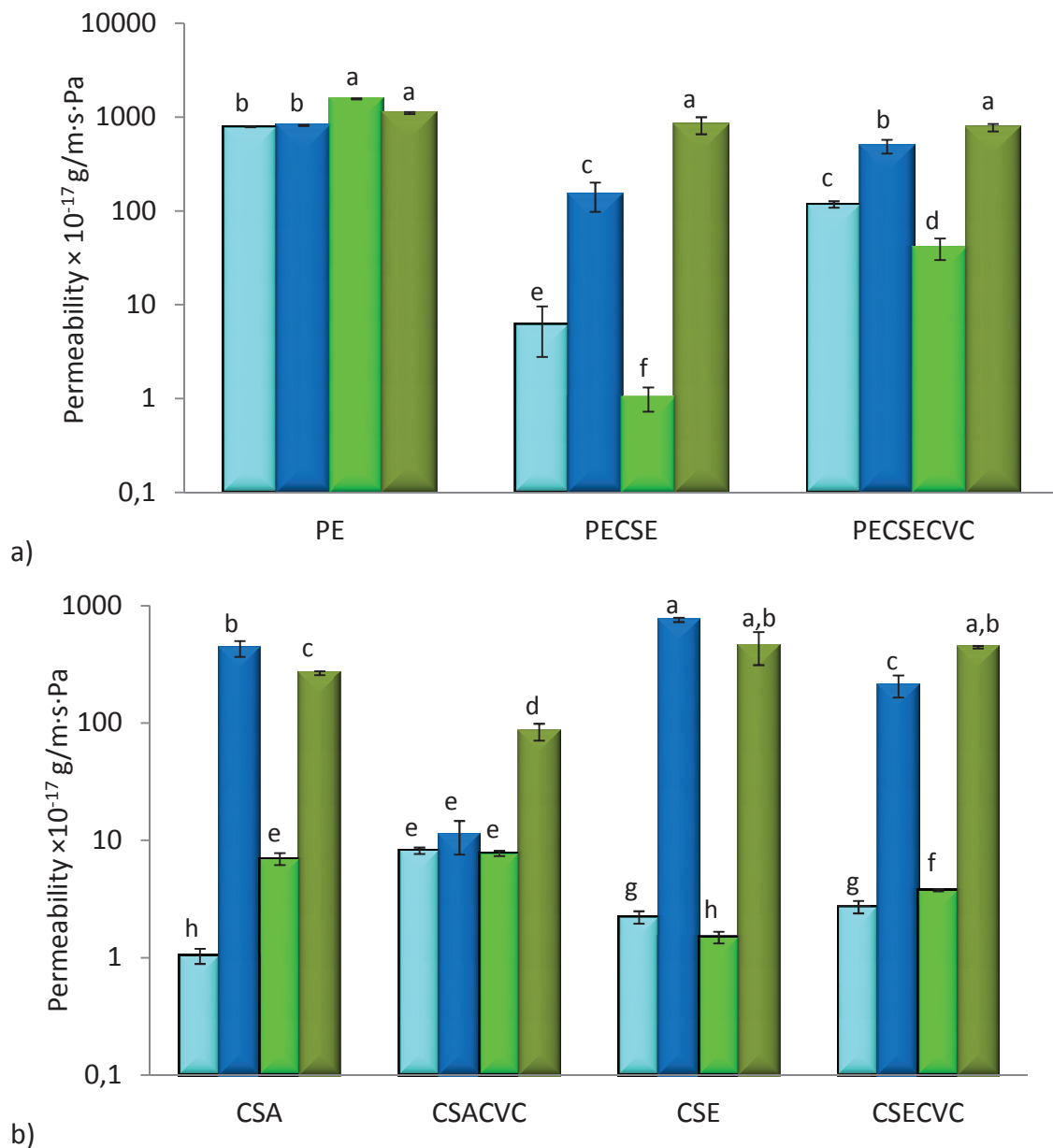


**Figure 8.5.** Oxygen and carbon dioxide permeability influenced by relative humidity of a) polyethylene and chitosan coated polyethylene films and b) chitosan and carvacrol activated chitosan self standing film. ■ O<sub>2</sub> dry (0% RH), ■ O<sub>2</sub> humid (>96% RH), ■ CO<sub>2</sub> dry (0% RH), ■ CO<sub>2</sub> humid (>96% RH).

<sup>a-h</sup> Different superscripts indicate significant differences between samples ( $p < 0.05$ ).

The  $PO_2$  and  $PCO_2$  of chitosan coated PE and self standing chitosan films are given in Figs. 8.5.a and 8.5.b. In dry conditions  $PCO_2$  ( $1 \times 10^{-17} \text{ g/m}\cdot\text{s}\cdot\text{Pa}$ ) was lower than  $PO_2$  ( $6 \times 10^{-17} \text{ g/m}\cdot\text{s}\cdot\text{Pa}$ ) for chitosan coated PE films. The gas permeability of PE films alone was not significantly affected by RH. At the temperatures of study, PE was probably in the rubbery state and as it is apolar material, it should not interact with

water molecules. On the contrary, for chitosan coated samples both  $PO_2$  and  $PCO_2$  were significantly higher at >96% RH, precisely 10 times for  $PO_2$  and 1000 times for  $PCO_2$ . The effect of RH was less pronounced for carvacrol containing coated PE. Already in dry conditions these films were less performing than PECSE.  $PO_2$  and  $PCO_2$  of PECSECVC at >96% increased for 4 and 19 times respectively, but still remained 1.6 and 1.5 times lower than PE film itself. Hagenmaier and Shaw (1991) also reported an exponential increase in  $PO_2$  of shellac coatings with increasing RH.

$PO_2$  and  $PCO_2$  changes with RH and composition of self standing chitosan films are given in Fig. 8.3.b. In dry conditions, the permeability of both gases increased with the incorporation of carvacrol. This was mostly due to microstructural changes in the chitosan network that became more mobile attributed to the presence of carvacrol microdroplets.

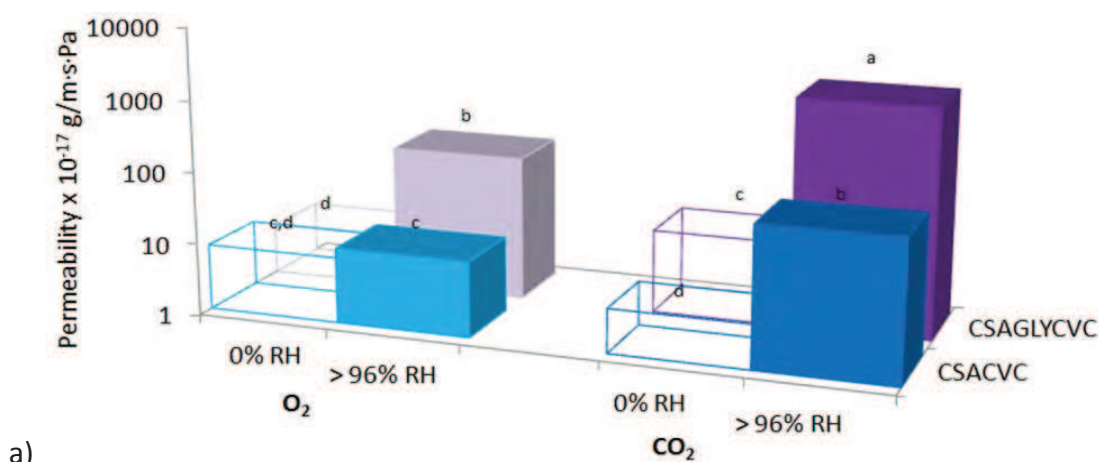
As the relative humidity increased, the  $PO_2$  and  $PCO_2$  of all samples significantly increased. Despond and co-workers (2001) found that  $PO_2$  and  $PCO_2$  increased by 12.9 and 172.7 times, respectively, when RH increased from 0 to 100%. In general, there is a competition between water and gas molecules. The plasticizing and/or swelling effect of moisture followed by self association of water molecules (clusters) might have induced rearrangements in the conformation, changes in crystallinity and mobility of the polymer chains and thus changed the permeation of gases through the chitosan film. CSACVC and CSECVC films were less permeable than CSA and CSE films. There are several explanations. First, at higher RH,  $T_{DS}$  for CSECVC films was higher comparing to pure chitosan films. Thus in humid environment, in the presence of carvacrol the decrease in  $PO_2$  can be associated with the increase of the crystallinity. Indeed, authors reported that in semi-crystalline chitosan, the mass transfer is primarily function of the amorphous phase, because the crystalline phase is usually assumed to be impermeable (Ziani et al., 2008). Second, at higher RH there is a competition between water molecules and carvacrol to be bonded with chitosan chains. Then, as mentioned previously, the plasticization effect of water was stronger in non activated samples and  $PO_2$  and  $PCO_2$  increased. CSACVC films (aqueous acid solvent) were less permeable than CSECVC (hydroalcoholic acid solvent). This can be attributed to the different molecular orientation of the polymeric chains due to solvent nature (Salame and Steingiser, 1977). Generally, when comparing gases, higher solubility of  $CO_2$  in the water leads to higher  $PO_2$  in humid conditions. In this study, in carvacrol containing samples,  $PCO_2$  was higher than  $PO_2$ , while in the pure chitosan films no significant

differences were observed (Fig. 5.3.b). Similarly, Bae and co-workers (1998) found that  $\text{CO}_2$  in wet chitosan membranes were 15-17 times more permeable than in the dry chitosan membrane.

## 8.6. Influence of glycerol and relative humidity on the gas and water vapour permeability of chitosan films with carvacrol

(Unpublished part of this chapter)

Oxygen, carbon dioxide and water vapour permeabilities of chitosan films containing either carvacrol or carvacrol and glycerol are given in the Figs. 8.6. and 8.7. Generally, plasticizers reduce intermolecular forces along the polymer chains, thus increasing free volume and chain movements. In previous chapters it was shown that addition of glycerol in chitosan/carcacrol film forming solutions led to some structural changes. Deviations in viscosity and particle size distribution were observed (Chapters 4 and 6). Then in section 8.2., structural changes were confirmed by ESEM. Likewise, it is to expect that these complex systems would change barrier properties of chitosan based films. Indeed, carbon dioxide permeability of CSACVC comparing to CSAGLYCVC films in dry and in humid environment was significantly increased (Fig. 8.6.a). The same behaviour was observed for oxygen permeability in humid environment, while in dry conditions no significant changes could be attributed. However, when hydroalcoholic acid solvent was used, no significant changes in gas barrier properties were observed (Fig. 8.6.b). This could be attributed to a better distribution of glycerol and carvacrol in hydroalcoholic systems as previously suggested (Chapters 4 and 6).



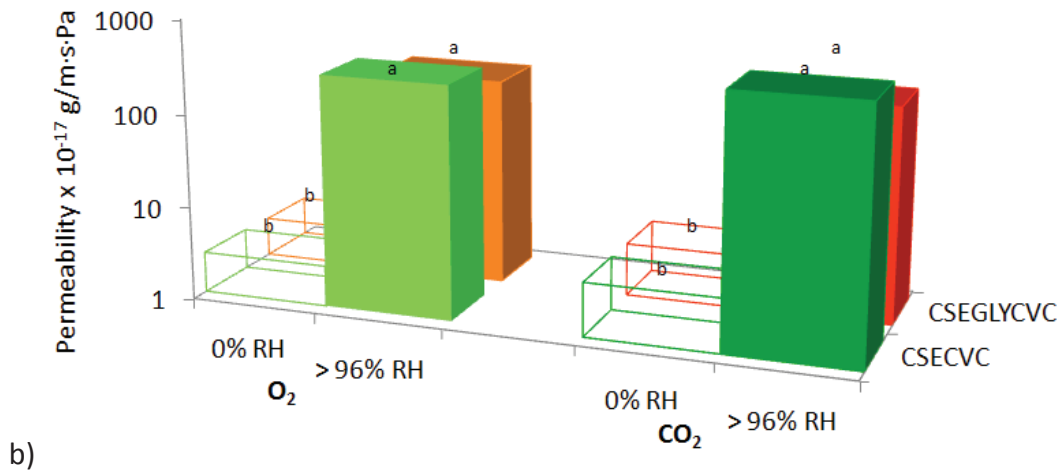


**Figure 8.6.** Oxygen and carbon dioxide permeability of carvacrol containing chitosan films in dry and humid environment as affected by the addition of glycerol: a) chitosan films prepared in aqueous acetic acid solvent (CSACVC); b) chitosan films prepared in hydroalcoholic acetic acid solvent (CSECVC).

<sup>a-d</sup> Different superscript indicate statistically significant difference between samples

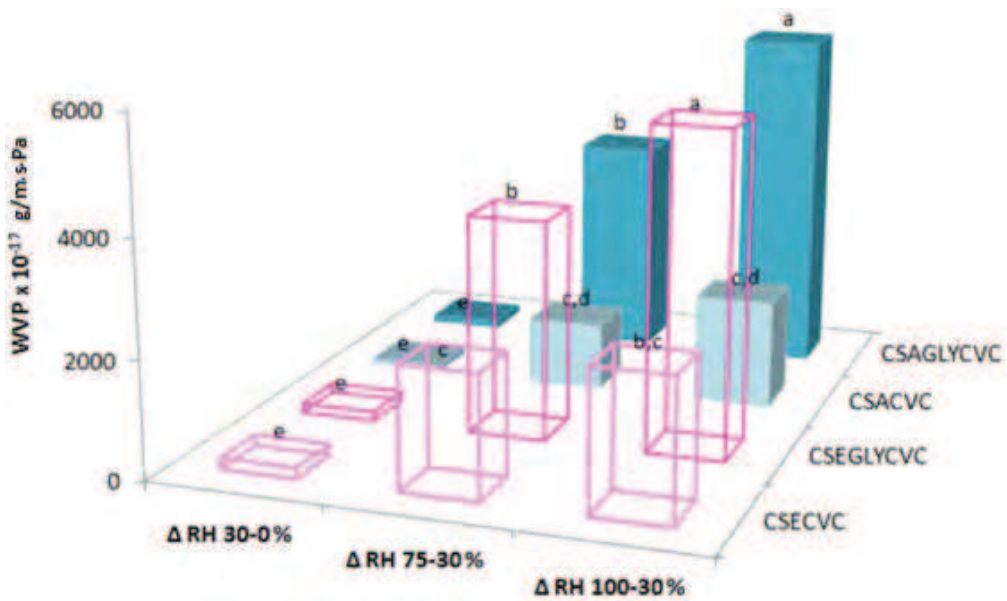


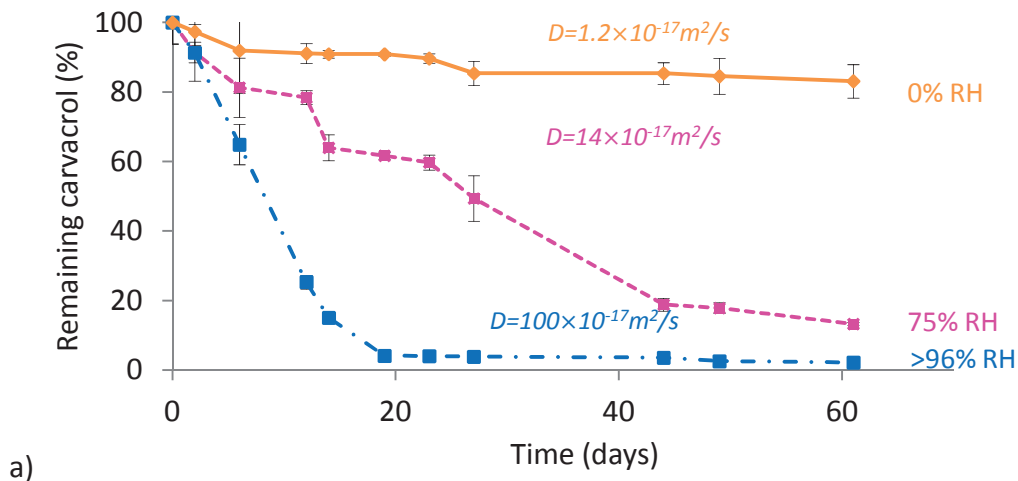
**Figure 8.7.** Water vapour permeability of chitosan films with carvacrol and glycerol at three different humidity differentials (CSAGLYCVC and CSEGLYCVC).

The majority of these anomalous behaviours arise due to the hydrophilic nature of glycerol that in complex systems with carvacrol induced the presence of inhomogeneities in its structure. Following this further, the water vapour permeability of CSAGLYCVC and CSEGLYCVC films was significantly increased at higher relative

humidity gradients (Fig. 8.7.). Solubilisation of carvacrol in glycerol seems to mask the protective hydrophobic effect of carvacrol, hence WVP was increased. Furthermore, glycerol increased the affinity of films to adsorb water, thus the plasticization by water was induced.

### 8.7. Release of carvacrol from chitosan films

In the development of active packaging, the remaining concentration of the active compound during processing and controlled-release of the same one from packaging materials is of major significance as it will extend the antimicrobial effect of the packaging film. Since the carvacrol release and diffusion from the chitosan matrix begins as soon as carvacrol is added to the film-forming solution, this point has been well reported in Chapter four (Kurek et al., 2012a). Diffusion can occur through the non hydrated chitosan matrix but will generally be facilitated as the polymer gradually swells in contact with water vapour. In order to quantify the effect of RH and temperature on the release of carvacrol from chitosan based films, release kinetics and apparent diffusivities of carvacrol were assessed for three relative humidities and three temperatures. Experimental (amounts of carvacrol) and calculated data (diffusion coefficient) are given in Fig. 8.8.



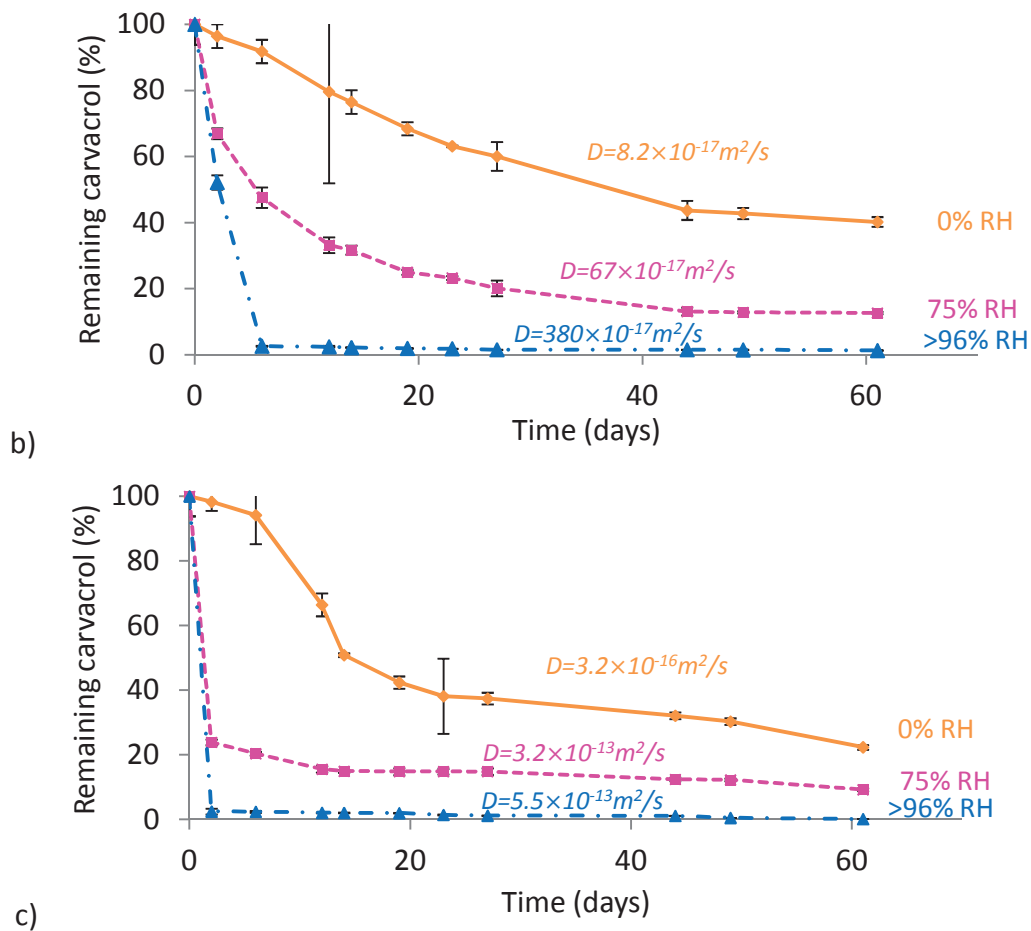


**Figure 8.8.** Kinetic of carvacrol release from chitosan based film during 2 months influenced by relative humidity (0, 75 and >96%) and temperature a) 4°C, b) 20°C and c) 37°C.

The experimental release kinetics at controlled RH (0, 75 and >96% RH) clearly showed that the release was greatly accelerated by saturating the system with the water vapour and increasing the temperature from 4 to 37°C. Thus after 60 days, the release was the lowest at 0% RH and the highest at >96% RH with almost complete exhaustion in the later. Moreover at 37°C and RH >96%, already after 2 days, more than 98% of carvacrol was lost, while at 0% RH this was significantly lower (only 2%). At 0% RH even after 60 days remaining carvacrol content was higher than 85% (for 4°C), 45% (for 20°C) and 20% (for 37°C). As long as the structure of the films was not significantly changed, a high retention of carvacrol was maintained. Effect of RH on carvacrol diffusivity was attributed to the plasticization of the chitosan matrix by water. In the high humidity environment, the release of the entrapped compound into the headspace is closely related to the adsorption of water in the material and hydration of the matrix (Whorton and Reinnecius, 1995). Thermodynamically, different

states of matter may be assigned to the chitosan chain in contact with water vapour molecules. With no doubt, hydrophilic content of the chitosan will affect the intermolecular forces responsible for diffusion and swelling (Ogawa et al., 2004). Water begins to penetrate the surface of the film, followed by cracks appearing near the surface, so subsequent release of carvacrol occurs. During the time, due to their hydrophilicity, the chitosan chains are significantly hydrated meaning that the interaction between water and chitosan increases. This facilitates water diffusion, leads to a greater swelling and thus to a greater release of carvacrol. The release mechanisms are quite important from the application point of view. When estimating the shelf life of the active packaging film we want to avoid active compound loss. On the contrary, as soon as the packaging will be put in the atmosphere of a 'real fresh food product', where  $a_w$  and thus RH in the packaging is high, accumulated water vapour would favour the release of carvacrol and thus induce the adsorption on the food surface. The antimicrobial effect will thus be obtained.

Depending on the RH and temperature, the diffusion coefficients (D) of carvacrol varied from  $1.2 \times 10^{-17} \text{ m}^2/\text{s}$  (at 0% RH and 4°C) to  $55000 \times 10^{-17} \text{ m}^2/\text{s}$  (at 100% RH and 37°C) (Fig. 8.8.). The slower release in the low  $a_w$  region is most likely due to the lower mobility of carvacrol molecules in the glassy state of the chitosan matrix. The activation energy ( $E_a$ ) for diffusion may be described as the energy required to create a hole large enough to let by a diffusing molecule. The calculated D was plotted against the reciprocal of absolute temperature (Fig. 8.9.).

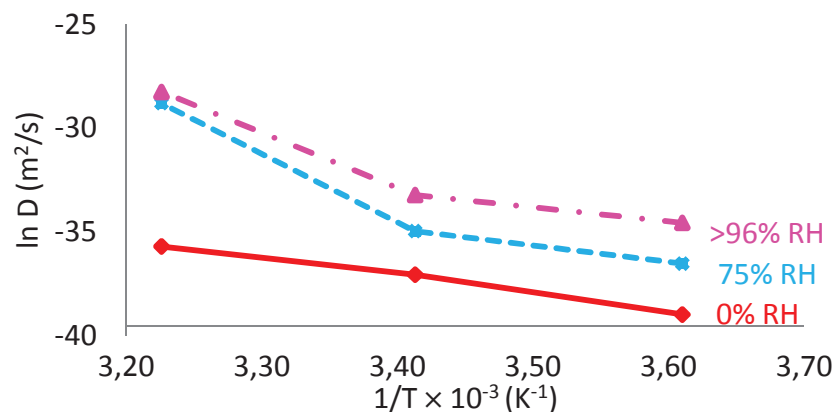


**Figure 8.9.** Influence of temperature and relative humidity on the diffusivity of carvacrol in chitosan film.

The diffusion rates significantly increased with the temperature and humidity increase. Tunc and Duman (2011) mentioned that temperature is very effective

parameter for controlling the loss of antimicrobial compounds from biopolymer based films. When sufficient amount of  $E_a$  is available in the system the diffusing molecule jumps from one position to another. For 0, 75 and >96% RH, the activation energies were 71, 167 and 136 kJ/mol respectively. The diffusivity values were a little bit higher than those obtained for the same compound in soy protein isolate based-matrix, where at 30°C and RH varying between 60% and 100%, D ranged from 0.02 to  $1.38 \cdot 10^{-14} \text{ m}^2/\text{s}$  (Chalier et al., 2009).

## **8.8. Conclusions of Chapter 8**

Chitosan films and coatings showed a great potential to be used as active aroma compound support matrices. These matrices can provide activity to food packaging films, by humidity and temperature induced release mechanisms. Changes in swelling properties, water vapour permeability and gas permeabilities at high humidity conditions, were mostly influenced by structure reorganization, presence of glycerol and plasticizing effect of water molecules. At low relative humidity gradients, the incorporation of carvacrol induced a plasticization of chitosan matrix, decreasing its barrier properties. These phenomena were confirmed by the changes in structural properties displayed by thermal analysis. In systems with both carvacrol and glycerol, irregularities in matrix structure degrade barrier performances of these films. Chitosan coatings significantly improved the gas permeability properties in dry conditions. For PECSE films,  $\text{PO}_2$  was still the lowest at high RH. Contrarily, lesser improvement was obtained for coatings with carvacrol, especially in the case of carbon dioxide. The release of the active compound was strongly enhanced by RH as required for the application. During the film storage, the most important was to avoid the active aroma compound loss. This is the reason why the diffusion coefficients had to be low at low RH. Contrarily, regardless of the temperature, as soon as the film is exposed to high humidity (foodstuff), the active compound will be fast released and will provide an immediate antimicrobial efficiency.

Chemically, the side groups of chitosan contribute greatly to the overall properties of this hygroscopic material. Polar in nature, these groups can also increase a large amount of free volume between neighbouring polymer molecules, because of their size and relative flexibility. Considering water to be a plasticizer for hydrophilic polymers, it may lead to further insight to an understanding of their swelling characteristics. To deepen analysis and to better understand affinity of chitosan films to water, water vapour sorption phenomena will be discussed in the following chapter.





*Chapter 9*  
*Water vapour sorption isotherms of chitosan  
based films and coatings: influence on their  
barrier and mechanical properties*

---

Publication: **Mia Kurek**, Thomas Karbowiak, Kata Galić, Andrée Voilley & Frédéric Debeaufort

Biomacromolecules, will be submitted



Since it is known that the addition or removal of water may cause phase transitions in the macromolecular structure (Schwartzberg, 1986; Torres, 1994), the knowledge of sorption isotherms has been important for predicting water sorption properties of hydrophilic films, stability and quality changes during packaging and storage, especially of intermediate and high moisture foods (Bell and Labuza, 2000). The ability of thin layer materials to adsorb water molecules strongly influences their structural, mechanical and barrier properties. The diffusion of penetrants can differ depending on polymeric systems. Therefore, the investigation of water sorption by chitosan is important because the presence of water can have preponderant effect on its physical properties and then on further applications. Water activity ( $a_w$ ) and consequently the humidity level inside the packaging is important to determine the stability criteria for foodstuffs and it is in function of both equilibrium moisture content and temperature. Water activity of the product affects microbial growth, browning, lipid oxidation, and some physical properties of foodstuff (such as colour, texture, aspect, etc.). Because of above mentioned effects, it is an important factor in the preservation of moisture sensitive packaging materials for food applications.

Due to specific interactions between water molecules and hydrophilic sites on the polymer backbone, water sorption in biopolymers is generally a complex phenomenon. Actually, adsorbed water molecules are partially dispersed into the polymer matrix and in part physically bonded to the hydrophilic sites (Netti et al., 1996). Because of film forming characteristics and as encapsulation capacity for active agents and drugs, susceptibility of chitosan to water has already been studied. Some recent works reported „anomalous diffusion“ (Despond et al., 2001), „degradation“ (Pereda et al., 2009) or „specific reorganisation“ (Bodek et al., 1999) of chitosan films during sorption experiments with water vapour. Up to now, there is no many data dealing with the thermodynamics of water vapour sorption over adsorption and desorption cycles, neither as with the kinetics aspect of water diffusivity in biopolymers. During experiment and storage, chitosan might encompass some phase transitions including polymorphism and re-crystallisation (Kawada et al., 1999).

### **9.1. Water vapour sorption kinetics in chitosan based films**

The complete kinetics of water vapour sorption by chitosan powder or chitosan film is displayed in Fig. 9.1. It gives the mass uptake of the samples as a function of time when the relative humidity is increased step by step from 0 to 80%. This kinetics

allows determining if equilibrium is achieved between each relative humidity change. From these data, an apparent diffusion coefficient for water can also be calculated assuming Fickian diffusion between each RH step.

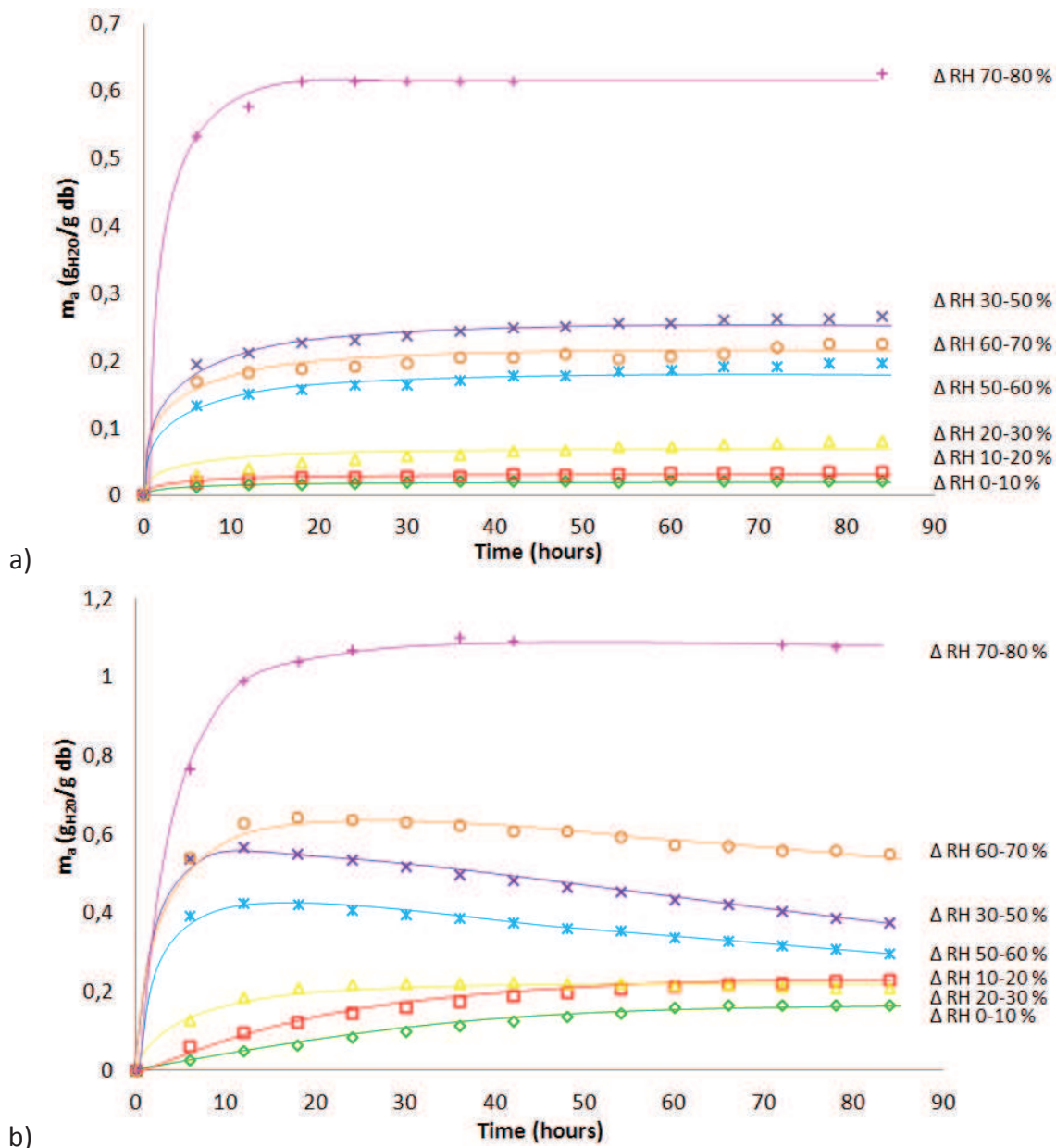


**Figure 9.1.** Curves of water vapour sorption kinetics for (a) chitosan powder and (b) chitosan based film (CSA). db= dry basis.

The initial study has involved a comparison of kinetic rates and equilibrium uptakes for water adsorption on chitosan powder and chitosan films. All chitosan films followed the same behaviour, thus in the following parts, only CSA film will be

presented as the model of both CSA and CSE. Chitosan powder (Fig. 9.1.a) and chitosan film (Fig. 9.1.b) did not show similar kinetics.

Firstly, the mass equilibrium was reached after around 12 hours for all relative humidity differentials for the chitosan powder. However, in all samples, it is evident that the amount of water adsorbed on chitosan powder at equilibrium (water adsorption capacity) increased with increasing RH. The adsorption may be approximately divided into three stages such as initial adsorption stage, gradually slowing adsorption stage and adsorption equilibrium stage. Moreover, three different regimes in this initial stage were observed depending on the relative humidity range. The slope of the kinetic curves, and thus the amount of adsorbed water was the lowest for 0-10%, 10-20% and 20-30% RH intervals and the highest for 70-80% RH intervals. The amount of water adsorbed in chitosan powder, rapidly increased with increasing the adsorption time in the initial adsorption stage. And then, in the gradually slowing adsorption stage, the  $m_a$  increasing rate turned slowly and gradually toward constant mass. After 12 hours of adsorption for chitosan powder, equilibrium was reached. In the initial adsorption stage, the water vapour pressure at the surface of chitosan powder was less than that in the environment. Then, the powder adsorbed water molecules from the environment rapidly, and as a result, the  $m_a$  was rapidly increased. With the progress of water adsorption experiment, the water vapour pressure in the chitosan surface gradually tended to equal to that in the environment. Then, the adsorption rate for chitosan to adsorb water molecules was slowed down to reach a dynamic equilibrium.

On the contrary, depending on the relative humidity differentials, the transient state seems to be variable in films. For example, it appears to be around 50 hours for relative humidity below 30% RH, but reduced to 9 hours between 30% and 70% RH, and increased again to 36 hours above 70% RH. We can reasonably think that the transient state for water transfer is therefore shortened in the case of powder, due to a greater surface area exposed compared to the film. However, considering the full kinetics and not only the first part up to which the equilibrium seems to be attained, it is worthy to note that another phenomenon superimposed to water sorption between 30% and 70% RH for the films. In this range, after a strong increase in mass during the first 9 hours, chitosan film displayed a very slight decrease in mass over time. This fact is very surprising and also points out that the equilibrium in mass was not perfectly reached for these relative humidity differentials. This also indicated that, for chitosan films adsorbing water a longer time was needed to reach equilibrium. In the case of

chitosan film, similar shape of kinetic curves was observed for 0-30% RH range and above 70% RH. However, as previously mentioned in the range from 30% to 70% RH, there was not the final equilibrium stage attained during the experiment.

The water vapour desorption kinetics for chitosan powder and chitosan film (CSA) are displayed in the Fig. 9.2.

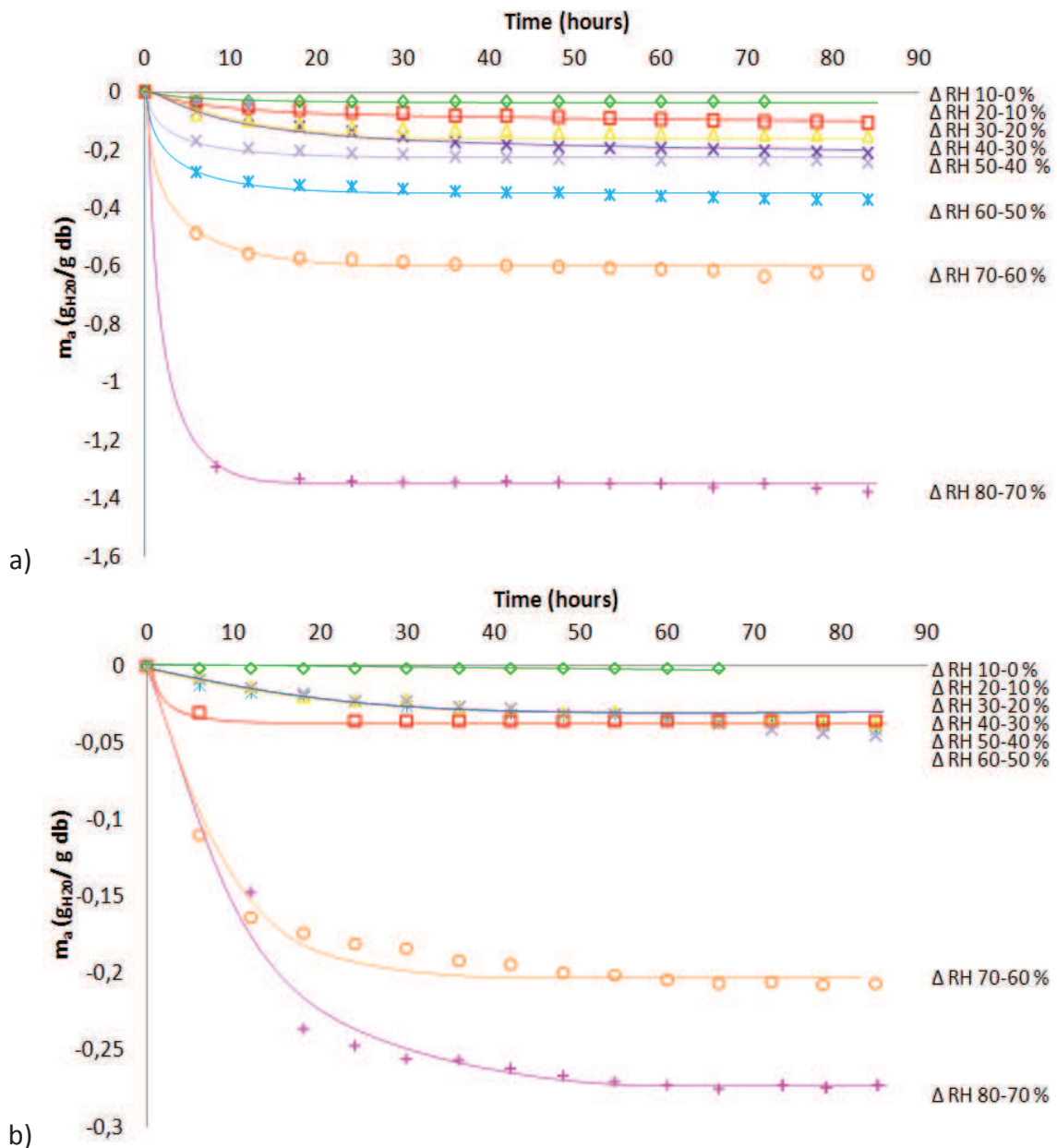


**Figure 9.2.** Curves of water vapour desorption kinetics for (a) chitosan powder and (b) chitosan based film (CSA).

Contrarily to the sorption, during the water vapour desorption from chitosan powder and chitosan films, similar kinetic behaviour was observed. In the initial desorption stages the mass loss was the highest and after a certain period, mass has reached the equilibrium. Contrarily to sorption kinetics, the constant mass seems to be reached faster for film samples (18 h) than for chitosan powder (around 50 h). However, two main regions were observed for both samples types, one above 70% RH where the mass loss was faster and the most important and the second one from 70% to 0% RH where mass lost was less important. Moreover, chitosan film samples displayed greater mass loss.

The moisture sorption isotherm (adsorption and desorption), is a way to characterize the solubility of water in the film matrix, so it is especially important for bio-based films. Even though chitosan is widely studied polymer and water vapour sorption isotherms were previously reported, very little work has been carried out on the kinetics of adsorption/desorption of water on chitosan films. The behaviour of water sorption in chitosan films obtained in this study is different from that reported in the literature. From kinetic results it is clear that for these systems very long times are required for reaching equilibrium. Thus it is very important to be careful when comparing the literature data. The experimental procedures as well as reported results may vary depending on the duration of the experiment, the weighting accuracy, and the determination of the chitosan samples dry weight. The former is key factor that makes questionable or doubtful some works which consider the only first part of the kinetics as the experimental period was much shorter (i.e. just 4 h in the work of Mucha et al. (2005)). The second dilemma comes out when comparing the determination of samples dry basis before sorption experiment. It has been reported that chitosan samples were dried at 95°C (Ludwiczak and Mucha, 2010), 100°C (Mucha et al., 2005; 2007) and 105°C (Suppakul et al., 2012) before sorption experiments. However, drying at high temperatures can result in the degradation and reorganisation of chitosan polymorph. Moreover, in this study, when films were dried at 105°C, colour modification was observed. This denoted some chemical reactions and possible structure change. That is why the determination of polymer dry basis in this study was performed by drying under the P<sub>2</sub>O<sub>5</sub> followed by drying under dry air flow (having a dew point -60°C that corresponds to <0.046% RH). All these factors must be taken into account for the following discussion.



In a similar study with chitosan films, a mass loss was reported during exposure to water vapour after 10 hours period (Pereda et al., 2009). Mass decrease observed after pseudo-equilibrium was hypothesised by these authors to result from the competition between polymer degradation and water sorption. However no experimental proof was given to confirm it. In another study, Epure et al. (2011) reported water uptake evolutions of unplasticized and glycerol plasticized chitosan over 35 days. Authors reported the attained equilibrium already after very short period (24 h). However, there is a trend that after the first equilibration, the mass of the samples for RH above 33% tended to decrease within the standard deviation, which is similarly to the results obtained in our study.

Interestingly, Martino et al. (2011) reported significant decrease in water content (from 67.3% to 10.1%) for chitosan films after 20 days of storage at 57% RH. This was attributed to a specific reorganisation of the material during its aging similarly to results reported in a study of Bodek et al. (1999). However, once again no experimental proof was given to confirm it.

In the present study, there are several hypotheses which could explain the mass loss in chitosan films. It can be attributed to the specific reorganization of chitosan matrix, changes in the chitosan polymorph and water removal action of acetic acid. First of all, during the film preparation, the addition of acetic acid aqueous solution allowed the partial protonation and destruction of chitosan plain powder which is favourable for its mixing and solubilisation. In result, hydrated crystals were formed. According to authors, hydrated crystals exist in the relaxed two-fold helical conformation with bonded two water molecules (Okuyama et al., 1997). As speculated by Demarger-Andre and Domard (1994), at room temperature, acetic acid might be removed from chitosan crystal. Then result of dehydration is anhydrous crystal (Fig. 2.4.). Even though authors reported that this removal is spontaneous, we must underline that in this study a certain hydration level (>20-30% RH) was required. The anhydrous polymorph is energetically a more stable conformation of chitosan polymorph, because of additional inter-chain hydrogen bonding formed upon the removal of loosely bound water molecules between chains (Ogawa et al., 1984; Saito et al., 1987). When dehydration occurs, chitosan macromolecular chains shift by breaking the bonds to fill up the spaces of previously existing water molecules. The re-crystallization into the anhydrous allomorph can then be favoured by a relatively higher molecular mobility in hydrated condition and result in the weight loss. Similar observations were reported by Osorio-Modraza et al. (2011). As during desorption in

all cases the equilibrium was reached, it could confirm that the removal of acetic acid was done during the sorption process and that specific re-organisation occurred.

To confirm this hypothesis, after desorption, the second water vapour sorption was performed. The mass gain values were almost superimposed to the desorption ones for the same RH gradient. Moreover, the mass of the sample was well equilibrated. This indicates irreversible re-organization in the film structure. As the binding capacity changed during the second sorption, mass gain was lower than during the first one. Special problems in sorption studies are typical for some low molecular carbohydrates such as lactose. If a sugar solution is dried below its saturation point an amorphous solid glass is formed. These amorphous non crystalline materials can bond water internally. During moisture sorption as  $a_w$  increases further crystallisation can occur, potentially leading to re-crystallisation of the entire matrix that causes water to be expelled from the matrix into the environment around it (Bell and Labuza, 2000).

From the kinetic results, water diffusion coefficients at relative humidity differentials from 0% to 85% in different chitosan films were determined. Results are given in the Table 9.1.

**Table 9.1.** Diffusion coefficients of water vapour in chitosan based films.

Film	Water diffusion coefficient $D \times 10^{-14} \text{ m}^2/\text{s}$							
	Relative humidity %							
	0-10	10-20	20-30	30-50	50-60	60-70	70-80	80-85
CSA	1.84±0.12	2.57±0.06	5.76±2.26	15.40±0.25	15.00±0.50	14.03±0.67	11.22±2.29	8.17±2.02
CSACVC	2.17±0.47	3.01±0.13	5.79±1.99	16.00±0.13	nd	14.33±0.11	11.79±0.60	7.22±0.14
CSAGLY	3.56±0.01	nd	12.86±2.49	14.10±0.73	14.37±0.98	13.58±0.89	8.88±3.11	6.69±1.73
CSE	1.80±0.05	2.84±0.52	7.23±0.48	16.09±0.88	14.41±1.59	13.39±0.85	9.98±1.84	6.90±1.54
CSECVC	2.51±0.05	3.30±0.12	4.00±0.01	13.65±1.02	nd	9.28±2.06	7.81±0.01	5.62±0.15
CSEGLY	1.91±0.20	nd	nd	15.83±0.50	14.06±0.69	13.57±0.80	9.06±2.27	7.07±0.01

nd = not determined

The transfer of water vapour through the chitosan films does not follow the Fick's law applied to transient state. For that reason, the ultimate value of water mass gain used in the fitting process in calculation of diffusion coefficients was taken at the moment when the tested sample started to lose its mass. This is an important choice and detail that must be considered in the interpretation of results. Examples of mentioned phenomena are given in the Fig. 9.3.

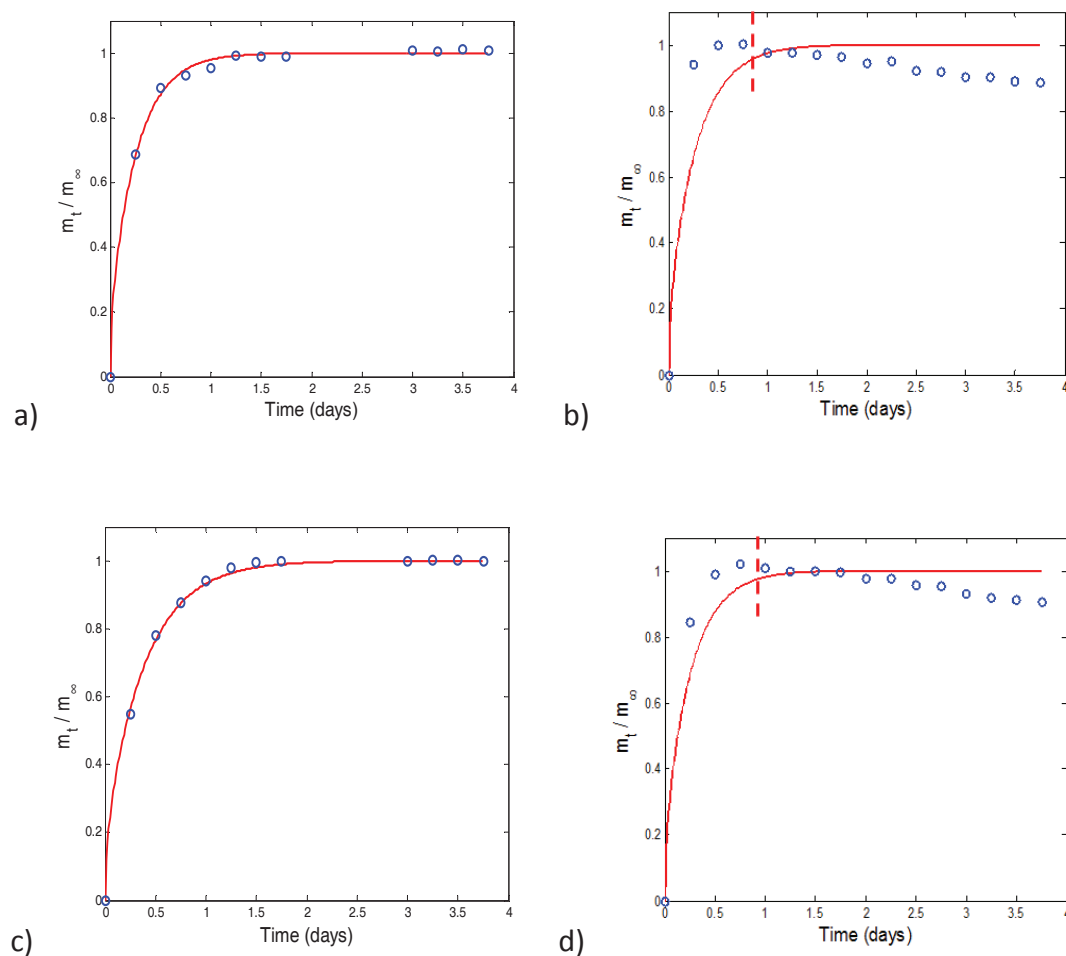


**Figure 9.3.** Water vapour sorption in chitosan based films. a) CSAGLY,  $\Delta RH$  70-80%; b) CSAGLY,  $\Delta RH$  50-60% c) CSEGLY,  $\Delta RH$  70-80%; d) CSEGLY,  $\Delta RH$  50-60%. Experimental data (o) and fitting data (-).

Moreover, for some samples the water vapour sorption was too fast. In other words, the transient state was too short and diffusion coefficient could not be determined (Fig. 9.4.). These results are considered as not detected (nd) (Table 9.1.).

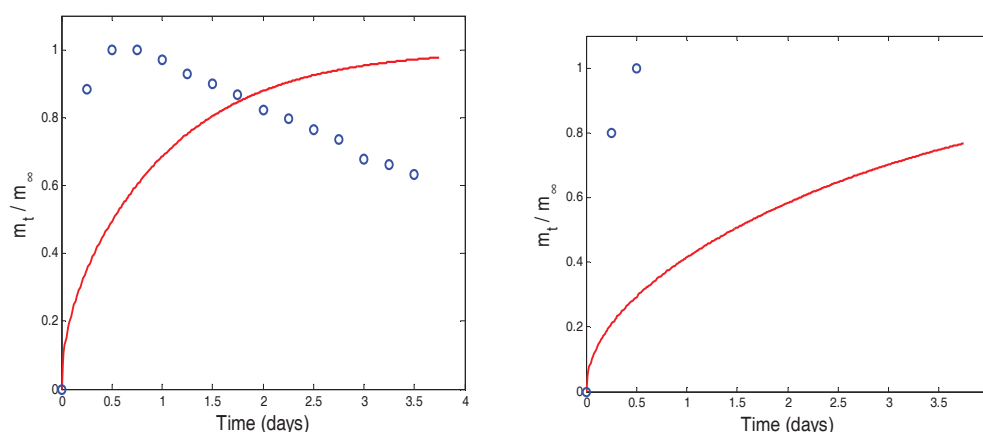


**Figure 9.4.** Water vapour sorption in CSAGLY film in relative humidity range 10-20%. Experimental data (o) and fitting data (-).

The diffusion of a water vapour through a polymer matrix is a consequence of random motions of individual molecules of the species. According to McHugh and Krochta (1994), anomalous diffusion occurs when penetrant diffusion and polymer relaxation rates are comparable. Relative humidity had strong impact on the moisture diffusivity in all chitosan-based films. The relation between relative humidity range and diffusion of water in different films is given in Table 9.1. and Fig. 9.5. All samples followed the same behaviour. The diffusivity increased gradually up to ten times, as the moisture content increased up to 50% when the maximum values were reached. It corresponded to the 10-20% of the moisture content in the chitosan films (depending on the sample type). Then, while the moisture content of films continued increasing,  $D$  gradually decreased. Depending on the relative humidity, moisture diffusivity at 25°C varied from  $1.84 \times 10^{-14}$  to  $15.4 \times 10^{-14}$  m<sup>2</sup>/s for pure chitosan films, from  $2.17 \times 10^{-14}$  to  $16.0 \times 10^{-14}$  m<sup>2</sup>/s for carvacrol containing films and from  $1.91 \times 10^{-14}$  to  $15.8 \times 10^{-14}$  m<sup>2</sup>/s for glycerol plasticized films. The solvents used for the film-forming solution did not significantly change the diffusivity of water in films. However,  $D$  in glycerol containing samples was significantly faster in the range from 10-30% relative humidity. In the RH range 10-20%, the diffusivity was so fast that the determination of diffusion coefficient was impossible, as previously mentioned.

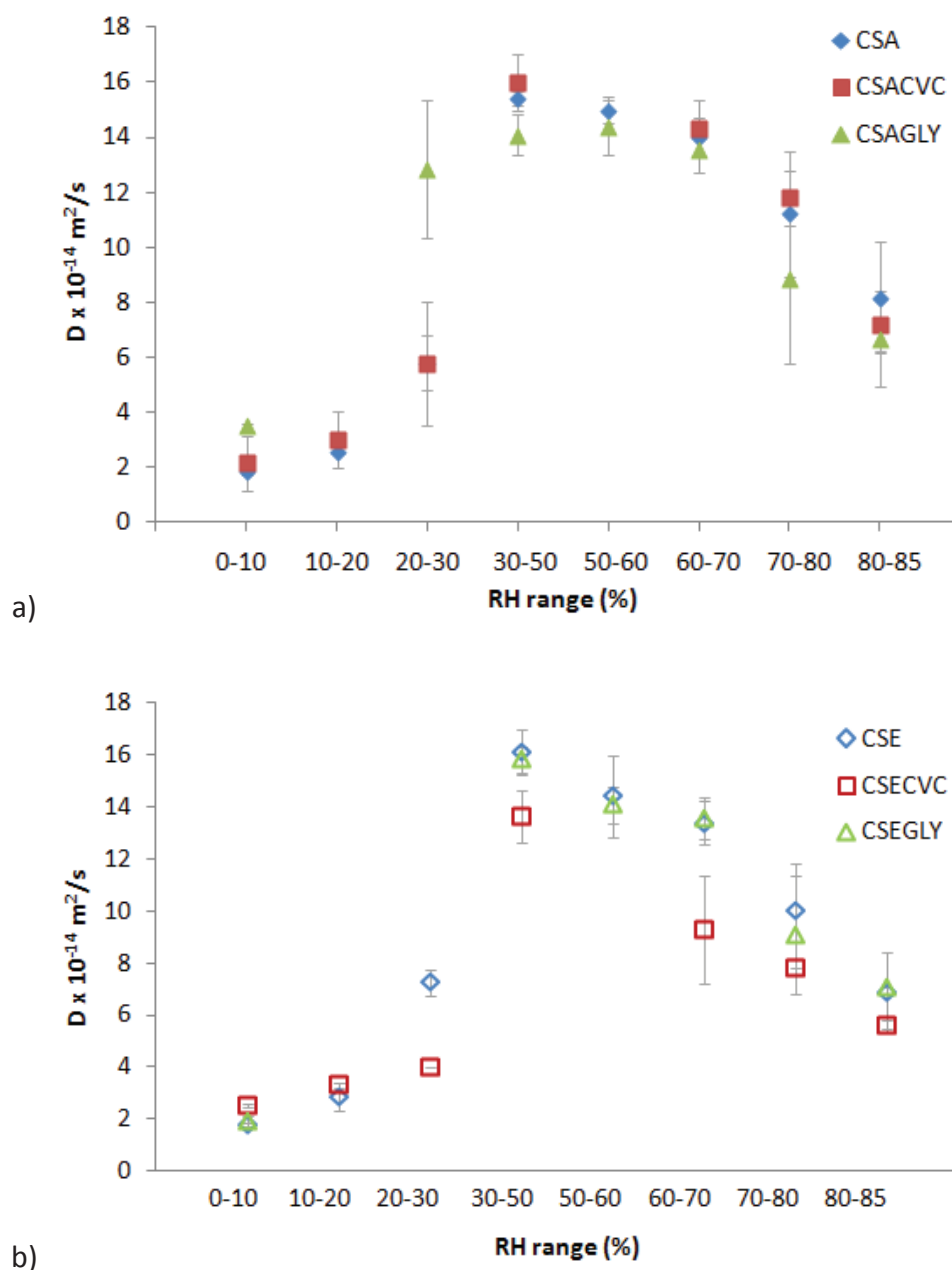


**Figure 9.5.** Diffusion of water in chitosan based films as a function of relative humidity: a) chitosan film prepared in aqueous acetic acid solvent, and b) chitosan films prepared in hydroalcoholic acid solvent.

Similar values of the effective diffusion coefficients for chitosan/glycerol films were reported by Pereda et al. (2009). In the mentioned study  $D$  was  $15 \times 10^{-14} \text{ m}^2/\text{s}$  at 75% RH. In another work, Despond et al. (2001) calculated the diffusion coefficients at lower partial pressures. In the RH range from 0% to 40%, according to authors, sorption was controlled by a Fickian mechanism. The reported values were in the same range as values in this study (from  $0.46$  to  $1.83 \times 10^{-14} \text{ m}^2/\text{s}$ ). According to same

authors, at low RH (<50%), water molecules are interacting with polar groups of chitosan by hydrogen bonding.

During the exposure to water vapours, water vapour plasticizes the chitosan films which swelled and then induced an increase of the mobility of both the chitosan polymer segments and water penetrant molecules. It is thought that anomalous effects observed in hydrophilic films could be due to glass transition-induced structural changes within films exposed to high RH gradients (McHugh and Krochta, 1994). Moreover in the presence of glycerol the network becomes open and flexible enough to allow the passage of the water molecules. Consequently,  $D$  was increased. It is possible that deviations from Fickian behaviour are the results of increased penetrant-polymer and penetrant-penetrant interactions. In other words this means that the association of water molecules can occur. At higher water activity weakly interacting water molecules are added. A positive deviation of equilibrium sorption from Henry's law sorption is generally interpreted by a clustering tendency of penetrates in the polymer material. Despond et al. (2001) reported that as the partial pressure increases water molecules are predominately clustered on active sites of hydrogen bonds. This was not confirmed experimentally but it was calculated from the GAB isotherm model. Similar behaviour of water clustering in cellulose-derivative films was also observed (Barrie, 1968; Debeaufort et al., 1994).

Consequently, decrease of  $D$  as the relative humidity increases above 50%, can be explained by a phenomenon of clusters formation. Below the concentration corresponding to the water monolayer, water interacts strongly with the chitosan macromolecular chains and/or hydrophilic glycerol, which explains the very large decrease in apparent diffusivity. Once the monolayer was formed, water no longer interacts with the polymeric system and the free water molecules associate to form clusters. As the molecular volume of these clusters increased, the water diffusivity decreased. Another explanation could be attributed to the higher density of hydrated chitosan amorph. Then interestingly, it can restrict the water diffusion rate (Okuyama et al., 2000). Thus, once again, bigger molecules could not penetrate and diffuse in the polymer. The diffusion decrease above 50 % perfectly corresponds to the humidity where structural reorganisation took place. The phenomenon of association of water molecules was initiated at polar centres and is especially important in hydrophilic polymers such as silicone, cellulose and its derivatives (Barrie et al., 1974).

## 9.2. Water vapour sorption isotherms

Water vapour sorption isotherms of chitosan powder and all chitosan based films are given in Figs. 9.6 and 9.7. All of them display a type II sigmoidal shape of the IUPAC classification (Fig. 3.15.).

The slope of adsorption isotherms, when the relative humidity tends to zero was rather low. This indicated a weak absorption affinity of water on chitosan films at low RH. When the relative humidity is above 60% and approaching 85%, the adsorbed amount of water increased for more than three times. These data are in agreement with other works reported in literature (Rosa et al., 2010; Sebti et al., 2007; Vargas et al., 2009).

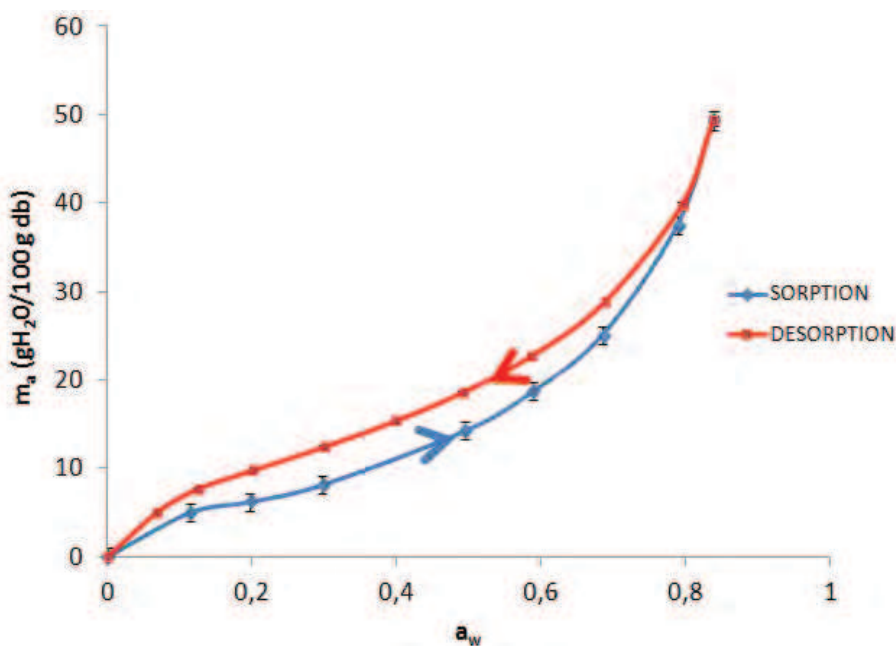
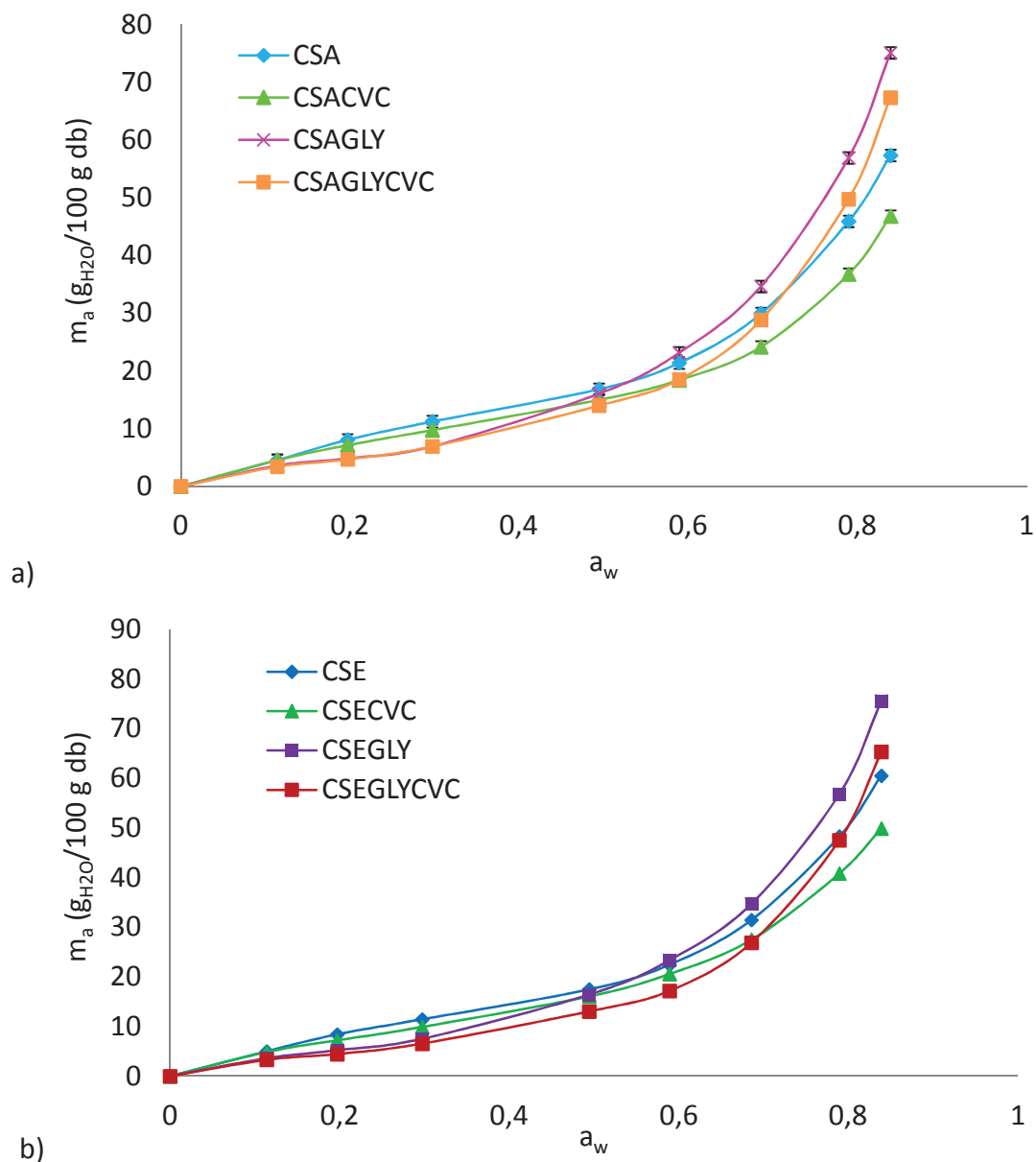


Figure 9.6. Water vapour sorption and desorption isotherms of chitosan powder.



**Figure 9.7.** Water vapour sorption isotherms of a) chitosan based films prepared with the aqueous acetic acid solvent (CSA); b) chitosan based films in hydroalcoholic acid solvent (CSE).

db= dry basis

The obtained sigmoidal shape shows an asymptotic trend when water activity tends toward 1. The sigmoid shape of water sorption isotherms was previously observed by other authors for pure chitosan films (Del Nobile et al., 2004; Wiles et al., 2000). Chitosan has three predominant adsorption sites: hydroxypropyl group, amine group and polymer chain end (composed of hydroxyl group or aldehyde group) (Fig. 2.3.). Analysis of the results of water sorption indicates significant differences in



water sorption capacity of chitosan powder (mass gain up to 45 g<sub>H<sub>2</sub>O</sub>/100 g db) and chitosan films (mass gain up to 75 g<sub>H<sub>2</sub>O</sub>/100 g db). Generally, water adsorption occurs into an amorphous phase of polymer. Crystallinity degree of chitosan powder decreased during the film formulation and freshly dry film had semi-crystalline structure (Li et al., 2011). This decrease is a consequence of the modification of inter- and intra-chain hydrogen bonds between the amino and hydroxyl groups due to the modification of the structure after the destructuration of chitosan crystal (Tanigawa et al., 2008).

For a RH >50% it is worthy to note that adsorbed amounts were higher on glycerol containing samples. Moreover, the maximum water uptake increased with the addition of glycerol, and decreased by the addition of carvacrol. Due to its hydrophilic character glycerol interacts both with chitosan and with water molecules through hydrogen bonds. As the resulting system has more water molecules, the equilibrium water contents were higher. According to Talja et al. (2007) films with higher glycerol concentrations could bind more water. Martino et al. (2011) found that chitosan/glycerol samples, preswelled in acetic acid solution, had 69.2% of water while neat chitosan had only 67.3%. Even that unplasticized and plasticized chitosan materials presented similar water uptake evolutions the glycerol containing samples, after 35 days had almost double values of water content as reported by Epure et al. (2011). Furthermore, in work of Pereda et al. (2009) the equilibrium moisture content of chitosan films increased with the glycerol concentration.

Furthermore, differences in mechanisms of sorption/desorption during the equilibration process were noticed, which could be due to a specific structure reorganisation of the material.

Adsorption isotherms on powder and on films exhibited a hysteresis loop. That is to say that the adsorption-desorption process was not reversible. However, different behaviour was observed in chitosan powder and chitosan films. For chitosan powder (Fig. 9.6.), during desorption process; the quantity of desorbed water was higher than that sorbed during the sorption. On the contrary, in all chitosan films these values were much lower (Fig. 9.8.). There is no many literature data reporting the existence of a hysteresis loop in the adsorption/desorption process in the chitosan film. The desorbed amounts were the highest in CSA films. Polymorph structure change and water removing due to competition between water and acetic acid could be postulated. We can assume in both hydroalcoholic samples, and those with both glycerol and carvacrol, there was less acetic acid in the system. Then, the acid was less

removed during sorption. Likewise during sorption, the equilibrium water content values were the highest for glycerol plasticized samples. Additionally, for both solvents, desorption isotherms were superposed for film with and without carvacrol. This indicated that carvacrol was completely desorbed at higher relative humidities (Chapter 8, Fig. 8.8.) and it didn't cause any significant structure change.

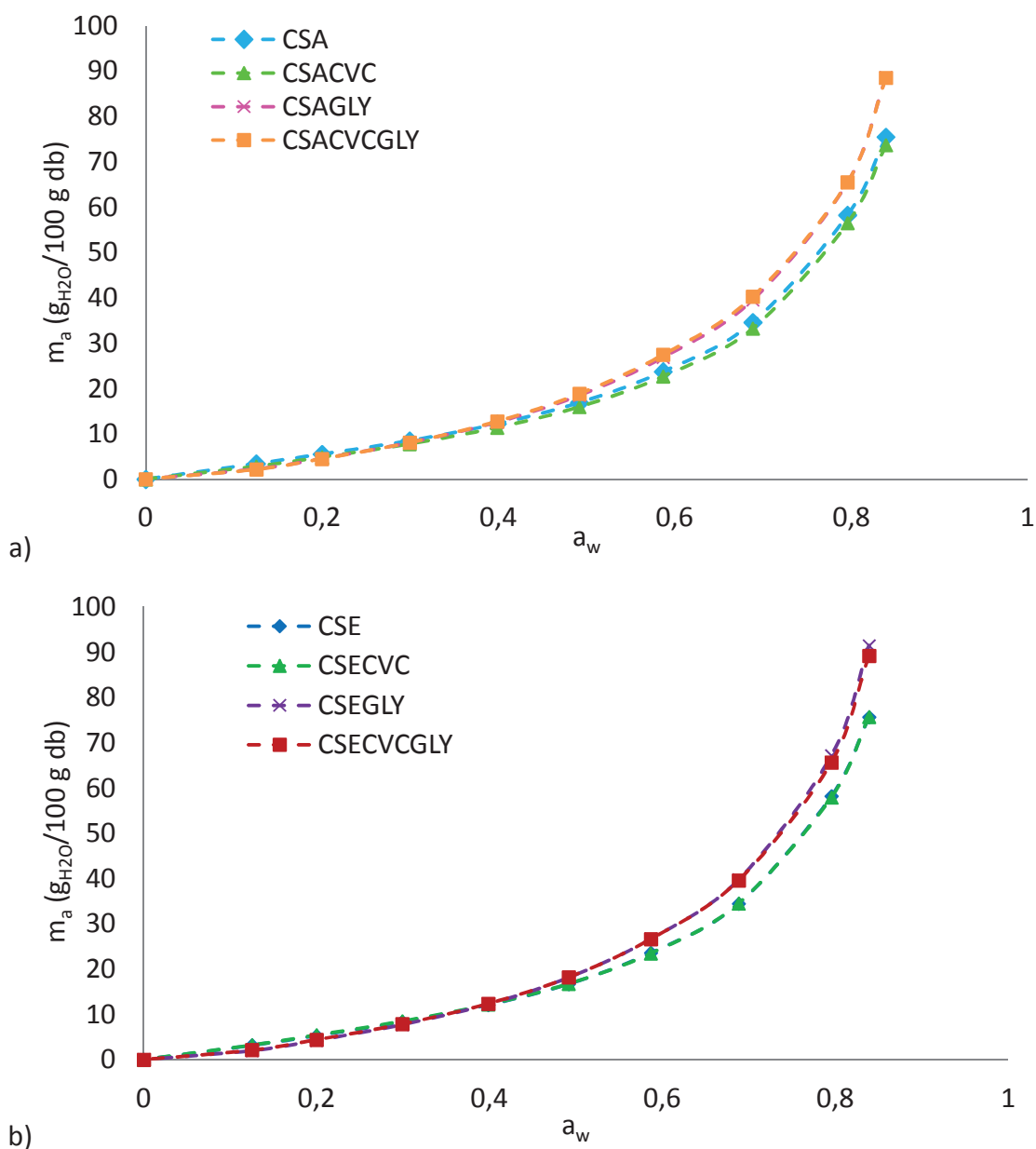


**Figure 9.8.** Water vapour desorption isotherms of a) chitosan based films prepared in aqueous acetic acid solvent (CSA); b) chitosan based films in hydroalcoholic acid solvent (CSE); containing carvacrol (CVC) or glycerol (GLY) or both (CVCGLY).

The data of water vapour sorption isotherms were fitted with the GAB model which gives accurate description of the adsorption process throughout the range of water vapour pressures explored (Fig. 9.9.). The GAB model parameters  $K_{GAB}$ ,  $C_{GAB}$  and  $m_m$  were determined on the way of adjustment of the curves of the equation with the experimental results. They are given in the Table 9.2. However, because of possible changes in material, desorption isotherms were not modelled.

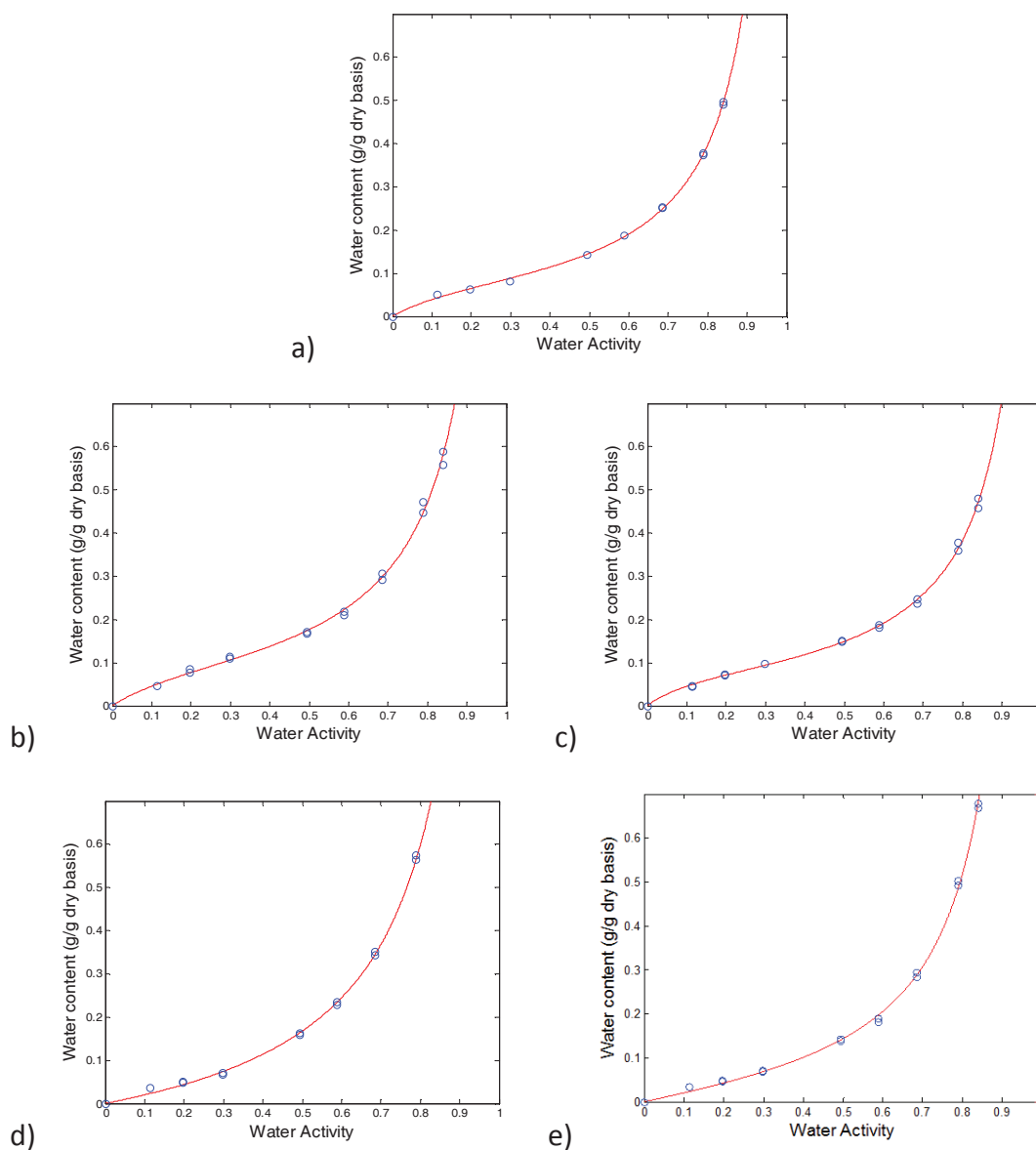


**Figure 9.9.** GAB model fitting of a) chitosan powder; b) CSA film; c) CSACVC film; d) CSAGLY film; and e) CSACVCGLY film. Experimental (o) and fitted (-).

**Table 9.2.** GAB model fitting parameters.

SAMPLE	$m_m$ (g/100 g db)	$C_{GAB}$	$K_{GAB}$	Maximum water uptake (g/100 g db) at 85% RH
CS powder	8.54	6.288	0.9916	49.32±0.54
CSA	10.60	5.7529	0.9811	57.32±2.28
CSACVC	8.54	8.3954	0.98	46.80±1.62
CSAGLY	16.83	1.1041	0.9708	75.10±0.90
CSAGLYCVC	10.92	1.764	1.0167	67.35±0.70
CSE	11.02	5.7356	0.9842	60.52±2.52
CSECVC	10.44	5.3448	0.9553	49.90±0.81
CSEGLY	15.06	1.3991	0.9856	75.56±1.84
CSEGLYCVC	9.81	1.8629	1.0279	65.32±0.31

The monolayer water content ( $m_m$ ) was the lowest in chitosan powder (8.54g/100g db) followed by carvacrol containing films (9.06 and 10.44g/100g db for CSACVC and CSECVC respectively). The highest monolayer water content was for plasticized chitosan films (16.83 and 15.06g/100g db for CSAGLY and CSEGLY, respectively). Constant  $C_{GAB}$ , related to the water–substrate interaction energy, was higher in pure carvacrol and carvacrol/chitosan films than for glycerol containing films. Significant drop, when glycerol was present in the film indicated that, as film became more hydrophilic, the water molecules were adsorbed with less energy. No significant changes were observed between the two solvents used. For more complex samples, where at the time there was both glycerol and carvacrol, constant  $C_{GAB}$  was lower than that of only carvacrol containing sample, but higher than glycerol- plasticized samples. These indicate changes in the structure and the competition between carvacrol and glycerol that were critical parameters influencing the final film properties.

### **9.3. Correlation between water vapour moisture isotherms and oxygen permeability in the relative humidity range from 0% to 96% of chitosan-based films and coatings**

As humidity is inescapable in many packaging situations, its effect cannot be overlooked. The humidity in the environment is often above 50% RH, and the humidity inside a food package can be nearly 100% RH. Significant changes in oxygen permeability when films were exposed in dry and completely humid environment (RH >96%) are already reported in previous chapters. To better understand the influence of hydration level on the oxygen permeability of chitosan films and to precise when exactly significant changes occur, in the following part the results of the tests performed over the whole humidity range from 0 to >96% RH are presented.

Oxygen permeability data for all chitosan based samples is given in Fig. 9.10. Within the studied range, two main regimes were observed. For RH <50%, O<sub>2</sub> permeability remained low and fairly constant. In all samples, in the range between 50 and 60% RH, slight decrease in permeability was observed. It's interesting that this corresponds to the same relative humidity range where unusual behaviour in water vapour sorption experiment occurred and a change in chitosan polymorph was proposed. Finally, at RH >60%, O<sub>2</sub> permeability increased exponentially up to very high values. There are several explanations for such behaviour. Firstly, when a polymer equilibrates with a humid environment, it absorbs water. Accordingly, above 60% RH, chitosan films swelled intensively and the average water content increased from 30% to 75% (w/w db) when humidity increased from 60% to 85%, respectively. Then high water content in the film at higher RH facilitated the gas solubility. Indeed, disruption of hydrogen bonds between molecules may create additional sites for the dissolution of oxygen and increase mobility of the O<sub>2</sub> molecules within the polymer bulk phase (Despond et al., 2001; Gennadios and Weller, 1990). Similar results were found for starch films which with less than 15% of water were shown to be good oxygen barriers, whereas those containing more than 20% water lost the oxygen barrier property (Forsell et al., 2002). Secondly, there is possible formation of water clusters. Zimm and Lundberg (1956) determined cluster functions for a variety of hydrophilic polymers over a large range of relative humidity. At low RH the initial water molecules were absorbed on specific sites. However, as RH increased the clustering occurred. Clustering leads to increases in the available free volume and in the permeability of polymeric matrix to test gases. The same phenomena could be postulated for chitosan

films. This might led to the appearance of greater gaps between macromolecular chains in chitosan films and diminished its cohesivity.

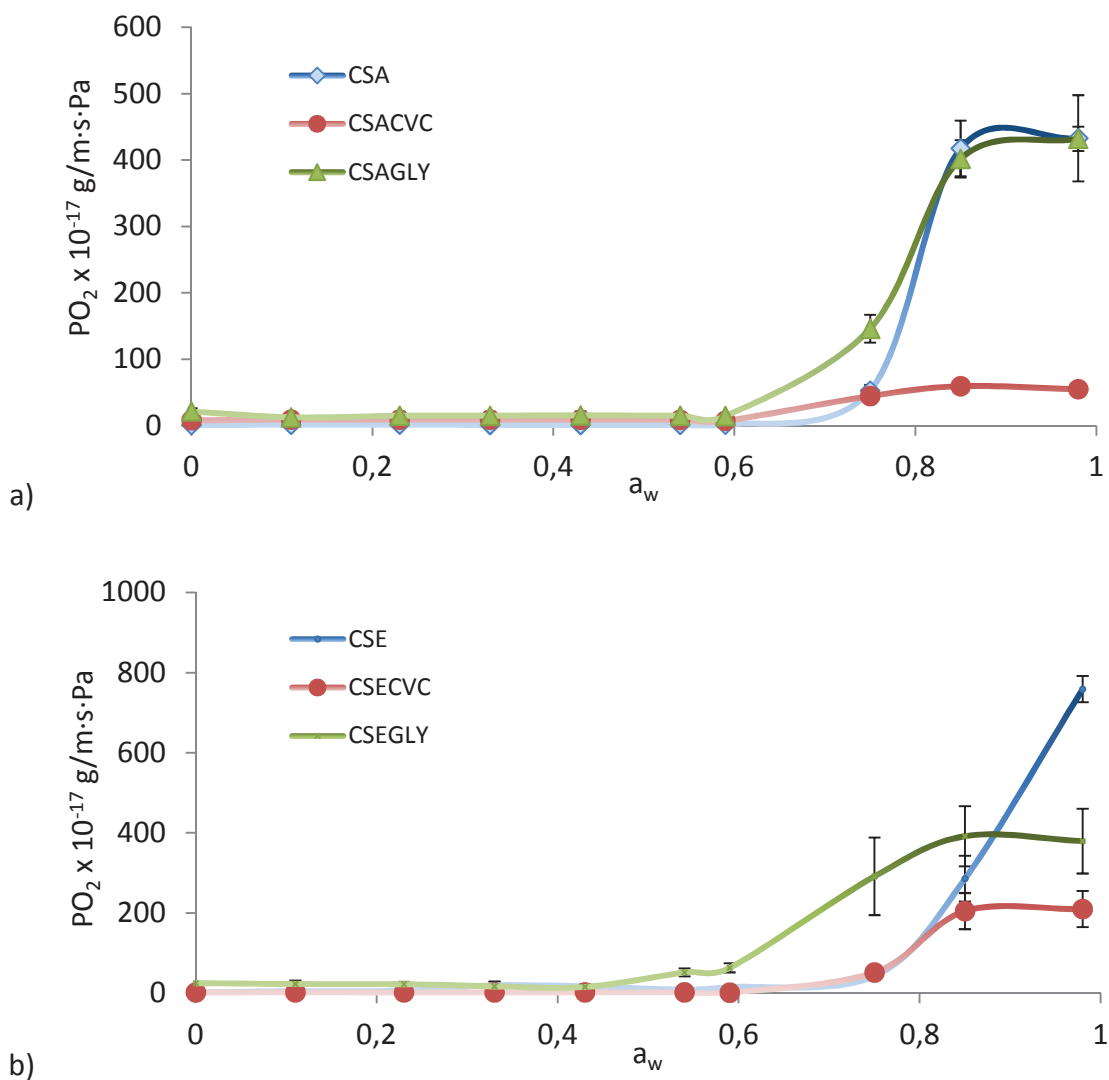


**Figure 9.10.** Oxygen permeability of chitosan based films as influenced by different relative humidities: a) chitosan based films prepared in aqueous acetic acid solvent (CSA); b) chitosan based films in hydroalcoholic acid solvent, containing either carvacrol (CVC) or glycerol (GLY).

In addition, the plasticization by carvacrol, by glycerol and/or by water was described in the Chapters 4 and 7. At lower relative humidities, carvacrol plasticized the polymer network. Then CSACVC and CSECVC films were more permeable. It was also noticed that when samples were equilibrated at high relative humidities ( $>75\%$  RH), changes in thermal degradation in carvacrol containing samples compared to pure

chitosan films occurred (Chapter 8). Water is the most effective plasticizer in hydrophilic films, and the amount of moisture in the films is related to the RH of the environment. Consequently, at RH >60% and film moisture content above 30%, plasticization with water was enhanced and higher  $PO_2$  of CSA and CSE was observed (Figs. 9.10.a,b).

Glycerol plasticized samples were more permeable in the RH humidity range from 0 to 80% RH (Fig. 9.10.). Here, once again the cluster theory can be postulated. Glycerol competes with water for active sites on chitosan molecule thus promoting water clustering at low moisture levels. Indeed, in a similar way, increased clustering with the presence of plasticizers resulted in increase in free volume within the collagen/glycerine matrix and subsequent increases in permeability as reported by Lieberman and Gilbert (1973). In addition, Epure et al. (2011) denoted that in glycerol-plasticized chitosan samples stored at 75% RH the crystallization process was inhibited due to materials' hydrophilicity and modification in hydrogen bonds interaction. For RH >85%, when samples were in completely humid environment, no significant changes for unplasticized and plasticized samples were observed. This was probably due to the competition of the greatest plasticizing effect of water than that of glycerol in high water containing materials. Similarly, hygroscopic materials: wheat gluten film (Gontard et al., 1994), starch (Gaudin et al., 2000), nylon 6 (Hernandez and Gavarra, 1994), cellophane (Krochta, 1992), methylcellulose (Rico Pena and Torres, 1991), etc., are significantly affected by the presence of moisture. The presence of hydroxyl groups (-OH) are responsible for the phenomena observed for most of these polymers.

Polyethylene, known to be good water barrier, was unaffected by humidity levels. Then, in pure polyethylene samples,  $PO_2$  was fairly constant in the whole RH range (Fig 9.11.).

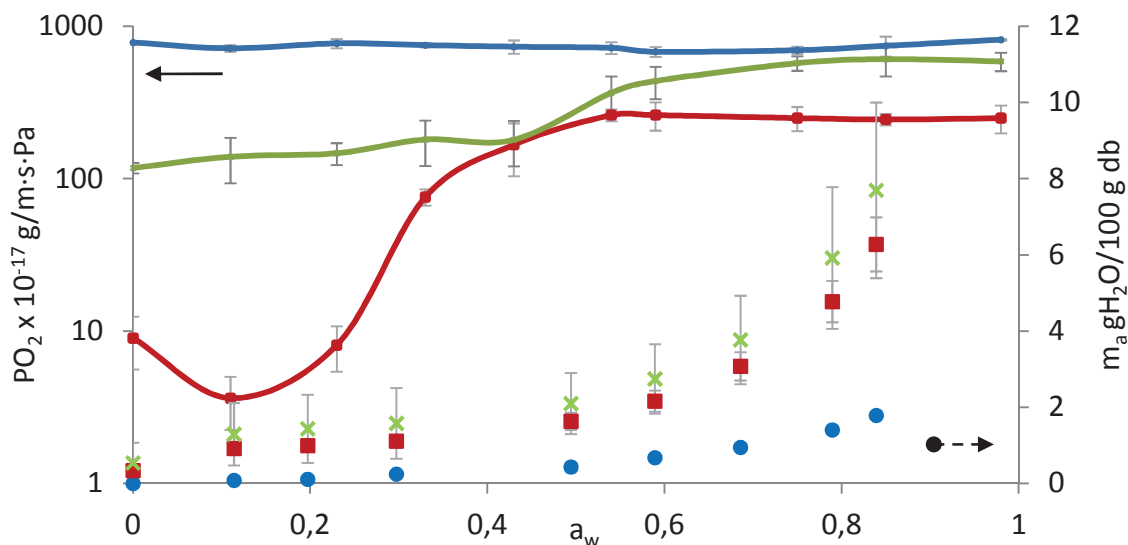


**Figure 9.11.** Relationship between water vapour sorption isotherms (symbols) and oxygen permeability (lines) of polyethylene (PE, blue), chitosan coated polyethylene (PECSE, green) and chitosan-carvacrol coated polyethylene (PECSECVC, red).

As it has been previously reported in Chapters 5 and 6, at low RH, all chitosan coatings significantly improved PE oxygen barrier properties. Furthermore, no significant changes in  $PO_2$ , neither in PECSE nor PECSECVC films in the range up to 40% RH were observed. Here, once again above 40% RH the  $PO_2$  increased rapidly. Interestingly, this corresponds to only 2% of sorbed water. At  $a_w$  above 0.6, small increases in humidity led to large mass gain of water. This suggested a swelling phenomenon as water activity increased. Logically, in the coated samples, the water uptake was mostly due to the presence of chitosan. Then, swelling together with its plasticization by water was critical outcome that result in important loss of barrier properties. Indeed, while pure polyethylene films sorbed less than 0.17% of water, chitosan coated (PECSE) and activated chitosan coated PE (PECSECVC) sorbed up to 6 and 8% of water, respectively. The  $PO_2$  values were higher from one to two orders of magnitude for chitosan coated and activated chitosan coated samples. Once again, at higher humidities PECSECVC samples were more permeable than PECSE films. This behaviour was previously attributed to the surface modification and roughness in the presence of carvacrol molecules. During fast drying of coated samples carvacrol molecules are evaporated and they might leave the holes on the chitosan surface. Thus an increase in surface heterogeneity supports the increase in oxygen permeability.



To conclude, permeability of chitosan films and films formed as coatings, increased at higher RH because of increasing moisture concentration within the film. In other words, relative humidity had an exponential effect on the oxygen permeability

The suitable use of packaging, apart from barrier properties is also strongly dependent on its favourable mechanical properties. Even that there is large information available on the mechanical properties of chitosan films; little information exists on the influence of moisture on the mentioned. Hence, the following discussion contributes to elucidate the relationship between mechanical properties and surrounding atmosphere of chitosan films.

#### **9.4. Effect of relative humidity on mechanical properties of chitosan based films and coatings**

Based on the requirements for packaging materials, films must have a certain degree of resistance. Mechanical properties reflect the ability of chitosan matrix to maintain a good integrity either as stand-alone films or applied as coatings on polyethylene.

Composition and hydration level changed the mechanical behaviour of all chitosan samples. The tensile strength (TS), the elongation at break (E) and the Young modulus (EM) could be used to describe how the mechanical properties are related to film's chemical structure. TS value indicates the maximum tensile stress that the film can sustain, E is the maximum change in length of a film before breaking, and EM is a measure of the stiffness of the film. The measured values are given in Table 9.3.

EM and E were significantly affected by increasing the relative humidity. While EM decreased the relative humidity generally affected E in the opposite way. At higher RH, water molecules were intensively sorbed into chitosan film. Thus increase in moisture content resulted in an extensive plasticization of chitosan matrix. Water molecules increased intermolecular spaces and reduced mechanical strength. In dry conditions (at RH <2%) all tested films were very brittle (Fig. 9.12.). Below 52% RH the addition of carvacrol and glycerol significantly increased the elongation at break of chitosan films. This was attributed to plasticization of the chitosan matrix in the presence of carvacrol and glycerol in dry conditions.

**Table 9.3.** Elongation at break (E), tensile strength (TS) and Young (elastic) modulus (EM) of chitosan-based films as a function of relative humidity.

Film	RH %	E %	TS (MPa)	EM (MPa)	Film	RH %	E %	TS (MPa)	EM (MPa)
CSA	<2	1.2 <sup>c</sup>	4.9 <sup>d</sup>	16.9 <sup>b</sup>	CSE	<2	0.6 <sup>c</sup>	16.6 <sup>b</sup>	30.6 <sup>a</sup>
	30	3.7 <sup>c</sup>	34.4 <sup>b,c</sup>	9.3 <sup>c</sup>		30	57.7 <sup>b</sup>	72.8 <sup>a</sup>	1.3 <sup>b</sup>
	52	71.1 <sup>a</sup>	50.8 <sup>b</sup>	0.7 <sup>e</sup>		52	72.8 <sup>b</sup>	50.5 <sup>a</sup>	0.7 <sup>c</sup>
	75	113.4 <sup>a</sup>	23.8 <sup>c</sup>	0.2 <sup>f</sup>		75	122.7 <sup>a</sup>	36.7 <sup>a,b</sup>	0.3 <sup>c</sup>
CSACVC	<2	2.3 <sup>c</sup>	57. <sup>b</sup>	25.9 <sup>a</sup>	CSECVC	<2	1.8 <sup>c</sup>	79.2 <sup>a</sup>	45.8 <sup>a</sup>
	30	49.2 <sup>b</sup>	55.2 <sup>b</sup>	1.1 <sup>d</sup>		30	72.8 <sup>b</sup>	76.4 <sup>a</sup>	1.1 <sup>b</sup>
	52	66.3 <sup>b</sup>	69.1 <sup>b</sup>	1.0 <sup>d</sup>		52	73.7 <sup>b</sup>	61.4 <sup>a</sup>	0.8 <sup>b</sup>
	75	110.4 <sup>a</sup>	17.9 <sup>c</sup>	0.2 <sup>f</sup>		75	128.0 <sup>a</sup>	21.9 <sup>b</sup>	0.2 <sup>c</sup>
CSAGLY	<2	2.7 <sup>c</sup>	63.2 <sup>a,b</sup>	22.6 <sup>a</sup>	CSEGLY	<2	2.8 <sup>c</sup>	81.2 <sup>a</sup>	0.3 <sup>c</sup>
	30	92.2 <sup>a</sup>	35.6 <sup>b,c</sup>	0.4 <sup>e</sup>		30	57.0 <sup>b</sup>	25.3 <sup>b</sup>	0.1 <sup>c</sup>
	52	43.3 <sup>b</sup>	18.9 <sup>c</sup>	0.4 <sup>e</sup>		52	55.9 <sup>b</sup>	12.8 <sup>b</sup>	0.2 <sup>c</sup>
	75	91.2 <sup>a</sup>	15.5 <sup>c</sup>	0.2 <sup>f</sup>		75	38.5 <sup>b</sup>	6.6 <sup>c</sup>	0.1 <sup>c</sup>
CSACVGLY	<2	3.4 <sup>c</sup>	99.9 <sup>a</sup>	30.0 <sup>a</sup>	CSECVGLY	<2	59.8 <sup>b</sup>	15.1 <sup>b</sup>	29.1 <sup>a</sup>
	30	103.2 <sup>a</sup>	48.5 <sup>b</sup>	0.5 <sup>e</sup>		30	51.0 <sup>b</sup>	6.9 <sup>c</sup>	0.4 <sup>c</sup>
	52	85.9 <sup>a</sup>	39.0 <sup>b</sup>	0.5 <sup>e</sup>		52	33.4 <sup>b</sup>	6.0 <sup>c</sup>	0.2 <sup>c</sup>
	75	75.5 <sup>a</sup>	13.2 <sup>c</sup>	0.2 <sup>f</sup>		75	45.3 <sup>b</sup>	6.0 <sup>c</sup>	0.2 <sup>c</sup>

<sup>a-f</sup> Different superscript within a column indicate significantly different result at  $p < 0.05$ .

The film stiffness is strongly affected by relative humidities higher than 52%, while film's capacity of stretching is significantly increased from 30% RH (Fig. 9.12.).

These effects could be explained by the glass transition of polymers inducing the structure change from glassy to rubbery, which can be estimated from the shape of stress-strain representations of the tensile curves. The work of Gibson and Ashby (1988) on the mechanical properties of synthetic polymers (solid materials) such as poly(vinyl chloride) shows that the shapes of tensile stress-strain curves are directly correlated to the structure characteristics of the polymer, and particularly to the glass transition. On the basis of the work of Gibson and Ashby (1988) (Fig. 3.7.), three different behaviours in chitosan based films as a function of both relative humidity and formulation were observed (Table 9.4.).

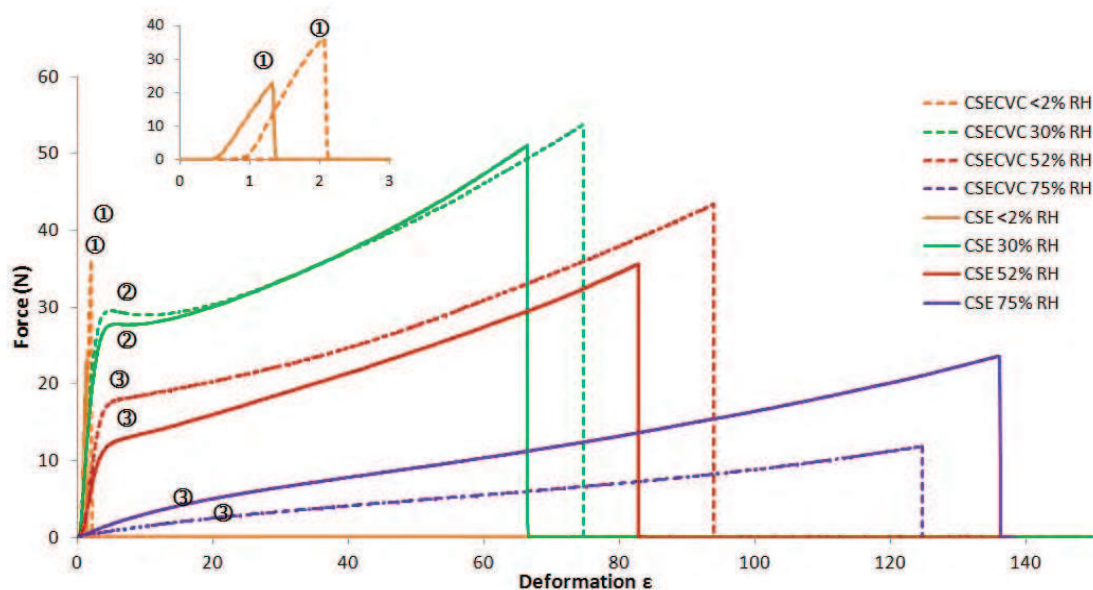


**Figure 9.12.** Tensile stress-strain curves of chitosan films in function of relative humidity and composition. CSE: film prepared in hydroalcoholic acid solvent, CVC: carvacrol containing films. Classification of Groups 1-3 was done according to Gibson and Ashby (1988) and it is given in Table 9.4.

**Table 9.4.** Classification<sup>a</sup> of mechanical properties and film structures as a function of ambient relative humidity and film composition.

Film	<2% RH	30% RH	52% RH	75% RH
CSA	1	2	3	3
CSACVC	1	2	2	3
CSAGLY	1	3	3	3
CSAGLYCVC	1	3	3	3
CSE	1	2	3	3
CSECVC	1	2	3	3
CSEGLY	1	3	3	3
CSEGLYCVC	1	3	3	3

<sup>a</sup>Group 1 brittle fracture, glassy polymer,  $T < 0.8 T_g$ . Group 2: extensive cold drawing, ductile polymer,  $T = T_g$ . Group 3: uniform viscous flow, rubbery polymer,  $T > 1.05 T_g$ .

Generally, the glass transition temperature of the polymer is decreased when the matrix is plasticized. When measurement temperature is lower than  $0.8 T_g$  (glass temperature of the film), polymers are linear-elastic to fracture, brittle, and in a glassy state (Group 1). At higher temperature ( $T = T_g$ ) the mode of failure changes from brittle

to ductile with large extensions (Group 2). Finally, in conditions corresponding to  $T > 1.05 T_g$  the polymer deforms homogeneously by viscous processes, giving a large extension to failure (Group 3). In the later, the interruption of the chitosan chain aggregations and plasticizing effect of both glycerol and water makes the chain displacement during stretching easier, which gives the film a greater ability to be deformed without breaking. An example of graphical determination is given in the Fig. 9.12. The similar trend was also found in previous studies for sodium caseinate and chitosan films (Fabra et al., 2010; Vargas et al., 2009). However, the real  $T_g$  value according the water content or RH couldn't be determined by classical techniques such as DSC.

## **9.5. Conclusions of Chapter 9**

In conclusion, the water vapour sorption in chitosan films was strongly influenced by relative humidity and film formulation. Powder and films did behave the same. At relative humidities from 20-70%, water sorption in chitosan films was not governed by Fickian mechanism, since sorption kinetics results revealed a decrease in mass. A deviation from Fickian sorption indicated an anomalous diffusion of water. The amount of sorbed water was mainly due to physical sorption on the active sites in chitosan chains, whereas at higher relative humidity, an additional contribution probable due to water clustering is observed. The diffusion coefficient of water vapour in chitosan films was not significantly influenced by solvent and carvacrol. However, the addition of glycerol seems to speed up the diffusion. Finally, glycerol increased the amount of water absorbed, as expected. The embedded carvacrol also tends to reduce the hygroscopicity of the films. However, the equilibrium moisture content in all films dramatically increased above  $a_w=0.6$ . The GAB model allows accurate description of all sorption isotherms. Film permeability changes in function of moisture concentration, which is related surrounding air's RH. Like for water sorption, two different domains were distinguished for oxygen permeation. Below 40% RH no significant changes were observed in all chitosan samples. However, for the water content in films higher than 20% (at RH >60%) exponential increase in oxygen permeability was induced. In the former region, differences in the permeabilities among samples were mainly due to the plasticization effects of both carvacrol and glycerol. However, at higher hydration levels the plasticization effect of water was predominant. The adsorption of water in chitosan coated polyethylene was totally attributed to the chitosan coating. Interestingly, even low amounts of sorbed water (around 6%) caused significant

decrease in oxygen barrier performance of coated polyethylene. Whatever the RH is, coated polyethylene film (PECSE) was shown to be better oxygen barrier than PE and PECSECVC (Fig. 9.11.).

The increase in moisture level significantly affected the mechanical properties, by lowering the tensile strength and the elastic modulus, while increasing the percentage of deformation. These changes were mainly due to the unavoidably important plasticizing effect of water, as confirmed by lowering the transition temperatures as speculated in Chapter 8.

In Chapters 8 and 9, it was clarified how water vapour significantly affected structural and barrier properties of chitosan based films and coatings. Moreover, in Chapter 7, the influence of storage parameters and release mechanism of active carvacrol compound was proposed. Also, the significance of formulation and of processing parameters in film design was underlined. The knowledge of these results is important for the development of antimicrobial films for food storage. Thus, to approach the real food and the industrial application of produced activated chitosan films and coatings, in the next two chapters, the study will be focused on their antimicrobial and sensory properties.

*Chapter 10*

*Antimicrobial efficiency of carvacrol vapour  
related to mass partition coefficient when  
incorporated in chitosan based films aimed for  
active packaging*

---

---

Publication: **Mia Kurek**, Sylvie Moundanga, Coralie Favier, Kata Galić, & Frédéric Debeaufort

Food Control, DOI 10.1016/j.foodcont.2012.11.049.

Unpublished part of this chapter:

10.3. Antimicrobial efficiency of chitosan based films against *Penicillium camemberti*

10.4. Antimicrobial efficiency of three chitosan based coatings with different concentrations of carvacrol in the vapour phase

All the experiments reported in this chapter were performed under the special supervision of Ms. Sylvie Moundanga, in the UMR PAM- lab. PMB.



The importance of composition and environmental conditions on physicochemical properties of chitosan based films and coatings were studied in previous chapters. Even that there is a large amount of available data on the antimicrobial efficiency of essential oils on different microorganisms, there are no many studies dealing with antimicrobial films that are active in the vapour phase. Most of the relevant studies have only evaluated measurement that provide protection when there is direct contact between microorganisms and active agents, which is not the case in most potential applications.

Moreover, no literature available data was found based on carvacrol/chitosan antimicrobial films. Carvacrol is a phenolic compound extracted from oregano and thyme oil. Its inhibitory effect on the growth of various microorganisms is well documented and described extensively. Different studies report its activity using either diffusion (Liolios et al., 2009) and/or contact methods (Lambert et al., 2001; Friedman et al., 2002). However, several works have been published concerning vapour-phase inhibition, i.e. vapour phase method (Ben Arfa et al., 2006; Nostro et al., 2009; Kloucek et al., 2011). Besides studies were performed on different food products such as fish (Kim et al., 1995), fruit juices (Kisko et al., 2005), meat (Skandamis and Nychas, 2002), and against different microorganisms such as *E. coli* (Friedman et al., 2002; Burt et al., 2007), *Bacillus* sp. (Ultee et al., 2000; Burt et al., 2007), *Listeria* sp. (Friedman et al., 2002), *Salmonella* sp. (Friedman et al., 2002), *Lactobacillus plantarum* (Ben Arfa et al., 2006) etc.. It can also be used to improve functional and antimicrobial properties of biopolymer films to extend product shelf-life (Ben Arfa et al., 2006; Mastromatteo et al., 2009). Ultee et al. (1999) showed that carvacrol has biological effects in the products associated with outbreaks of *B. cereus* (e.g., rice, pasta, and soup). Thus, it could be applied both as an antimicrobial and as a flavouring compound.

The increasing numbers of foodborne illness outbreaks caused by some pathogens and the antibiotic resistance of some strains have captured the attention of regulatory agencies. Most reporting cases of foodborne illness have documented significant increases over past few decades in the incidence caused by microorganisms in food, including pathogens such as *Salmonella* sp., *Listeria* sp., and enterohaemorrhagic *Escherichia coli*, parasites such as cryptosporidium, cryptospora, trematodes and fungi (Viazis et al. 2011, Amalaradjou et al., 2012; Olaimat et al., 2012; Pires et al., 2012). *Salmonella* species have become the major cause of foodborne diseases which has raised a great safety concern to public health. *Escherichia coli* O157:H7 and sporulating *Bacillus* species are a concern to public health on a global scale and are found in a wide variety of foodstuffs. Pasteurization and cooking are



adequate methods of ensuring that viable cells are eliminated, but heat treatment is not desirable for all foods and cross-contamination cannot always be prevented. Controlling the numbers and growth of *E. coli* and *Bacillus* sp. therefore remains an important objective for sectors of the food production industry (Burt, 2007).

In this chapter, the antimicrobial potential of carvacrol vapours will be studied. First of all, the inhibition of *Bacillus subtilis*, *Escherichia coli*, *Listeria innocua* and *Salmonella Enteritidis* by the only vapour phase using volatile carvacrol incorporated into chitosan-based films was assessed. The concentrations of carvacrol in the chitosan-based films after drying were determined. In addition, the mass partition coefficients were also detected. These systems were used to control the concentration of carvacrol in the vapour phase. From the quantification of the aroma compounds in the air, minimum inhibitory concentration of studied films was reported. In the second part of this chapter, the study was expanded on the determination of antimicrobial efficiency against a fungus: *Penicillium camemberti*. Pursuing this further, in the third part, the antimicrobial efficiency of chitosan coated polyethylene is given.

### **10.1. Film characterization**

The film composition and the physico-chemical characterization of the system are given in Table 10.1. Five chitosan based films having various compositions were used as carvacrol support matrix and allowed to fix the air/film mass partition coefficient ( $K_{\text{mass}}$ , ratio between the aroma compound concentration in the air and the aroma compound concentration in the film) and the carvacrol concentration in the headspace above culture media. In relation to the effectiveness of antimicrobial food packaging, it is very important to know the amount of active compound retained in the film matrix after processing. Most of the reported data only consider the initial quantities of the active substance in the FFS and scarcely in the film after drying. Therefore it is not easy to compare the reported values. Carvacrol initially added in the FFS was significantly lost (from 50 to 99%) during film processing and drying (formation of the film matrix and solvent evaporation). Carvacrol concentration in films after drying varied from 0.04% to 10.75% (w/w) (Table 10.1.).

Its retention and release are influenced by film structure and composition at the tested temperature of 25°C. In Chapter four it was pointed out that  $K_{\text{mass}}$  is inversely exponential to the retention capacity during film processing. Then it directly affected carvacrol vapour phase concentration. It was attributed to the release mechanism from the chitosan-based matrix. The partition coefficient of films tested in this study,

depending on the carvacrol retention and its concentration in the headspace, varied from  $10^{-8}$  to  $10^{-4}$ . Indeed, carvacrol partitioning is influenced by aroma compound properties (e.g. volatility, vapour pressure, etc.), by the properties of food product inside the packaging ( $a_w$ , fat content, etc.) and by the chitosan film properties (composition, physico-chemical properties of the matrix and intra-network interactions) (Chillo et al., 2008). Thereby, the presence of arabic gum, nanoclays, glycerol and lecithin changed the overall thermodynamic behaviour and release kinetic of carvacrol reflecting its ability to reach a gaseous phase above food product. Then the reduction of food spoilage bacteria might be increased when the  $K_{mass}$  and carvacrol concentration in the headspace rose. In this study, volatile carvacrol molecules were easily released into the vapour phase with resultant significantly increased antimicrobial properties (AF1). The highest carvacrol vapour concentration ( $1.08 \times 10^{-7}$  g/mL) was found for the film with the highest  $K_{mass}$  (AF1) and the lowest ( $6.28 \times 10^{-9}$  g/mL) for the film with the lowest  $K_{mass}$  (AF5). Besides, from previously observed phenomena (Chapters four to nine) fast diffusion to the vapour phase could be due to the structural changes in chitosan matrix. Then it favoured the antimicrobial efficiency. Antimicrobial tests and observations permitted a comparison of the antimicrobial potential of chitosan-based films and examination of its relationship with  $K_{mass}$ .

**Table 10.1.** Properties of chitosan based films used in antimicrobial study.

Film code	Film composition	$K_{mass}$	Concentration of carvacrol in the dry film % (w/w)	Concentration of carvacrol in the headspace at equilibrium $g_{carvacrol}/mL_{air}$
AF 1	Chitosan/arabic gum/glycerol/carvacrol	$1.01 \times 10^{-4a}$	0.09 <sup>d</sup>	$1.08 \times 10^{-7a}$
AF 2	Chitosan/glycerol/carvacrol	$6.50 \times 10^{-5b}$	0.04 <sup>d</sup>	$3.13 \times 10^{-8c}$
AF 3	Chitosan/arabic gum/glycerol/lecithine/carvacrol	$1.13 \times 10^{-6c}$	3.45 <sup>c</sup>	$4.62 \times 10^{-8b,c}$
AF 4	Chitosan/glycerol/montmorillonite/carvacrol	$5.06 \times 10^{-7d}$	10.75 <sup>a</sup>	$6.41 \times 10^{-8b}$
AF 5	Chitosan/arabic gum/glycerol/carvacrol	$6.81 \times 10^{-8e}$	7.79 <sup>b</sup>	$6.28 \times 10^{-9d}$

<sup>a-e</sup> Different superscripts indicate significant differences between samples at  $p < 0.05$ .

## 10.2. Antimicrobial efficiency

In this study, the growth of bacterial colonies exposed to pure carvacrol in the vapour phase and carvacrol containing chitosan films was monitored by using different investigation methods. For macroscopic observations pictures of Petri dishes were recorded over the incubation period. Further measurement of colonies diameter by image analysis was performed. In addition, the rate of cultivability was determined. Up to date, direct liquid contact studies for antimicrobials were mostly performed. In the gaseous phase, the antimicrobial efficiency of tested vapours depends upon the volatility of each compound while in liquid phase it depends upon the “diffusability” and solubility of the active compounds into the agar (Goñi et al., 2009). Carvacrol is a volatile compound and therefore it could be highly active in the packaging headspace. Presence in a gaseous phase could facilitate the solubilisation of lipophilic carvacrol in the cell membranes, thereby causing high damages such as permeabilization (Inouye et al., 2001).

### 10.2.1. Macroscopic observations

Fig. 10.1. presents some pictures of the control film and two chitosan-based films with carvacrol. The antimicrobial effect of the two films of the extreme  $K_{mass}$  (AF1 with the highest  $K_{mass}$  and AF5 with the lowest  $K_{mass}$ ) against Gram-positive bacteria, *B. subtilis* and *L. innocua* and Gram-negative bacteria, *S. Enteritidis* and *E. coli* is presented. For control samples with and without Parafilm<sup>®</sup> no significant differences were observed (data not presented) for all tested bacteria. Then a decrease of microbial growth cannot be attributed to potential anoxia. First of all, pictures given in Fig. 10.1. show that a macroscopic observation allows an approximate estimation of the antimicrobial efficiency of carvacrol since drastic differences appeared especially comparing pictures obtained for colonies exposed to AF1 and AF5.

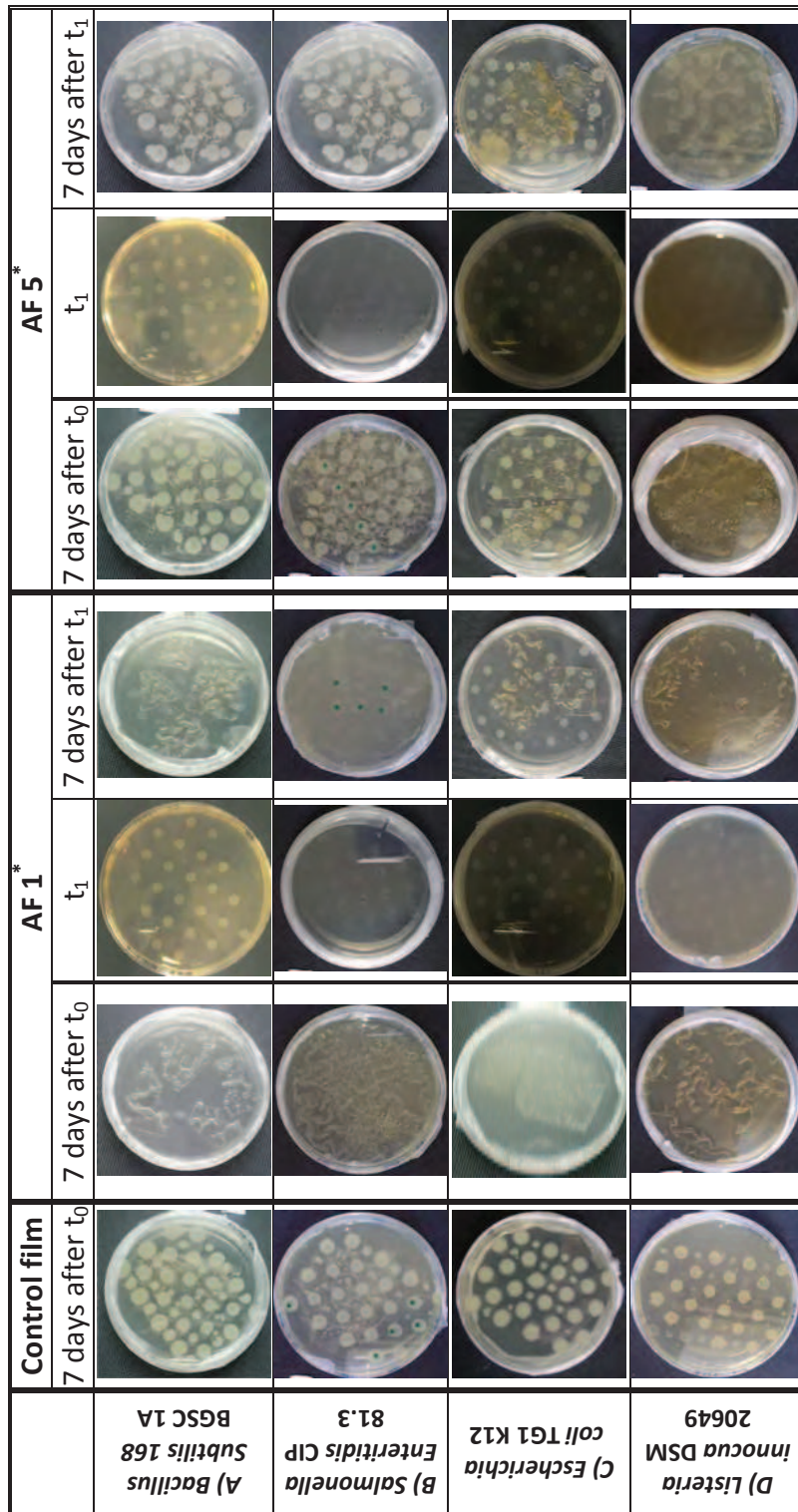


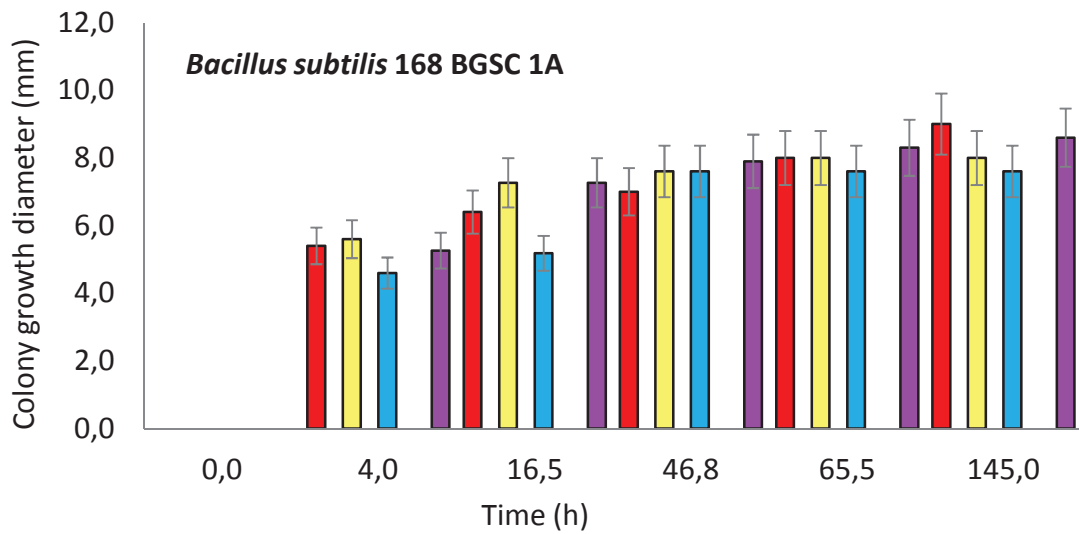
**Figure 10.1.** Photos of A) *Bacillus subtilis* 168 BGSC 1A, B) *Salmonella Enteritidis* CIP 81.3, C) *Escherichia coli* TG1 K12 and D) *Listeria innocua* DSM 20649 after the exposure to the vapour of two antimicrobial films AF1\* and AF5\* and control film (chitosan-based film without carvacrol).

\* Film type and definition is given in Table 1. t<sub>0</sub>-start of the incubation; t<sub>1</sub>-microbial culture after an initial incubation phase (allowing to obtain cellular colonies)\*\* . Film was put in the vapour contact with the already grown culture at t<sub>1</sub>\*\* the incubation time for *B. subtilis* and *E. coli* was 4 h and for *S. Enteritidis* and *L. innocua* 6 h. Green marks on some photos are marks of a pen used for labeling during the sampling and counting.

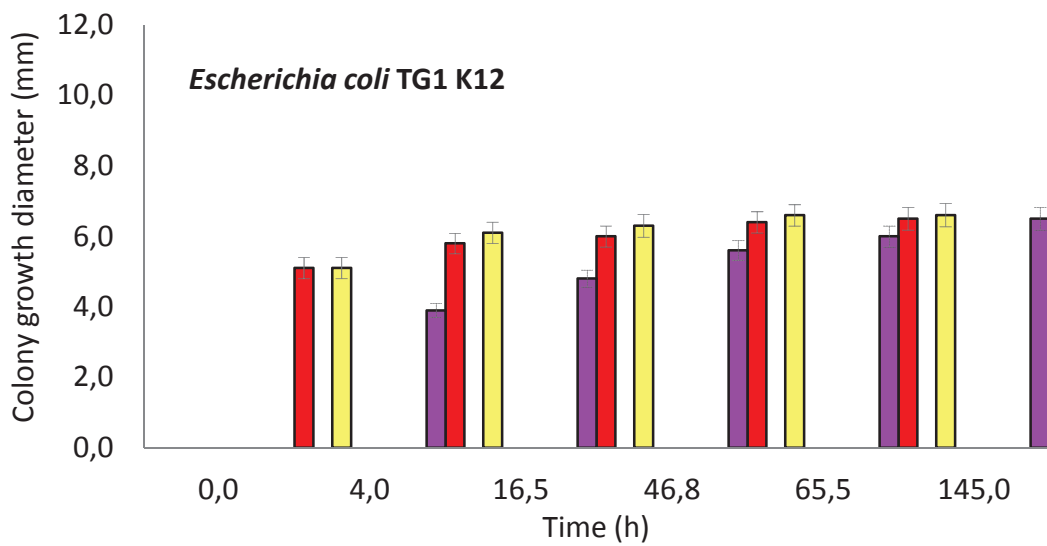
From all the results it was observed that the AF1, with the highest  $K_{mass}$ , was strongly efficient against all microorganisms tested. This film totally inhibited growth of just inoculated bacteria ( $t_0$ ) since no colony was observed on nutrient plates. This high antimicrobial efficiency was confirmed on already grown colonies ( $t_1$ ) compared to the control. In the case of *L. innocua*, carvacrol was even able to kill the bacteria, probably by permeabilization of the cell membrane and to lyse the cells since no more colonies were visible on the nutrient agar plate after seven days of exposure. The complete reduction was confirmed after counting (CFU/mL was equal to zero, this will be discussed later). It seemed to be slightly less efficient against already formed colonies of *S. Enteritidis* and *E.coli*. Indeed, after seven days of film exposure, colonies seemed to be a bit larger in diameter and thicker than at the initial time of exposure. On the contrary, in a previous work, Burt et al. (2007) evaluated carvacrol vapours against foodborne *Salmonella* species in meat products. Pathogen counts were reduced to extended limit and significantly increased product shelf-life. Different experimental conditions used (size of inoculum, culture media, etc.) could explain different efficiency of carvacrol against *Salmonella* species observed in these two studies. In our research, in the experiment performed at  $t_0$ , the microbial cells were at the beginning of the lag phase. The AF5, with the lowest  $K_{mass}$ , appeared not to be efficient. Growth of just inoculated cells and the growth of already formed colonies followed the same behaviour. Therefore, the concentration of carvacrol released in the vapour phase from this film was not high enough to inhibit or stop the growth of the tested microorganisms.

### 10.2.2. Chitosan/carvacrol film antimicrobial efficiency in lag phase of bacterial growth

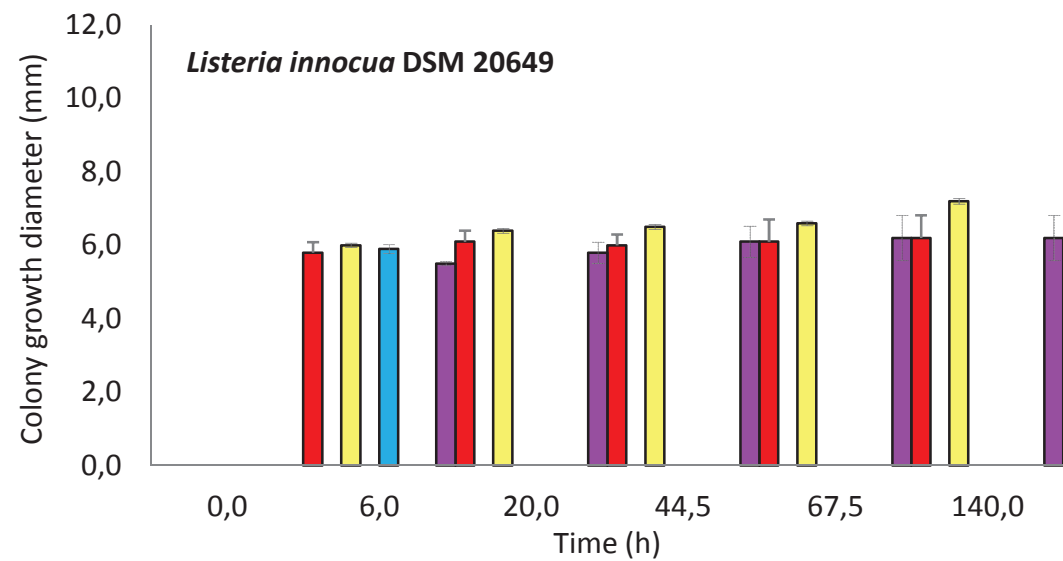
From the photos of Petri dishes, colony diameter was measured using image analysis software. Same examples of photos are given in Fig. 10.1. Radial colony diameters of *B. subtilis*, *E. coli*, *L. innocua* and *S. Enteritidis* as a function of incubation time were recorded (Figs. 10.2. and 10.3.). The colony size diameter ratio was determined from the ratio  $d_x/d_t$ .  $d_x$  is the average colony size diameter and  $d_1$  is the colony diameter at a time when films were put in the vapour contact with the inoculated medium.



a)



b)



c)



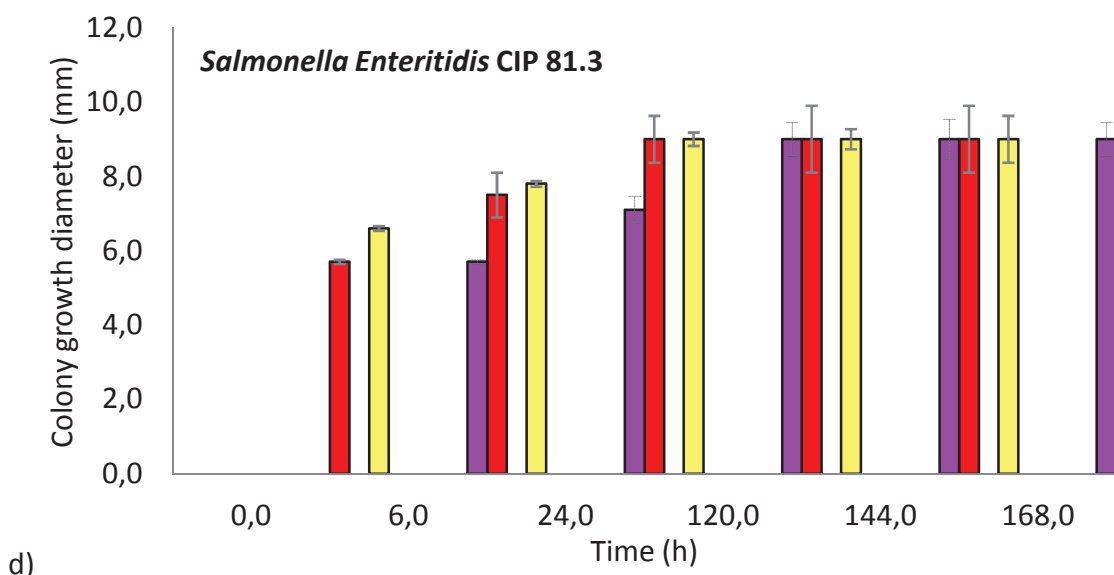


**Figure 10.2.** Average colony size diameter of bacterial strains put in the vapour contact with five active chitosan-based films, control film and pure carvacrol vapours at  $t_0$  during seven days exposure of a) *Bacillus subtilis* 168 BGSC 1A; b) *Escherichia coli* TG1 K12; c) *Listeria innocua* DSM 20649; and d) *Salmonella Enteritidis* CIP 81.3.

$t_0$  - films or aroma compound were put in the Petri dish lid at the same time as the incubation started

■ microbial cells without treatment; ■ pure carvacrol vapour; ■ chitosan-based film without carvacrol; ■ AF1\* ; ■ AF2\* ; ■ AF3\* ; ■ AF4\* ; ■ AF5\* .

\* Film type definition and characteristics are given in Table 10.1.

For not visible columns colony growth diameter was equal to zero.

Measurements of the colony size diameter allowed a first estimation of the antimicrobial efficiency of the carvacrol. Indeed, carvacrol has been shown to cause the cell permeabilization, but it also induces modifications in the bacterial morphology. The cell surface structure of Gram-positive and Gram-negative bacteria changes after contact with carvacrol. An increase in cell surface roughness and a decrease of both length and diameter of bacteria cells due to the leakage of cytoplasmic contents were previously reported (La Storia et al., 2011; Sousa et al., 2012). Furthermore, the sub-lethal levels of carvacrol prevent the development of flagella in *E. coli* O157:H7 (Burt et al., 2007), causing cell to be non-motile, and completely inhibit the motility of *Salmonella* (Inamuco et al., 2012). This absence of flagellum may lead to the altered morphology of bacterial colonies making them more rugose (Watnick et al., 2001). Mendelson and Salhi (1996) found a relationship between colony form and *Bacillus subtilis* motility attributed to response to the local signals during colony development



and to global conditions. However, in our study no modification in colonies form was observed. Nevertheless, to exclude the impact of the variations of the size and the shape of colonies according to the stress, further measurements of the cultivability were performed to confirm the antimicrobial activity of carvacrol.

The first part of the presented results gives the data about the experiments performed at  $t_0$  (inoculation and vapours exposition at the same time). At  $t=6h$ , all the bacteria were in the exponential growth phase. In control samples (non-exposed cells and exposed to the chitosan films without carvacrol) colony growth diameters increased with time for all tested bacteria. After this exponential phase the mean diameter increase rate remained low (stationary phase). Chitosan-based films without carvacrol were not efficient, since no significant differences appeared with respect to the control plates. The maximal radial growth of control samples after seven days was 9 mm, 6.5 mm, 6.2 mm and 9 mm for *B. subtilis*, *E. coli*, *L. innocua* and *S. Enteritidis*, respectively. For all tested microorganisms, after six hours exposure to AF1, AF3, AF4 and pure carvacrol vapours ( $1 \times 10^{-7} \text{ g}_{\text{carvacrol}}/\text{mL}_{\text{air}}$ ) colony diameters were significantly different (equal to zero) from the control samples (Fig. 10.2.).

**Table 10.2.** Cultivability (expressed as percentage of bacterial cells having reproduction ability, %) and inactivation ability of carvacrol in various chitosan-based antimicrobial films against *Bacillus subtilis* 168 BGSC 1A, *Escherichia coli* TG1 K12, *Listeria innocua* DSM 20649 and *Salmonella Enteritidis* CIP 81.3. Reported results are mean values ( $p < 0.05$ ) of the results obtained 7 days after exposure at  $t_0$  and  $t_1$ .

	<i>Bacillus subtilis</i> 168 BGSC 1A		<i>Escherichia coli</i> TG1 K12		<i>Listeria innocua</i> DSM 20649		<i>Salmonella</i> <i>Enteritidis</i> CIP 81.3	
	$t_0$	$t_1$	$t_0$	$t_1$	$t_0$	$t_1$	$t_0$	$t_1$
<b>Control</b>	100	100	100	100	100	100	100	100
<b>Pure carvacrol vapour</b>	0	0	0	0	0	0	0	0
<b>Chitosan film without aroma</b>	100	100	100	100	100	100	100	100
<b>AF 1</b>	0	0	0	0	0	0	0	16
<b>AF 2</b>	84	96	0	100	0	100	0	100
<b>AF 3</b>	0	0	0	0	0	0	0	84
<b>AF 4</b>	0	0	0	0	0	0	0	100
<b>AF 5</b>	100	100	100	63	100	100	100	100

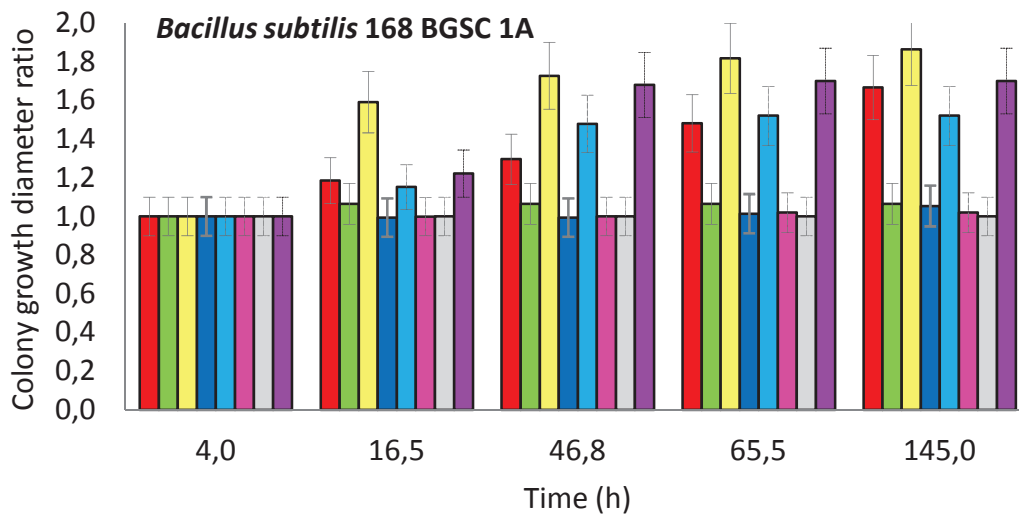
$t_0$  – the films and carvacrol were put in the Petri dish at the same time as the incubation started;  $t_1$  – the films and carvacrol were put in the Petri dish after the incubation started. Incubation time as described in Materials and methods.

Furthermore, after 7 days inactivation was observed (Table 10.2.) and statistically no significant differences could be seen among the active samples. These three films, AF1, AF3 and AF4, were then efficient to inhibit the growth of just inoculated *B. subtilis*, *E. coli*, *L. innocua* and *S. Enteritidis*. For AF2 *B. subtilis* diameter increased up to 7.6 mm (Figs. 10.1.a and 10.2.a) while for *E. coli* and *S. Enteritidis* no growth was observed. Furthermore, in *L. innocua* plates different pattern was noticed (Fig. 10.2.c). This strain has a particularly short lag phase and short generation time (results shown later) which could explain that carvacrol was less active on this strain at the beginning of exposure. Weissinger et al. (2001) found significantly greater influence for longer incubation periods (1h<7h). During first several hours, “the aroma compound had more time” to reach the headspace above the inoculated agar. Carvacrol entered and damaged microbial cells before they started to divide. Thus, films were active even at lower carvacrol concentrations. Indeed, it was reported that antimicrobial efficiency via headspace was obtained from the combined effect of direct vapour absorption on microorganisms and indirect effect through the medium that absorbed the vapour (Inouye et al., 2006). In the first six hours, AF2 presented a less marked antimicrobial efficiency (average colony size up to 5.6 mm). However accumulation of carvacrol vapour over time might lead later to a complete inactivation and reduction in cells cultivability (Fig. 10.2.c, Table 10.2).

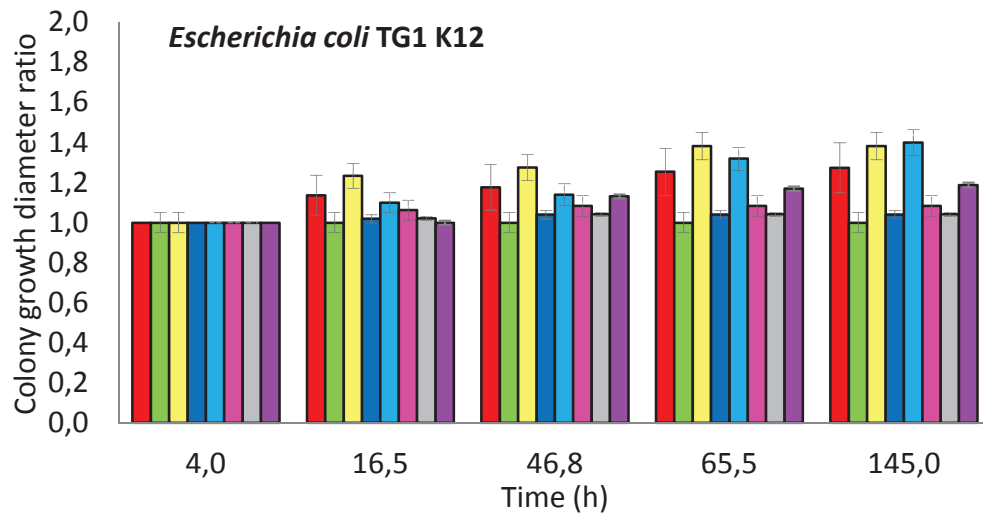
Film AF5 was not efficient against *E. coli*, *B. subtilis*, *L. innocua* and *S. Enteritidis*. Thus, for AF5, *B. subtilis* diameter increased up to 8.6 mm, *E. coli* up to 6.5 mm, *L. innocua* up to 6.2 mm and *S. Enteritidis* up to 9 mm (Figs. 10.1.b and 10.2.b-d). It was attributed to the low carvacrol concentration in the AF5 and low partitioning between the headspace and the film (Table 10.1.). López et al. (2007b) reported that polymer structure directly influenced the diffusion of carvacrol, thymol, and cinnamaldehyde during the first six hour through the polymeric matrix. As a conclusion for  $t_0$  samples, chitosan films with  $K_{mass}$  of  $10^{-4}$ ,  $10^{-6}$  and  $10^{-7}$  (AF1, AF3 and AF4, respectively) had antimicrobial efficiency against all tested microorganisms (*B. subtilis*, *E. coli*, *L. innocua* and *S. Enteritidis*). Moreover no significant differences were observed underneath pure carvacrol vapours and in the plates coated with these active films. AF2 exhibited efficiency against all the tested strains except *B. subtilis*, while AF5 was inefficient against all five tested microorganisms. Thus, the less marked antimicrobial effect was for the lowest  $K_{mass}$  ( $10^{-8}$ , AF5).

### 10.2.3. Chitosan/carvacrol film antimicrobial efficiency in the exponential phase of bacterial growth

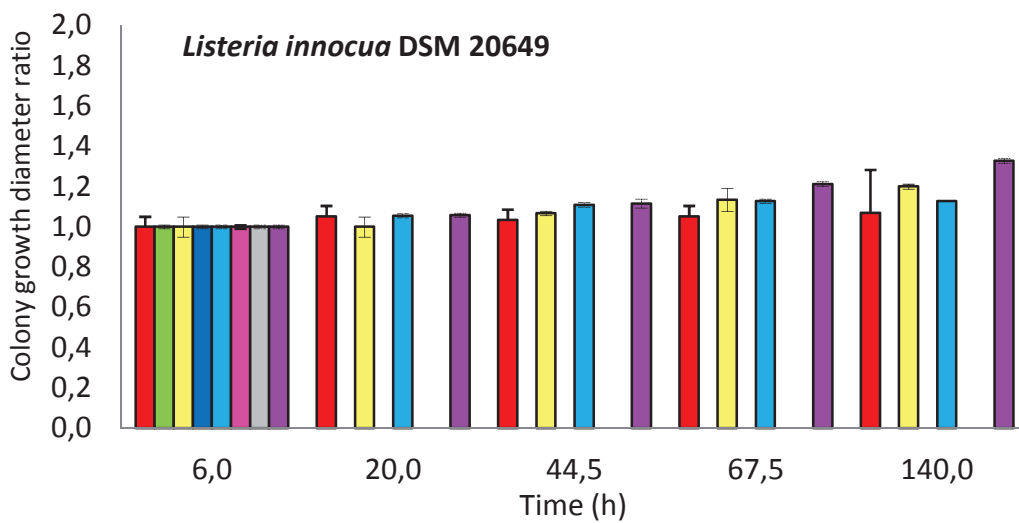
The results of antimicrobial efficiency at  $t_1$  are presented in Fig. 10.3. and Table 10.2. This second part of the study allowed estimating the efficiency of the antimicrobial films against bacteria in their exponential phase. Parameters concerning microorganisms such as inoculum sizes, bacteria physiological state and storage conditions (temperature, culture media and relative humidity) are important to explain the antimicrobial efficiency of both carvacrol and chitosan films (Lambert et al., 2001). Tests were performed when visible round colonies could be macroscopically observed (Fig. 10.1.). The growth curves for all tested strains were obtained in another experiment (data not shown). At  $t_1$  all bacteria were in exponential phase. To be active, antimicrobial has to damage bacterial cells before they start to divide. Then time delay for carvacrol to reach cells has to be shorter than their generation time. Generation times vary for different bacterial strains. So, at this experimental part, different film activities were observed for different bacteria. Fernandez-Saiz, et al. (2009) also reported that bacteria were more sensitive when inoculated in the mid-log phase. At the end of experiment, only pure carvacrol could maintain complete inhibition. Accordingly, as the most resistant, *S. Enteritidis* grew during the whole tested period, except after exposure to the pure carvacrol vapours when the growth was stopped (Fig. 10.3.d). Besides, *E. coli* was more sensitive than *S. Enteritidis*. For AF1 among tested bacteria only *S. Enteritidis* was not completely inactivated (16% cultivability) for AF1. Still it can be considered as efficient.



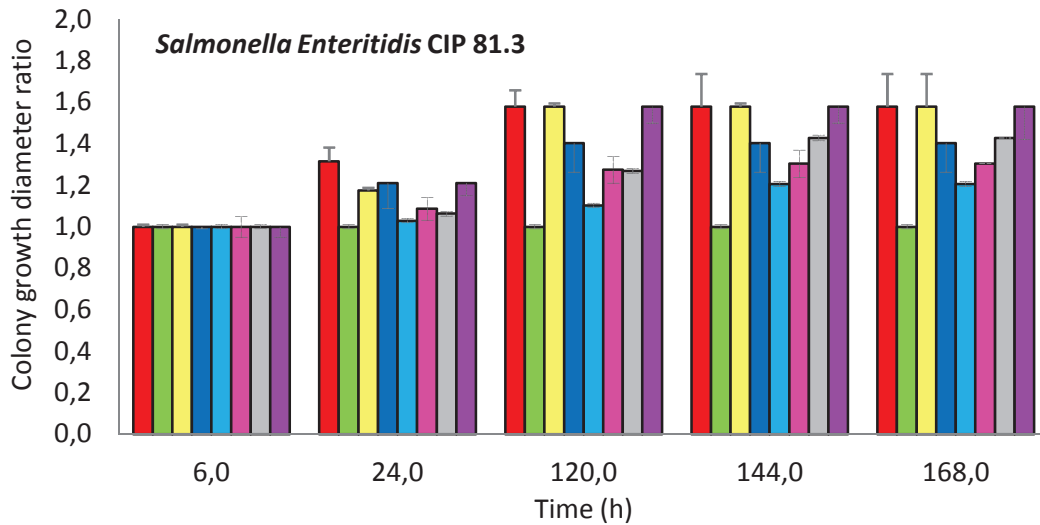
a)



b)



c)



d)

**Figure 10.3.** Average colony size diameter ratio of bacterial strains put in the vapour contact with five active chitosan-based films, control film and pure carvacrol vapours at  $t_1$  during seven days exposure of a) *Bacillus subtilis* 168 BGSC 1A; b) *Escherichia coli* TG1 K12; c) *Listeria innocua* DSM 20649; and d) *Salmonella Enteritidis* CIP 81.3.

$t_1$  - films or aroma compound were put in the Petri dish lid after an initial incubation phase of 4 h for *B. subtilis* and *E. coli* and 6 h for *S. Enteritidis* and *L. innocua*

■ microbial cells without treatment; ■ pure carvacrol vapour; ■ chitosan-based film without carvacrol; ■ AF1\* ; ■ AF2\* ; ■ AF3\* ; ■ AF4\* ; ■ AF5\* .

\* Film type definition and characteristics are given in Table 10.1.

Gram-negative bacteria tested are found to be more resistant to carvacrol than Gram-positives tested. This result is in accordance with the results of most works where the antimicrobial effect of essential oils and their components was studied (Lanciotti et al., 2003; Burt, 2004). This fact is attributed to the hydrophobicity of the lipopolysaccharides that are predominately contained in their outer membrane. However these results are not sufficient to conclude that carvacrol is more efficient against Gram-positive bacteria. As discussed by Burt (2004), in some studies no evidence for a difference in the sensitivity between Gram-negative and Gram-positive bacteria was found (Deans & Ritchie, 1987), whereas in other studies Gram-negatives appeared to be even more susceptible (Hao et al., 1998; Wan et al., 1998). Furthermore, even if the ability of carvacrol to permeabilize and to depolarize the cytoplasmic membrane is a sine qua non condition for antimicrobial activity, the mechanism of bacterial resistance to carvacrol does not only concern the cell envelopes. Indeed, Burt et al. (2007) first demonstrated that carvacrol induces production of HSP60 in *Escherichia coli* O157:H7 and more recently Ait-Ouazzou and

co-workers (2012) showed that genetic factors such as *rpoS* or *sigB* also influence the cell resistance to this antibacterial. For these reasons inter-specific but also intra-specific differences in the resistance of Gram-positive and Gram-negative bacteria can be observed.

According to Nebe-Von-Caron et al. (2000) cultivable cells require both metabolic activity and membrane integrity to reproduce themselves. Contrarily, even if they are alive, “viable but not cultivable cells” that are in an eclipsed state do not necessarily show their reproductive capacity on growth media. Attributed to its hydrophobicity, carvacrol was accumulated in the cells membranes. Hydrogen bonding modification of the membranes resulted in the cell death. When AF3 and AF4 were used, the inactivation of *B. subtilis*, *E. coli* and *L. innocua* was observed, while they had no significant effect against *S. Enteritidis* (Fig. 10.3. and Table 10.2.). In this experimental part, AF2 and AF5 films were not effective against all tested bacteria. From all results, minimal vapour inhibitory concentration in this study was considered as  $4.62 \times 10^{-8}$   $\text{g}_{\text{carvacrol}}/\text{mL}_{\text{air}}$  ( $K_{\text{mass}}=1.13 \times 10^{-6}$ ) for *B. subtilis*, *E. coli* and *L. innocua*,  $1.08 \times 10^{-7}$   $\text{g}_{\text{carvacrol}}/\text{mL}_{\text{air}}$  ( $K_{\text{mass}}=1.01 \times 10^{-4}$ ) for *S. Enteritidis*. Values reported in the present study are lower than previously reported. López et al. (2007b) found MIC for *L. monocytogenes* of  $2.13 \times 10^{-5}$   $\text{g}_{\text{carvacrol}}/\text{mL}_{\text{air}}$ . Authors observed significant antimicrobial effect of vapours of *Thymus vulgaris* ( $1.27 \times 10^{-5}$   $\text{g}_{\text{carvacrol}}/\text{mL}_{\text{air}}$ ) against several pathogenic bacteria, *L. monocytogenes*, *E. coli* and *S. Enteritidis* (Inouye et al., 2001; Nedorostova et al., 2009). Even though this essential oil had carvacrol as a principal component, significantly lower values in our study may be caused by the different methods used and possible different mode of action of complex essential oils and isolated compound.

### 10.3. Antimicrobial efficiency of chitosan based films against *Penicillium camemberti*

(unpublished part of this chapter)

The shelf life of different food products, especially sliced cheese and meat can be compromised by fungi. For example, cheese is a good substrate for the growth of certain adaptive fungal species due to its low pH, elevated salt concentration and low water activity (Pitt and Hocking, 1997). Molds can produce mycotoxins which have potential adverse health effects. In addition, they can cause an unsightly appearance, objectionable flavour and cause textural changes in food product. In addition to

Gram-positive and Gram-negative bacteria, it was also interesting to check the antimicrobial efficiency of carvacrol vapours against fungi. *Penicillium camemberti* was used as an example of fungi species.

In this study, the growth of fungal mycelium exposed to pure carvacrol in the vapour phase and to films containing this antimicrobial compound was monitored by macroscopic observations. Fig. 10.4. presents some pictures of the control and two chitosan-based films with carvacrol.

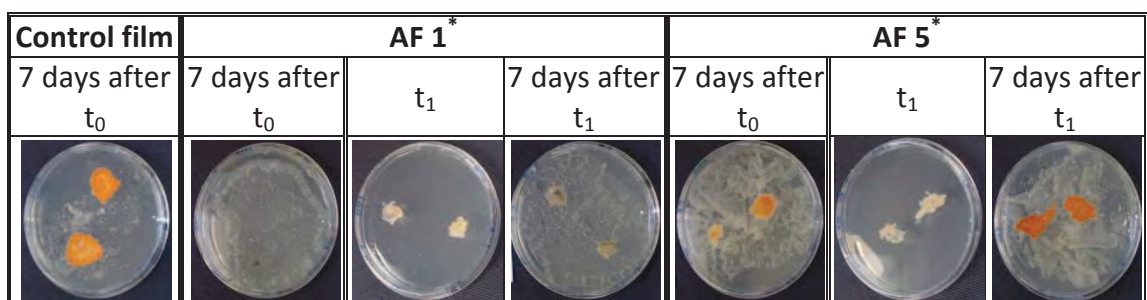


**Figure 10.4.** Photos of *Penicillium camemberti* DSM 1233 after the exposure to the vapour of two antimicrobial films AF1\* and AF5\* and control film (chitosan-based film without carvacrol).

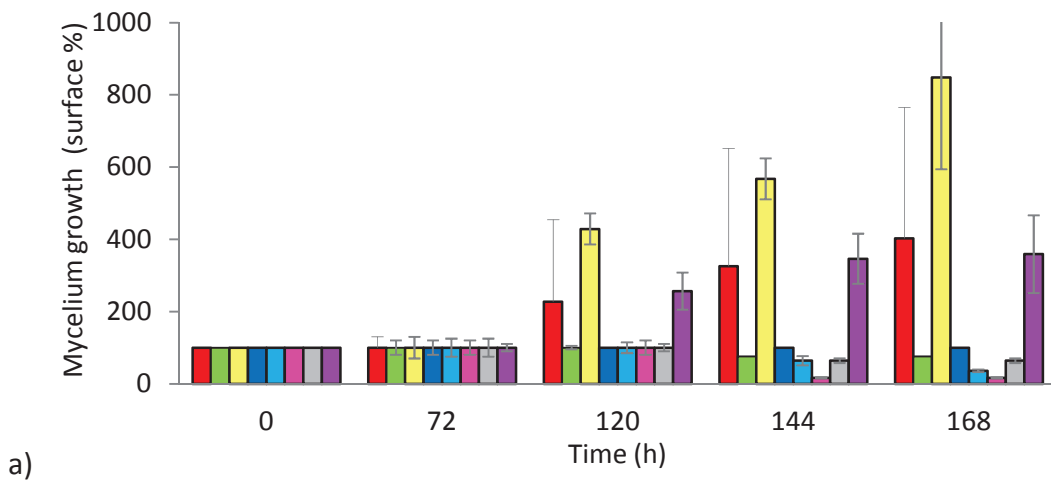
t<sub>0</sub> - start of the incubation; t<sub>1</sub> - microbial culture after an initial incubation phase of 48 h. Tested film\* was put in the vapour contact with the already grown fungus at t<sub>1</sub>.

\* Film type definition is given in Table 10.1.

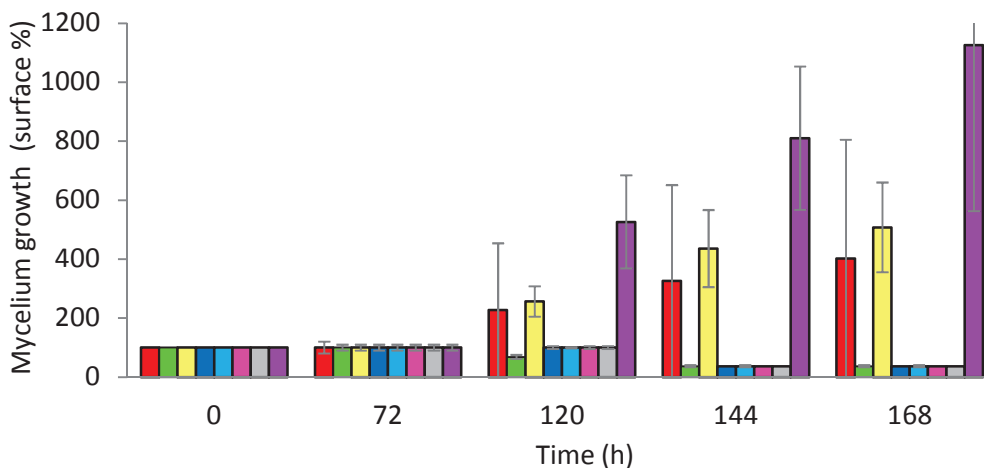
The antimicrobial effect of two films of the extreme  $K_{mass}$  (AF1 with the highest  $K_{mass}$  and AF5 with the lowest  $K_{mass}$ ) against *P. camemberti* is presented. It can be observed that the AF1, with the highest  $K_{mass}$ , was strongly efficient against *P. camemberti*. For all active samples, after 7 days exposure to carvacrol vapours, mycelia seemed to be completely destroyed. The inhibited molds had black colour contrary to the orange colour of living molds. This high antimicrobial activity was confirmed on already grown mycelium (t<sub>1</sub>) as shown on picture presented on the column four compared to the control (column one). AF1 film stopped the growth of *P. camemberti*, probably from the beginning of the antimicrobial exposure, since the mycelium size decreased and was black, as can be seen on the pictures presented on the columns three and four. Then only black colour biomass could be observed. However, the AF5, with the lowest  $K_{mass}$ , appeared not to be efficient. Therefore, the concentration of carvacrol released in the vapour phase from this film was too low to stop the growth of *P. camemberti*.

From the photos presented in Fig. 10.4. and others, mean mycelium surface was measured and it was taken into account in determination of antimicrobial efficiency (Fig. 10.5.).

The first part of the presented results gives the data about the experiments performed at  $t_0$  (inoculation and vapours exposition at the same time). Growth of *P. camemberti* was followed over 168 h. Only macroscopic observations were performed (Fig. 10.4.) and global aspect was taken into account. Inoculation was carried out by transferring a loopful of mycelium with fungal spores to agar plates. Then, the initial spore number and the initial mycelium size were not very well controlled. The lack of precision explains the differences between film without carvacrol and control (Fig. 10.5.). For all samples no visible changes were observed within the first 72 h. This was generally due to long growth dynamics for fungus species. After 144 h, the mycelium size decreased when exposed to AF1, AF2, AF3 and AF4, while samples with AF5 continued growing (Fig. 10.5.a). After 168 h, it reached the size more than five times bigger than at the beginning of the experiment which was coherent with control samples. In brief, for  $t_0$  samples, chitosan films with  $K_{\text{mass}}$  of  $10^{-4}$ ,  $10^{-6}$  and  $10^{-7}$  (AF1, AF2, AF3 and AF4, respectively) were efficient against *P. camemberti*.







b)

**Figure 10.5.** Inhibition of *Penicillium camemberti* DSM 1233 at a)  $t_0$  and b)  $t_1$ .

■ microbial cells without treatment; ■ pure carvacrol vapour; ■ chitosan-based film without carvacrol; ■ AF1\* ; ■ AF2\* ; ■ AF3\* ; ■ AF4\* ; ■ AF5\* .

$t_0$  - films or aroma compound were put in the Petri dish lid at the same time as the incubation started;  $t_1$  - films or aroma compound were put in the Petri dish lid after an initial incubation phase.

\* Film type definition and characteristics are given in Table 10.1.

In the second part, tests were performed when eye-visible orange/yellow mycelium could be macroscopically observed (Fig. 10.4.). When already grown *P. camemberti* was exposed to the active films vapours, mycelium size was significantly reduced for pure carvacrol vapours and AF1, AF2, AF3 and AF4, as compared to the control samples (Fig. 10.5.b). Control film without carvacrol and AF5 did not show any activity. The destruction of the fungal mycelium could be attributed to the carvacrol lipophilic nature (Rasooli et al., 2006). Among tested carvacrol containing films, only AF5 film with  $K_{mass} < 10^{-8}$  did not show any antifungal activity. Thus, the MIC of carvacrol vapour against *P. camemberti* determined in this study was about  $3.2 \times 10^{-8} \text{ g}_{\text{carvacrol}}/\text{mL}_{\text{air}}$ .

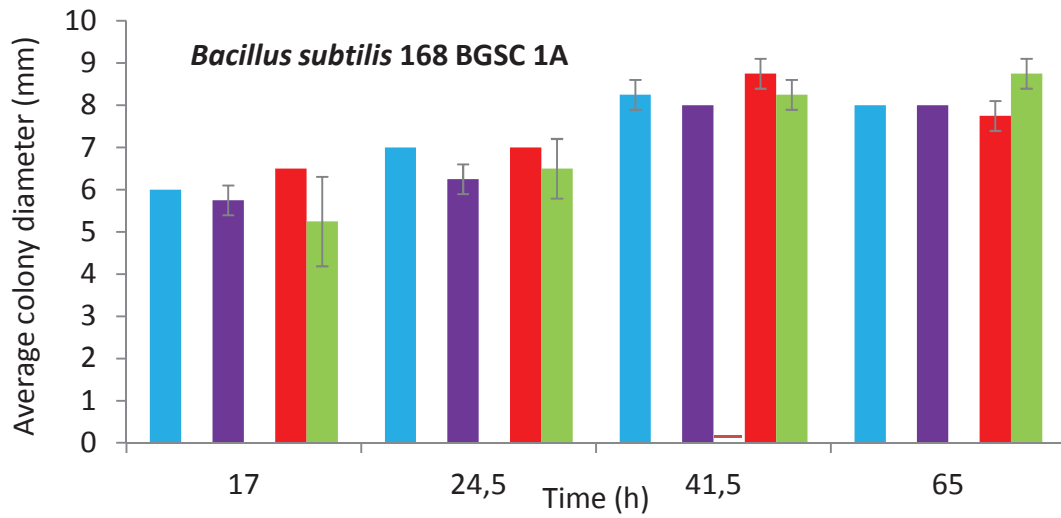
To summarize, chitosan based self standing films with carvacrol showed antimicrobial efficiency against tested Gram-positive, tested Gram-negative bacteria and tested fungus. The antimicrobial effect in the vapour phase could be controlled by mass partition coefficient as it determines the quantity of the carvacrol in the headspace. However, the efficiency is also dependent on the experimental conditions and processing parameters. Since application objective of this work is the packing of products using chitosan coated polyethylene, it was unavoidably important to test the antimicrobial efficiency of these systems.

#### 10.4. Antimicrobial efficiency of three chitosan coated polyethylene films with different concentrations of carvacrol in the vapour phase

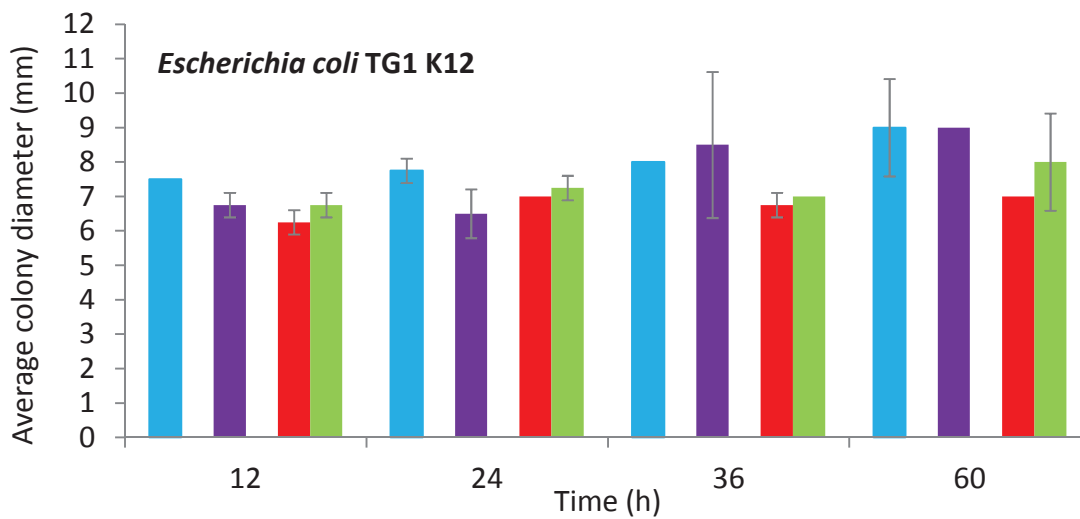
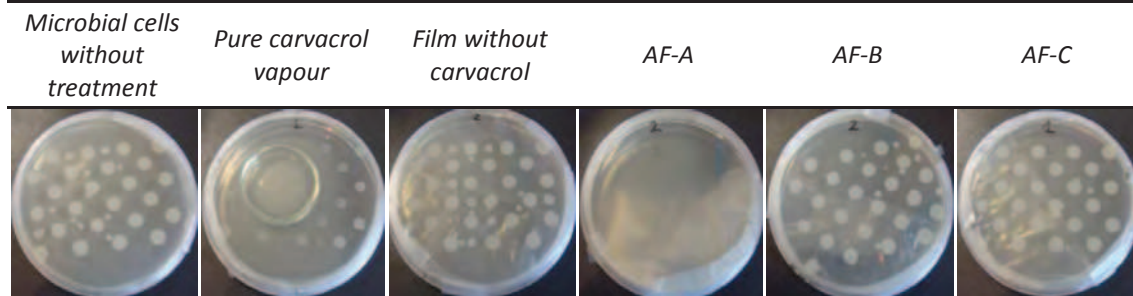
(unpublished part of this chapter)

Three chitosan coated polyethylene films with different concentrations of carvacrol in the vapour phase, AF-A ( $2.82 \times 10^{-7} \text{ g}_{\text{carvacrol}}/\text{mL}_{\text{air}}$ ), AF-B ( $4.44 \times 10^{-9} \text{ g}_{\text{carvacrol}}/\text{mL}_{\text{air}}$ ) and AF-C ( $2.58 \times 10^{-10} \text{ g}_{\text{carvacrol}}/\text{mL}_{\text{air}}$ ) were tested against *Bacillus subtilis*, *Escherichia coli*, *Lactobacillus plantarum* and *Penicillium camemberti*. These films were chosen because their vapour concentrations were close to the films used for the sensory evaluation (Chapter 11). That is to say that microbial cell was exposed to the vapours (atmosphere) above coated-film or pure carvacrol at the same time as the agar was inoculated. The average colony size diameter was followed during 65 h for *Bacillus subtilis*, 60 h for *Escherichia coli*, 70 h for *Lactobacillus plantarum* and 144 h for *Penicillium camemberti*.

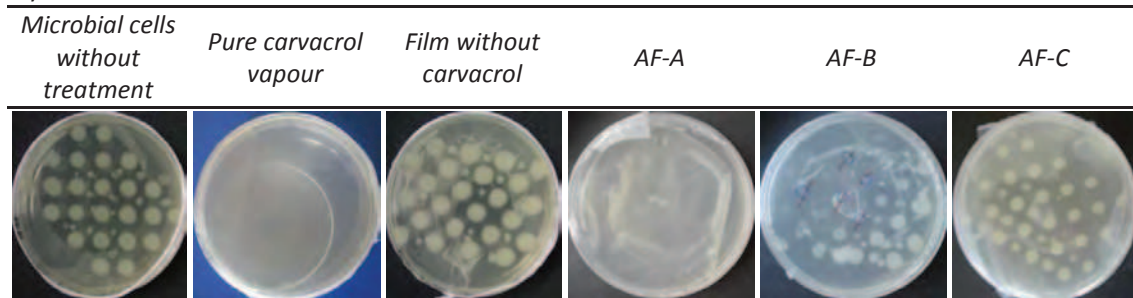
Average colony/mycelium size and photos of Petri dishes at the end of experiment are given in Fig. 10.6. The same behaviour was observed for all tested microorganisms. Differences in the average colony size diameter among different strains were due to the different development and formation of colonies for each bacterium. However, among the same species, no significant changes in control samples (film without aroma compound) with respect to control cells were observed. From the Fig. 10.6., it can be seen that in samples treated with pure carvacrol vapours and AF-A, no visible colonies were formed on the agar. Contrarily, in all other samples, round whitish colonies were developed. *Penicillium camemberti* was the less resistant (Fig. 10.6. h-j). For this fungus, along AF-A (highest concentration) and pure carvacrol vapours, AF-B film was also efficient. In these samples, only small black particles could be seen on the agar plates. These were probably residues of the biomass of the destroyed mycelium. In summary, among three tested films, only AF-A ( $2.82 \times 10^{-7} \text{ g}_{\text{carvacrol}}/\text{mL}_{\text{air}}$ ,  $K_{\text{mass}}=1.01 \times 10^{-5}$ ) was efficient against all four tested microorganisms. AF-B was efficient against *P. camemberti*, while AF-C did not show any effect. The concentration of carvacrol in the vapour phase is of  $2.82 \times 10^{-7} \text{ g}_{\text{carvacrol}}/\text{mL}_{\text{air}}$  could be considered close to the minimal vapour inhibitory concentration in this experiment that provoked antimicrobial effect for *E. coli*, *B. subtilis* and *L. plantarum*, and that of  $4.4 \times 10^{-9} \text{ g}_{\text{carvacrol}}/\text{mL}_{\text{air}}$  could be considered as the minimal vapour inhibitory concentration for *P. camemberti*.



a)



b)



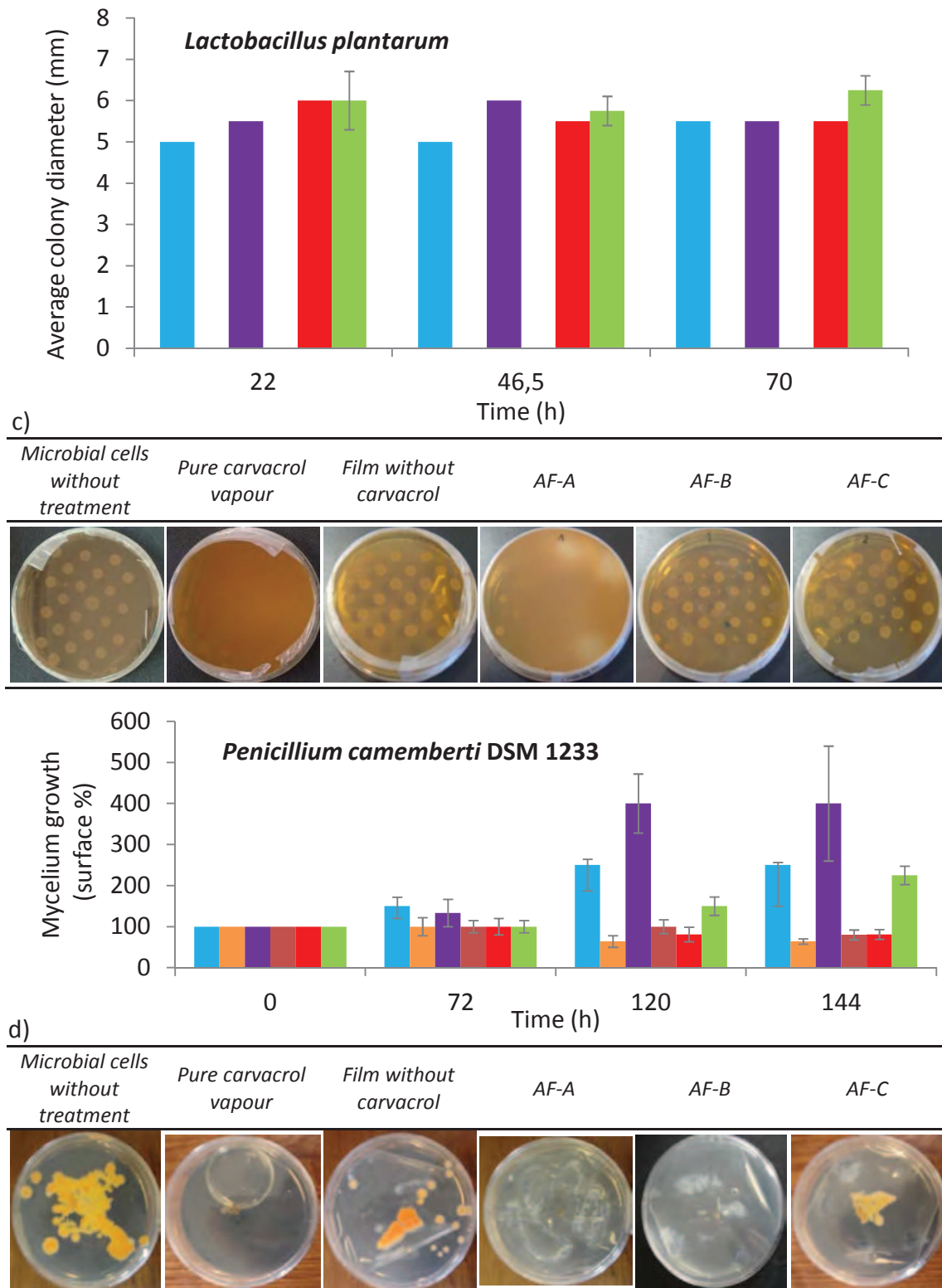


**Figure 10.6.** Antimicrobial efficiency of three chitosan coated polyethylene films against (a,b) *B. subtilis* 168 BGSC 1A, (c,d) *E. coli* TG1 K12, (e,f) *L. plantarum* and (g,h) *P. camemberti* DSM 1233. ■ untreated cells; ■ film without carvacrol; ■ pure carvacrol vapours ; ■ AF-A; ■ AF-B; ■ AF-C.

Chapter 10 only presents a small part of work done on microbiology aspects. A lot of other experiments and trials have been conducted in parallel and partially done by Ms. Moundanga (2012) from lab UMR-PAM-PMB. These complementary works deal with experimental parameters influencing antimicrobial efficiency of produced films and determination of minimal inhibitory concentrations in the vapour phase.

Parameters concerning microorganisms such as inoculums sizes, bacteria physiological state and storage conditions (temperature, culture media and relative humidity) are important to explain the antimicrobial activity of carvacrol and different chitosan films (Lambert et al., 2001). During the experiments, it was observed that the efficiency of both pure carvacrol vapours and those released from films were significantly affected by the distance from the testing sample in the Petri dish. This result is of key importance for the application, since the aim of developed films was the antimicrobial action by the vapour phase and not by diffusion within the product. Furthermore this pointed out that during packaging of a food product, packaging film with incorporated active compound should cover the whole surface above product. In real conditions, fluctuation in temperature and possible contamination of food products in food supply chain during opening/reclosing of the packaging may occur. Some other experiments and trials were then performed to verify the effect of temperature and inoculum size on antimicrobial efficiency of carvacrol vapours. This part greatly helps to determine and then to optimize the efficiency of the active packaging systems developed in this project. However, all the data are under confidentiality.

## **10.7. Conclusions of Chapter 10**

To summarize, antimicrobial efficiency of films varied as a function of both type of microorganisms and characteristics of the film matrix where carvacrol was included. The antimicrobial effect can be controlled by  $K_{mass}$ . Among five different active films that varied in composition, and consequently in the final carvacrol concentration in the film after drying, those with highest  $K_{mass}$  were the most active. From presented results, it can be seen that AF1 film ( $1.08 \times 10^{-7} \text{ g}_{carvacrol}/\text{mL}_{air}$ ) exhibits antimicrobial effect against all tested microorganisms both during their latent and exponential phase. AF3 ( $4.62 \times 10^{-8} \text{ g}_{carvacrol}/\text{mL}_{air}$ ) and AF4 ( $6.41 \times 10^{-8} \text{ g}_{carvacrol}/\text{mL}_{air}$ ) films had also strong antimicrobial effect at  $t_0$  and  $t_1$  except for *S. Enteritidis* that was the most resistant bacterium. AF2 film was efficient at  $t_0$  but not at  $t_1$ . AF5 film ( $6.28 \times 10^{-9} \text{ g}_{carvacrol}/\text{mL}_{air}$ ) did not exhibit any antimicrobial effect against *E. coli*,

*B. subtilis*, *L. innocua*, *S. Enteritidis* and *P. camemberti*, both at  $t_0$  and  $t_1$ . Even though the antimicrobial mechanisms are not fully understood, active compounds are thought to exert their effect during the lag phase. This can explain better antimicrobial efficiency and lower inhibitory concentrations for those samples exposed to vapours as soon as they were inoculated ( $t_0$ ). The antimicrobial tests and observations permitted a comparison of the bioactive potential of chitosan films and examination of relationship between the antimicrobial activity and mass partition coefficient ( $K_{\text{mass}}$ ).

Chitosan based films and coatings on polyethylene used in a vapour phase showed potential to inhibit the development of different microorganisms. However, the effect of the background on the inhibition of microbes is in dispute. This could be due to the fact that much of this knowledge is derived from laboratory media simulating the unique conditions of a “real” environment in which there is diversity among microbes, as well as changes impact on their physiological status or concentration level of contaminations or synergistic effect with food components such as salt. Depending on the concentration, carvacrol vapours are efficient against large spectrum of microbes. However, these concentrations should be better studied and evaluated in real food products. Moreover, by synergistic action of different compounds it could be possible to reduce the concentrations needed to stop the microbial proliferation. Additive effects between the antimicrobials and their use in the vapour phase may permit the use of relatively low amounts of each antimicrobial and thereby reduce cost of the antimicrobial treatment while improving the antimicrobial efficiency.

Following the microbial approach in this study, the next chapter focuses on the sensory analysis of food packed with different chitosan coated polyethylene films to assess the organoleptic impact.



*Chapter 11*

*Application of carvacrol as active compound on  
real food products: Validation of sensory impact*

---

---

Publication: **Mia Kurek**, Anne Endrizzi, Jean Marie Delaitre, Kata Galić & Frédéric Debeaufort

Journal of Food Technology, Biotechnology and Nutrition, will be submitted





### **11.1. Impact of essential oils on organoleptic properties of packaged food products**

Quality of food product is a complex issue. Sensory properties are the most apparent to the consumers, so the majority of consumer complaints relates directly to sensory quality failures. In contrast to the large amount of information on the effectiveness of films and coatings containing essential oils against a wide spectrum of microorganisms, little is known about their possible impact on organoleptic food properties. The major drawback is their strong flavour, which could change the original taste of foods. Understanding of the sensory impacts due to interactions between food and packaging materials can lead to innovations in quality and to increase shelf-life of food systems. Thus, sensory evaluation of real food products packed with antimicrobial films should be performed.

Sensory impact from food packaging interactions is probably more prevalent than acknowledged. Sensory evaluation has been defined as a scientific method used to evoke, measure, analyze and interpret those responses to products as perceived through the senses of sight, smell, touch, taste, and hearing (Stone and Sidel, 1993). This definition has been accepted and authorised by sensory evaluation committees within various professional organizations such as the Institute of Food Technologists.

In the previous chapter, use of carvacrol as antimicrobial agent in food preservation has been assessed. Due to specific taint, essential oils containing carvacrol are used as flavour ingredients, seasonings in food preparations, in perfumery, in pharmaceuticals and cosmetics while preserving capabilities, potential health benefits, antioxidant activity, and antimicrobial effects (Burt, 2004). Carvacrol is approved food additive, particularly as flavouring agent, in Europe ((EC) No 1334/2008) and USA (FDA CFR - Code of Federal Regulations Title 21) and is included in the European Union list of flavouring substances ((EC) No 2232/96 and Commission Decision 1999/217/EC). The regulatory status of thyme, oregano and their phenolic constituents suggest minimal safety concerns when used as food antimicrobial. Cinnamaldehyde, carvacrol, carvone and thymol appear to have no significant or marginal effects in vivo whilst in vitro they exhibit mild to moderate toxic effects at the cellular level. Genotoxicity data appear not to raise concern in view of the present levels of use (Stammati et al., 1999). However, some essential oils and their components can cause allergic contact dermatitis in people who use them frequently. So, preventive measures may be needed if these substances were to be used on a larger scale (Carson and Riley, 2001).

The concentration of oregano oil in food applications varies from about 320 to 3200 ppm (Tucker and Maciarelo, 1994). In practice, carvacrol is added to different products, e.g., baked goods (15.75 ppm), non alcoholic beverages (28.54 ppm/0.18 mM), and chewing gum (8.42 ppm) (Fenaroli, 1995). Thymol, an isomer of carvacrol, is generally used for flavouring purposes in food and beverages at levels of 5-78 ppm (Burdock, 2005).

Up to date, no many consumer acceptance tests or other sensory studies have been published on jambon blanc (ham), feta cheese, jambon persillé (parsley ham), terrine or paté en croute (meat paté pie) packed with antimicrobial films. However, sensory studies have been conducted on related food products and antimicrobial films containing some natural antimicrobials. Foods generally associated with herbs, spices or seasonings would be the least affected by non wanted flavouring phenomenon (Burt, 2004). As it is not always evident to find a literature data on sensory analysis of food products treated with carvacrol, the collected data both for pure carvacrol as well as for essential oils where carvacrol is the main component are given in Table 11.1.

For example, the flavour of beef fillets treated with 0.8% v/w oregano oil was found to be acceptable after 15 days storage at 5°C and cooking (Tsigarada et al., 2000). According to Ultee and others (2000), carvacrol is capable of inhibiting *B. cereus* in soup, but at an approximately 50-fold higher concentration than needed to reach the same effect as in broth. On fish, carvacrol is said to produce a 'warmly pungent' aroma; citral was 'lemon-like' and geraniol 'rose-like' (Kim et al., 1995). Thyme and oregano oils, spread on whole asian sea bass at 0.05% (v/v), also imparted a herbal odour, which became more pronounced after 33 days storage at 0-2°C (Harpaz et al., 2003). Similar concentrations, however, may be less acceptable in other foods (Burt and Reinders, 2003). For example, the incorporation of thyme oil (1.8%) as an antimicrobial coating for pre-cooked shrimps reduced the acceptability scores for taste and odour (Ouattara et al., 2001).

Roller and Seedhar (2002) demonstrated that carvacrol and cinnamic acid were effective in reducing and inhibiting microbial growth on fresh cut kiwi fruit and honeydew melon, respectively, without determinable sensory effects. However, it has been mentioned that carvacrol rapidly reduced acceptability of fresh-cut jalapeno peppers and carvacrol treated samples had the lowest shelf life (Ruiz-Cruz et al., 2010).

**Table 11.1.** Collected data on sensory impact of carvacrol and carvacrol containing essential oils in different food products. The upper part of a table gives the acceptable scores, while the lower part gives literature data for unacceptable sensory score.

Active compound	Food product	Sensory note	Reference
Oregano oil (0.8% v/w)	Beef fillets	Acceptable	Tsigarida et al., 2000
Oregano oil (1% v/w)	Minced beef	Undetectable	Skandamis and Nychas, 2001
Thyme and oregano oils 0.05% (v/v)	Asian sea bass	Herbal odour	Harpaz et al., 2003
Oregano oils (1%)	Ready-to-eat soups	Acceptable	Ultee and Smid, 2001
Oregano oil (0.05% v/w)	Cod fillets	Pleasant effect	Mejlholm and Dalgaard, 2002
Carvacrol (250 ppm)	Lettuce	Acceptable	Gutierrez et al., 2009a
Carvacrol (150 ppm)	Carrot broth	Acceptable	Valero and Giner, 2006
Carvacrol (3%)	Fish	Warmly pungent	Kim et al., 1995
Thyme oil (1.8%)	Pre-cooked shrimps	Changes in appearance, odour and taste	Ouattara et al., 2001
Carvacrol (5–15 mM)	Fresh cut kiwi fruit Honeydew melon	Adverse sensory consequences	Roller and Seedhar, 2002
Carvacrol (2.5 mM)	Fresh-cut jalapeno peppers	Strong negative effect	Ruiz-Cruz et al., 2010
Thyme oil (1%)	Chopped bell peppers	Adverse sensory properties	Uyttendaele et al., 2004
Carvacrol (2.5µL/mL)	Vegetable broth	„Like slightly" "neither like nor dislike“	Sousa et al., 2012

Sousa et al. (2012) determined influence of carvacrol and 1,8-cineole on the sensory characteristics of vegetables. Sensory evaluation revealed that scores of the most-evaluated attributes felt between "like slightly" and "neither like nor dislike." As application of carvacrol and 1,8-cineole in vegetable broth caused a significant decrease ( $p < 0.05$ ) in bacterial count over 24 h, the combination of carvacrol and 1,8-cineole at sub-inhibitory concentrations could constitute an interesting approach to sanitizing minimally processed vegetables.

Linalool and methycavicol have been embedded in LDPE to test both the antimicrobial effects of as well as sensory impacts on wrapped cubed Cheddar cheese over 6 weeks of storage at 4°C (Suppakul et al., 2008). Linalool embedded in LDPE did not impact flavour of the cheddar cheese over 6 week storage as panellists could not

detect the difference between cheeses stored in LDPE or linalool/LDPE. While the microbial shelf life of cheese was improved with use of methylcavicol as compared to linalool, the sensory effects were noticeable with the use of this compound illustrating the potential for reducing the commercial success of the antimicrobial material.

This chapter focuses on the sensory evaluation and potential for the application of chitosan/carvacrol coated polyethylene on five typical Burgundy food products. The sensory evaluation of: ham-jambon blanc, jellied ham with parsley - "jambon persillé", "paté en croute"- meat paté pie, "terrine" and feta cheese were performed. It was aimed to identify whether a sensory difference, if any, has resulted from the active packaging treatments and how panellists detected and described the difference.

### **11.2. Effect of carvacrol/chitosan coated polyethylene on sensory quality of "jambon blanc", „jambon persillé“, „paté en croute“, „terrine“ and feta cheese**

A sensory test was conducted to determine if the application of activated chitosan coated polyethylene films causes a difference in odour and overall acceptability of real food. Better understanding of the odour thresholds of antimicrobial agents has a great importance in order to assess the possibility of using active packaging treatments in preservation of cheese and meat products. Tested fresh food products had high water activity ( $a_w > 0.97$ ), and therefore they could change the atmospheric conditions inside the packaging. Consequently the release mechanism from packaging material significantly changed. Moreover, food with high protein and lipid content are good aroma supports and able to absorb flavour compounds.

Characteristics of active packaging films used in sensory evaluation are given in Table 11.2. Depending on the carvacrol concentration, carvacrol activated chitosan coated polyethylene films were classified as AF1, AF2 and AF3. The carvacrol in the vapour and carvacrol incorporated in chitosan matrix was in following order AF1>AF2>AF3.

**Table 11.2.** Characteristics of three active packaging films used in sensory evaluation.

	AF1	AF2	AF3
Film forming solution (w/v)	0.35	0.035	0.0035
Aroma quantity in dry film ( $\text{mg}_{\text{cvc}}/\text{g}_{\text{film}}$ )	4.78	0.270	0.023
Headspace ( $\times 10^{-2} \mu\text{g}_{\text{cvc}}/\text{mL}_{\text{air}}$ )	6.53	0.727	0.0538
$K_{\text{mass}} (\times 10^{-5})$	1.15	2.27	1.95

Sensory analysis based on a series of triangle tests was conducted to discriminate the products packed in different active films. This was carried out to determine the lowest level of carvacrol that could be detected by panellists.

Parallel to the sensory evaluation, the quantification of carvacrol as the active compound in both films and products was performed (Fig. 11.1.).

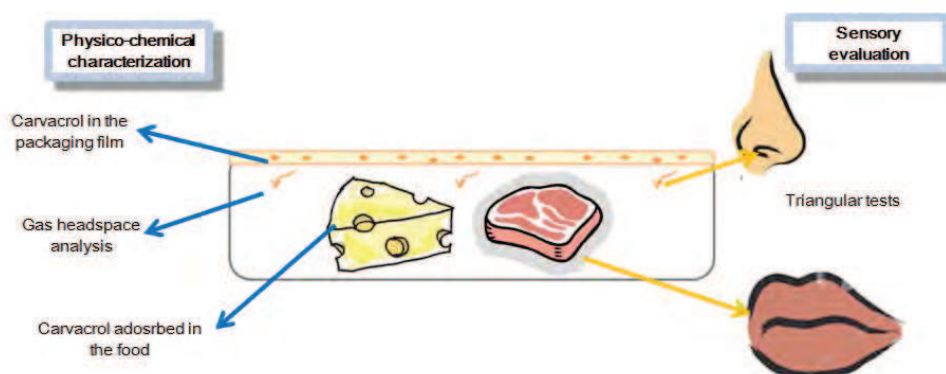


**Figure 11.1.** Schematic view of tests performed in order to characterize the influence of active films on organoleptic impact in food products.

Presence of carvacrol was tested in the headspace, in the films before and after products conditioning (Fig. 11.2.), and finally in the product itself (Fig. 11.3.)

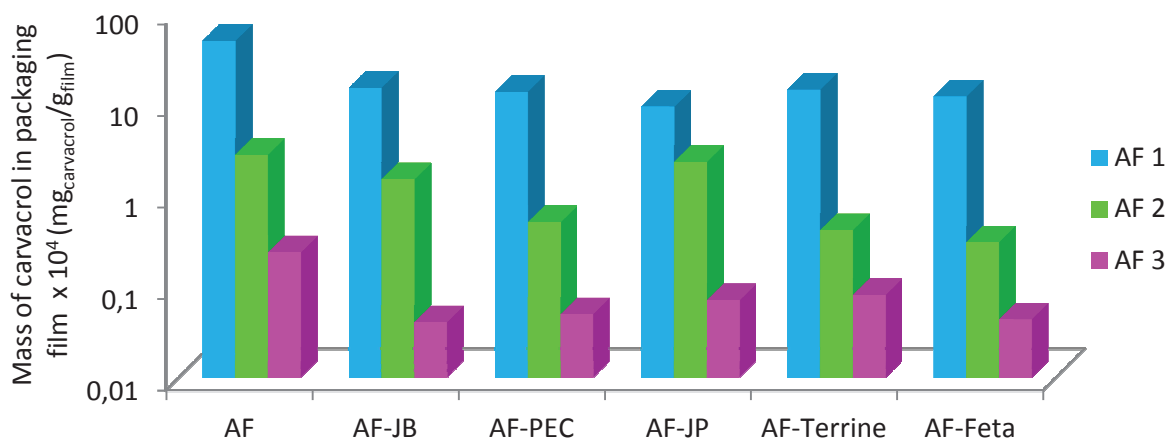


**Figure 11.2.** Mass of carvacrol in different films after 15 days of storage of ham, “paté en croûte”, “jambon persillé”, “terrine” and feta cheese.

AF=active film; AF-JB=active film in which ham was packed; AF-PEC=active film in which Paté en croûte was packed; AF-JP=active film in which “jambon persillé” was packed; AF-Terrine=active film in which terrine was packed; AF-Feta=active film in which feta cheese was packed.

The results of remaining concentrations in three packaging films tested after the application with ham, “paté en croûte”, “jambon persillé”, “terrine” and feta cheese are given in Fig. 11.2. During storage, carvacrol was significantly released from packaging films. Concentrations that remained in the films after conditioning were approximately ten times lower than at the beginning of the evaluation.

Since carvacrol has its own characteristic flavour and interactions among the compounds it may generate unique flavours and impact sensory attributes of packed foodstuff. Some amounts of carvacrol were sorbed by food product. Depending on the concentration in the vapour phase and on the product composition, different amounts of carvacrol were found after the extraction (Fig. 11.3.). This could be attributed to different diffusion rates and to the repartition of carvacrol in the samples. Indeed, Han (2005) reported that variable activity in foods due to interactions of essential oils with food components occur and then limit their use.

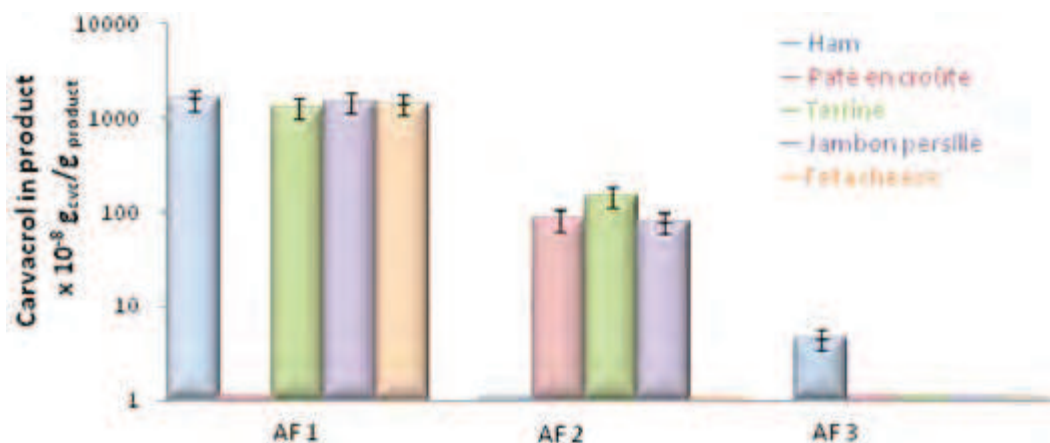


**Figure 11.3.** The amounts of carvacrol found in food products after the storage in three different active films.

Tests of differences were used to determine, whether or not, a difference in some specific attribute exists between two samples, or to determine if one sample is preferred to another. These types of tests are the simplest and the most sensitive tests that can be used. However, they cannot tell us anything about how large the difference is or how great the preference between the samples is. In order to better understand how the panellists perceived the differences in the products; a sensory evaluation based on quantitative descriptive analysis was also carried out.

When high concentrations of natural active agents are incorporated in films, the film may have a strong flavour due to the incorporated active agents (Han et al., 2005). The odour and taste thresholds of carvacrol were determined in order to assess the possibility of detecting these attributes at low concentrations by the panellists. The detection odour thresholds are summarized in Table 11.3. For a products packed in AF1, intensive odour was detected immediately after opening the packages, which disappeared a few time after because of the evaporation at room temperature. On the contrary, for AF2 and AF3 packages, after their opening, no significant differences have been attributed to carvacrol in the product atmosphere.

After smelling the product, some panellists perceived the presence of carvacrol for all tested concentrations (AF1, AF2 and AF3) (Fig. 11.4.). Statistically, some significant differences between active packaging and control films were found only for AF1 packed products. This was the highest concentration tested. The same observation was for all packed products. Then, the odour threshold in the product was determined to be around 15 ppm.



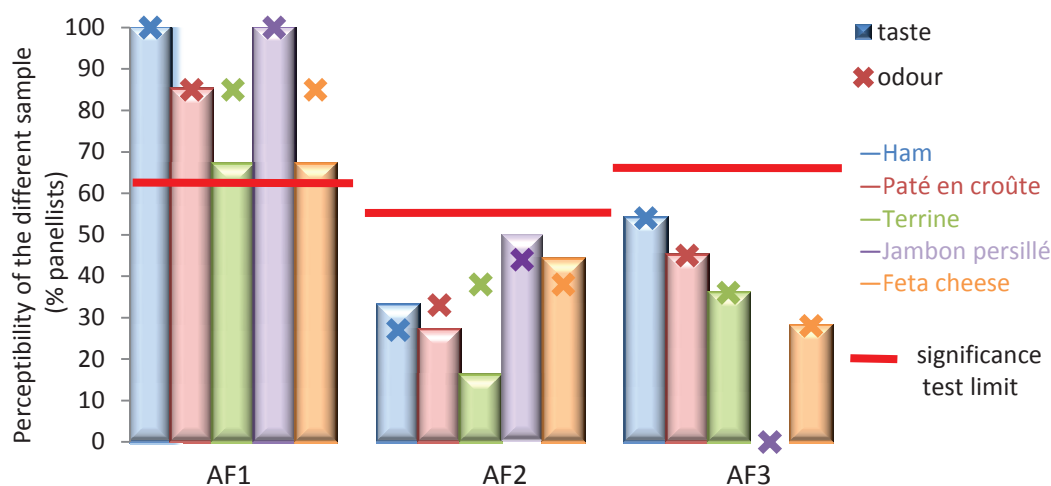


**Figure 11.4.** Results from taste and odour triangle test of five products packed in three packaging materials with different concentration of carvacrol (AF1, AF2, AF3). The significance limit is based on a difference tests ( $\alpha$  risk of 5%).

The detected odour thresholds reported in this study are different from odour thresholds published in the literature (Table 11.3.). Actually, threshold values suffer from lack of reproducibility due to differences in methodology and training of panellists.

**Table 11.3.** Odour thresholds of carvacrol.

	Detected odour threshold (ppm)		Reference
	This study	literature	
In the packaging headspace	65.3	2.29	Burdock, 2005
After smelling the product	15.9	124	Bitar et al., 2008

After tasting the products packed in AF1, which was the system with the highest carvacrol concentration, persistence of characteristic aroma was detected (Fig. 11.4.). Already after 3 days of storage, the strong impact on taste and smell was detected for ham and ham with parsley. Only weak, but still significant differences were seen on the “paté en croûte” and feta cheese. For “terrine”, the differences were more easily perceived by smell than taste. General description remarks were recognition of oregano taint and hot/spicy taste. Finally, both taste and odour descriptors were fairly above significance limit.

For AF2 and AF3 packaging, the overall scores were better than in AF1 and below the significant detection level (Fig. 11.4.). To better understand “unpleasantness” detected by panellists who answered correctly, descriptive analysis was performed and comments are summarized in the Tables 11.4. and 11.5.

**Table 11.4.** Odour and taste descriptors after triangle tests performed with AF2 after 3 and 15 days of storage.

ACTIVE PACKAGING			CONTROL FILM		
day	odour	taste	odour	taste	
jambon blanc	3	ND	„stronger“, „less strong“	ND	
	15	„somewhat different“	„fresh“, „stronger“	„less salty“, „firmer“	
„paté en croûte“	3	ND	„more intense“	„more intense flavour“	
	15	„less pronounced“	„less strong“	ND	
„jambon persillé“	3	ND	„less intense“	ND	
	15	„more pronounced product“, „irritating“	„parsley less pronounced“, „slightly spicy“	„less juicy“, „less taste“, „parsley less pronounced“	
„terriner“	3	„more pronounced“	„cooler“, „less spicy“	„normal“, „unflavoured“, „firmer“, „pretty bland“, „less salty“	
	15	ND	„smell of a meat“	„more bland product“, „fresher taste“	
Feta	3	„more odour“, „more neutral“	ND	„less strong“	
	15	„spicy“, „less sweet“	„less pronounced“, „pungent“	„less pronounced“, „sweet“	

ND=not described/detected by panellists

**Table 11.5.** Odour and taste descriptors after triangle tests performed with AF3 after 3 and 15 days of storage.

ACTIVE PACKAGING			CONTROL FILM		
day	odour	taste	odour	taste	
jambon blanc	3	ND	ND	ND	
	15	„stronger smell“	„saltier“	„firmer“, „less salty“	
„paté en croûte“	3	ND	ND	ND	
	15	ND	„less firmly“, „less salty“	„different taste“	
„jambon persillé“	3	ND	ND	ND	
	15	ND	ND	ND	
„terriner“	3	ND	„slightly different smell“	ND	
	15	ND	ND	ND	
feta	3	ND	ND	ND	
	15	ND	„salty“, „more neutral“	ND	

ND=not described/detected by panellists

Both after 3 and 15 days, the odour differences for AF2 were not significant. To confirm it, more panellists should be involved. After 15 days, all products repacked in active packaging and in the control package were similar. Moreover, within the same samples, some contradictory answers were found. For example, for a ham at the same time “less pronounced” and “more pronounced” odour descriptions are given. Similarly, no significant differences in taste were found both after 3 and 15 days. To conclude, recognition of carvacrol in both odour and taste was below the significance level (Fig. 11.5.)

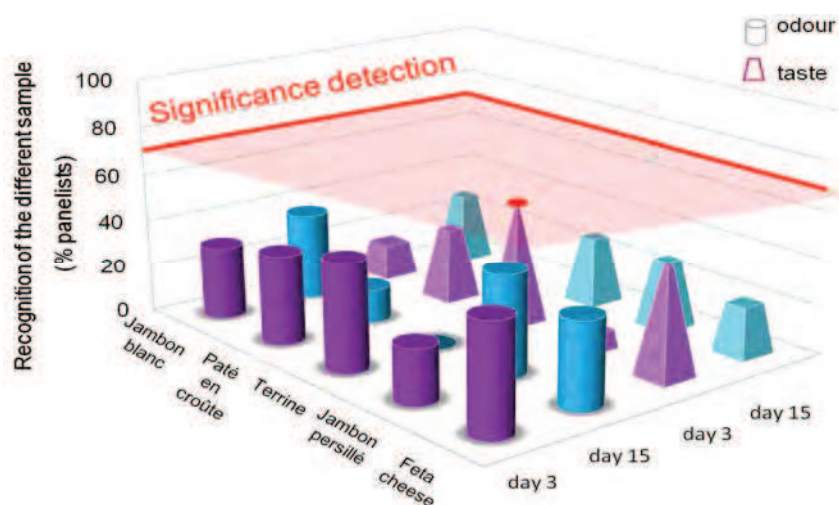


**Figure 11.5.** Changes in odour and taste of different product packed in chitosan coated AF2 after sensory evaluation. Obtained values are result of triangular test with  $\alpha = 5\%$ .

For the lowest concentration of carvacrol in packaging films (AF3), no significant differences in odour and taste could be detected. Even that these concentrations are lower than that required for antimicrobial efficiency, the understanding of the odour and of the taste thresholds in food products is of a great merit. However, it implies the complementarities between the antimicrobial efficiency and sensory impact in real food products and points out a great interest for future research.

### 11.3. Conclusions of Chapter 11

Sensory analysis based on a triangle test helps to differentiate between the products packaged in active packaging films containing higher concentrations of carvacrol from those packaged in control films. It was previously reported that the

required levels for essential oils and their constituents to maintain an antimicrobial effect in food products are usually higher than the amount used in flavouring applications. So, they may result in adverse sensorial effects (Bagamboula et al., 2004; Smith-Palmer et al., 2001). However, activated bio-based coatings can be an interesting application in packaging sector.

The addition of higher concentrations of carvacrol clearly imparted a noticeable odour and taste to products during storage. In Chapter 10 only higher levels of carvacrol were shown to be effective against different spectrum of microorganisms. However in this chapter, it was not compatible with packed meat and cheese products.

Maximally absorbed concentration of carvacrol that was significantly detected by panellists in different products was about 15 ppm. This corresponds to around 65 ppm in the headspace. When the concentration in the headspace dropped ten times, detection ability approached the limit values for “paté en croûte” and “jambon persillé”. This could be due to the odour detection thresholds that were shaped by the molecular architecture of chemical stimuli (Bitar et al., 2008). For carvacrol concentrations less than 7 ppm, no significant changes in organoleptic properties were found.

Sensory studies associated with antimicrobial tests can provide the information required for getting the best new active material. Nowadays, sensory evaluation becomes a tool irreplaceable in food industry while interacting with the key sectors in food production. To overcome organoleptic impact of carvacrol, further investigations can follow some literature approaches. For example, Bagamboula et al. (2004) suggested that the strong aroma associated with essential oils and their compounds could be reduced by the use of de-aromatization methods. Particular essential oil could be replaced with its principal constituents that may be equally antimicrobial effective but with milder flavouring attributes (Lambert et al., 2001; Smith-Palmer et al., 2001). The addition of a flavourless additive to the essential oil mixture can increase the antimicrobial efficacy and enable a lower essential oil concentration to be used (Burt and Reinders, 2003; Mejlholm and Dalgaard, 2002). Furthermore, Gutierrez et al. (2009) suggested that combinations of essential oils can minimize application of higher concentrations by synergism of compounds. Consequently, any adverse sensory impact in food will be reduced. Additionally, microencapsulation process can be used. In these systems, active compounds can be trapped and their odour and flavour will be masked until they will be slowly released into the atmosphere at constant low doses. However in this case, slowed release would also impact the antimicrobial effect. This

technique must be taken with precaution and an additional antimicrobial test should be performed.

To overcome the barrier between the antimicrobial effectiveness of new packaging systems with natural antimicrobial compounds, and their efficacy in the real food systems, further researches and investigations on larger industrial scales are needed and envisaged.

*Chapter 12*  
*Overall conclusions and perspectives*

---



Research on bio-based materials that have been forgotten for decades in favour of those derived from petrochemicals has steadily increased in recent years. On one hand, awareness of environmental risks and the depletion of oil resources have increased the value of research on agricultural resources. On the other hand, consumers' awareness for new, natural, chemically free products with increased food shelf life are main issues that the food industry is fighting with on daily level. It is within this context that this research was focused on the validation of chitosan, carbohydrate polymer, as a bio-based material for food packaging applications. More specifically, the food industry is addressing the issue by gradually incorporating natural essential oils into food/headspace/packaging to replace the more traditionally used synthetic chemical preservatives. In order to make for both food and packaging change from the use of synthetic sources to purely natural sources, this research is focussed to the optimization of film processing, the use of hurdle technology, the release systems, the functional and barrier properties, the limits of antimicrobial activity, the most effective concentration and the validation of active compound on the real food products. While literature research provides knowledge about antimicrobial activity of materials in direct contact with a food product, there are still many areas where information is lacking. In particular links between structure, function and active compound released in a headspace are rarely made.

This work contributes to a better understanding of the mass transfers from and through packaging material. It aimed to correlate involved mechanisms and factors, a prerequisite for its application, as described in Fig. 12.1. During this study, the focus was made on the analysis of transfer mechanisms through material and identification of parameters that are crucial at different scales, from macroscopic to molecular investigations. Incorporated substances may affect the physical properties, processability and applicability of the packaging material. So performance of packaging materials must be maintained after addition of active compounds.

Composition parameters, film structure and film production in relation to its functional properties was assessed. First, it was necessary to characterize the film forming materials that were aimed to be the support matrix for carvacrol used as the model active/antimicrobial compound. Importance of chitosan film design was pointed out. Drying procedure, optimization of formulations and production of bio-based chitosan films was performed.



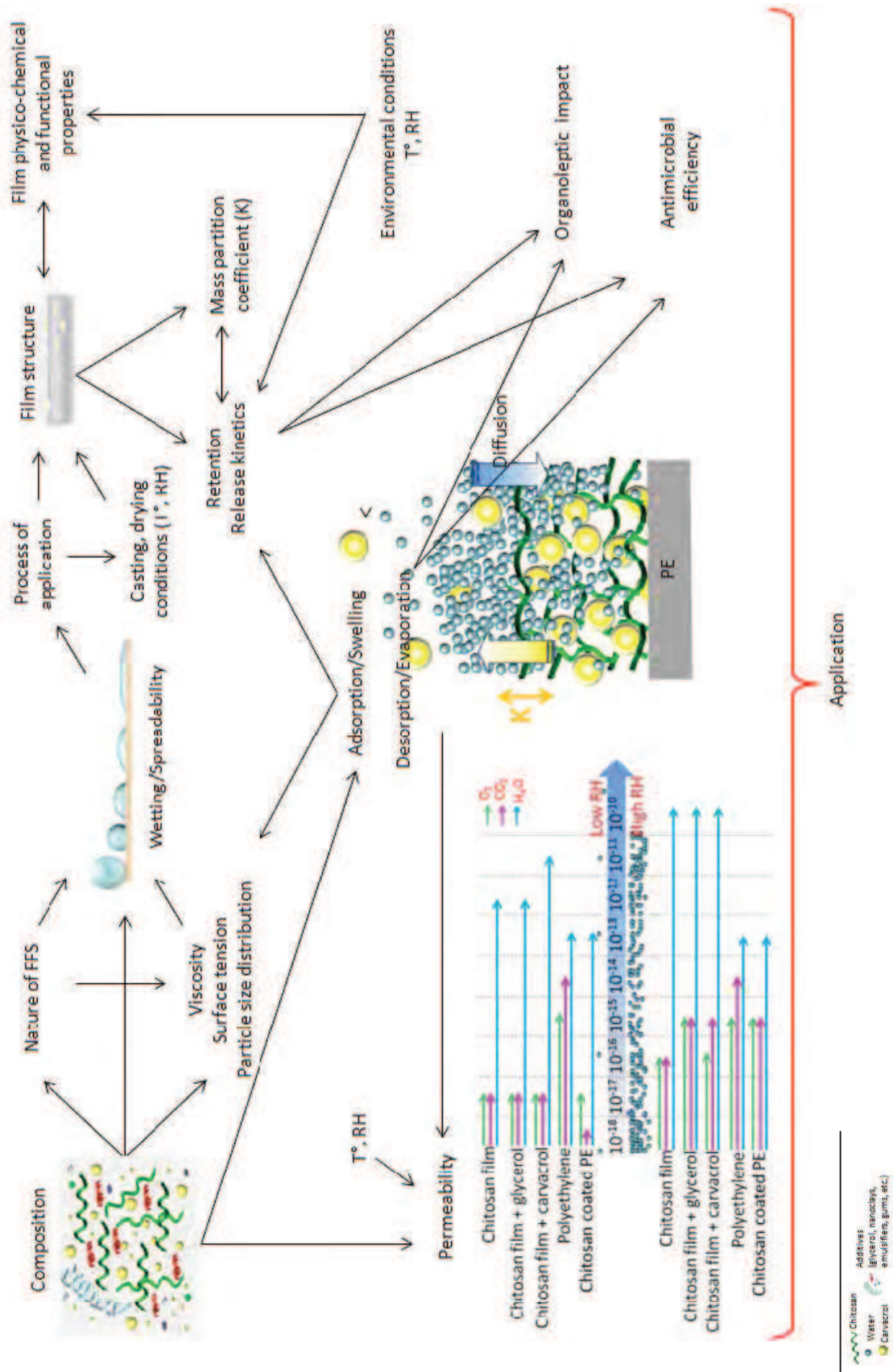


Figure 12.1. Schema of the most important parameters influencing active bio-based film production and application

In relation to the effectiveness of potential antimicrobial films, the most important was to know the amount of active compound retained in the film matrix after processing. Lower temperatures (20°C) and average relative humidity (30%), hydroalcoholic acid solvent, arabic gum and nanoclays strongly influenced carvacrol retention in chitosan matrix. In a life cycle of packaging film, there are two main stages when active compound might be lost, in particular during the drying period and the storage/application period. In the first chapter, deeper study of drying system already quantified the relative importance of water transfers within the chitosan matrix. Carvacrol was preferentially lost at higher water contents. In this stage, chitosan chains are still far away from each other, and all the volatiles including carvacrol are progressively evaporated. At water content lower than 10%, mass transfers were slower. Moreover, the water diffusion coefficients in this range were ten times lower than in humidified systems. Certainly, the loss of carvacrol was greatly influenced not only by the water content, but also with the composition of film matrix. The retention was found to be oppositely related to the mass partition coefficient. When less carvacrol was retained in the film, this indicated higher mass partition coefficient. So the greater release occurred in the headspace.

The composition of film forming solution is important for solution casting. Changes in solvent polarity and structural changes at the interface of chitosan globules in the film forming solution have influenced surface tension. It is depending on its polar and apolar components. Ethanol and carvacrol lowered the surface tension of film forming solutions. Thereby, the spreadability onto the non polar/hydrophobic polyethylene was improved. As the cohesion coefficient was higher than the adhesion coefficient, spreading of chitosan solution occurred. This has permitted optimization of the coating process of polyethylene films by thin chitosan layers. The drying technique and environmental parameters have influenced the drying time, film structure, film appearance, carvacrol retention and film functional properties. Addition of ethanol does not only change the polarity of film forming solutions but also improve the solubility of carvacrol and glycerol. Furthermore it reduced, for about 10%, the time needed to obtain dry films during oven drying. The solvent evaporation led to changes in the film surface properties and its composition. The support sides of self-standing chitosan films were more hydrophobic than air drying sides. Glycerol and carvacrol influenced the phase separation during drying. In dry films, carvacrol looked like small droplets that were easily seen in the microscopic scale. In addition, evaporation of carvacrol towards air surface increased the surface heterogeneity. So, depending on

the composition, all chitosan films swelled in a lesser (pure chitosan films) or larger (chitosan films with glycerol) extent.

Fast drying technique was applied for industrial production of chitosan coated polyethylene. This process did not significantly change the structural and thermal properties of supporting material. Nonetheless, in dry environment the gas permeability of coated polyethylene was improved up to three orders of magnitude. Meanwhile, water vapour permeability was not significantly affected. Actually, polyethylene alone is a rather good water vapour barrier. So, thin chitosan coatings on PE did not drastically decrease its water barrier performance. However due to its hygroscopic nature, even 3-6  $\mu\text{m}$  thin chitosan films absorbed up to 6% of water vapour that condensed on the chitosan/PE interface and presented water reservoir. When environmental relative humidity was above 60%, a significant increase in gas permeation occurred, but it still remained lower than the uncoated polyethylene. As gas permeation through pure polyethylene films is not affected by environmental humidity, this increase was then attributed to chitosan only. Thus, particular attention was made on the water vapour impact on the chitosan matrix.

Deepen analysis of mass transfers that occurs on the surface of chitosan film exposed to water vapour was performed and possible explanations were given. The sorption of water vapour in chitosan matrix led to some structural changes. Water was shown to be the most ubiquitous plasticizer for chitosan films. Already during early stage of the drying, high carvacrol loss was induced by the matrix plasticization. This also led to changes in the strength and the nature of interactions between chitosan chains. Moreover, according to Ogawa et al. (2000), during drying, water molecules help the structuration of the chitosan crystals. Then, a hydrated chitosan crystal was formed with a shape of two fold helix. As this system is energetically more stable than the anhydrous polymorph, the complete removal of water molecules from the chitosan crystal is rather difficult. This was observed in the water vapour sorption experiment. Once completely dry, with 0% of water in a film, increasing the number of water molecules in the environment led to the increased amount of sorbed water. Non ordinary phenomenon was observed from 30 to 70% relative humidity. In this humidity range, moisture has induced some removal of acetic acid, so re-crystallisation/re-organisation of chitosan chains was observed. Above 60% RH, the sorbing capacity exponentially increased. This amount of environmental water was also crucial for barrier performances of both self-standing chitosan film and coatings on PE. The monomolecular layer of sorbed water has increased with the addition of glycerol. This hydrophilic plasticizer is known for its water attracting attributes so water molecules

were sorbed with less energy. Higher water contents in the film led to plasticization and formation of water clusters that caused an increase in gas and water vapour permeabilities. At lower relative humidities, chitosan was plasticized by both glycerol and carvacrol, while at higher relative humidities water had a stronger impact and masked the other plasticizers. This hypothesis resulted from series of experiments. At lower relative humidities, the dissociation temperature was lowered for carvacrol containing samples. Lowering the transition temperatures is a specific attribute of plasticizing agents. The dissociation temperature was also lowered for glycerol containing samples. On the contrary, in the pure chitosan films, the lower temperatures were observed at higher relative humidities indicating the plasticization by water. However, the real glass transition temperature for chitosan films was not determined, because in this study it could not be displayed by thermal analysis. Barrier performances of chitosan films changed depending on the composition and on the environmental conditions. In dry environment, the increase in oxygen and carbon dioxide permeability was observed for carvacrol and glycerol containing samples. Nevertheless, in dry conditions, all chitosan films were fairly good gas barriers (about  $10^{-17}$  g/m·s·Pa). The gas permeability of chitosan coated PE was up to 1000 times lower than uncoated polyethylene films. The increase in the environmental humidity above 60% and up to 96% (that represents the conditions of a real fresh food packaging system), has significantly increased gas permeability in all chitosan films. Finally, mechanical tests confirmed that when the relative humidity was increased, structural changes were induced. This indicated an extensive water plasticization of chitosan matrix.

Even that the water significantly decreased the barrier performances of chitosan films and changed the integrity of film matrix, this phenomenon is desirable for the antimicrobial film performance. Indeed, during application, water plays an important role in the release of the active compound from chitosan matrix. Swelling of chitosan in contact with the water vapour increases the gaps between chitosan macromolecular chains and thus facilitates the release of carvacrol. Diffusion coefficients of carvacrol from chitosan film increased up to 1000 times when humidity went up from 0% to 100%. Water vapour triggered the release of carvacrol in the vapour phase. So it indicated the importance of controlling the environmental conditions in the packaging, at the time of the application but also during the active film storage. The release of active compound is defined by a mass partition coefficient. This parameter can be used to control the concentration of carvacrol in the vapour phase.

Comprehension of the physico-chemical mechanisms involved in such complex system is crucial to control the release and the concentrations of active volatile compound. Indeed, kinetics and thermodynamics of mass transfers are key factors to control the composition of the vapour phase between the foodstuff and packaging material. Only the knowledge of these transfer phenomena allows to measure and to understand the antimicrobial efficiency of volatile compound. The antimicrobial efficiency is a concentration dependent parameter. In other words, there is a certain minimal concentration required to obtain the antimicrobial effect. However, films with carvacrol concentrations in the vapour phase above  $2 \times 10^{-7}$  g/mL<sub>air</sub> were extremely active against large spectrum of bacteria, including Gram positive bacteria, Gram negative bacteria and fungi. In some instances the concentration that was required (around 124 ppm) for carvacrol antimicrobial efficiency, it was not organoleptically acceptable to consumers. Due to its deliberate interaction with the food, the migration of carvacrol even at low doses represents an organoleptic problem. Therefore, efforts need to be made to use essential oil such as carvacrol in very low amounts (much lower than reported in the literature), in order to be effective in controlling microorganisms without contributing to an overwhelming flavour and/or odour notes to food products.

To optimise mass transfers in antimicrobial system during the application, transfers of carvacrol in the vapour phase, in the agar and through agar have been assessed in a parallel study. These experiments are part of those on the long trail to better understand the importance of the surface of exposure and the distance (or air gap) between film and surface contaminated with microorganisms. Thus modelling of the data will provide sufficient information for the improvement of the antimicrobial effect. Consequently, this way is important for the final application and validation in industrial scale.

In the scopes of this project, multilayered films were also produced. These films are made of an antimicrobial compound incorporated in the synthetic polymer. Additionally, they are coated with activated chitosan. Multilayer systems can be efficient to control the release of the active compound. On one hand, this active compound that is incorporated in the synthetic polymer has low partitioning. So this system serves as a long term active compound reservoir. On the other hand, the chitosan layer that is exposed to product atmosphere will provide a fast release at the time of the application. In this way, the concentration of the active compound within

the packaging could be maintained over a long period. However, further investigation on mass transfers is needed to resolve these hypotheses.

This work opens many possible investigation trails concerning the chitosan based films development.

First of all, a further investigation about the structural changes of chitosan matrix by a water vapour is envisaged. Indeed, finer analyses of network organisation by X-ray diffraction or circular dichroism are envisaged. This will help to better understand the phenomena that occur in the chitosan/water interface. Besides, in this way, functional film properties that are governed by water vapour could be clarified.

Being an excellent gas barrier in dry conditions gives a potential to chitosan to be used as an inner layer in conventional multilayer plastic films. So, further investigations could be focused on substitution of polymers like ethylene vinyl alcohol, polyvinylidene chloride or polyamide. Not only that chitosan would provide a barrier against gases, but also, as it is natural and a water sensitive polymer, it would improve recyclability of laminates normally used in multilayered packaging films.

Controlled releasing systems are of a top subjects not only in the food packaging industry but also for medical purposes. Therefore, chitosan based systems studied in this work, could be potentially used as supports of some pharmaceutical products and in tissue engineering.

Even if chitosan, as a bio-sourced and naturally derived material, has been extensively studied in the literature, no many available data exist on its biodegradation. A study on the biodegradation of chitosan films can be considered to define the parameters that govern its degradation kinetics depending on whether it takes place in a ground or in compost. Also, it would be interesting to study the consequences of real biodegradation of these materials on the environment.

All along this work, the word “active” was the main thought. It supposes that the active compound will improve the product shelf life because of antimicrobial efficiency and due to its deliberate interaction with the food and/or its environment. The migration of substances can represent a food safety concern. So first of all, finding appropriate methods for migration tests accomplished with toxicology testing, could also be of a great interest for both scientific community and industrial forces.



## *References*

---





- Abdollahi, M., Rezaei, M., & Farzi, G. (2012). A novel active bionanocomposite film incorporating rosemary essential oil and nanoclay into chitosan. *Journal of Food Engineering*, 111(2), 343-350.
- Abugoch, L.E., Tapia, C., Villamán, M.C., Yazdani-Pedram, M., & Díaz-Dosque, M. (2011). Characterization of quinoa protein chitosan blend edible films. *Food Hydrocolloids*, 25, 879-886
- Aday, M.S., & Caner, C. (2012). The shelf life extension of fresh strawberries using an oxygen absorber in the biobased package. *LWT - Food Science and Technology*, ISSN 0023-6438, 10.1016/j.lwt.2012.06.006.
- Ahmad, M., Benjakul, S., Sumpavapol, P., & Nirmal, N.P. (2012a). Quality changes of sea bass slices wrapped with gelatin film incorporated with lemongrass essential oil. *International Journal of Food Microbiology*, 155(3), 171-178.
- Ahmad, M., Benjakul, S., Prodpran, T., & Agustini, T.W. (2012b). Physico-mechanical and antimicrobial properties of gelatin film from the skin of unicorn leatherjacket incorporated with essential oils. *Food Hydrocolloids*, 28, 189-199.
- Ahvenainen R., Vermeiren L., Heirligs L., Delieghere F., & Debevere J. (2003). Novel food packaging techniques. Woodhead Publishing Limited: Cambridge England, 1-52.
- Aider, M. (2010) Chitosan application for active bio-based films production and potential in the food industry: review. *LWT-Food Science and Technology*, 43, 837-842.
- Ait-Ouazzou, A., Espina, L., Gelaw, T.K., de Lamo-Castellví, S., Pagán, R. & García-Gonzalo, D. (2012). New insights in mechanisms of bacterial inactivation by carvacrol. *Journal of Applied Microbiology*, doi: 10.1111/jam.12028.
- Alcantara, C.R., Rumsey, T.R., & Krochta, J.M. (1998). Drying rate effect on the properties of whey protein films. *Journal of Food Process Engineering*, 21, 387-405.
- Aloui, H., Khwaldia, K., Ben Slama, M., & Hamdi, M. (2011). Effect of glycerol and coating weight on functional properties of biopolymer-coated paper. *Carbohydrate Polymers*, 86, 1063-1072.
- Altiook, D., Altiook, E., & Tihminlioglu, F. (2010). Physical, antibacterial and antioxidant properties of chitosan films incorporated with thyme oil for potential wound healing applications. *The Journal of Materials Science: Materials in Medicine*, 21, 2227-2236.
- Amalaradjou, M.A.R., & Bhunia, A.K. (2012). Chapter Five - Modern Approaches in Probiotics Research to Control Foodborne Pathogens. In: J. Henry (Ed.), *Advances in Food and Nutrition Research* (pp. 185-239). Academic Press.
- Anderson, R.B. (1946). Modifications of the Brunauer, Emmett and Teller equation. *Journal of American Chemical Society*, 68(4), 686-691.
- Andreuccetti, C., Andreuccetti, R., Carvalho, A., Galicia-García, T., Martínez-Bustos, F., & Grosso, C.R.F. (2011). Effect of surfactants on the functional properties of gelatin-based edible films. *Journal of Food Engineering*, 103, 129-136.
- Anker, M. (1996). Edible and biodegradable films and coatings for food packaging literature review. Report no. 623, SIK, Göteborg, 5-60.
- Anker, M. (2000). Edible and Biodegradable Whey Protein Films as Barriers in Foods and Food Packaging, in Department of Food Science. 2000, Chalmers University of Technology: Göteborg.

- Anker, M., Bensten, J., Hermansson, A. & Stading, M. (2002). Improved water vapor barrier of whey protein films by addition of an acetylated monoglyceride. *Innovative Food Science and Emerging Technologies*, 3, 81-92.
- Anonymus, <http://www.bohemia-grafia.de>, Accesed July, 2012.
- Appelqvist, I.A.M., Cooke, D., Gidley, M.J., & Lune, S.J. (1993.) Thermal properties of polysaccharides at low moisture: 1-An endothermic melting process and water-carbohydrate interactions. *Carbohydrate Polymers*, 20(4), 291-299.
- Appendini, P., & Hotchkiss, J.H. (2002). Review of antimicrobial food packaging. *Innovative Food Science and Emerging Technologies*. 3(2), 113-126
- Aranaz, I., Mengibar, M., Harris, R., Paños, I., Miralles, B., Acosta, N., Galed, G., & Heras, A. (2009). Functional characterization of chitin and chitosan. *Current Chemical Biology*, 3, 203-230.
- Arora, D.K., Hansen, A. P., & Armagost, M.S. (1991). Sorption of flavor compounds by low-density polyethylene film. *Journal of Food Science*, 56(5), 1421-1423.
- Arvanitoyannis, I., & Biliaderis, C.G. (1998). Physical properties of polyol-plasticized edible films made from sodium caseinate and soluble starch blends. *Food Chemistry*, 62, 333-342.
- Arvanitoyannis, I.S., Nakayamab, A., & Aibab, S. (1998). Chitosan and gelatin based edible films: state diagrams, mechanical and permeation properties. *Carbohydrate Polymers*, 37, 371-382.
- Ashley, R.J. (1985). Permeability and plastic packaging. In J.Commyrn (Ed.), *Polymer permeability* (pp. 269-307). New York: Elsevier Applied Science publishers.
- Atarés L., De Jesús C., Talens P., & Chiralt A. (2010). Characterization of SPI-based edible films incorporated with cinnamon or ginger essential oils. *Journal of Food Engineering*, 99, 384-391.
- Avila-Sosa, R., Palou, E., Jiménez Munguía, M.T., Nevárez-Moorillón, G.V., Navarro Cruz, A.R., & López-Malo, A. (2012). Antifungal activity by vapor contact of essential oils added to amaranth, chitosan, or starch edible films. *International Journal of Food Microbiology*, 153, 66-72.
- Ayranci, E., & Tunc, S. (2003). A method for the measurement of the oxygen permeability and the development of edible films to reduce the rate of oxidative reactions in fresh foods. *Food Chemistry*, 80(3), 423-431.
- Azevedo, S., Cunha, L.M., Mahajan, P.V., & Fonseca, S.C. (2011). Application of simplex lattice design for development of moisture absorber for oyster mushrooms. *Procedia Food Science*, 1, 184-189.
- B.O.** (2003). Vocabulaire de la chimie physique, couches et films minces, liquides ou solides, et des interfaces. Bulletin Officiel du ministere de la jeunesse, de l'education nationale et de la recherche, 45: 2746-2758.
- Bae, S.Y., Lee, K.H., Yi, S.C., Kim, H.T., Kim, Y.H., & Kumazawa, H. (1998). CO<sub>2</sub>, N<sub>2</sub> gas sorption and permeation behavior of chitosan membrane. *Korean Journal of Chemical Engineering*, 15, 223-226.
- Bagamboula, C.F., Uyttendaele, M. J., Debevere, J. (2004). Inhibitory effect of thyme and basil essential oils, carvacrol, thymol, estragol, linalool and p-cymene towards *Shigella sonnei* and *S. flexneri*. *Food Microbiology*, 21, 33-42.

- Baines, Z.V., & Morris, E.R. (1987). Flavour/taste perception in thickened systems: The effect of guar gum above and below  $c^*$ . *Food Hydrocolloids*, 1(3), 197–205.
- Balasubramanian, A., Rosenberg, L.E., Yam, K., & Chikindas, M.L. (2009). Antimicrobial packaging: potential vs. reality—A Review. *Journal of Applied Packaging Research*, 3(4), 193–221
- Balau, L.G.L., Popa, M.I., Tura, V., & Melnig, V. (2004). Physico-chemical properties of chitosan films. *Central European Journal of Chemistry*, 2(4), 638–647.
- Bangs, W.E., & Reineccius, G.A. (1982). Influence of dryer infeed matrices on the retention of volatile flavour compounds during spray drying. *Journal of Food Science*, 47(1), 254–259.
- Barrer, R.M. (1937). Nature of the diffusion process in rubber. *Nature*, 140, 106–107.
- Barrie, J.A. (1968) Water in polymers. In J. Crank, & G.S. Park (Eds.), *Diffusion in polymers* (pp. 259–313). Academic press, New York, USA.
- Barrie, J.A., Nunn, A., & Sheer, A. (1974). Sorption and diffusion of water in polyurethane elastomers. In H.P. Hopfenberg (Ed.), *Permeability of plastic films and coatings to gases, vapors and liquids* (pp. 167–182), Plenum Press, New York, USA.
- Batista, L.M., Rosa, C.A., & Pinto, L.A.A. (2007). Diffusive model with variable effective diffusivity considering shrinkage in thin layer drying of chitosan. *Journal Food Engineering*, 81, 127–132.
- Bauer K., Garbe, D., & Surburg, H. (2001). *Common Fragrance and Flavor Materials: Preparation, Properties and Uses*. Wiley-VCH, Weinheim.
- Beaudry, R. M. (1999). Effect of O<sub>2</sub> and CO<sub>2</sub> partial pressure on selected phenomena affecting fruit and vegetable quality. *Postharvest Biology and Technology*, 15, 293–303.
- Bégin, A., & Van Calsteren, M.R. (1999). Antimicrobial films produced from chitosan. *International Journal of Biological Macromolecules*, 26, 63–67.
- Bell L.N., & Labuza T.P. (2000). *Moisture Sorption: Practical Aspects of Isotherm measurement and Use*, 2nd Ed., American of Cereal Chemists Inc.: St.Paul, MN, 2000.
- Ben Arfa, A., Combes, S., Preziosi-Belloy, L., Gontard, N., & Chalier, P. (2006). Antimicrobial activity of carvacrol related to its chemical structure. *Letters in Applied Microbiology*, 43, 149–154.
- Benavides, S., Villalobos-Carvajal, R., & Reyes, J.E. (2012). Physical, mechanical and antibacterial properties of alginate film: Effect of the crosslinking degree and oregano essential oil concentration. *Journal of Food Engineering*, 110(2), 232–239.
- van der Berg, C. (1984). Description of water activity of foods for engineering purposes. In: B.M. McKenna (Ed.), *Engineering and food* (pp. 311–321). Elsevier Applied Science, New York.
- Bernkop-Schnürch, A., & Dünnhaupt, S. (2012). Chitosan-based drug delivery systems. *European Journal of Pharmaceutics and Biopharmaceutics*, 81(3), 463–469.
- Bertuzzi, M.A., Armada, M., & Gottifredi, J.C. (2007) Physicochemical characterization of starch based films. *Journal of Food Engineering*, 82, 17–25.
- Bettini, R., Romani, A.A., Morgani, M.M., & Borghetti, A.F. (2008). Physicochemical and cell adhesion properties of chitosan films prepared from sugar and phosphate-containing solutions. *European Journal of Pharmaceutics and Biopharmaceutics*, 68, 74–81.

- Biesheuvel, P.M., & Cohen Stuart, M.A. (2004). Cylindrical cell model for the electrostatic free energy of polyelectrolyte complexes. *Langmuir*, 20 (11), 4764–4770.
- Bifani, V., Ramirez, C., Ihl, M., Rubilara, M., Garcia, A., & Zaritky, N. (2007). Effects of murta (*Ugni molinae* Turcz) extract on gas and water vapor permeability of carboxymethylcellulose-based edible film. *LWT*, 40, 1473–1481.
- Bitar, A., Ghaddar, T., Malek, A., Haddad, T., & Toufeili, I. (2008). Sensory thresholds of selected phenolic constituents from thyme and their antioxidant potential in sunflower oil. *Journal of the American Oil Chemists Society*, 85, 641-646.
- Bodek, K.H., & Bak, G.W. (1999). Ageing phenomena of chitosan and chitosan-diclofenac sodium system detected by low-frequency dielectric spectroscopy. *European Journal of Pharmaceutics and Biopharmaceutics*, 48, 141–148.
- Boland, A.B., Buhr, K., Giannouli, P., & van Ruth, S.M. (2004). Influence of gelatin, starch, pectin and artificial saliva on the release of 11 flavour compounds from model gel systems. *Food Chemistry*, 86, 401-411.
- Bonilla, J., Atarés, L., Vargas, M., & Chiralt, A. (2012). Effect of essential oils and homogenization conditions on properties of chitosan-based films. *Food Hydrocolloids*, 26, 9-16.
- Bravin, B., Peressini, D., & Sensidoni, A. (2004). Influence of emulsifier type and content on functional properties of polysaccharide lipid-based edible films. *Journal of Agricultural and Food Chemistry*, 52, 6448–6455.
- Briassoulis, D. (2006). Mechanical behaviour of biodegradable agricultural films under real field conditions. *Polymer Degradation and Stability*, 91, 1256-1272.
- Brody, A.L., Bugusu, B., Han, J.H., Koelsch Sand, C., & McHugh, T.H. (2008). Innovative Food Packaging Solutions. *Journal of Food Science*, 73, R107-R116.
- Brody, A.L., Strupinsky, E.R., & Kline, L.R. (2001). Active packaging for food applications, Technomic Pub. Co., Lancaster, Pa., xviii, 218.
- Broumand, A., Emam-Djomeh, Z., Hamedi, M., & Razavi, S.H. (2011). Antimicrobial, water vapour permeability, mechanical and thermal properties of casein based Zataria multiflora Boiss Extract containing film. *LWT - Food Science and Technology*, 44(10), 2316-2323.
- Brown, C.D., Kreilgaard, L., Nakakura, M., Caram-Lelham, N., Pettit, D.K., & Gombotz, W.R. (2001). Release of PEGylated granulocyte–macrophage colony-stimulating factor from chitosan/glycerol films. *Journal of Controlled Release*, 72, 35-46.
- Buonocore, G.G., Conte, A., Corbo, M.R., Sinigaglia, M., & Nobile, M.A. (2005). Mono and multilayer active films containing lysozyme as antimicrobial agent. *Innovative Food Science and Emerging Technologies*, 6, 459-464
- Buonocore, G.G., Del Nobile, M.A., Panizza, A., Corbo, M.R., & Nicolais, L. (2003). A general approach to describe the antimicrobial agent release from highly swellable films intended for food packaging applications. *Journal of Controlled Release*, 90, 97–107.
- Burdock, G.A. (2005). Fenaroli's handbook of flavour ingredients. 5 ed. CRC Press, Boca Raton, FL.

- Burgentzlè, D., Duchet, J., Gerard, J.F., Jupin, A., & Fillon, B. (2004). Solvent-based nanocomposite coatings. I. Dispersion of organophilic montmorillonite in organic solvents. *Journal of Colloid and Interface Science*, 278, 26–39.
- Burt, S. (2004). Essential oils: Their antibacterial properties and potential applications in foods – A review. *International Journal of Food Microbiology*, 94(3), 223-253.
- Burt, S.A., & Reinders, R.D. (2003). Antibacterial activity of selected plant essential oils against *Escherichia coli* O157:H7. *Letters in Applied Microbiology*, 36, 162-167.
- Burt, S.A., Van der Zee, R., Koets, A.P., de Graaff, A.M., van Knapen, F., Gaastra, W., Haagsman, H.P., & Veldhuizen, E.J.A. (2007). Carvacrol induces heat shock protein 60 and inhibits synthesis of flagellin in *Escherichia coli* O157:H7. *Applied and Environmental Microbiology*, 73, 4484-4490.
- Busolo, M.A., Lagaron, J.M. (2012). Oxygen scavenging polyolefin nanocomposite films containing an iron modified kaolinite of interest in active food packaging applications. *Innovative Food Science and Emerging Technologies*, <http://dx.doi.org/10.1016/j.ifset.2012.06.008>.
- Butler, B.L., Vergano, P.L., Testin, R.F., Bunn, J.M., & Wiles, J.L. (1996). Mechanical and barrier properties of edible chitosan film as affected by composition and storage. *Journal of Food Science*, 61, 953–961.
- Buttery, R.G., Bomben, J.L., Gaudagni, D.G., & Ling, L.C. (1971). Volatilities of organic flavour compounds in foods. *Journal of Agricultural and Food Chemistry*, 19(6), 1045-1048.
- Çagri, A., Ustunol, Z. & Ryser, E. (2004). Antimicrobial edible films and coatings: A review. *Journal of Food Protection*, 67(4), 833-848.
- Cameron, A.C., Beaudry, R.M., Banks, N.H., & Yelanich, M.V. (1994). Modified atmosphere packaging of blueberry fruit: modelling respiration and package oxygen partial pressures as a function of temperature. *Journal of the American Society for Horticultural Science*, 119, 534–539.
- Caner, C., Vergano, P.J., & Wiles, J.L. (1998). Chitosan film mechanical and permeation properties as affected by acid, plasticizer, and storage. *Journal of Food Science*, 63, 1049-1053.
- Cantín, C.M., Palou, L., Bremera, V., Michailides, T.J., & Crisosto, C.H. (2011). Evaluation of the use of sulfur dioxide to reduce postharvest losses on dark and green figs. *Postharvest Biology and Technology*, 59(2), 150–158.
- Cárdenas, G., Díaz, J., Meléndrez, M.F., & Cruzat, C. (2008). Physicochemical properties of edible films from chitosan composites obtained by microwave heating. *Polymer Bulletin*, 61, 737-748.
- Carelli, A. A., Crapiste, G. H., & Lozano, J. E. (1991). Activity coefficients of aroma compounds in model solutions simulating apple juice. *Journal of Agricultural and Food Chemistry*, 39(9), 1636–1640.
- Carson, C.F., & Riley, T.V. (2001). Safety, efficacy and provenance of tea tree (*Melaleuca alternifolia*) oil. *Contact Dermatitis*, 45, 65– 67.
- Carson, C.F., Hammer, K.A., & Riley, T.V. (1995). Broth microdilution method for determining the susceptibility of *Escherichia coli* and *Staphylococcus aureus* to the essential oil of *Melaleuca alternifolia* (tea tree oil). *Microbios*, 82, 181-185.



- Casareigo A., Souza, B.W.S., Vicente, A.A., Teixeira, J.A., Cruz, L., & Diaz, R. (2008). Chitosan coating surface properties as affected by plasticizer, surfactant and polymer concentrations in relation to the surface properties of tomato and carrot. *Food Hydrocolloids*, 22, 1452-1459.
- Casareigo, A., Souza, B.W.S., Cerqueira, M.A., Teixeira, J.A., Cruz, L., Diaz, R., & Vicente, A.A. (2009). Chitosan/clay films' properties as affected by biopolymer and clay micro/nanoparticles' concentrations. *Food Hydrocolloids*, 23, 1895–1902.
- Castelló, R., Ferreira, A.R., Costa, N., Fonseca, I.M., Alves, V.I., & Coelho, I.M. (2010.) Nanocomposite films obtained from carrageenan/pectin biodegradable. International conference on Food Innovation, Food Innova, 2010.
- Cayot, N. (2007). Sensory quality of traditional foods. *Food Chemistry*, 102, 445-453.
- Cerqueira, M.A., Souza, B.W.S., Teixeira, J.A., & Vicente, A.A. (2012). Effect of glycerol and corn oil on physicochemical properties of polysaccharide films - A comparative study. *Food Hydrocolloids*, 27(1), 175-184.
- Cha, D.S., Cooksey, D.K., Chinnan, M.S. & Park, H.J. (2003). Release of nisin from various heat-pressed and cast films. *LWT-Food Science and Technology*, 36, 209–213.
- Cháfer, M., Sánchez-González, L., González-Martínez, C., & Chiralt, A. (2012). Fungal decay and shelf life of oranges coated with chitosan and bergamot, thyme, and tea tree essential oils. *Journal of Food Science*, 77, E182–E187.
- Chalier, P., Ben Arfa, A., Guillard, V., & Gontard, N. (2009). Moisture and temperature triggered release of a volatile active agent from soy protein coated paper: effect of glass transition phenomena on carvacrol diffusion coefficient. *Journal of Agricultural and Food Chemistry*, 57, 658-665.
- Chandra, R., & Rustgi, R. (1998). Biodegradable Polymers. *Progress in Polymer Science*, 23, 1273-1335.
- Charve, J., & Reineccius, R.A. (2009). Encapsulation performance of proteins and traditional materials for spray dried flavors. *Journal of Agricultural and Food Chemistry*, 57(6), 2486–2492.
- Chen, R. H., & Hwa, H. D. (1996). Effect of molecular weight of chitosan with same degree of deacetylation on the thermal, mechanical and permeability properties of prepared membrane. *Carbohydrate Polymers*, 29, 353–358.
- Chen, R. H., Lin, J. H., & Yang, M. H. (1994). Relationships between the chain flexibilities of chitosan molecules and the physical properties of their casted films. *Carbohydrate Polymers*, 24, 41-46.
- Chen, R.H., Domard, A., Muzzarelli, R.A.A., Tokura, S., Wang, D.M. (2011). Advances in chitin/chitosan science and their applications. *Carbohydrate Polymers*, 84(2), 695.
- Cheng, L.H., Abd Karim, A., & Seow, C.C. (2008) .Characterisation of composite films made of konjac glucomannan (KGM), carboxymethyl cellulose (CMC) and lipid. *Food Chemistry*, 107, 411-408.
- Chillo, S., Flores, S., Mastromatteo, M., Conte, A., Gerschenson, L., & Del Nobile, M.A. (2008). Influence of glycerol and chitosan on tapioca starch-based edible film properties. *Journal of Food Engineering*, 88, 159–168.
- Cho, Y., Kim, J.T., Park, H.J. (2012). Size-controlled self-aggregated N-acyl chitosan nanoparticles as a vitamin C carrier. *Carbohydrate Polymers*, 88(3), 1087-1092.

- Choi, W.Y., Park, H.J., Ahn, D.J., Lee, J., & Lee, C.Y. (2002). Wettability of chitosan coating solution on 'Fuji' apple skin. *Journal of Food Science* 67(7), 2667-2672.
- Chuang, W-Y., Young, T-H., Yao, C-H., & Chiu, W-Y. (1999). Properties of the poly(vinyl alcohol)/chitosan blend and its effect on the culture of fibroblast in vitro. *Biomaterials*, 20, 1479-1487.
- Chung, D., Papadakis, S.E., & Yam, K.L. (2001). Release of propyl paraben from a polymer coating into water and food simulating solvents for antimicrobial packaging applications. *Journal of Food Protection*, 25, 71-87.
- Coelho, S., Moreno-Flores, S., Toca-Herrera, J.L., Coelho, M.A.N., Pereira, M.C., & Rocha, S. (2011). Nanostructure of polysaccharide complexes. *Journal of Colloid and Interface Science*, 363, 450-455.
- Contini, C., Katsikogianni, M.G., O'Neill, F.T., O'Sullivan, M., Dowling, D.P., & Monahan, F.J. (2011). Development of active packaging containing natural antioxidants. *Procedia Food Science*, 1, 224-228.
- Crank, J. (1975). The mathematics of diffusion. 2nd Edition, Clarendon Press, Oxford, London.
- Cunha, A.G., Fernandes, S.C.M., Freire, C.S.R., Silvestre, A.J.D., Neto, C.P., & Gandini, A. (2008). What is the real value of chitosan's surface energy?. *Biomacromolecules*, 9 (2), 610-614.
- Cuq, B., Gontard, N., Cuq, J.L., & Guilbert, S. (1996) Functional properties of myofibrillar protein-based biopackagings as affected by film thickness. *Journal of Food Science*, 61, 1-15.
- Dainelli, D., Gontard, N., Spyropoulos, D., Zondervan-van den Beuken, E., & Tobback, P. (2008). Active and intelligent food packaging: legal aspects and safety concerns. *Trends in Food Science and Technology*, 19(1), S103-S112.
- Dan, J.R. (1970). Forces involved in the adhesive process 1. Critical surface tensions of polymeric solids as determined with polar liquids. *Journal of Colloids and Interface Science*, 32(2), 302-319.
- Darder, M., Colilla, M., & Ruiz-Hitzky, E. (2003). Biopolymer-clay nanocomposites based on chitosan intercalated in montmorillonite. *Chemistry of Material*, 15, 3774-3780.
- Davey, H.M., & Winson, M.K. (2003) Using flow cytometry to quantify microbial heterogeneity. *Current Issues in Molecular Biology*, 5, 9-15.
- Davidson, P.M., & Juneja, V.K. (1990). Antimicrobial agents. In: Branen, A.L. Davidson, & P.M., Salminen (Eds.), *Food Additives* (pp. 83-137). Marcel Dekker Inc., New York.
- de Kruijf, N., Beest, M. V., Rijk, R., Sipilainen-Malm, T., Losada, P. P. & Meulenaer, B. D. (2002). Active and intelligent packaging: applications and regulatory aspects. *Food Additives and Contaminants*, 19, 144-162.
- Deans, S. G., & Ritchie, G. (1987). Antibacterial properties of plant essential oils. *International Journal of Food Microbiology*, 5, 165-180.
- Debeaufort, F., Martin-Polo, M.O. & Voilley, A. (1993). Polarity homogeneity and structure affect water vapor permeability of model edible films. *Journal of Food Science*, 58, 426-434.



- Debeaufort, F., Voilley, A., & Meares, P. (1994). Water vapor permeability and diffusivity through methylcellulose edible films. *Journal of Membrane Science*, 91, 125-133.
- Del Nobile, M.A., Buonocore, G.G., & Conte, A. (2004). Oscillatory sorption tests for determining the water-transport properties of chitosan-based edible films. *Journal of Food Science*, 69: FEP44–FEP49.
- Demarger-Andre, S., & Domard, A. (1994). Chitosan carboxylic acid salts in solution and in the solid state. *Carbohydrate Polymers*, 23, 211–219.
- Denavi, G., Tapia-Blácido, D.R., Añón, M.C., Sobral, P.J.A., Mauri, A.N., & Menegalli, F.C. (2009). Effects of drying conditions on some physical properties of soy protein films. *Journal of Food Engineering*, 90, 341-349.
- Deng, Y., Zhu, L.W., Luo, W., Xiao, C.L., Song, X.Y., & Chen, J.S. (2009). Changes in physical properties of chitosan films at subzero temperatures. *Italian Journal of Food Science*, 21(4), 487–497.
- Desobry, S., & Debeaufort, F. (2011). Encapsulation of flavors, nutraceuticals and antibacterials. In J Bai, R Hagenmaier and L Baldwin (Eds), *Edible films and coatings for food and other applications* (Chapter 11). Technomic Publishing Co.
- Despond, S., Espuche, E., & Domard, A. (2001). Water sorption and permeation in chitosan films: Relation between gas permeability and relative humidity. *Journal of Polymer Science Part B: Polymer Physics*, 39, 3114-3127.
- Dhanikula, A.B., & Panchagnula, R. (2004). Development and characterization of biodegradable chitosan films for local delivery of Paclitaxel. *AAPS*, 6, DOI: 10.1208/aapsj060327.
- di Gioia, L., & Guilbert, S. (1999). Corn protein-based thermoplastic resins: effect of some polar and amphiphilic plasticizers. *Journal of Agricultural and Food Chemistry* 47, 1254–1261.
- Di Pierro, P., Sorrentino, A., Mariniello, L., Valeria, C., Giosafatto, L., & Porta, R. (2011) Chitosan/whey protein film as active coating to extend Ricotta cheese shelf-life. *LWT - Food Science and Technology*, 44(10), 2324-2327.
- DiBenedetto, A.T., & Paul, D.R. (1964). Interpretation of gaseous diffusion through polymers using fluctuation theory. *Journal of Polymer Science Part A: Polymer Chemistry*, 2, 1001-1015.
- Dorman, H.J.D., & Deans, S.G. (2000). Antimicrobial agents from plants: antibacterial activity of plant volatile oils. *Journal of Applied Microbiology*, 88, 308–316.
- Drelich, J. (1997). Static contact angles for liquids at heterogeneous rigid solid surfaces. *Polish Journal of Chemistry*, 71, 525-549.
- Du, W.X., Olsen, C.W., Avena-Bustillos, R.J., McHugh, T.H., Levin, C.E., & Friedman, M. (2009). Effects of allspice, cinnamon, and clove bud essential oils in edible apple films on physical properties and antimicrobial activities. *Journal of Food Science*, 74(7), M372-8.
- Duan, J., Park, S.L., Daeschel, M.A., & Zhao, Y. (2007). Antimicrobial chitosan lysozyme (CL) films and coatings for enhancing microbial safety of Mozzarella cheese. *Journal of Food Science*, 72, M355-M362.
- Dupre, A. (1869). *Theorie Mecanique de La Chaleur*. Gauthier-Villan, Paris, France.

Dutta, P.K., Tripathi, S., Mehrotra, G.K., & Dutta, J. (2009). Perspectives for chitosan based antimicrobial films in food applications. *Food Chemistry*, 114, 1173-1182.

El-Azzami, L.A., & Grulke, E.A. (2007). Dual mode model for mixed gas permeation of CO<sub>2</sub>, H<sub>2</sub> and N<sub>2</sub> through a dry chitosan membrane. *Journal of Polymer Science: Part B: Polymer Physics*, 45(18), 2620-2631.

El-Hefian, E.A., Elgannoudi, E.S., Mainal, A., & Yahaya, A.H. (2010). Characterization of chitosan in acetic acid: Rheological and thermal studies. *Turkish Journal of Chemistry*, 34, 47-56.

Elsabee, M.Z., Morsi, R.E., & Al-Sabagh, A.M. (2009). Surface active properties of chitosan and its derivatives. *Colloids and Surfaces B: Biointerfaces*, 74, 1–16.

Emirođlu, Z.K., Yemiř, G.P., Cořkun, B.K., & Candođan, K. (2010). Antimicrobial activity of soy edible films incorporated with thyme and oregano essential oils on fresh ground beef patties. *Meat Science*, 86(2), 283-288.

Epure, V., Griffon, M., Pollet, E., & Averous, L. (2011). Structure and properties of glycerol-plasticized chitosan obtained by mechanical kneading. *Carbohydrate Polymers*, 83, 947–952.

Ettre, L. S., & Kolb, B. (1991). Headspace - gas chromatography: the influence of sample volume on analytical results. *Chromatographia*, 32(1/2), 5–12.

European Commission (1996) Regulation (EC) No 2232/96 of the European Parliament and of the Council of 28 October 1996 laying down a Community procedure for flavouring substances used or intended for use in or on foodstuffs. Official Journal of the European Communities L299/1.

European Commission (1999) Commission Decision 1999/217/EC of 23 February 1999 adopting a register of flavouring substances used in or on foodstuffs drawn up in application of Regulation 2232/96/EC of the European Parliament and of the Council of 28 October 1996 (1999/217/EC). Official Journal of the European Communities L84/1.

European Commission (2004) Regulation (EC) No 1935/2004 of the European Parliament and of the Council of 27 October 2004 on materials and articles intended to come into contact with food and repealing Directives 80/590/EEC and 89/109/EEC Regulation. Official Journal of the European Union L338/4.

European Commission (2006) Council Regulation (EC) No 509/2006 of 20 March 2006 on agricultural products and foodstuffs as traditional specialities guaranteed. Official Journal of the European Union L93/1.

European Commission (2006) Council Regulation (EC) No 510/2006 of 20 March 2006 on the protection of geographical indications and designations of origin for agricultural products and foodstuffs.

European Commission (2008) Regulation (EC) No 1333/2008 of the European Parliament and of the Council of 16 December 2008 on food additives. Official Journal of the European Union L354/16.

European Commission (2008) Regulation (EC) No 1334/2008 of the European Parliament and of the Council of 16 December 2008 on flavourings and certain food ingredients with flavouring properties for use in and on foods and amending Regulation (EC) No 1601/91 of the Council, Regulations (EC) No 2232/96 and (EC) No 110/2008 and Directive 2000/13/EC. Official Journal of the European Union L354/34.

- European Commission (2009) Commission Regulation (EC) No 450/2009 of 29 May 2009 on active and intelligent materials and articles intended to come into contact with food (Text with EEA relevance). Official Journal of the European Union L135/3.
- Exama, A., Arul, J., Lencki, R.W., Lee, L.Z., & Toupin, C. (1993) Suitability of plastic films for modified atmosphere packaging of fruits and vegetables. *Journal of Food Science*, 58, 1365–1370.
- Fabra, M.J., Talens, P., & Chiralt, A. (2010). Water sorption isotherms and phase transitions of sodium caseinate–lipid films as affected by lipid interactions. *Food Hydrocolloids*, 24, 384–391.
- Fabra, M.J., Talens, P., Gavara, R., & Chiralt, A. (2012). Barrier properties of sodium caseinate films as affected by lipid composition and moisture content. *Journal of Food Engineering*, 109, 372-379.
- Fajardo, P., Martins, J.T., Fuciños, C., Pastrana, L., Teixeira, J.A., & Vicente, A.A. (2010). Evaluation of a chitosan-based edible film as carrier of natamycin to improve the storability of Saloio cheese. *Journal of Food Engineering*, 101(4), 349-356.
- Farris, S., Introzzi, L., & Piergiovanni, L. (2009) Evaluation of a biocoating as a solution to improve barrier, friction and optical properties of plastic films. *Packaging Technology and Science*, 22, 69-83.
- Farris, S., Introzzi, L., Biagioni, P., Holz, T., Schiraldi, A., & Piergiovanni L. (2011). Wetting of biopolymer coatings: contact angle kinetics and image analysis investigation. *Langmuir*, 27, 7563–7574.
- FDA US Food and Drug Administration, CFR - Code of Federal Regulations Title 21. Food and Agriculture Organization of the United Nations, Acceced May 2012, <http://www.fao.org/ag/agn/jecfa-flav/details.html?flavId=3538>
- Fenaroli, G. (1995). Fenaroli's handbook of flavor ingredients. 3rd ed. Boca Raton, Fla: CRC Press, Inc.
- Fernandes, L.P., Oliveira, W.P., Sztatisz, J., & Novák, C. (2008). Thermal properties and release of Lippia Sidoides essential oil from gum arabic/maltodextrin microparticles. *Journal of Thermal Analysis and Calorimetry*, 94(2), 461–467.
- Fernández Cervera, M., Heinämäki, J., Krogars, K., Jörgensen, A.C., Karjalainen, M., Colarte, A.I.C., & Yliruusi, J. (2004). Solid-state and mechanical properties of aqueous chitosan-amylose starch films plasticized with polyols. *AAPS Pharmaceutical Science & Technology*, 5(1), 1-6.
- Fernandez, M., Heinämäki, J., Räsänen, M., Antikainen, O., Nieto, O.M., & Iraizoz, A. (2004) Determination of tackiness of chitosan film-coated pellets exploiting minimum fluidization velocity. *International Journal of Pharmaceutics*, 281, 119-127.
- Fernandez-Saiz, P., Lagaron, J.M., & Ocio, M.J. (2009). Optimization of the biocide properties of chitosan for its application in the design of active films of interest in the food area. *Journal of Food Hydrocolloids*, 23, 913-921.
- Fernandez-Saiz, P., Soler, C., Lagaron, J.M., Ocio, M.J. (2010). Effects of chitosan films on the growth of *Listeria monocytogenes*, *Staphylococcus aureus* and *Salmonella* spp. in laboratory media and in fish soup. *International Journal of Food Microbiology*, 137(2-3), 287-294.

- Flores, S., Haedo, A.S., Campos, C., & Gerschenson, L. (2007). Antimicrobial performance of potassium sorbate supported in tapioca starch edible films. *European Food Research and Technology*, 225, 375-384.
- Floros, J.D., Dock, L.L., & Han, J.H. (1997). Active packaging technologies and applications. *Food Cosmetics and Drug Packaging*, 20(1), 10-7.
- Forsell, P., Lahtinen, R., Lahelin, M., & Myllärinen, P. (2002). Oxygen permeability of amylose and amylopectin films. *Carbohydrate Polymers*, 47(2), 125-129.
- Francois, K., Devlieghere, F., Smet, K., Standaert, A.R., Geeraerd, J.F., Van Impe, J.F., & Debevere, J. (2005). Modelling the individual cell lag phase: effect of temperature and pH on the individual cell lag distribution of *Listeria monocytogenes*. *International Journal of Food Microbiology*, 100, 41-53.
- Friedman, M., Henika, P.R., & Mandrell, R.E. (2002). Bactericidal activities of plant essential oils and some of their isolated constituents against *Campylobacter jejuni*, *Escherichia coli*, *Listeria monocytogenes*, and *Salmonella enterica*. *Journal of Food Protection*, 65, 1545-1560.
- Galdeano, M.C., Grossmann, M.V.E., Mali, S., Bello-Perez, L.A., Garcia, M.A., & Zamudio-Flores, P.B. (2009). Effects of production process and plasticizers on stability of films and sheets of oat starch. *Materials Science and Engineering*, 29, 492-498.
- Galić, K., Čurić, D., & Gabrić, D. (2009). Shelf life of packaged bakery goods--a review. *Critical Reviews in Food Science and Nutrition*, 49(5), 405-26.
- Galić, K., Ščetar, M., & Kurek, M. (2011). The benefits of processing and packaging. *Trends in Food Science Technology*, 22(2-3), 127-137.
- Garcia, M.A., Martino, M.N., & Zaritzky, N.E. (2000a). Lipid addition to improve barrier properties of edible starch-based films and coatings. *Journal of Food Science*, 65(6), 941-947.
- Garcia, M.A., Martino, M.N., & Zaritzky, N.E. (2000b). Microstructural characterization of plasticized starch-based films. *Starch-Stärke*, 52, 118-124.
- Garrido Assis, O. B. & de Britto, D. (2011). Evaluation of the antifungal properties of chitosan coating on cut apples using a non-invasive image analysis technique. *Polymer International*, 60, 932-936.
- Gaudin, S., Lourdin, D., Forsell, P.M., & Colonna, P. (2000). Antiplasticisation and oxygen permeability of starch-sorbitol films. *Carbohydrate Polymers*, 43, 33-37.
- Gemili, S., Yemenicioğlu, A., & Altınkaya, S.A. (2010). Development of antioxidant food packaging materials with controlled release properties. *Journal of Food Engineering*, 96(3), 325-332.
- Gennadios, A. & Weller, C.L. (1990). Edible films and coatings from wheat and corn proteins. *Food Technology*, 44, 63-69.
- Gennadios, A. (2002). Protein-based films & coatings. CRC Press.
- Gennadios, A., Weller, C.L., & Gooding, C.H. (1994). Measurement error in water vapor permeable, hydrophilic edible films. *Journal of Food Engineering*, 21, 395-409.
- Gennadios, A., Weller, C.L., & Testin, R.F. (1993). Temperature effect on oxygen permeability of edible protein-based films. *Journal of Food Science*, 58, 212-214.
- Ghanbarzadeh, B., Musavi, M., Oromiehie, A.R., Rezayi, K., Rad, E.R., & Milani, J. (2007). Effect of plasticizing sugars on water vapor permeability, surface energy and

microstructure properties of zein films. *LWT - Food Science and Technology*, 40(7), 1191-1197.

Ghorpade, V.M., Li, H., Gennadios, A., & Hanna, M.A. (1995). Chemically modified soy protein films. *Transactions of the ASAE*, 38, 1805–1808.

Gibson, L.J., & Ashby, M.F. (1988). *Cellular Solids: Structures & Properties*, Pergamon Press, Cambridge, MA.

Godshall, M. A. (1997). How carbohydrates influence food flavour. *Food Technology*, 51(1), 63–67.

Gómez-Estaca, J., López de Lacey, A., López-Caballero, M.E., Gómez-Guillén, M.C., & Montero, P. (2010). Biodegradable gelatin–chitosan films incorporated with essential oils as antimicrobial agents for fish preservation. *Food Microbiology*, 27(7), 889-896.

Goñi, P., López, P., Sánchez, C., Gómez-Lus, R., Becerril, R., & Nerín, C. (2009). Antimicrobial activity in the vapour phase of a combination of cinnamon and clove essential oils. *Food Chemistry*, 116, 982-989.

Gontard, N., & Guilbert, S. (1992). Edible wheat gluten films: influence of the main process variables on film properties using response surface methodology. *Journal of Food Science*, 57(1), 190–195.

Gontard, N., Duchez, C., Cuq, J.L., & Guilbert, S. (1994). Edible composite films of wheat gluten and lipids: water vapour permeability and other physical properties. *International Journal of Food Science and Technology*, 29, 39–50.

Gontard, N., Thibault, R., Cuq, B., & Guilbert, S. (1996). Influence of relative humidity and film composition on oxygen and carbon dioxide permeabilities of edible films. *Journal of Agricultural and Food Chemistry*, 44, 1064-1069.

Griffin, S. G., Wyllie, S. G., Markham, J. L. & Leach, D. (1999). The role of structure and molecular properties of terpenoids in determining their antimicrobial activity. *Flavour and Fragrances Journal*, 14, 322–332.

Guichard, E. (2002). Interactions between flavor compounds and food ingredients and their influence on flavor perception. *Food Reviews International*, 18, 49–70.

Guilbert, S., & Gontard, N. (2005). Agro-polymers for edible and biodegradable films: review of agricultural polymeric materials, physical and mechanical characteristics. In J.H. Han (Ed.), *Innovations in Food Packaging* (pp.263-274). Elsevier Academic Press: New York.

Günister, E., Pestreli, D., Ünlü, C.H., Atici, O., & Güngör, N. (2007). Synthesis and characterization of chitosan-MMT biocomposite systems. *Carbohydrate Polymers*, 67, 358–365.

Gutierrez, J., Bourke, P., Lonchamp, J., & Barry-Ryan, C. (2009). Impact of plant essential oils on microbiological, organoleptic and quality markers of minimally processed vegetables. *Innovative Food Science and Emerging Technologies*, 10(2), 195-202.

Gutiérrez, L., Sánchez, C., Batlle, R., López, P., & Nerín, C. (2009) New antimicrobial active package for bakery products. *Trends in Food Science and Technology*, 20(2), 92–99.

Ha, J.U., Kim, Y.M., & Lee, D.S. (2001). Multilayered antimicrobial polyethylene films applied to the packaging of ground beef. *Packaging Technology and Science*, 14(2), 55-62.



- Hagenmaier, R.D., & Baker, R.A. (1993). Reduction in gas exchange of citrus fruit by wax coatings. *Journal of Agriculture and Food Chemistry*, 41, 283-287.
- Hagenmeier, R. & Shaw, P. (1991). Permeability of shellac coatings to gases and water vapor. *Journal of Agricultural and Food chemistry*, 39, 825-829.
- Hambleton A., Debeaufort F., Beney L., Karbowiak T. & Voilley A. (2008). Protection of active aroma compound against moisture and oxygen by encapsulation in biopolymeric emulsion-based edible films. *Biomacromolecules*, 9(3), 1058-1063.
- Hambleton, A., Perpiñan-Saiz, N., Fabra, M.J., Voilley, A., & Debeaufort F. (2011). The Schroeder paradox or how the state of water affects the moisture transfers through edible films. *Food Chemistry*, 132 (4), 1671–1678.
- Han, J. H. (2003). Antimicrobial food packaging. In R. Ahvenainen (Ed.), *Novel food packaging techniques*. Woodhead; CRC Press, Cambridge, Boca Raton, FL.
- Han, J. H. (2005). Antimicrobial packaging systems. In Jung H. Han (Ed.), *Innovations in food packaging* (pp. 81–107). Amsterdam: Elsevier Academic Press.
- Han, J.H. (2000). Antimicrobial food packaging. *Food Technology*, 54(3), 56-65.
- Hao, Y.Y., Brackett, R.E. & Doyle, M.P. (1998). Efficacy of plant extracts in inhibiting *Aeromonas hydrophila* and *Listeria monocytogenes* in refrigerated cooked poultry. *Food Microbiology*, 15, 367-378.
- Harpaz, S., Glatman, L., Drabkin, V., & Gelman, A. (2003). Effects of herbal essential oils used to extend the shelf life of freshwaterreared Asian sea bass fish (*Lates calcarifer*). *Journal of Food Protection*, 66(3), 410–417.
- Hernandez, R. J., & Gavara, R. (1994). Sorption and transport of water in nylon-6 films. *Journal of Polymer Science Part B: Polymer Physics*, 32, 2367–2374.
- Hernández-Muñoz, P., López-Rubio, A., Del-Valle, V., Almenar, E., & Gavara, R. (2004). Mechanical and water barrier properties of glutenin films influenced by storage time. *Journal of Agricultural and Food Chemistry*, 52, 79-83.
- Hong, S.I. & Krochta, J.M. (2006). Oxygen barrier performance of whey–protein coated plastic films as affected by temperature, relative humidity, base film and protein type. *Journal of Food Engineering*, 77, 739-745.
- Hook, P., Heimlich, J.E., 2006. *A History of Packaging*, CDFS-133.
- Imran, M., Revol-Junelles, A.M., René, N., Jamshidian, M., Akhtar, M.J., Arab-Tehrany, E., Jacquot, M., & Desobry, S. (2012). Microstructure and physico-chemical evaluation of nano-emulsion-based antimicrobial peptides embedded in bioactive packaging films. *Food Hydrocolloids*, 29(2), 407-419.
- Inamuco, J., Veenendaal, A.K.J., Burt, S.A., Post, J.A., Tjeerdsma-van Bokhoven, J.L.M., Haagsman, H.P., & Veldhuizen, E.J.A. (2012). Sub-lethal levels of carvacrol reduce *Salmonella Thyphimurium* motility and invasion of porcine epithelial cells. *Veterinary Microbiology*, 157(1-2), 200-207.
- Inouye, S., Takizawa, T., & Yamaguchi, H. (2001). Antibacterial activity of essential oils and their major constituents against respiratory tract pathogens by gaseous contact. *Journal of Antimicrobial Chemotherapy*, 47, 565-573.
- Inouye, S., Uchida, K., & Abe, S. (2006). Vapor activity of 72 essential oils against a Trichophyton mentagrophytes. *Journal of Infection and Chemotherapy*, 12, 210-216.

- Ito, A., Sato, M., & Anma, T. (1997). Permeability of CO<sub>2</sub> through chitosan membrane swollen by water vapor in feed gas. *Die Angewandte Makromolekulare Chemie*, 248, 85-94.
- Iturriaga, L., Olabarrieta, I., & Martínez de Marañón, I. (2012). Antimicrobial assays of natural extracts and their inhibitory effect against *Listeria innocua* and fish spoilage bacteria, after incorporation into biopolymer edible films. *International Journal of Food Microbiology*, 158(1), 58-64.
- IUPAC 1985. Reporting physisorption data for glass/solid systems. *Pure and Applied Chemistry*, 57, 603-619.
- Janssen, L.P.B.M., & Moscicki, L. (2009). Thermoplastic Starch. WILEY-VCH Verlag GmbH & Co. KGaA, Weinheim.
- Jeon, Y-J., Kamil, J.Y.V.A., & Shahidi, F. (2002). Chitosan as an edible invisible film for quality preservation of herring and atlantic cod. *Journal of Agricultural and Food Chemistry*, 50, 5167-5178.
- Joerger, R.D. (2007). Antimicrobial films for food applications: a quantitative analysis of their effectiveness. *Packaging Technology and Science*, 20, 231-273.
- Kaelble, D. H. (1970). Dispersion-polar surface tension properties of organic solids. *Journal of Adhesion*, 2, 66-81.
- Kam, H. M., Khor, E., & Lim, L. Y. (1999). Storage of partially deacetylated chitosan films. *Journal of Biomedical Materials Research*, 48 (6), 881-888.
- Kanatt, S. W., Chander, R., & Sharma, A. (2008). Chitosan-glucose complex—a novel food preservative. *Food Chemistry*, 106, 521-528.
- Kanatt, S.R., Rao, M.S., Chawla, S.P., & Sharma, A. (2012). Active chitosan-polyvinyl alcohol films with natural extracts. *Food Hydrocolloids*, 29(2), 290-297.
- Karbowiak, T., Debeaufort, F., & Voilley, A. (2006). Importance of surface tension characterization for food, pharmaceutical and packaging products: A Review. *Critical Reviews in Food Science and Nutrition*, 46, 1-17.
- Karbowiak, T., Gougeon, R.D., Rigolet, S., Delmotte, L., Debeaufort, F., & Voilley, A. (2008). Diffusion of small molecules in edible films: Effect of water and interactions between diffusant and biopolymer. *Food Chemistry*, 106, 1340-1349.
- Karbowiak, T., Ferret, E., Debeaufort, F., Voilley, A., & Cayot, P. (2011). Investigation of water transfer across thin layer biopolymer films by infrared spectroscopy. *Journal of Membrane Science*, 370(1-2), 82-90.
- Kasaai, M.R., Charlet, G., Paquin, P., & Arul, J. (2003). Fragmentation of chitosan by microfluidization process. *Innovative Food Science and Emerging Technologies*, 4, 403-413.
- Kawada, J., Abe, Y., Yui, T., Okuyama, K., & Ogawa, K. (1999). Crystalline Transformation of chitosan from hydrated to anhydrous polymorph via chitosan monocarboxylic acid salts. *Journal of Carbohydrate Chemistry*, 18(5), 559-571.
- Kaya, S., & Kaya, M. (2000). Microwave drying effect on properties of whey protein isolate edible films. *Journal of Food Engineering*, 43, 91-96.
- Keawchaon, L., & Yoksqn, R. (2011). Preparation, characterization and in vitro release study of carvacrol-loaded chitosan nanoparticles. *Colloids and Surfaces B: Biointerfaces*, 84, 163-171.

- Kechichian, V., Ditchfield, C., Veiga-Santos, P., & Tadini, C.C. (2010). Natural antimicrobial ingredients incorporated in biodegradable films based on cassava starch *LWT - Food Science and Technology*, 43(7), 1088-1094.
- Keller, & Heckman (2002). LLP's Packaging Practice Group, Accessed: August, 2012. <http://www.packaginglaw.com>.
- Kester, J.J. & Fennema, O.R. (1986). Edible films and coatings: a review. *Food Technology*, 54, 47- 58.
- Kim, J.M., Marshall, M.R., Cornell, J.A., Preston, J.F., & Wei, C.I. (1995). Antibacterial activity of carvacrol, citral, and geraniol against *Salmonella typhimurium* on culture medium and on fish cubes. *Journal of Food Science*, 60(6), 1364–1374.
- Kinsella, J. E. (1989). Flavour perception and binding to food components. In D.B. Min, & T. H. Smousse (Eds.), *Aroma research* (pp. 376–403). Champaign, IL: American Oil Chemist's Society.
- Kisko, G., & Roller, S. (2005). Carvacrol and p-cymene inactivate *Escherichia coli* O157:H7 in apple juice. *BMC Microbiology*, 5, 36-44.
- Klopffer, M.H., & Flaconnèche, B. (2001). Transport properties of gases in polymers: bibliographic review. *Oil & Gas Science and Technology – Rev. IFP*, 56(3), 223-244
- Kloucek, P., Smid, J., Frankova, A., Kokoska, L., Valterova, I., & Pavela, R. (2011). Fast screening method for assessment of antimicrobial activity of essential oils in vapor phase. *Food Research International*, 47(2), 161–165.
- Kokoszka, S., Debeaufort, F., Hambleton, A., Lenart, A., & Voilley, A. (2010). Protein and glycerol contents affects physico-chemical properties of soy protein isolate-based edible films. *Innovative Food Science and Emerging Technologies*, 11, 503-510.
- Kolb, B., Welter, C., & Bichler, C. (1992). Determination of partition coefficients by automatic equilibrium headspace gas chromatography by vapor phase calibration. *Chromatographia*, 34(5/8), 235–240.
- Kong, M., Chen, G.X., Xing, K., & Park, J.H (2010). Antimicrobial properties of chitosan and mode of action: A state of the art review. *International Journal of Food Microbiology*, 144(1), 51-63.
- Koutsoumanis, K.P., & Sofos, J.N. (2005). Effect of inoculum size on the combined emperature, pH and limits for growth of *Listeria monocytogenes*. *International Journal of Food Micorbiology*, 104, 83-91.
- Krishnan, S., Kshirsagar, A.C., & Singhal, R.C. (2005). The use of gum arabic and modified starch in the microencapsulation of a food flavoring agent. *Carbohydrate Polymers*, 62, 309–315.
- Krochta, J.M., & De Mulder-Johnston, C.D. (1997). Edible and biodegradable polymer films: challenges and opportunities. *Food Technology*, 51, 61-74.
- Krochta, J.M., Baldwin, E.A., & Nisperos-Carriedo, M.O. (1994). Edible coatings and films to improve food quality, Lancaster: Technomic Publishing Co. Inc.
- Kühne, B., Vanhonacker, F., Gellynck, X. & Verbeke, W. (2010). Innovation in traditional food products in Europe: Do sector innovation activities match consumers' acceptance? *Food Quality and Preference*, 21(6), 629-638.



- Kumirska, J., Weinhold, M.X., Thöming, J., & Stepnowski, P. (2011). Biomedical activity of chitin/chitosan based materials—influence of physicochemical properties apart from molecular weight and degree of N-acetylation. *Polymers*, 3(4), 1875-1901.
- Kurek, M., Klepac, D., Scetar, M., Galić, K., Valić, S., Lin, Y., & Yong, W. (2011) Gas barrier and morphology characteristic of linear low density polyethylene and two different polypropylene films. *Polymer Bulletin*, 67, 1293-1309.
- Kurek, M., Descours, E., Galić, K., Voilley, A., & Debeaufort, F. (2012a) How composition and process parameters affect volatile active compounds in biopolymer films. *Carbohydrate Polymers*, 88(2), 646-656.
- Kurek, M., Ščetar, M., Voilley, A., Galić, K., & Debeaufort, F. (2012b). Barrier properties of chitosan coated polyethylene. *Journal of Membrane Science*, 404-405, 162-168.
- Kurek, M., Brachais, C.-H., Ščetar, M., Voilley, A., Galić, K., Couvercelle, J.-P., & Debeaufort, F. (2012c). Carvacrol affects interfacial, structural and transfer properties of chitosan coated polyethylene. *Carbohydrate Polymers*, submitted.
- Ladet, S., David, L., & Domard, A. (2008). Multi-membrane hydrogels. *Nature*, 452(7183), 76-79.
- Lambert, R.J., & Pearson, J. (2000). Susceptibility testing accurate and reproducible minimum inhibitory concentration (MIC) and non-inhibitory concentration (NIC) values. *Journal of Applied Microbiology*, 88(5), 784-790.
- Lambert, R.J.W., Skandamis, P.N., Coote, P.J., & Nychas, G.J.E. (2001). A study of the minimum inhibitory concentration and mode of action of oregano essential oil, thymol and carvacrol. *Journal of Applied Microbiology*, 91(3), 453-462.
- Lanciotti, R., Gianotti, A., Patrignani, F., & Belletti, N. (2003). Use of natural aroma compounds to improve shelf-life and safety of minimally processed fruits. *Trends in Food Science and Technology*, 15, 201-208.
- La Storia, A., Ercolini, D., Marinello, F., Di Pasqua, R., Villani, F. & Mauriello, G. (2011). Atomic force microscopy analysis shows surface structure changes in carvacrol-treated bacterial cells. *Research in Microbiology*, 162(2), 164-172.
- Lavorgna, M., Piscitelli, F., Mangiacapra, P., & Buonocore, G.G. (2010). Study of the combined effect of both clay and glycerol plasticizer on the properties of chitosan films. *Carbohydrate Polymers*, 82, 291-298.
- Li, F.H., Chen, Y.M., Li, L., Bai, X.L., & Li, S. (2011). Starch-chitosan blend films prepared by glutaraldehyde cross-linking. *Advanced Materials Research*, 415-417, 1626-1629.
- Lichter, A., Zutkhy, Y., Sonogo, L., Dvir, O., Kaplunov, T., Sarig, P., & Ben-Arie, R. (2002). Ethanol controls postharvest decay of table grapes. *Postharvest Biology and Technology*, 24, 301-308.
- Lide, D.R. (1998). Handbook of Chemistry and Physics (87 ed.). Boca Raton, FL: CRC Press. pp. 3–346.
- Lide, D.R. (2007-2008). CRC handbook of Chemistry and Physics Online. In: D.R. Lide (Ed.), CRC press.
- Lieberman, E.R., & Gilbert, S.G. (1973). Gas permeation of collagen films as affected by cross-linkage, moisture, and plasticizer content. *Journal of Polymer Science*, 41, 33-43.

- Limjaroen, P., Ryser, E., Lockhart, H., & Harte, B. (2003). Development of a food packaging coating material with antimicrobial properties. *Journal of Plastic Film and Sheeting*, 19, 95-109.
- Liolios, C.C., Gortzi, O., Lalas, S., Tsaknis, J., & Chinou, I. (2009). Liposomal incorporation of carvacrol and thymol isolated from the essential oil of *Origanum dictamnus* L. and invitro antimicrobial activity. *Food Chemistry*, 112, 77-83.
- Liu, T.L. (2008). Edible films from starch and chitosan: Formulation and Gas Permeabilities. Doctoral dissertation.
- Loget, F. (2002). Wallis entre Hobbes et Newton – La question de l'angle de contact chez les Anglais. *Revue d'histoire des mathématiques*, 8, 207-262.
- López, P., Sánchez, C., Batlle, R., & Nerín, C. (2007a). Development of flexible antimicrobial films using essential oils as active agents. *Journal of Agricultural and Food Chemistry*, 55(21), 8814–8824.
- Lopez, P., Sanchez, C., Batlle, R., & Nerin, C. (2007b). Vapour-phase activities of cinnamon, thyme, and oregano essential oils and key constituents against foodborne microorganisms. *Journal of Agricultural and Food Chemistry*, 55, 4348-4356.
- López-de-Dicastillo, C., Catalá, R., Gavara, R., & Hernández-Muñoz, P. (2011). Food applications of active packaging EVOH films containing cyclodextrins for the preferential scavenging of undesirable compounds. *Journal of Food Engineering*, 104(3), 380-386.
- López-de-Dicastillo, C., Gómez-Estaca, J., Catalá, R., Gavara, R., & Hernández-Muñoz, P. (2012). Active antioxidant packaging films: Development and effect on lipid stability of brined sardines. *Food Chemistry*, 131(4), 1376-1384.
- Lopez-Rubio, A., Almenar, E., Hernandez-Munoz, P., Lagaron, J.M., Catala, R., & Gavara, R. (2004). Overview of active polymer-based packaging technologies for food applications. *Food Reviews International*, 20, 357-87.
- Lovergen, N.V., & Feuge, R.O. (1954). Permeability of acetostearin products to water vapour. *Journal of Agricultural Food Chemistry*, 2, 558-563.
- Lubbers, S., Landy, P., & Voilley, A. (1998). Retention and release of aroma compounds in foods containing proteins. *Food Technology*, 52(1), 68–74.
- Ludwiczak, S., & Mucha, M. (2010). Modeling of water sorption isotherms of chitosan blends. *Carbohydrate Polymers*, 79, 34–39.
- Luo, Y., Teng, Z., Wang, Q.J. (2012). Development of zein nanoparticles coated with carboxymethyl chitosan for encapsulation and controlled release of vitamin D3. *Journal of Agricultural and Food Chemistry*, 60(3):836-43.
- Ma, X.F., Chen, M., Meng, K., & Li, F.F. (2012). Effect of temperature on barrier properties of soy protein isolate films. *Advanced Materials Research*, 380, 270-273.
- Mahdi Ojagh, S., Rezaei, M., Razavi, S.H., & Hosseini, S.M.H. (2010). Effect of chitosan coatings enriched with cinnamon oil on the quality of refrigerated rainbow trout. *Food Chemistry*, 120(1), 193-198.
- Martínez-Camacho, A.P., Cortez-Rocha, M.O., & Ezquerro-Brauer, J.M. (2010). Chitosan composite films: thermal, structural, mechanical and antifungal properties. *Carbohydrate Polymers*, 82, 305-315.

- Martino, V.P., Pollet, E., & Averous, L. (2011). Novative biomaterials based on chitosan and poly (ε-caprolactone): Elaboration of porous structures. *Journal of Polymers and the Environment*, 19, 819–826.
- Martins, J.T., Cerqueira, M.A., & Vicente, A.A. (2012). Influence of α-tocopherol on physicochemical properties of chitosan-based films. *Food Hydrocolloids*, 27, 220–227.
- Martins, J.T., Cerqueira, M.A., Vicente, A.A. (2010). Influence of α-tocopherol on chitosan-edible film properties. *International Conference on Food Innovation*, Food Inova, 2010.
- Masana, M.O., & Baranyi, J. (2000). Growth/no growth interface of *Brochothrix hermosphacta* as a function of pH and water activity. *Food Microbiology*, 17, 485–493.
- Mascheroni, E., Chalier, P., Gontard, N., & Gastaldi, E. (2010). Designing of a wheatgluten/montmorillonite based system as carvacrol carrier: rheological and structural properties. *Food Hydrocolloids*, 24(4), 406–413.
- Massouda, D.F., Visioli, D., Green, D.A., & Joerger, R.D. (2011). Extruded blends of chitosan and ethylene copolymers for antimicrobial packaging. *Packagaging Technology and Science*, DOI: 10.1002/pts.980
- Mastromatteo, M., Barbuzzi, G., Conte, A., & Del Nobile, M.A. (2009). Controlled release of thymol from zein based film. *Innovative Food Science and Emerging Technologies*, 10, 222–227.
- Maté, J.I., & Krochta, J.M. (1996). Comparison of oxygen and water vapor permeabilites of whey protein isolate and β-lactoglobulin edible films. *Journal of Agricultural and Food Chemistry*, 44, 3001–3004.
- Maté, J.I., & Krochta, J.M. (1998). Oxygen uptake model for uncoated and coated peanuts. *Journal of Food Engineering*, 35, 299–312.
- Matsui, T., Ono, A., Shimoda, M., & Osajima, Y. (1992). Thermodynamic elucidation of depression mechanism on sorption of flavor compounds into elecron beam irradiated LDPE and EVA films. *Journal of Agricultural and Food Chemistry*, 40, 479–483.
- Mauriello, G., Ercolini, D., La Stora, A., Casaburi, A., & Villani, F. (2004). Development of polythene films for food packaging activated with an antilisterial bacteriocin from *Lactobacillus curvatus* 32Y. *Journal of Applied Microbiology*, 97(2), 314–322.
- Mayachiev, P., & Devahastin, S. (2010). Effects of drying methods and conditions on release characteristics of edible chitosan films enriched with Indian gooseberry extract. *Food Chemistry*, 118, 594–601.
- McHugh, T.H., & Krochta, J.M. (1994a). Sorbitol- vs glycerol-plasticized whey protein edible films: integrated oxygen permeability and tensile property evaluation. *Journal of Agricultural and Food Chemistry*, 42, 841–845.
- McHugh, T.H., Aujard, J.-F. & Krochta, J.M. (1994b). Plasticized whey protein edible films: water vapor permeability properties. *Journal of Food Science*, 59: 416–419.
- Meares, P. (1954). The diffusion of gases through polyvinyl acetate. *Journal of the American Chemical Society*, 76, 3415–3422.
- Mejlholm, O., & Dalgaard, P. (2002). Antimicrobial effect of essential oils on the seafood spoilage micro-organism *Photobacterium phosphoreum* in liquid media and fish products. *Letters in Applied Microbiology*, 34, 27–31.

- Mendelson, N.H. & Salhi, B. (1996). Patterns of reporter gene expression in the phase diagram of *Bacillus subtilis* colony forms. *Journal of Bacteriology*, 178(7), 1980-1989.
- Mengatto, L.N., Helbling, I.M., & Luna J.A (2012). Recent advances in chitosan films for controlled release of drugs. *Recent patents on drug delivery & formulation*, 6(2), 156-70.
- Mensitieri, G., Di Maio, E., Buonocore, G.G., Nedi, I., Oliviero, M., Sansone, L. & Iannace, S. (2011). Processing and shelf life issues of selected food packaging materials and structures from renewable resources. *Trends in Food Science and Technology*, 22, 72-80.
- Metz, S.J., van de Ven, W.J.C., Mulder, M.H.V., & Wesslin, M. (2005). Mixed gas water vapour/N<sub>2</sub> transport in poly(ethylene oxide) poly(butylene terephthalate) block copolymers. *Journal of Membrane Science*, 266, 51–61.
- Miller, K.S. & Krochta, J.M. (1997). Oxygen and aroma barrier properties of edible films: A review. *Trends in Food Science and Technology*, 8(7), 228-237.
- Min, S., & Krochta, J.M. (2005). Inhibition of *Penicillium commune* by edible whey protein films Incorporating lactoferrin, lactoferrin hydrosylate, and lactoperoxidase systems. *Journal of Food Science*, 70(2), 87-94.
- Mir, S., Yasin, T., Halley, P.J., Siddiqia, H.M., & Nicholson, T. (2011). Thermal, rheological, mechanical and morphological behavior of HDPE/chitosan blend. *Carbohydrate Polymers*, 83(2), 414-421.
- Montebault, A., Viton, C., & Domard, A. (2005a). Physico-chemical studies of the gelation of chitosan in a hydroalcoholic medium. *Biomaterials*, 26(8), 933-943.
- Moradi, M., Tajik, H., Razavi Rohani, S.M., Rasoul Oromiehie, A., Malekinejad, H., Aliakbarlu, & Hadian, J.M. (2012). Characterization of antioxidant chitosan film incorporated with *Zataria multiflora* Boiss essential oil and grape seed extract. *LWT - Food Science and Technology*, 46, 477-484.
- Moreira, M.R., Pereda, M., Marcovich, N.E., & Roura, S.I. (2011). Antimicrobial effectiveness of bioactive packaging materials from edible chitosan and casein polymers: assessment on carrot, cheese, and salami. *Journal of Food Science*, 76(1), M54-63.
- Morillon, V., Debeaufort, F., Blond, G., Capelle, M. & Voilley, A. (2002). Factors affecting the moisture permeability of lipid-based edible films: A review. *Critical Reviews in Food Science and Nutrition*, 42(1), 67–89.
- Moundanga, S. (2012). Personal communication, EMAC Project, Confidential data.
- Mucha, M., & Ludwiczak, S. (2007). Water sorption by biodegradable chitosan/polylactide composites. *Polish Chitin Society, Monograph XII*, 41-48.
- Mucha, M., Ludwiczak, S., & Kawinska, M. (2005). Kinetics of water sorption by chitosan and its blends with poly(vinyl alcohol). *Carbohydrate Polymers*, 62, 42–49.
- Mujica-Paz, H., & Gontard, N. (1997). Oxygen and carbon dioxide permeability of wheat gluten film: effect of relative humidity and temperature. *Journal of Agricultural and Food Chemistry*, 45, 4101-4105.
- Murray, K.A., Kennedy, J.E., McEvoy, B., Vrain, O., Ryan, D., & Higginbotham, C.L. (2012). The effects of high energy electron beam irradiation on the thermal and

structural properties of low density polyethylene. *Radiation Physics and Chemistry*, 81(8), 962-966.

Muzzarelli, R. A. A. (1977). Chitin. Oxford, UK: Pergamon Pres, 103–108.

Muzzarelli, R., Tarsi, R., Filippini, O., Giovanetti, E., Biagini, G., & Varaldo, P.E. (1990). Antimicrobial properties of N-carboxybutyl chitosan. *Antimicrobial Agents and Chemotherapy*, 34, 2019-2023.

Muzzarelli, R.A.A., Boudrant, J., Meyer, D., Manno, N., DeMarchis, M., & Paoletti, M.G. (2012). Current views on fungal chitin/chitosan, human chitinases, food preservation, glucans, pectins and inulin: A tribute to Henri Braconnot, precursor of the carbohydrate polymers science, on the chitin bicentennial. *Carbohydrate Polymers*, 87(2), 995-1012.

Muzzarelli, R.A.A., Isolati, A., & Ferrero, A. (1974). Chitosan membranes: Ion exchange and membranes. Vol. 1. London: Gordon and Breach Science Publishers. P 193-196.

Myllärinen, P., Partanen, R., Seppälä, J., & Forssell, P. (2002). Effect of glycerol on behavior of amylose and amylopectin films. *Carbohydrate Polymers*, 50, 355-361.

Navarro, R., Torre, L., Kenny, J.M., Jiménez, A. (2003). Thermal degradation of recycled polypropylene toughened with elastomers. *Polymer Degradation and Stability*, 82, 279-290.

Nebe-Von-Caron, G., Stephens, P.J., Hewitt, C.J., Powell, J.R., & Badley, R.A. (2000). Analysis of bacterial function by multi-colour and single cell sorting. *Journal of Microbiological Methods*, 42, 97-114.

Nedorostova, L., Kloucek, P., Kokoska, L., Stolcova, M., & Pulkrabek, J. (2009). Antimicrobial properties of selected essential oils in vapour phase against foodborne bacteria. *Food Control*, 20(2), 157–160.

Neogi, P. (1996). Diffusion in polymers. Dekker, New York.

Nerin, C., Tovar, L., Djenane, D., Camo, J., Salafranca, J., Beltran, J.A., & Roncales, P. (2006). Stabilization of beef meat by a new active packaging containing natural antioxidants. *Journal of Agricultural and Food Chemistry*, 54, 7840-7846.

Neto, C.G.T., Giacometti, J.A., Job, A.E., Ferreira, F.C., Fonseca, J.L.C., & Pereira, M.R. (2005). Thermal Analysis of Chitosan Based Networks. *Carbohydrate Polymers* 62(2), 97-103.

Netti, P.A., Del Nobile, M.A., Mensitieri, G., Ambrosio, L., & Nicolais, L. (1996). Water transport in hyaluronic acid esters. *Bioactive and Compatible Polymers*, 11(4), 312–327.

Nostro, A., Marino, A., Blanco, A.R., Cellini, L., Di Giulio, M., Pizzimenti, F., Roccaro, A.S., & Bisignano, G. (2009). In vitro activity of carvacrol against staphylococcal preformed biofilm by liquid and vapour contact. *Journal of Medical Microbiology*, 58, 791-797.

Nostro, A., Scaffaro, R., D'Arrigo, M., Botta, L., Filocamo, A., Marino, A., & Bisignano, G. (2012). Study on carvacrol and cinnamaldehyde polymeric films: mechanical properties, release kinetics and antibacterial and antibiofilm activities. *Applied Microbiology and Biotechnology*, DOI: 10.1007/s00253-012-4091-3.

Ogawa, K., Hirano, S., Miyanishi, T., Yui, T., & Watanabe, T. (1984). A new polymorph of chitosan. *Macromolecules*, 17(4), 973–975.



- Ogawa, K. (1991) Effect of heating an aqueous suspension of chitosan on the crystallinity and polymorphs. *Agricultural and Biological Chemistry*, 55 (9), 2375–2379.
- Ogawa, K., Oka, K., & Yui, T. (1993). X-ray study of chitosan–transition metal complexes. *Chemistry of Materials*, 5 (5), 726–728
- Ogawa, K., Yui, T., & Okuyama, K. (2004). Three D structures of chitosan. *International Journal of Biological Macromolecules*, 34, 1–8.
- Oh, E., & Luner, P.E. (1999). Surface free energy of ethycellulose films and the influence of plasticizers. *International Journal of Pharmaceutics*, 188, 203-219.
- Ojagh, S.M., Rezaei, M., Razavi, S.H., & Hosseini, S.M.H. (2010). Development and of a novel biodegradable film made from chitosan and cinnamon essential oil with low affinity toward water. *Food Chemistry*, 122, 161-166.
- Okuyama, K., Noguchi, K., Hanafusa, Y., Osawa, K., & Ogawa, K. (1999). Structural study of anhydrous tendon chitosan obtained via chitosan/acetic acid complex. *International Journal of Biological Macromolecules*. 26(4), 285-293.
- Okuyama, K., Noguchi, K., Kanenari, M., Egawa, T., Osawa, K., & Ogawa, K. (2000). Structural diversity of chitosan and its complexes. *Carbohydrate Polymers*, 41, 237–247.
- Okuyama, K., Noguchi, K., Miyazawa, T., Yui, T., & Ogawa, K. (1997). Molecular and crystal structure of hydrated chitosan. *Macromolecules*, 30, 5849–5855.
- Olaimat, A.N., & Holley, R.A. (2012). Factors influencing the microbial safety of fresh produce: A review. *Food Microbiology*, 32(1), 1-19.
- Osorio-Madrado, A., David, L., Trombotto, S., Lucas, J.M., Peniche-Covas, C., & Domard, A. (2011). Highly crystalline chitosan produced by multi-steps acid hydrolysis in the solid-state. *Carbohydrate Polymers*, 83, 1730–1739.
- Ouattara, B., Simard, R.E., Piette, G., Begin, A., & Holley, R.A. (2000). Diffusion of acetic and propionic acids from chitosan-based antimicrobial packaging films. *Food Chemistry and Toxicology*, 65(5), 768-773.
- Ousallah, M., Caillet, S. Salmieri, S., Saucier, L. & Lacroix, M. (2004). Antimicrobial and antioxidant effects of milk protein based film containing essential oils for the preservation of whole beef muscle. *Journal of Agricultural and Food Chemistry*, 52, 5598-5605.
- Oussalah, M., Caillet, S., Salmiéri, S., Saucier, L., & Lacroix, M. (2006). Antimicrobial effects of alginate-based film containing essential oils for the preservation of whole beef muscle. *Journal of Food Protection*, 69(10), 2364-2369.
- Owens, D.K. & Wendt, R.C. (1969). Estimation of the surface free energy of polymers. *Journal of Applied Polymer Science*, 13, 1741-1747.
- Oxford University Chemical Safety Data, [www.msds.chem.ox.ac.uk](http://www.msds.chem.ox.ac.uk), acces May 2012.
- Ozdemir, M., & Floros J.D. (2004). Active food packaging technologies. *Critical Reviws in Food Science and Nutrition*, 44, 185–193.
- Park, H. M., Liang, X., Mohanty, A. K., Misra, M., & Drzal, L. T. (2004a). Effect of compatibilizer on nanostructure of the biodegradable cellulose acetate/organoclay nanocomposites. *Macromolecules*, 37, 9076-9082.
- Park, H.J., & Chinnan, M.S. (1995). Gas and water vapor barrier properties of edible films from protein and cellulosic materials. *Journal of Food Engineering*, 25(4), 497-507.

- Park, J.H. (1999). Development of advanced edible coatings for fruits. *Trends in Food Science and Technology*, 10, 254-260.
- Park, S. Y., Marsh, K. S., & Rhim, J. W. (2002). Characteristics of different molecular weight chitosan films affected by the type of organic solvents. *Journal of Food Science*, 67(1), 194–197.
- Park, S.I., & Zhao, Y. (2004). Incorporation of a high concentration of mineral or vitamin into chitosan-based films. *Journal of Agricultural and Food Chemistry*, 52, 1933-1939.
- Park, S.Y., Jun, S.T., & Marsh, K.S. (2001). Physical properties of PVOH/chitosan-blended films cast from different solvents. *Food Hydrocolloids*, 15, 499–502.
- Pawlak, A., & Mucha, M. (2003). Thermogravimetric and FTIR studies of chitosan blends. *Thermochimica Acta*, 396(1-2,5), 153-166.
- Pelissari, F.M., Grossmann, M.V.E., Yamashita, F., & Pineda, E.A.G. (2009). Antimicrobial, mechanical, and barrier properties of cassava starch-chitosan films incorporated with oregano essential oil. *Journal of Agricultural and Food Chemistry*, 57, 7499-7504.
- Pelissari, F.M., Yamashita, F., Garcia, M.A., Martino, W.N., Zaritzky, N.E., & Grossmann, M.V.E. (2012). Constrained mixture design applied to the development of cassava starch–chitosan blown films. *Journal of Food Engineering*, 108, 262-267.
- Percot, A., Viton, C., & Domard, A. (2003). Optimization of chitin extraction from shrimp shells. *Biomacromolecules*, 4, 12–18.
- Perdones, A., Sánchez-González, L., Chiralt, A., & Vargas, M. (2012). Effect of chitosan–lemon essential oil coatings on storage-keeping quality of strawberry. *Postharvest Biology and Technology*, 70, 32-41.
- Pereda, M., Amica, G., & Marcovich, N.E. (2012). Development and characterization of edible chitosan/olive oil emulsion films. *Carbohydrate Polymers*, 87, 1318-1325.
- Pereda, M., Aranguren, M.I., & Marcovich, N.E. (2009). Water vapor absorption and permeability of films based on chitosan and sodium caseinate. *Journal of Applied Polymer Science*, 111, 2777-2784.
- Pereda, M., Aranguren, M.I., & Marcovich, N.E. (2010). Caseinate films modified with tung oil. *Food Hydrocolloids*, 24, 800-808.
- Perisco, P., Abroggi, V., Carfagna, C., Cerruti, P., Ferrocino, I., & Mauriello, G. (2009). Nanocomposite polymer films containing carvacrol for antimicrobial active packaging. *Polymer Engineering and Science*, 49, 1447–1455.
- Petrou, S., Tsiraki, M., Giatrakou, V., Savvaidis, I.N. (2012). Chitosan dipping or oregano oil treatments, singly or combined on modified atmosphere packaged chicken breast meat. *International Journal of Food Microbiology*, 156(3), 264-271.
- Phan, T.D., Debeaufort, F., Luu, D., & Voilley, A. (2005). Functional properties of edible agar-based and starch-based films for food quality preservation. *Journal of Agricultural and Food Chemistry*, 53, 973-981.
- Picón, A., Martínez-Jávega, J.M., Cuquerella, J., Del Río, M.A., & Navarro, P. (1993). Effects of precooling, packaging film, modified atmosphere and ethylene absorber on the quality of refrigerated Chandler and Douglas strawberries. *Food Chemistry*, 48(2), 189-193.

- Pillai, C.K.S., Paul, W., & Sharma, C.P. (2009). Chitin and chitosan polymers: Chemistry, solubility and fiber formation. *Progress in Polymer Science*, 34, 641–678.
- Pires, C., Ramos, C., Teixeira, B., Batista, I., Nunes, M.L., & Marques, A. (2013). Hake proteins edible films incorporated with essential oils: Physical, mechanical, antioxidant and antibacterial properties. *Food Hydrocolloids*, 30(1), 224-231.
- Pires, S.M., Vieira, A.R., Perez, E., Wong, D.L.F., & Hald, T. (2012). Attributing human foodborne illness to food sources and water in Latin America and the Caribbean using data from outbreak investigations. *International Journal of Food Microbiology*, 152(3), 129-138.
- Pitt, J.I., & Hocking, A.D. (1997). Fungi and food spoilage. Cambridge, UK: Cambridge Univ Press. 593.
- Pranoto, Y., Rakshit, S.K., & Salokhe, V.M. (2005a). Enhancing antimicrobial activity of chitosan films by incorporating garlic oil, potassium sorbate and nisin. *LWT*, 38, 859-865.
- Pranoto, Y., Salokhe, V.M., & Rakshit, S.D. (2005b). Physical and antibacterial properties of alginate-based edible film incorporated with garlic oil. *Food Research International*, 38(3), 267-272.
- Pushpadass, H.A., Kumar, A., Jackson, D.S., Wehling, R.L., Dumais, J.J., & Hanna, M.A. (2009). Macromolecular changes in extruded starch-films plasticized with glycerol, water and stearic acid. *Starch – Stärke*, 61, 256-266.
- Qi, Z. H., & Xu, A. (1999). Starch based ingredients for flow encapsulation. *Cereal Food World*, 44, 460–465.
- Quintavalla, S. & Vicini, L. (2002). Antimicrobial food packaging in meat industry. *Meat Science*, 62, 373-380.
- Quirijns, E.J., van Boxtel, A.J.B., van Loon, W.K.P., & van Straten, G. (2005). Sorption isotherms, GAB parameters and isosteric heat of sorption. *Journal of the Science of Food and Agriculture*, 85, 1805-1814.
- Rabel, W. (1971). Einige aspekte der benetzungstheorie und ihre anwendung auf die untersuchung und veränderung der oberflächeneigenschaften von polymeren. *Farbe und Lack*, 77(10), 997-1006.
- Ramos, M., Jiménez, A., Peltzer, M., & Garrigós, M.C. (2012) Characterization and antimicrobial activity studies of polypropylene films with carvacrol and thymol for active packaging. *Journal of Food Engineering*, 109(3), 513-519.
- Rasooli, I., Rezaei, M.B., & Allameh, A. (2006). Growth inhibition and morphological alterations of *Aspergillus niger* by essential oils from *Thymus eriocalyx* and *Thymus xporlock*. *Food Control* 17, 359-364.
- Ratto, J., Hatakeyama, T., & Blumstein, R.B. (1995). Differential scanning calorimetry investigation of phase transition in water/chitosan systems. *Polymers*, 36, 2915-2919.
- Raviv, U., Giasson, S., Kampf, N., Gohy, J.F., Jerome, R., & Klein, J. (2003). Lubrication by charged polymers. *Nature*, 425, 163-165.
- Reinholdt, M., Miehé-Brendlé, J., Delmotte, L., Le Dred, R., & Tuilier, M.H. (2005). Synthesis and characterization of montmorillonite-type phyllosilicates in a fluoride medium. *Clay Minerals*, 40, 177–190.



- Rhim, J-W., Hong, S-I., Park, H-M., & Ng, P.K.W. (2006). Preparation and Characterization of Chitosan-Based Nanocomposite Films with Antimicrobial Activity. *Journal of Agricultural and Food Chemistry*, 54(16), 5814–5822.
- Ribeiro, C., Vicente, A.A., Teixeira, J.A., & Miranda, C. (2007). Optimization of edible coating composition to retard strawberry fruit senescence. *Postharvest Biology and Technology*, 44(1), 63-70.
- Richard, A., & Cooksey, K. (2012). Extruded antimicrobial film targeting Gram-positive pathogens. IAFP 2012 Conference proceedings.
- Rico-Pena, D.C., & Torres, J.A. (1991). Sorbic acid and potassium sorbate permeability of an edible film methylcellulose-palmitic acid film: water activity and pH effects. *Journal of Food Science*, 56, 1991–1995.
- Rinaudo, M., & Domard, A. (1989). Solution properties of chitosan. In G. Skjåk-Bræk, T. Anthonsen, & P. Sandford (Eds.), *Chitin and Chitosan* (pp. 71–86). Elsevier, London, UK.
- Roberts, D. D., Stephen Elmore, J., Langley, K., & Bakker, J. (1996). Effects of sucrose, guar gum and carboxymethylcellulose on the release of volatile flavour compounds under dynamic conditions. *Journal of Agricultural and Food Chemistry*, 44(5), 1321–1326.
- Robertson, G.L. (1993). *Food Packaging Principles and Practice*, Marcel Dekker Inc, New York.
- Robertson, G.L. (2006). *Food Packaging Principles and Practice*. CRC Press.
- Rodríguez, M., Osés, J., Ziani, K., & Maté, J.I. (2006). Combined effect of plasticizers and surfactants on the physical properties of starch based edible films. *Food Research International*, 39, 840–846.
- Rodríguez, M.S., Albertengo, L.A., & Agulló, E. (2002). Emulsification capacity of chitosan. *Carbohydrate Polymers*, 48(3), 271-276.
- Rogers, C.E. (1985). Permeation of gases and vapours in polymers. In J. Comyn (Ed.), *Polymer permeability* (Vol. 2) (pp. 11-73). Elsevier Applied Science Publishers, New York.
- Rojas-Graü, M.A., Avena-Bustillos, R.J., Olsen, C., Friedman, M., Henika, P.R., Martín-Belloso, O., Pan, Z., & McHugh, T.H. (2007a). Effects of plant essential oils and oil compounds on mechanical, barrier and antimicrobial properties of alginate-apple puree edible films. *Journal of Food Engineering*. 81, 634- 641.
- Rojas-Graü, M., Raybaudi-Massilia, R.M., Soliva-Fortuny, R.S., Avena-Bustillos, R.J., McHugh, T.H., & Martín-Belloso, O. (2007b). Apple puree-alginate edible coating as carrier of antimicrobial agents to prolong shelf-life of fresh-cut apples. *Postharvest Biology and Technology*, 45, 254-264.
- Rojas-Graü, M.A., Soliva-Fortuny, R., & Martín-Belloso, O. (2009). Edible coatings to incorporate active ingredients to fresh-cut fruits: a review. *Trends in Food Science and Technology*, 20(10), 438-447.
- Roller, S. (2003). *Natural antimicrobials for the minimal processing of foods* CRC Press, Boca Raton, FL.
- Roller, S., & Seedhar, P. (2002). Carvacrol and cinnamic acid inhibit microbial growth on fresh-cut melon and kiwifruit at 4 degrees and 8 degrees C. *Letters in Applied Microbiology*, 35(5), 390-394.

- de Roos, K. B. (2003). Effect of texture and microstructure on flavour retention and release. *International Dairy Journal*, 13, 593–605.
- Rosa, G.S., Moraes, M.A., Pinto, L.A.A. (2010). Moisture sorption properties of chitosan *LWT - Food Science and Technology*, 43, 415–420.
- Roudaut, G., & Debeaufort, F. (2010). Moisture loss, gain and migration in foods. In L. Skibsted, J. Risbo, & M. Andersen (Eds.), *Chemical deterioration and physical instability of food and beverages* (pp 143-185). Woodhead Publishing.
- Ruiz-Cruz, S., Alvarez-Parrilla, E., de la Rosa, L.A., Martinez-Gonzalez, A.I., de Jesus Ornelas-Paz, J., Mendoza-Wilson, A.M., & Gonzalez-Aguilar, G.A. (2010). Effect of different sanitizers on microbial, sensory and nutritional quality of fresh-cut Jalapeno peppers. *American Journal of Agricultural and Biological Sciences*, 5(3), 331-341.
- Rulon, J. & Robert, H. (1993). Wetting of low-energy surfaces. In J.C. Berg (Ed.), *Wettability* (pp. 4-73), Seattle: Marcel Dekker Inc.
- Saito, H., Tabeta, R., & Ogawa, K. (1987). High-resolution solid-state carbon-13 NMR study of chitosan and its salts with acids: Conformational characterization of polymorphs and helical structures as viewed from the conformation-dependent carbon-13 chemical shifts. *Macromolecules*, 20(10), 2424–2430.
- Sakurai, K., Maegawa, T., & Takahashi, T. (2000). Glass transition temperature of chitosan and miscibility of chitosan/poly(n-vinyl pyrrolidone) blends. *Polymer*, 41, 7051-7056.
- Salame, M. (1986). Barrier polymers. In M. Bakker (Ed.), *The Wiley Encyclopaedia of Packaging Technology* (pp. 51-52.). John Wiley and Sons Inc., New York, 1986.
- Salame, M., & Steingiser, S. (1977). Barrier polymers. *Polymer-Plastics Technology and Engineering*, 8, 155-175.
- Salamone J.C. (1996). *Polymeric Material Encyclopedia*, CRC Press Inc.
- Sánchez-González, L., Cháfer, M., Chiralt, A., & González-Martínez, C. (2010a). Physical properties of edible chitosan films containing bergamot essential oil and their inhibitory action on *Penicillium italicum*. *Carbohydrate Polymers*, 82(2), 277-283.
- Sánchez-González, L., González-Martínez, C., Chiralt, A., & Cháfer, M. (2010b). Physical and antimicrobial properties of chitosan–tea tree essential oil composite films. *Journal of Food Engineering*, 98(4), 443-452.
- Sánchez-González, L., González-Martínez, C., Chiralt, A., & Cháfer, M. (2011a). Antimicrobial activity of polysaccharide films containing essential oils. *Food Control*, 22, 1302-1310.
- Sánchez-González, L., Cháfer, M., González-Martínez, C., Chiralt, A., & Desobry, S. (2011b). Study of the release of limonene present in chitosan films enriched with bergamot oil in food simulants. *Journal of Food Engineering*, 105(1), 138-143.
- Sánchez-González, L., Pastor, C., Vargas, M., Chiralt, A., González-Martínez, C., & Cháfer, M. (2011c). Effect of hydroxypropylmethylcellulose and chitosan coatings with and without bergamot essential oil on quality and safety of cold-stored grapes. *Postharvest Biology and Technology*, 60(1) 57-63.
- Saravacos, G., & Moyer, J. C. (1968). Volatility of some aroma compounds during vacuum-drying of fruit juice. *Food Technology*, 22, 623–627.

- Sathivel, S., Liu, Q., Huang, J., & Prinyawiwatukul, W. (2007). The influence of chitosan glazing on the quality of skinless pink salmon (*Oncorhynchus gorboscha*) fillets during frozen storage. *Journal of Food Engineering*, 83, 366-373.
- Schulz, H., Ozkan, G., Baranska, M., Kruger, H., & Ozcan, M. (2005). Characterisation of essential oil plants from Turkey by IR and Raman spectroscopy. *Vibrational Spectroscopy*, 39, 249-56.
- Schwartzberg, H.G. (1986). Modeling of gas and vapour transport through hydrophilic films. In M. Mathlouthi (Ed.), *Food packaging and preservation: theory and practice* (pp.115). Elsevier, London.
- Scott, G. (1999). Polymers in modern life. Polymers and the Environment. Cambridge, UK: The Royal Society of Chemistry.
- Sebti, I., Ripoche Carnet, A., Blanc, D., Saurel, R., & Coma, V. (2003). Controlled diffusion of an antimicrobial peptide from a biopolymer film. *Trans IChemE*, 81, Part A.
- Sebti, I., Chollet, E., Degrave, P., Noel, C., & Peyrol, E. (2007). Water sensitivity, antimicrobial, and physicochemical analyses of edible films based on HPMC and/or chitosan. *Journal of Agricultural and Food Chemistry*, 55, 693-699.
- Secouard, S., Malhiac, C., Grisel, M., & Decroix, B. (2003). Release of limonene from polysaccharide matrices: Viscosity and synergy effects. *Food Chemistry*, 82(2), 227–234.
- Seuvre, A.-M., Philippe, E., Rochard, S., & Voilley, A. (2006). Retention of aroma compounds in food matrices of similar rheological behaviour and different compositions. *Food Chemistry*, 96(1), 104–114.
- Seydim, A.C., & Sarikus, G. (2006). Antimicrobial activity of whey protein based edible films incorporated with oregano, rosemary and garlic essential oils. *Food Research International*, 39(5), 639-644.
- Shanmugaraj, A. M., Rhee, K. Y., & Ryu, S. H. (2006). Influence of dispersing medium on grafting of aminopropyltriethoxysilane in swelling clay materials. *Journal of Colloid Interface Science*, 298, 854–859.
- Shin, G.H., Lee, Y.H., Lee, J.S., Kim, Y.S., Choi, W.S., & Park, H.J. (2002). Preparation of plastic and biopolymer multilayer films by plasma source ion implantation. *Journal of Agricultural and Food Chemistry*, 50(16), 4608-4614.
- Simantos, D. (2002). Propriétés de l'eau dans les produits alimentaires: activité de l'eau, diagrammes de phases d'états. In M. Le Meste, D. Lorient, & D. Simantos (Eds.), *L'eau dans les Aliments* (pp. 49-79). Tec. & Doc-Lavoisier, Paris (France).
- Siripatrawan, U., & Harte, B.R. (2010). Physical properties and antioxidant activity of an active film from chitosan incorporated with green tea extract. *Food Hydrocolloids*, 24, 770-775.
- Siripatrawan, U., & Noipha, S. (2012). Active film from chitosan incorporating green tea extract for shelf life extension of pork sausages. *Food Hydrocolloids*, 27(1), 102-108.
- Skandamis, P.N., & Nychas, G.-J.E. (2001). Effect of oregano essential oil on microbiological and physico-chemical attributes of minced meat stored in air and modified atmospheres. *Journal of Applied Microbiology*, 91, 1011–1022.

- Skandamis, P.N., & Nychas, G.J.E. (2002). Preservation of fresh meat with active and modified atmosphere packaging conditions. *International Journal of Food Microbiology*, 79, 35-45.
- Skandamis, P.N., Stopforth, J.D., Kendall, P.A., Belk, K.E., Scanga, J.A., Smith, G.C., & Sofos, J.N. (2007). Modeling the effect of inoculum size and acid adaptation on growth/no growth interface of *Escherichia coli* O157:H7. *International Journal of Food Microbiology*, 120, 237-249.
- Smith, S.A. (1986). Polyethylene, low density. In M. Bakker (Ed.), *The wiley encyclopedia of packaging technology* (pp.514-523). New York: John Wiley & Sons.
- Smith-Palmer, A., Stewart, J., & Fyfe, L. (2001). The potential application of plant essential oils as natural food preservatives in soft cheese. *Food Microbiology*, 18, 463-470.
- Sollogoub, C., Guinault, A., Bonnebat, C., Bennjima, M., Akrou, L., Fauvarque, J.F., & Ogier, L. (2009). Formation and characterization of crosslinked membranes for alkaline fuel cells. *Journal of Membrane Science*, 335, 37-42.
- Song, B., & Springer, J. (1996a). Determination of interfacial tension from the profile of a pendant drop using computer-aided image processing 1. Theoretical. *Journal of Colloid and Interface Science*, 184(1), 64-76.
- Song, B., & Springer, J. (1996b). Determination of interfacial tension from the profile of a pendant drop using computer-aided image processing 1. Experimental. *Journal of Colloid and Interface Science*, 184(1), 77-91.
- Soottitawatt, A., Takayama, K., Okamura, K., Muranaka, D., Yoshii, H., Fururta, T., Ohkaware, M., & Linko, P. (2005). Microencapsulation of l-menthol by spray drying and its release characteristics. *Innovative Food Science and Emerging Technologies*, 6, 163-170.
- Sothornvit, R., & Krochta, J.M. (2005). Plasticizers in edible films and coatings. In J.H. Han (Ed.), *Innovations in food packaging*. San Diego, Calif.: Elsevier Academic Press. pp. 403-33.
- Sothornvit, R., & Pitak, N. (2007). Oxygen permeability and mechanical properties of banana films. *Food Research International*, 40, 365-70.
- Sothornvit, R., Rhim, J. W., & Hong, S. I. (2009). Effect of nano-clay type on the physical and antimicrobial properties of whey protein isolate/clay composite films. *Journal of Food Engineering*, 91, 468-473.
- Sousa, J.P., Azerêdo, G.A., de Araújo Torres, R., da Silva Vasconcelos, M.A., da Conceição, M.S., de Souza, E.L. (2012). Synergies of carvacrol and 1,8-cineole to inhibit bacteria associated with minimally processed vegetables. *International Journal of Food Microbiology*, 154(3), 145-151.
- Srinivasa, P.C., Revathy, B., Ramesh, M.N., Prashanth, K.V.H., & Tharanathan, R.N. (2002). Storage studies of mango packed using biodegradable chitosan films. *European Food Research and Technology*, 215, 504-508.
- Srinivasa, P.C., Ramesh, M.N., Kumar, K.R., & Tharanathan, R.N. (2004). Properties of chitosan films prepared under different drying conditions. *Journal of Food Engineering*, 63, 79-85.

- Srinivasa, P.C., Ramesh, M.N., & Tharanathan, R.N. (2007). Effect of plasticizers and fatty acids on mechanical and permeability characteristics of chitosan films. *Food Hydrocolloids*, 21, 1113-1122.
- Stammati, A., Bonsi, P., Zucco, F., Moezelaar, R., Alakomi, H.-L., & Von Wright, A. (1999). Toxicity of selected plant volatiles in microbial and mammalian short-term assays. *Food and Chemical Toxicology*, 37, 813-823.
- Stannett, V. (1968). Simple Gases, in *Diffusion in Polymers*, Crank, J. and Park, G.S. (eds.), Academic Press, London and New York, 41-73.
- Stannett, V. (1978). The transport of gases in synthetic polymeric membranes - An historic perspective. *Journal of Membrane Science*, 3, 97-115.
- Stone, H., & Sidel, J.L. (1993). *Sensory Evaluation Practices*. 2nd ed. Academic Press: San Diego.
- Suppakul, P., Chalernsook, B., Ratisuthawat, B., Prapasitthi, S., & Munchukangwan, N. (2012). Empirical modeling of moisture sorption characteristics and mechanical and barrier properties of cassava flour film and their relation to plasticizing and antiplasticizing effects, *LWT - Food Science and Technology* doi.org/10.1016/j.lwt.2012.05.013.
- Suppakul, P., Miltz, J., Sonneveld, K., & Bigger, S. W. (2003). Antimicrobial properties of basil and its possible application in food packaging. *Journal of Agricultural and Food Chemistry*, 51, 3197-3207.
- Suppakul, P., Miltz, J., Sonneveld, K., & Bigger, S.W. (2003). Active packaging technologies with an emphasis on antimicrobial packaging and its applications. *Journal of Food Science*, 68(2), 408-420.
- Suppakul, P., Miltz, J., Sonneveld, K., & Bigger, S.W. (2006). Characterization of antimicrobial films containing basil extracts. *Packaging Technology and Science*, 19(5), 259-268.
- Suppakul, P., Sonneveld, K., Bigger, S.W., & Miltz, J. (2008). Efficacy of polyethylenebased antimicrobial films containing principal constituents of basil. *LWT - Food Science and Technology*, 41(5), 779-788.
- Suyatma, N.E., Tightzert, L., & Copinet, A. (2005). Effects of Hydrophilic Plasticizers on Mechanical, Thermal, and Surface Properties of Chitosan Films. *Journal of Agricultural and Food Chemistry*, 53, 3950-3957.
- Šćetar, M., Kurek, M., & Galić, K. (2010). Trends in fruit and vegetable packaging – a review. *Croatian Journal of Food Technology, Biotechnology and Nutrition*, 5, 69-86.
- Talens, P., Pérez-Masía, R., Fabra, M.J., Vargas, M., & Chiralt, A. (2012). Application of edible coatings to partially dehydrated pineapple for use in fruit-cereal products. *Journal of Food Engineering*, 112(1-2), 86-93.
- Talja, R.A., Helén, H., Roos, Y.H., & Jouppila, K. (2007). Effect of various polyols and polyol contents on physical and mechanical properties of potato starch-based films. *Carbohydrate Polymers*, 67, 288-295.
- Tanigawa, J., Miyoshi, N., & Sakurai, K. (2008). Characterization of chitosan/citrate and chitosan/acetate films and applications for wound healing. *Journal of Applied Polymer Science*, 110, 608-615.
- Thangvaravut, H., Chiewchan, N., & Devahastin, S. (2012). Inhibitory effect of chitosan films incorporated with 1,8-Cineole on *Salmonella* attached on model food surface. *Advanced Materials Research*, 506, 599-602.



- Tharanathan, R.N. (2003). Biodegradable films and composite coatings: past, present and future. *Trends in Food Science and Technology*, 14, 71–78.
- Tihminlioglu, F., Atik, D., & Özen, B. (2010). Water vapor and oxygen-barrier performance of corn–zein coated polypropylene films. *Journal of Food Engineering*, 96, 342-347.
- Tongnuanchan, P., Benjakul, S., & Prodpran, T. (2012). Properties and antioxidant activity of fish skin gelatin film incorporated with citrus essential oils. *Food Chemistry*, 134(3), 1571-1579.
- Torres, J.A. (1994). Edible coating and films from proteins. In Hettiarachchy, A., Iegler, G. (Ed). *Protein functionality in food systems*. IFT/Marcel Dekker Press, New York, p. 467.
- Torres, M.A., Aimoli, C.G., Beppu, M.M., & Frejlich J. (2005). Chitosan membrane with patterned surface obtained through solution drying. *Colloid Surface A*, 268, 175-179.
- Tsigarida, E., Skandamis, P., & Nychas, G.J. (2000). Behaviour of *Listeria monocytogenes* and autochthonous flora on meat stored under aerobic, vacuum and modified atmosphere packaging conditions with or without the presence of oregano essential oil at 5 degrees C. *Journal of Applied Microbiology*, 89(6), 901-909.
- Tucker, A.O., & Maciarello, M.J. (1994). Oregano: botany, chemistry and cultivation. In G. Charalambous (Ed.), *Spices, herbs and edible fungi* (pp.439-456). Elsevier Science, Amsterdam, The Netherlands.
- Tunc, S., & Duman, O. (2010). Preparation and characterization of biodegradable methyl cellulose/montmorillonite nanocomposite films. *Applied Clay Science*, 48(3), 414 - 424.
- Tunç, S., & Duman, O. (2011). Preparation of active antimicrobial methyl cellulose/carvacrol/montmorillonite nanocomposite films and investigation of carvacrol release. *LWT - Food Science and Technology*, 44, 465-472
- Tunc, S., Angellier, H., Cahyana, Y., Chalier, P., Gontard, N., & Gastaldi, E. (2007). Functional properties of wheat gluten/montmorillonite nanocomposite films processed by casting. *Journal of Membrane Science*, 289, 159-168.
- Turhan, K.N., & Sahbaz, F. (2004). Water vapour permeability, tensile properties and solubility of methylcellulose-based edible film. *Journal of Food Engineering*, 61, 459-466.
- Tzoumaki, M.V., Biliaderis, C.G., & Vasilakakis, M. (2009). Impact of edible coatings and packaging on quality of white asparagus (*Asparagus officinalis*, L.) during cold storage. *Food Chemistry*, 117, 55–63.
- Ultee, A., Kets, E.P.W. & Smid, J. (1999). Mechanisms of action of carvacrol on the food-borne pathogen *Bacillus cereus*. *Appl Environ Microbiol* 65, 4606–4610.
- Ultee, A., & Smid, E.J. (2001). Influence of carvacrol on growth and toxin production by *Bacillus cereus*. *International Journal of Food Microbiology*, 64, 373–378.
- Ultee, A., Kets, E.P.W., Alberda, M., Hoekstra, F.A., & Smith, E.J. (2000). Adaptation of the food-borne pathogen *Bacillus cereus* to carvacrol. *Archives of Microbiology*, 174, 233-238.
- Uspenskii, S.A., Vikhoreva, G.A., Sonina, N.A., & Gal'braikh, L.S. (2010). Properties of acetic-acid alcohol-containing solutions of chitosan. *Fibre Chemistry*, 42(2), 88-91.

- Uyttendaele, M., Neyts, K., Vanderswalmen, H., Notebaert, E., & Debevere, J. (2004). Control of *Aeromonas* on minimally processed vegetables by decontamination with lactic acid, chlorinated water, or thyme essential oil solution. *International Journal of Food Microbiology*, 90(3), 263-271.
- Valderrama Solano, A.C., & de Rojas Gante, C. (2011). Two different processes to obtain antimicrobial packaging containing natural oils. *Food and Bioprocess Technology*, 5(6), 2522-2528.
- Valero, M., & Giner, M.J. (2006). Effects of antimicrobial components of essential oils on growth of *Bacillus cereus* INRA L2104 in and the sensory qualities of carrot broth. *International Journal of Food Microbiology*, 106(1), 90-94.
- Van Oss, C.J. (1994). Interfacial forces in aqueous media. New York: Marcel Dekker.
- Vargas, M., Albors, A., & Chiralt, A. (2011a). Application of chitosan-sunflower oil edible films to pork meat hamburgers. *Procedia Food Science*, 1, 39-43.
- Vargas, M., Albors, A., Chiralt, A., & González-Martínez, C. (2009). Characterization of chitosan–oleic acid composite films. *Food Hydrocolloids*, 23, 536-547.
- Vargas, M., Albors, A., Chiralt, A., Gonzalez-Martinez, C. (2006). Quality of cold-stored strawberries as affected by chitosan–oleic acid edible coatings. *Postharvest Biology and Technology*, 41, 164–171.
- Vargas, M., Perdones, A., Chiralt, A., Cháfer, M. & González-Martínez, C. (2011b). Effect of homogenization conditions on physicochemical properties of chitosan-based film-forming dispersions and films. *Food Hydrocolloids*, 25, 1158–1164.
- Vermeiren, L., Heirlings, L., Devlieghere, F., & Debevere, J. (2003). Oxygen, ethylene and other scavengers. I. R. Ahvenainen (Ed.), *Novel food packaging techniques*, Woodhead Publishing Limited/CRC Press LLC.
- Viazis, S., & Diez-Gonzalez, F. (2011). Chapter one - Enterohemorrhagic *Escherichia coli*: The Twentieth Century's Emerging Foodborne Pathogen: A Review. In: D.L. Sparks (Ed.), *Advances in Agronomy* (pp. 1-50). Academic Press.
- Villalobos, R., Hernández-Muñoz, P., & Chiralt, A. (2006). Effect of surfactants on water sorption and barrier properties of hydroxypropyl methylcellulose films. *Food Hydrocolloids*, 20, 502–509.
- Vogler, E.A. (1998). Structure and reactivity of water at biomaterial surfaces *Advances in Colloid and Interface Science*, 74 (1-3) 69-117.
- Voilley, A., & Simatos, D. (1980). Retention of aroma compounds during freeze and air drying. In P. Linko, Y. Malkki, J. Olkku, & J. Larinkari (Eds.), *Food process engineering* (pp. 371–384). London: Applied Sciences.
- Von Bahr, M., Tiberg, F., & Zhmud, B.V. (1999). Spreading dynamics of surfactant solutions. *Langmuir*, 15, 7069-7075.
- Wan, J., Wilcock, A. & Coventry, M.J. (1998). The effect of essential oils of basil on the growth of *Aeromonas hydrophila* and *Pseudomonas fluorescens*. *Journal of Applied Microbiology*, 84, 152-158.
- Wang, S. F., Shen, L., Tong, Y. J., Chen, L., Phang, I. Y. & Lim, P. Q. (2005). Biopolymer chitosan/montmorillonite nanocomposites: Preparation and characterization. *Polymer Degradation and Stability*, 90, 123–131.

Wang, X., Du, Y., Luo, J., Lin, B., & Kennedy, J.F. (2007). Chitosan/organic rectorite nanocomposite films: Structure, characteristic and drug delivery behaviour. *Carbohydrate Polymers*, 69, 41–49.

Wareing, V.M. (1999). Thickening and gelling agents for food. In A. Imeson (Editor), *Exudate gums* (pp. 86-99). Gaithersburg, MD: Aspen Publishers.

Watnick, P.I., Lauriano, C.M., Klose, K.E., Croal, L. & Kolter, R. (2001). The absence of a flagellum leads to altered colony morphology, biofilm development and virulence in *Vibrio cholerae* O139. *Molecular Microbiology*, 39(2), 223-235.

Weber, C.J. (2000). Biobased packaging materials for the food industry. Food Biopack. project EU Directorate 12.

Weinkauff, D.H., & Paul, D.R. (1990). Effects of structure order on barrier properties. In W.J. Koros (Ed.), *Barrier polymers and structures* (pp. 60-91). American Chemical Society: Washington, DC.

Weissinger, W.R., McWatters, K.H., & Beuchat, L.R. (2001). Evaluation of volatile chemical treatments for lethality to *Salmonella* on alfalfa seeds and sprouts. *Journal of Food Protection*, 64(4), 442-450.

Weon, J.I. (2010). Effects of thermal ageing on mechanical and thermal behaviors of linear low density polyethylene pipe. *Polymer Degradation and Stability*, 95(1), 14-20

Whorton, C. & Reineccius, G. (1995). Evaluation of the mechanisms associated with the release of encapsulated flavor materials from maltodextrin matrices. In S.J. Risch & G.A. Reineccius (Eds.), *Encapsulation and controlled release of food ingredients* (pp. 143-160). Washington: ACS Symposium Series, American Chemical Society.

Wiles, J.L., Vergano, P.J., Barron, F.H., Bunn, J.M., & Testin, R.F. (2000). Water vapor transmission rates and sorption behavior of chitosan films. *Journal of Food Science*, 65, 1175– 1179.

Wilke, C.R., & Chang, P. (1955). Correlation of diffusion coefficients in dilute solutions. *AIChE Journal*, 1, 264-27.

Wong, D.W.S., Gastineaut, F.A., Gregorski, K.S., Tillin, S.J., & Pavlath, A.E. (1992). Chitosan-lipid Films: microstructure and surface energy. *Journal of Agricultural and Food Chemistry*, 40, 540-544.

Xiao, C.B., Zhang, Z.J., Zhang, J.H., Lu, Y.S., & Zhang, L. (2003). Properties of regenerated cellulose films plasticized with alpha-monoglycerides. *Journal of Applied Polymer Science*, 89, 3500-3505.

Xu, Y., Ren, X., & Milford, A. (2006). Chitosan/clay nanocomposite film preparation and characterization. *Journal of Applied Polymer Science*, 99, 1684-1691.

Yakimets, I., Paes, S.S., Wellner, N., Smith, A.C., Wilson, R.H., & Mitchell, J.R. (2007). Effect of water content on the structural reorganization and elastic properties of biopolymer films: a comparative study. *Biomacromolecules*, 8, 1710-1722.

Yalpani, M., Johnson, F., & Robinson, L. E. (1992). *Advance in chitin and chitosan*. Elsevier Applied Science, London.

Young, T. (1805). An essay on the cohesion of fluids. *Philosophical Transactions of the Royal Society*, 95, 65-87.

Zanetti, M., Bracco, P., & Costa, L. (2004). Thermal degradation behaviour of PE/clay nanocomposites. *Polymer Degradation and Stability*, 85, 657-665.



- 
- Zenkiewicz, M. (2007). Methods for the calculation of surface free energy of solids. *Journal of Achievements in Materials and Manufacturing Engineering*, 24(1), 137-145.
- Zhao, Z., Li, Q.S., Di, Y.B., Wang, X., & Hong, W. (2012). Effect of chitosan as antimicrobial agent on flame retardant protein viscose fiber. *Advanced Materials Research*, 427, 32-37.
- Ziani, K., Oses, J., Coma, V., & Maté, J.I. (2008). Effect of the presence of glycerol and Tween 20 on the chemical and physical properties of films based on chitosan with different degree of deacetylation. *LWT - Food Science and Technology*, 41, 2159-2165
- Zimm, B.H., & Lundberg, J.L. (1956). Sorption of vapors by high polymers. *Journal of Physical Chemistry*, 60, 425-428.
- Zinoviadou, K.G., Koutsoumanis, K.P., & Biliaderis, C.G. (2009). Physico-chemical properties of whey protein isolate films containing oregano oil and their antimicrobial action against spoilage flora of fresh beef. *Meat Science*, 82, 338-345.
- Zisman, W.A. (1964). Contact angle wettability and adhesion. In R.F. Gould (Ed.), *Advances in chemistry series* (pp. 1-5). Washington, DC: American Chemical Society.
- Zivanovic, S., Chi, S., & Draughon, A.F. (2005). Antimicrobial activity of chitosan films enriched with essential oils. *Journal of Food Science*, 70(1), M45-M51.
- Zohuriaan, M.J., & Shokrolahi, F. (2004). Thermal studies on natural and modified gums. *Polymer Testing*, 23(5), 575-579.

